UNIVERSIDAD NACIONAL AUTÓNOMA DE MÉXICO

PROGRAMA DE MAESTRÍA Y DOCTORADO EN CIENCIAS BIOQUÍMICAS

Efecto de la preadministración de N-acetilcisteína en la función mitocondrial y la S-glutationilación en la insuficiencia renal aguda experimental

TESIS

PARA OPTAR POR EL GRADO DE:

Doctor en Ciencias

PRESENTA:

M. C. Omar Emiliano Aparicio Trejo

TUTOR PRINCIPAL:
Dr. José Pedraza Chaverri
Facultad de Química

MIEMBROS DEL COMITÉ TUTOR:
Dra. Perla D. Maldonado Jiménez
Instituto Nacional de Neurología Neurocirugía
Dr. Salvador Uribe Carvajal
Instituto de Fisiologia Celular

Ciudad de México, Septiembre, 2020

7-9-2020

Resumen del proyecto

Dado que la función renal depende de la homeostasis mitocondrial, recientemente se ha sugerido que la disfunción mitocondrial, específicamente alteraciones en la bioenergética y estado redox, podrían ser un factor común involucrado en la génesis y progresión del daño renal. En este sentido, el daño renal inducido por ácido fólico (FA) es un modelo experimental ampliamente utilizado para estudiar los mecanismos involucrados en el daño renal agudo (AKI). Aunado a esto, la AKI inducida por FA puede evolucionar en un corto tiempo hacia la enfermedad renal crónica (CKD), por lo que este modelo permite también estudiar la transición AKI-CKD. Sin embargo, los mecanismos moleculares relacionados a las alteraciones mitocondriales, su evolución a lo largo del tiempo y su participación en el génesis de la AKI y su posible progresión hacia la CKD siguen siendo poco conocidos. Por otro lado, se ha sugerido que la N-acetilcisteína (NAC) podría ser un agente protector capaz de prevenir la disfunción mitocondrial y por lo tanto, el deño renal. Esto dada la capacidad de la NAC para aumentar la cantidad de glutatión mitocondrial, regulando así los niveles de S-glutationilación, modificación postraduccional reversible que ha surgido como un mecanismo protector, capaz de vincular el metabolismo energético con la homeostasis redox mitocondrial. Sin embargo, esta hipótesis tampoco se ha explorado.

El presente trabajo está dividido en dos partes. En la primera demostramos por primera vez que, a las 24 h posteriores a su administración, el FA induce alteraciones en la bioenergética, estado redox y dinámica mitocondrial, así como una mitofagia disfuncional. Dichos mecanismos favorecen en conjunto el desarrollo de la AKI. Por su parte, el pretratamiento con NAC previene dichas alteraciones mitocondriales a las 24 h y, por lo tanto, el desarrollo de la AKI. Estos efectos protectores de la NAC están relacionados con la capacidad observada de esta molécula para preservar la S-glutationilación de las proteínas y los niveles de glutatión en las mitocondrias. En la segunda parte de este trabajo, se procedió evaluar temporalmente las alteraciones en la bioenergética y estado redox mitocondrial en la progresión hacia la CKD. El estudio de la función mitocondrial en diferentes puntos de tiempo reveló que, durante el intervalo de tiempo evaluado, existe un deterioro sostenido en la capacidad de fosforilación oxidativa y en la β-oxidación mitocondrial, atribuibles a la disminución en la actividad de los complejos mitocondriales I y III. Esto junto con la permanencia del desacoplamiento y un estado pro-oxidante en dicho organelo, favorece la transición AKI-CKD. Aún más, la protección mitocondrial ejercida por la NAC en la AKI no sólo previene el deterioro de la función mitocondrial a largo plazo, sino también el desarrollo de la CKD. Tomados en conjunto, nuestros resultados no sólo respaldan la idea de que estos mecanismos mitocondriales pueden ser un blanco terapéutico para prevenir el desarrollo de la AKI, sino que también respaldan la idea de que preservar la función mitocondrial durante un evento de AKI puede ser una estrategia útil para prevenir el desarrollo de la CKD.

Abstract

Kidney function highly depends on mitochondrial homeostasis. Therefore, it has been suggested that mitochondrial dysfunction, specifically alterations in bioenergetics and redox state, are a common factor involved in the genesis and progression of kidney damage. In this way, folic acid (FA) induced kidney damage model is widely used to study the mechanisms involved in the acute kidney damage (AKI). Furthermore, FA-induce AKI can quickly evolve into chronic kidney disease (CKD), allowing us to study the AKI-CKD transition. However, the molecular mechanisms related to the mitochondrial alterations, their evolution over time and their participation in the genesis of AKI and its progression towards CKD remain poorly understood. On the other hand, it has been suggested that N-acetylcysteine (NAC) administration can be able to prevent mitochondrial dysfunction and the posterior kidney damage. Thus, given the NAC ability of increase the mitochondrial glutathione concentration and consequently regulating the levels of S-glutathione, a reversible post-translational modification that has emerged as a protective mechanism, able to link energy metabolism with mitochondrial redox homeostasis. However, this hypothesis has not been explored.

The present work is divided into two parts. In the first one, it is demonstrated for the first time that FA induces alterations in mitochondrial bioenergetics, redox state, dynamics and mitophagy at 24 h after its administration. Furthermore, together these alterations favor the AKI development. Meanwhile, NAC pretreatment prevents these mitochondrial alterations at 24 h, avoiding AKI development. These NAC protective effects are related to its ability of preserve the S-glutathionylation and glutathione levels in mitochondria. In the second part, we proceeded to temporarily evaluate the alterations in mitochondrial bioenergetics and redox state along the AKI-CKD transition. This reveals a sustained impairment in the oxidative phosphorylation capacity and in mitochondrial β-oxidation during the evaluated time, which is attributable to the complex I and III activities decrease. Which, together with the permanence of the decoupling and a pro-oxidant state in this organelle, favors the AKI-CKD transition. Furthermore, the mitochondrial protection exerted by NAC in AKI prevents not only the long-term deterioration of mitochondrial function, but also the CKD development. Taken together, our data support the idea that these mitochondrial mechanisms are therapeutic targets to prevent the AKI development, furthermore, preserving mitochondrial function during an AKI event can be a useful strategy to prevent CKD development.

Agradecimientos

Se agradece al **Consejo Nacional de Ciencia y Tecnología (CONACYT)** por la beca para realizar mis estudios de doctorado y por el apoyo económico (*proyecto A1-S-7495*), al **Programa de Apoyo a Proyectos de Investigación e Innovación Tecnológica (PAPIIT)** con *número de proyecto IN202219* y al programa de **Apoyo a la Investigación y Posgrado (PAIP)** *5000-9105* de la Facultad de Química por la ayuda recibida para la elaboración de este trabajo.

Se agradece también al **Programa de Apoyo a los Estudios del Posgrado (PAEP)** por el apoyo recibido para presentar este proyecto en la *20th European Bioenergetics Conference* en agosto del 2018 Budapest, Hungría.

Dedicatorias personales

Con especial dedicación a mis padres, por todo el apoyo, amor y confianza que me han procurado durante toda mi vida, sin el que no hubiera sido posible este y cada uno de los logros que he alcanzado durante mi vida. Porque ustedes siempre han sido mi ejemplo de conciencia social, dedicación, trabajo, principios, perseverancia y lucha frente a las desigualdades sociales.

"Cuando el jilguero no puede cantar,
Cuando el poeta es un peregrino,
Cuando de nada nos sirve rezar.
Caminante no hay camino,
Se hace camino al andar.
Golpe a golpe, verso a verso...
Golpe a golpe, verso a verso..."

A Miriam, mi pareja durante todos estos años. Por todo el apoyo, amor, tiempo y cariño que me has brindado.

"Comenzamos felices a juntar cicatrices,
como buenas señales de los años
y peldaño a peldaño, levantamos paisaje".

A mi hermana, mis abuelos y al resto de mi familia, gracias por su apoyo, tiempo y cariño.

A la doctora Tapia, al doctor Molina-Jijón y al doctor Pedraza gracias por su orientación. Agradezco también a los doctores, técnicos y compañeros del laboratorio 315 y de los diferentes laboratorios involucrados en este proyecto, por su apoyo experimental, orientación y comentarios que ayudaron a enriquecer este trabajo.

Índice de abreviaturas y acrónimos

AKI	Las siglas en ingles de daño renal agudo
ADP	Adenosina-5-difosfato
ATP	Adenosina-5-trifosfato
BSA	Las siglas en ingles de albúmina sérica bovina
BUN	Las siglas en ingles de nitrógeno ureico en sangre
CI	Complejo I del sistema de transporte de electrones
CII	Complejo II del sistema de transporte de electrones
CIII	Complejo III del sistema de transporte de electrones
CIV	Complejo IV del sistema de transporte de electrones
CKD	Las siglas en ingles de insuficiencia renal crónica
CCCP	Las siglas en ingles de m-clorocarbonilcianuro fenilhidrazona
CT	Las siglas en ingles de túbulos coletores
DCPIP	Sal de sodio de hidrato de 2,6-diclorofenol
DHE	Las siglas en ingles de dihidroetidio
DMEM	Medio de cultivo *Dulbecco's Modified Eagle's*
DPI	Las siglas en ingles de cloruro de difeniliodonio
Drp1	Proteína 1 relacionada a la dinamina
DT	Las siglas en ingles de túbulo distal
DuB	Decilubiquinona
EGTA	Ácido etilenglicol-bis(β-aminoetiléter)-N,N,N',N-tetraacético
EDTA	Ácido etilendiaminotetracético
ETS	Las siglas en ingles de sistema de transporte de electrones
FA	Las siglas en ingles de ácido fólico
FF	Fracción de filtración
FBS	Las siglas en ingles de suero fetal bovino
Fis1	Proteína de fisión 1
GFR	Las siglas en ingles de tasa de filtración glomerular
GPx	Glutatión peroxidasa
GR	Glutatión reductasa
GSH	Glutatión reducido
GSSG	Glutatión disulfuro u oxidado
GST	Glutatión S-transferasa
Grx	Glutaredoxina
G6PDH	Glucosa-6-fosfato deshidrogenasa
H_2O_2	Peróxido de hidrógeno
HEPES	Ácido 4-(2-hidroxietil)-1-piperazina etanosulfónico
HIF	Las siglas en ingles de factor inducible por la hipoxia
HRP	Las siglas en ingles de peroxidasa de "rábano picante"
H&E	Tinción de hematoxilina y eosina
RCI	Las siglas en ingles de índice de control respiratorio
KCN	Cianuro de potasio
L-NAME	N^G-nitro-L-arginina metil éster
MAP	Las siglas en ingles de presión arterial media
MDA	Marcador de lipoeroxidación malondialdehído
MOM	Las siglas en ingles de membrana externa mitocondrial

Mfn1	Mitofusina 1
Mfn2	Mitofusina 2
MPTs	Las siglas en ingles de modificaciones post-traduccionales
NAC	N-acetilcisteína
NEM	N-etilmaleimida
NDUFB8	Subunidad beta 8 de la NADH deshidrogenasa
Nos	Sintasa de óxido nítrico
Nox	NADPH oxidasa
NRF1	Factor nuclear respiratorio 1
NRF2	Factor nuclear respiratorio 2
$O_2^{\bullet-}$	Anión superóxido
Opa1	Proteína de atrofia óptica 1
OXPHOS	Las siglas en ingles de fosforilación oxidativa
P	Respiración asociada a la OXPHOS
PBS	Solución salina taponeada con fosfatos
Pink1	Cinasa putativa inducida por PTEN 1
PGC-1α	Coactivador-1 alfa del receptor *gamma* activado por proliferadores de peroxisomas
Prx	Peroxiredoxina
PT	Las siglas en ingles de túbulo proximal
RBF	Las siglas en ingles de flujo sanguíneo renal
RVR	Las siglas en ingles de resistencia vascular renal
RPF	Las siglas en ingles de flujo plasmático renal
ROS	Las siglas en ingles de especies reactivas de oxígeno
snGFR	Filtración glomerular por nefrona
SOD	Superóxido dismutasa
SDS	Dodecilsulfato de sodio
S3	Estado 3 respiratorio
S4o	Estado 4 respiratorio inducido por oligomicina
TAL	Las siglas en ingles de segmento grueso ascendente del asa de Henle
TDL	Las siglas en ingles de segmento delgado descendente del asa Henle
TFAM	Factor A de la transcripción mitocondrial
TMPD	Tetrametil-p-fenilendiamina
VAS2870	3-bensoxazol-2-il-3-bencil-3H-[1,2,3]triazolo[4,5-d]pirimidin-7-il sulfuro, inhibidor de la Nox
V	Vehículo
VDAC	Canal aniónico dependiente de voltaje
4-HNE	4-hidroxinonenal, marcador de estrés oxidante
ΔΨm	Potencial de membrana mitocondrial

Tabla de contenido

Resumen del proyecto 2
Abstract 3
Agradecimientos 4
Dedicatorias personales 5
Índice de abreviaturas y acrónimos 6
Tabla de contenido 8
1.Introducción 11
1.1. El riñón y su estructura 11
..... 13
1.2. La mitocondria en el riñón 13
2. Antecedentes 16
2.1. La insuficiencia renal aguda (AKI) y la enfermedad renal crónica (CKD) 16
2.1. Las mitocondrias y su papel en la enfermedad renal 17
2.1.1. Alteraciones en la bioenergética mitocondrial en la AKI y la CKD 17
2.1.2. Las ROS mitocondriales y el estrés oxidante 18
2.1.3. Dinámica mitocondrial y recambio en el daño renal 20
2.2. La S-glutationilación y la regulación de la homeostasis mitocondrial 21
2.3. El modelo de daño renal por ácido fólico (FA) y la N-acetilcisteína (NAC) 22
3. Justificación 24
4. Hipótesis 25
5. Objetivos 25
5.1. Objetivo general 25
5.2. Objetivos particulares 25
6. Materiales y métodos 25
6.1. Reactivos 25
6.2. Modelo experimental 27
6.3. Marcadores de daño renal y parámetros hemodinámicos 29
6.4. Estudios histológicos y de microscopia electrónica de trasmisión 30
6.5. Aislamiento de mitocondrias 31
6.6. Consumo de O_2 y β-oxidación mitocondriales 31

6.7. Potencial de membrana mitocondrial (ΔΨm) 32
6.8. Actividad de los complejos mitocondriales 32
6.8.1. Actividad del complejo I (CI) 32
6.8.2. Actividad del CII. 32
6.8.3. Actividad del CIII. 33
6.8.4. Actividad del CV. 33
6.9. Actividad de la ATP sintasa. 33
6.10. Producción de H_2O_2 mitocondrial 34
6.11. Marcadores de estrés oxidante 35
6.12. Actividad de las enzimas antioxidantes 35
6.12.1. Superóxido dismutasa (SOD) 35
6.12.2. Glutatión peroxidasa (Gpx) 36
6.12.3. Peroxiredoxina (Prx) 37
6.12.4. Catalasa 38
6.13. Niveles de GSH y actividad de las enzimas del sistema de S-glutationilación 38
6.13.1. Contenido total de glutatión, GSH y GSSG 38
6.13.2. Actividad de la Grx 38
6.13.3. Actividad de la GST 39
6.13.4. Actividad de la GR 40
6.14. Aislamiento de PT y DT 40
6.15. Determinación de la producción de ROS por la NADPH oxidasa (Nox) y la sintasa de óxido nítrico (Nos) 41
6.16. Extracción de proteína y Western Blot 41
6.17. Cultivo celular 42
6.18. Consumo de oxígeno en células completas 42
6.18. Análisis estadístico 42
7. Resultados 43
7.1. La AKI inducida por FA 43
7.1.1. El pretratamiento con NAC evita la AKI inducida por FA 43
7.1.2. LA NAC previene las alteraciones en la bioenergética mitocondrial relacionadas con la disfunción del CI en la AKI inducida por FA 45
7.1.3. La NAC previene el estrés oxidante mitocondrial en la AKI inducida por FA 49
7.1.4. La NAC inhibe el aumento de la producción de ROS en los segmentos tubulares en la AKI inducida por FA 52

7.1.5. La NAC previene la pérdida de la S-glutationilación en el proteoma mitocondrial en la AKI inducida por FA 54
7.1.6. La NAC evita el desplazamiento de la dinámica mitocondrial hacia la fisión en la AKI inducida por FA 56
7.1.7. El FA induce en la AKI una disminución en la biogénesis mitocondrial y una mitofagia alterada 59
7.1.8. Anexos primera parte. 61
7.2. La transición AKI-CKD inducida por el FA 64
7.2.1. El efecto de la NAC en la transición AKI-CKD inducida por el FA 64
7.2.2. El FA induce la persistencia de la disfunción en la bioenergética mitocondrial durante la transición AKI-CKD 66
..... 68
7.2.3. El FA induce una disfunción persistente en la β-oxidación durante la transición de AKI a CKD 68
7.2.4. El FA induce un estado pro-oxidante permanente en las mitocondrias durante la transición de AKI-CKD 71
7.2.5. Anexo segunda parte. Transicion de AKI-CKD 73
8. Discusión 75
8.1. La NAC previene las alteraciones mitocondriales asociadas a la pérdida de la S-glutationilación en la AKI inducida por AF 75
8.2. La evolución temporal del deterioro en la bioenergética y estado redox inducida por el FA favorece la transición AKI-CKD 81
9. Conclusiones 86
10. Perspectivas 87
11. Referencias 88
12.Indice de figuras. 100

1.Introducción

1.1. El riñón y su estructura

Los riñones son dos órganos pares que se encuentran situados detrás del peritoneo a ambos lados de la columna vertebral, implicados en el mantenimiento de la homeostasis corporal mediante la conservación del equilibrio osmótico y la eliminación de desechos metabólicos, entre otros múltiples procesos. Dichos órganos reciben cerca del 25% del gasto cardiaco a través de la arteria renal [1], la cual se ramifica en un sistema de arteriolas que regulan la entrada del flujo sanguíneo a las unidades funcionales del riñón: las nefronas [2]. Una persona adulta posee entre 1.5 y 2 millones de nefronas, el 80% de las cuales se conocen como corticales y poseen estructuras denominadas "asas de Henle" cortas, las cuales penetran una distancia corta dentro de la médula. El otro 20% de las nefronas reciben el nombre de yuxtamedulares y poseen asas de Henle largas, que penetran profundamente en la médula [3].

Cada nefrona está compuesta de un corpúsculo renal encargado del proceso de filtración y una serie de segmentos tubulares adjuntos (ver Fig. 1). El corpúsculo renal está conformado por un enramado capilar, conocido como glomérulo, y una esfera que lo encierra, la cápsula de Bowman. Por otro lado, la parte tubular comprende el túbulo proximal (PT), el segmento delgado descendente del asa de Henle (TDL), el segmento grueso ascendente del asa de Henle (TAL), el túbulo distal (DT) y los túbulos colectores (CT) [2,4]. El glomérulo tiene como principal función la filtración del plasma sanguíneo para producir el ultrafiltrado, a través de tres membranas que forman la barrera de filtración glomerular [2]. La primera, el endotelio fenestrado, está conformado por células que forman poros con un diámetro aproximado de 70 a 100 nm, y su función es evitar el cruce de las células sanguíneas y moléculas cargadas negativamente [5]. La segunda, la membrana basal glomerular, repele moléculas cargadas negativamente [4]. Finalmente, las ranuras de filtración de los podocitos poseen prolongaciones del citoplasma conocidas como pendículos, los cuales se entrelazan entre sí y se enrollan alrededor de los capilares glomerulares, donde forman ranuras de filtración de 25 a 60 nm [6].

El fluido que entra al lumen de la nefrona a partir de la filtración glomerular posee una composición muy similar a la del plasma. Sin embargo, dentro de los segmentos tubulares se modifica la composición del filtrado a partir de los procesos de reabsorción y secreción. La reabsorción hace referencia al movimiento de solutos del lumen tubular de vuelta al plasma, esta se inicia en el PT, el cual representa el segmento más largo de la nefrona y constituye la mayor parte de la corteza renal [5]. En él se efectúa la mayoría de la reabsorción de solutos como sodio, cloro, glucosa, aminoácidos, péptidos y bicarbonato. El PT está constituido por dos partes, la “inicial contorneada” que está unida directamente al corpúsculo renal en la corteza y realiza la mayor parte de la reabsorción, y la “parte recta”, que desciende en dirección a la medula [4].

Desde el PT, el líquido desciende hacia el asa de Henle. En este punto el fluido que entra en el asa de Henle es isotónico con respecto al plasma, sin embargo, durante

su paso por este segmento, se produce el alto gradiente osmótico que permite al agua ser removida a medida que atraviesa la médula renal mediante el mecanismo conocido como flujo a contracorriente. Por su parte, la porción ascendente del asa de Henle es un continuo con el TD, por lo cual algunos autores lo consideran como parte del mismo [4]. El TD es inicialmente impermeable al agua y posee un transporte activo considerable [2]. El siguiente segmento del DT es conocido como "contorneado", este segmento participa en la reabsorción activa de calcio, ya que tiene la mayor actividad de la Ca^{2+}-ATPasa en la nefrona [7]. Finalmente, la región conectora del DT desemboca en el túbulo colector cortical, donde se lleva a cabo el control hormonal de la reabsorción de agua por medio de la hormona antidiurética [2].

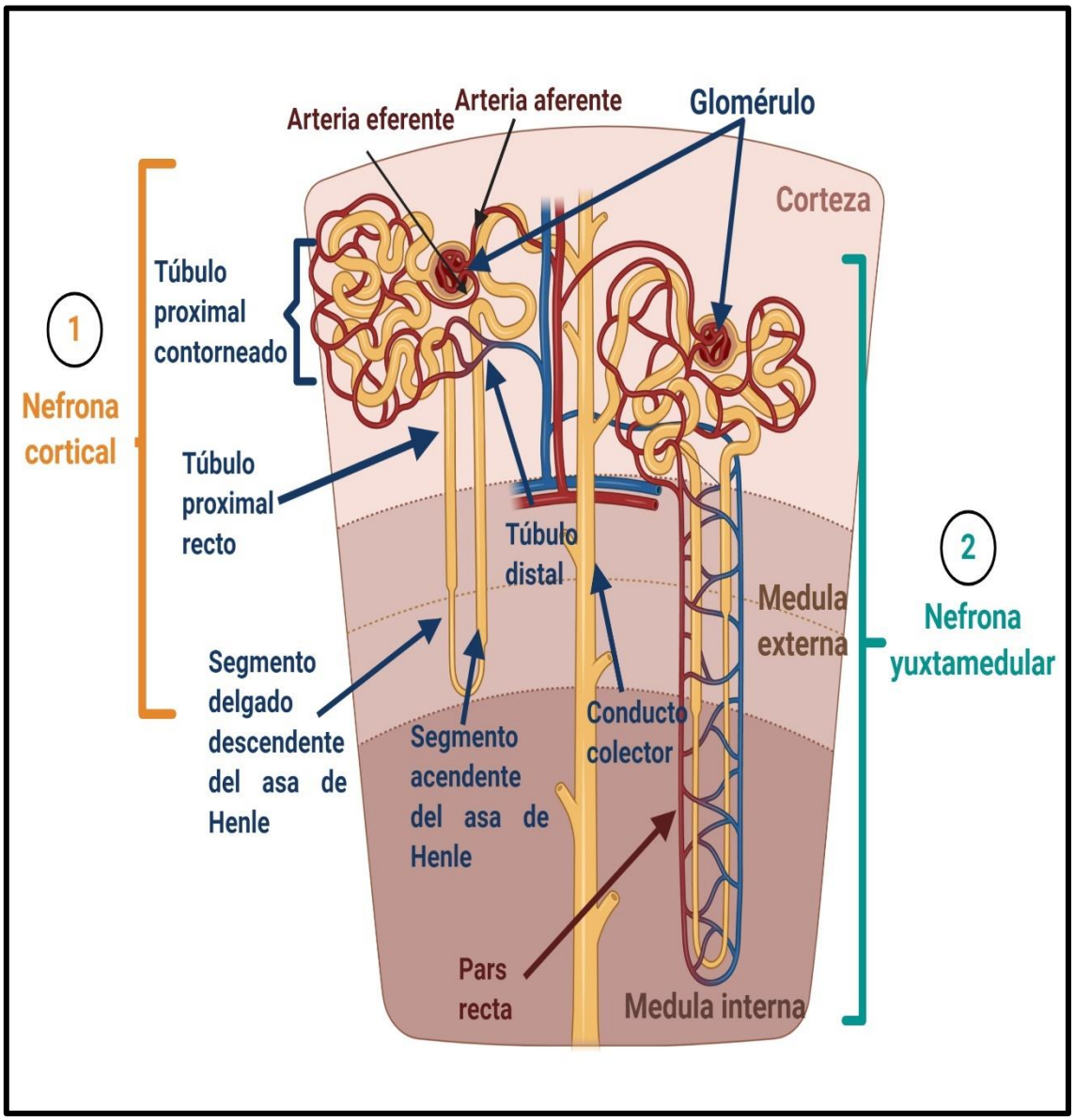

Figura 1. Estructura de la nefrona. La unidad funcional del riñón se conoce como nefrona. En la imagen superior observamos los dos tipos de nefronas. **(1)** La primera conocida como cortical, se extiende desde la corteza hasta la medula interna. **(2)** La nefrona yuxtamedular, se extiende desde la corteza hasta la medula interna. Ambos tipos de nefronas están abastecidas del flujo sanguíneo a partir de una serie de capilares que desembocan en la arteria aferente, la cual suministra de sangre al primer segmento de la nefrona, el glomérulo. El cual restituye los elementos no filtrados por medio de la arteria eferente. Por su parte el filtrado glomerular viaja a través de una serie de segmentos tubulares (flechas azules) donde se lleva acabo los procesos de reabsorción y secreción, dando origen a la concentración final de la orina. En el caso de las nefronas yuxtamedulares, de manera paralela a los segmentos tubulares corre una red de vasos sanguíneos conocida como pars recta.

1.2. La mitocondria en el riñón

En los riñones, los procesos de transporte activo son la fuerza motriz que hace posible la reabsorción de los distintos solutos, por lo que este órgano posee una demanda energética alta, utilizando alrededor del 7% del oxígeno total consumido por el cuerpo [8]. La mayor contribución al consumo de oxígeno renal está dada por el transporte activo de sodio, el cual depende de la actividad mitocondrial [9]. Debido a los diferentes requerimientos energéticos a lo largo de la nefrona, cada segmento tubular tiene una abundancia mitocondrial diferente [8,10,11], teniendo una mayor densidad mitocondrial aquellos segmentos con mayor tasa de reabsorción, como el PT contorneado y la TAL [10].

Por otro lado, la actividad del sistema de fosforilación oxidativa (OXPHOS) mitocondrial también depende del tipo y disponibilidad de sustratos [12]. Si bien en el riñón la demanda energética es predominantemente sostenida por la β-oxidación de ácidos grasos [13], existe una preferencia de cada segmento de la nefrona por ciertos sustratos. En el caso del PT, la OXPHOS es mantenida predominantemente por la β-oxidación de ácidos grasos de cadena media y larga, seguidos por los cuerpos cetónicos, el ácido láctico e intermediarios del ciclo del ácido cítrico como el malato [14,15], siendo el aporte glucolítico de ATP casi inexistente en este segmento [8]. Por su parte, el TDL posee una densidad mitocondrial pobre y un aporte de la OXPHOS limitado, siendo los sustratos preferidos el piruvato y la glucosa [8]. Mientras que en la parte medular, la glicólisis anaerobia tiene una mayor contribución [8]. Al contrario, en la TAL y el TD, el alto consumo de oxígeno genera un enriquecimiento mitocondrial, en donde se oxidan ácidos grasos, cuerpos cetónicos, glucosa, lactato, glutamato y glutamina pero no malato, succinato o citrato [11]. Finalmente en el caso de los conductos colectores, los experimentos de deprivación de sustratos revelan que estos son capaces de mantener el contenido de ATP intracelular incluso después de 30 minutos de deprivación [16], sugiriendo que poseen una alta actividad glicolítica, así como reservas endógenas de sustratos.

Estudios de microscopía confocal multifotónica han demostrado que el potencial de membrana mitocondrial ($\Delta\Psi m$) también cambia a lo largo de la nefrona. En estos estudios en ratones anestesiados, se reveló un mayor $\Delta\Psi m$ en el PT, seguido por

la TAL [17,18]. Además, en estados patológicos como la hipoxia, el ΔΨm rápidamente colapsa en el PT, pero no en el DT [18]; lo cual es consistente con la pobre capacidad de PT para obtener energía de la glucólisis [8]. La función renal depende en gran parte del equilibrio entre los procesos que regulan la dinámica y recambio mitocondrial (fisión, fusión, biogénesis y mitofagia) [8,19], por lo que las patologías mitocondriales son un factor muy importante en el desarrollo de diversas enfermedades renales [20–22].

El riñón se considera como el segundo órgano con mayor capacidad de gluconeogénesis solo después del hígado [23]. En condiciones fisiológicas normales, la contribución del riñón a la glucosa en sangre es del 25%, sin embargo esta puede llegar hasta cerca del 45% después de ayuno prolongado [24]. Esto se ha asociado principalmente a la capacidad del riñón sintetizar glucosa a partir de precursores no carbohidratos como los ácidos carboxílico y los amino ácidos [25]. En condiciones normales sustratos representan el 90% de la gluconeogénesis en el riñón: lactato, glutamina, glicerol y alanina. Sin embargo, estas contribuciones pueden llegar a variar durante periodos de ayuno [24,25]. Para el análisis de la gluconeogénesis renal, dicho órgano puede considerarse divido en dos compartimientos separados, la corteza donde produce y libera glucosa principalmente por el PT, y la medula en la que la gluconeogénesis es mínima y se utilizan altas cantidades glucosa [26]. El PT, en especial el segmento S3 del mismo, reabsorbe glucosa y sintetiza la mayor cantidad de glucosa, pero no es capaz de metabolizarla, dada la falta de actividad y abundancia de enzimas glucolíticas como la hexocinasa en este segmento [26]. En contraste, en las regiones medulares de la nefrona como el asa de Henle, la glucosa en el fluido tubular es mínima y así como la gluconeogénesis, sin embargo estas regiones usan glucosa proporcionado por el TP y entregada por del flujo sanguíneo [24,26]. Por otro lado, la mitocondria renal tiene un papel fundamental en la a gluconeogénesis en los segmentos corticales, esto a partir del aporte de ATP necesario para esta vía biosintética [24–26]. De hecho, la abundancia mitocondrial en estos segmentos correlaciona con la expresión y actividad de las enzimas gluconeogenicas como la fosfoenolpiruvato carboxiquinasa, así el consumo de lactato, glutamina y alanina en los mismos [23,26]. Así mismo, el suministro de piruvato a partir de amino ácidos como la glutamina y el glutamato, depende de las transaminasas mitocondriales y del correcto flujo en el ciclo de Krebs [23,26]. Aún más, dicha producción es sensible a inhibidores del ETS como la antimicina A [24–26], confirmando el papel fundamental de la mitocondria en la regulación de esta vía metabólica.

Adicionalmente, las mitocondrias se consideran como un eje central en la regulación redox celular en el riñón, dado que dicho organelo es uno de los principales sitios de producción de especies reactivas de oxígeno ROS en la célula [21,27]. En las mitocondrias, la producción de ROS, incluso en condiciones no patológicas, depende directamente de la actividad de las deshidrogenasas del sistema de transporte de electrones (ETS), de la β-oxidación y del ciclo de Krebs [28,29]. Por lo que, múltiples sitios de producción de ROS han sido identificados hasta ahora, cuyas contribuciones dependen de la disponibilidad de sustratos y el balance energético, entre otros factores [12,28]. De igual manera, la mitocondria y las ROS

producidas por dicho organelo también pueden regular la activación el inflamosoma NLRP3 y el desencadenamiento de la muerte celular por apoteosis [30]. La activación mitocondrial del inflamosoma NLRP3 lleva a la activación de la señalización mediada por el factor nuclear kappa B (NF-κB) en células proinflamatorias como los macrófagos, monocitos y neutrófilos [30], contribuyen así a los procesos regenerativos o fibróticos en el riñón [31,32]. Aunado a esto, la mitocondria junto con la aldosterona, median la transición epitelio-mesenquimo en las células tubulares [33], regulando la respuesta al daño renal.

Por otro lado, 98% –99% de la carga filtrada por la nefrona de Ca^{2+} es reabsorbida por los túbulos renales a partir del transporte activo secundario dependiente de la producción de ATP mitocondrial [34]. Dicho organelo no solamente sostiene la absorción del Ca^{2+} en los segmentos tubulares, si no que junto con el retícula endoplásmico (ER) es considerado como uno de uno de los sitios principales de regulación de la concentración intracelular de Ca^{2+} [35,36]. En condiciones de reposo, la concentración mitocondrial de Ca^{2+} es de aproximadamente 100-200 nM. Sin embargo, bajo estimulación, las mitocondrias pueden acumular de 10 a 20 veces más Ca^{2+} que el compartimento citosólico [36]. La membrana externa mitocondrial (MOM) es altamente permeable al Ca^{2+} gracias a los altos niveles del canal selectivo de aniones dependientes de voltaje (VDAC). Mientras que la entrada de Ca^{2+} a través de la membrana interna mitocondrial (MIM) está regulada principalmente por el complejo del uniportador mitocondrial de Ca^{2+} (MCU) y está regulada por el $\Delta\Psi m$ [35,36]. Por último, las mitocondrias interactúan física y funcionalmente con una gran cantidad de organelos, siendo la interacción con el ER de particular interés para la regulación celular [37]. La comunicación entre estos orgánulos es a través de las membranas mitocondrias-ER asociadas (MAM), las cuales tiene un papel fundamental en las funciones celulares como la señalización de Ca^{2+}, el transporte de lípidos, el metabolismo energético y la muerte [37,38]. Por tal motivo, cualquier alteración en los segmentos renales hay una estrecha correlación entre las funciones mitocondriales y del ER [39].

2. Antecedentes

2.1. La insuficiencia renal aguda (AKI) y la enfermedad renal crónica (CKD)

El término insuficiencia renal aguda (AKI) se utiliza para englobar un conjunto de patologías que se caracterizan por un deterioro repentino de las funciones renales en un intervalo de tiempo relativamente corto, generando un aumento en la creatinina en sangre, así como la desregulación en la homeostasis ácido-base y osmótica del riñón [40,41]. A nivel mundial, se ha observado un aumento creciente en el número de casos de AKI durante las últimas dos décadas [42], estimándose que anualmente 13 millones de personas experimentan episodios de AKI [43]. Esto genera un escenario alarmante, puesto que la AKI se asocia con altas tasas de mortalidad en pacientes con complicaciones cardiovasculares [44]. Si bien existen diversas causas de la AKI, las más comunes son: procesos isquémicos o de oclusión, así como el consumo de ciertos fármacos y la exposición a contaminantes ambientales, son [45–48].

Por otro lado, la enfermedad renal crónica (CKD) se da como resultado de una serie de insultos agudos y/o continuos, que generan la pérdida inicial de nefronas. En un intento por compensar dicha pérdida, el riñón desencadena cambios hemodinámicos, vasculares e inflamatorios, que conducen a una mayor pérdida de nefronas, generando así daños a largo plazo y la pérdida progresiva de la función renal [49,50]. De acuerdo con la *Kidney Disease Outcomes Quality Initiative* (KDOQI) de la Fundación Nacional Americana del Riñón, que toma como principal parámetro de referencia a la tasa de filtración glomerular (GFR), la CKD en humanos puede definirse como: una GFR menor a 60 mL/min/1.73 m^2 por 3 meses o más, junto con anormalidades funcionales y estructurales en el riñón, que puede o no manifestarse por el incremento en los marcadores clínicos de daño renal [51]. La naturaleza progresiva de la enfermedad llevó a la KDOQI a clasificarla en 5 estadios tomando como parámetro la caída en la GFR, donde menos de 15 mL/min/1.73m^2 se considera como estadio 5 o enfermedad renal en etapa terminal, punto en el cual el paciente precisa de diálisis o trasplante para sobrevivir.

En las últimas décadas, el número de pacientes con CKD ha aumentado dramáticamente, pasando a la lista de las principales causas de mortalidad a nivel mundial, del puesto 27 en 1990 al puesto 18 en 2014 [52,53]. En México, la CKD representa la octava causa de defunción en varones y la sexta en mujeres de entre 20 a 59 años. La situación en nuestro país es alarmante debido a que presenta el mayor incremento en el número de pacientes por millón de habitantes de América Latina [54,55] y las mayores tasas de mortalidad en pacientes [56,57]. En estudios realizados en poblaciones americanas se ha identificado a la hipertensión, la diabetes mellitus, la hiperlipidemia, la proteinuria, la obesidad, el tabaquismo y el uso indiscriminado de medicamentos como los principales factores de riesgo en la población [49,51,58].

Así mismo, se ha demostrado tanto en modelos animales como en pacientes, que un episodio fuerte de AKI o una serie de ellos puede resultar en el desarrollo de CKD [5,50,51]. Dado que ambas enfermedades están consideradas como problemas crecientes de salud pública en todo el mundo [59–61] y al hecho de que

los enfoques clínicos muchas veces son insuficientes para prevenir el avance de estas enfermedades [49,51,62], se ha propuesto la idea de que para desarrollar mejores terapias se debe partir de una visión más integrativa de los procesos involucrados en la génesis de la AKI y su progresión hacia la CKD [40,63].

2.1. Las mitocondrias y su papel en la enfermedad renal

Los riñones tienen una alta demanda energética y un alto consumo de oxígeno asociado a la OXPHOS [8,26]. Además de ser las principales productoras de ATP en el riñón, las mitocondrias modulan funciones celulares relacionadas a la homeostasis de calcio, apoptosis y señalización celular [21,64–66] y se les considera como uno de los principales sitios de generación de ROS [28], las cuales en exceso contribuyen al desarrollo y progresión de diversas enfermedades. Dado que la homeostasis mitocondrial es esencial para el mantenimiento de la función renal [66], en los últimos años ha tomado fuerza la idea de que la disfunción mitocondrial juega un papel fundamental en la génesis y el desarrollo de enfermedades renales [22,66–68].

2.1.1. Alteraciones en la bioenergética mitocondrial en la AKI y la CKD

Se ha demostrado en los modelos *in vivo* de AKI inducidos por cisplatino, isquemia/reperfusión [17], gentamicina [17] y maleato [69], que los segmentos tubulares ricos en mitocondrias como el PT y TAL son los más propensos a sufrir daño. Además, en estos modelos existe una correlación entre el daño tubular y alteraciones mitocondriales tales como: la disminución en el $\Delta\Psi m$, la caída en los niveles de ATP y un desplazamiento de la dinámica mitocondrial hacia la fisión [17,69]. Aunado a esto, las alteraciones en la bioenergética mitocondrial se han relacionado con defectos tubulares en pacientes con patologías renales, como el síndrome de Fanconi, el síndrome de Bartter y la enfermedad renal quística, entre otros [20,70].

En el caso de la CKD, esta se desarrolla como resultado de un conjunto de mecanismos patológicos, que incluyen variaciones hemodinámicas, hipertrofia, inflamación, fibrosis y estrés oxidante [50]. Por lo que la pérdida continua de nefronas desencadena una hipertrofia compensatoria y el aumento en la síntesis de biomacromoleculas en el riñón [50]. Así mismo, la GFR por nefrona (snGFR) aumenta, favoreciendo mayores tasas de reabsorción de solutos y por tanto mayor consumo de energía por nefrona [71,72]. El aumento en la reabsorción de solutos y la hipertrofia compensatoria generan una demanda excesiva de ATP en los segmentos tubulares, lo cual se ha postulado que induce estrés en las mitocondrias [50,73–75]. En la literatura existe un consenso de que las mitocondrias en la progresión hacia la CKD no son capaces de responder efectivamente a este aumento en la demanda de ATP [73,76,77], como lo demuestra la acumulación de fosfato inorgánico, los bajos niveles de ATP, el aumento en el consumo de oxígeno y la disminución del transporte de sodio en el riñón. Dichos cambios se han descrito ampliamente en pacientes con CKD [78–80] y son particularmente mayores en los segmentos altamente dependientes del ATP mitocondrial, como el PT [81–84].

En el caso de los modelos de CKD por nefrectomía, en estudios realizados a 8, 12 y 13 semanas después de la cirugía, se observaron menores niveles de ATP en la

corteza renal, un menor ΔΨm, alteraciones en el ETS y específicamente una menor actividad de los complejos mitocondriales I (CI) y III (CIII) y la pérdida de la definición de las crestas mitocondriales en el PT [32,85,86]. Lo que sugiere que en estadios avanzados hay una acumulación de mitocondrias disfuncionales y con producción ineficiente de ATP [32,74,85–88]. En comparación, a 9 meses de evolución en la CKD inducida por isquemia/reperfusión, se observó la acumulación de mitocondrias pequeñas, con crestas anormales y signos de degradación proteolítica [89,90]. Aunado a esto, evidencias recientes sugieren que el ciclo de Krebs renal también se encuentra disfuncional en la CKD. En las biopsias renales de pacientes con CKD se ha descrito una reducción en los niveles de mRNA de las proteínas del ciclo de Krebs y de los metabolitos de esta vía en orina [80].

En conjunto, estos datos sugieren que las alteraciones en la bioenergética mitocondrial son un mecanismo común involucrado en la progresión hacia la CKD. Sin embargo, nuestro conocimiento sobre las alteraciones en la bioenergética mitocondrial renal y su participación en la progresión hacia la CKD es limitado, dado que la información existente en la literatura es escasa. Aunado a esto, los datos acerca de las mediciones bioenergéticas y del consumo de oxígeno mitocondrial realizadas por oximetría de baja resolución en algunos casos son contradictorios [91–93] y los trabajos existentes se han realizado en un solo tiempo [73,74,93]. Por lo que, hasta la fecha, no existe una descripción temporal de los cambios que ocurren en las mitocondrias a lo largo de la progresión hacia la CKD.

2.1.2. Las ROS mitocondriales y el estrés oxidante

Los niveles excesivos de ROS mitocondriales conducen al estrés oxidante, definido como un desequilibrio entre la producción de ROS y el sistema antioxidante [94]. El cual se ha asociado ampliamente con cambios en la bioenergética mitocondrial [73,91,95] y con la alteración en los procesos que regulan la dinámica y recambio mitocondriales [96,97]. De hecho, el estrés oxidante se ha relacionado con la génesis y la progresión de diversas patologías renales incluidas la AKI y la CKD [98–100]. En el caso de la AKI, en diversos modelos animales se ha descrito que el aumento del estrés oxidante precede a la pérdida del ΔΨm y al aumento en los marcadores de daño renal clínicos [20,101–104]. Por su parte en los estudios de progresión hacia la CKD, la participación del estrés oxidante, y en especial el mitocondrial, está menos estudiada. En el caso de los modelos de nefrectomía, a las 24 h posteriores a la cirugía, se describió un aumento en la producción mitocondrial de ROS y un aumento en los niveles de los marcadores de estrés oxidante en la mitocondria [73]. Por su parte, en estadios más avanzados, posteriores a los 28 días, se ha reportado que los niveles de ROS mitocondriales y los marcadores de estrés permanecen altos, así como una disminución en los niveles de glutatión reducido (GSH) y una actividad reducida de la superóxido dismutasa (SOD) mitocondrial [32,85,86,88,105]. Tomados en conjunto, estos datos sugieren un estado pro-oxidante permanente en las mitocondrias a lo largo de la progresión hacia la CKD, sin embargo, esta hipótesis no ha sido mediante estudios temporales.

Recientemente se propuso que en condiciones patológicas, las mitocondrias integran un mecanismo de retroalimentación positiva de producción de ROS con la NADPH oxidasa (Nox) en el riñón, la cual presenta subunidades membranales tanto en la membran citoplásmica como mitocondrial [87,106,107]. Como se describe en la figura 2, en modelos murinos las ROS mitocondriales son capaces de activar a la proteína cinasa C (PKC), lo que conduce a la fosforilación de la subunidad p47phox de la Nox y por tanto a la activación de esta enzima [108,109]. Por su parte, el aumento excesivo en la producción de ROS por la Nox puede inducir la disfunción del ETS mitocondrial, principalmente en el CI, favoreciendo así el aumento en la producción de ROS mitocondriales [107,109]. Este mecanismo es particularmente importante ya que la sobreactivación de la Nox ha sido ampliamente reportada en diversos modelos de CKD y se ha relacionado fuertemente con el daño tubular, la

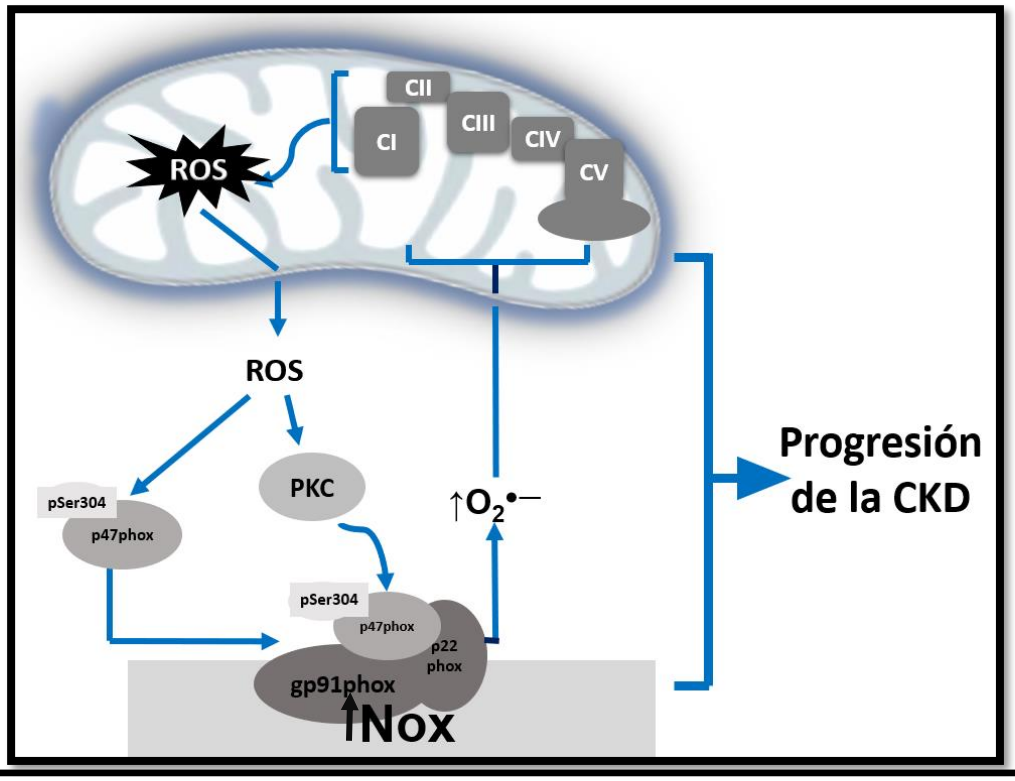

Figura 2. Mecanismo Nox/mitocondria de aumento de la producción de ROS. La sobre activación de la Nox aumenta la producción de superóxido ($O_2^{\cdot-}$), el cual genera estrés oxidante en las mitocondrias. Dicho estrés promueve modificaciones postraduccionales irreversibles en proteínas mitocondriales, especialmente en componentes del ETS, desacoplando a la mitocondria y aumentando la producción de ROS mitocondriales. Por su parte, las ROS mitocondriales activan a la Nox, mediante la activación de diversas isoformas de la PKC. Esto desencadena la fosforilación de la subunidad p47phox de Nox, que aumenta la activación de esta enzima y por tanto la producción de $O_2^{\cdot-}$. Este círculo vicioso de producción de ROS induce el estrés oxidante y contribuye a la progresión hacia la CKD. ETS= sistema de transporte de electrones; CI-CV= complejos mitocondriales I a V; Nox= NADPH oxidasa, PKC= proteína cinasa C; ROS= especies reactivas de oxígeno; pSer304 = fosforilación de serina 304.

glomeruloesclerosis, el aumento en las citocinas proinflamatorias y los factores profibróticos [110–112], así como la sobreactivación del sistema renina-angiotensina II [113–115].

Adicionalmente, se sabe que las ROS mitocondriales son capaces de promover diversos procesos relacionados con la progresión de la CKD. Tal es el caso del factor inducible por la hipoxia (HIF), el cual puede ser estabilizado por las ROS tanto en normoxia como en hipoxia [82,116]. Aunado a esto, se sabe que HIF activa procesos como la inflamación, la apoptosis y posteriormente la fibrosis, relacionados a la pérdida progresiva de la función renal [117]. Así mismo, las ROS mitocondriales también pueden activar al inflamasoma NLRP3, el cual aumenta la respuesta inflamatoria activando la señalización mediada por el factor nuclear *kappa* β (NF-κB), contribuyendo aún más al proceso fibrótico [31,32]. De igual manera, las ROS mitocondriales junto con la aldosterona favorecen la transición epitelio-mesénquima en las células tubulares [118], promoviendo así el proceso fibrótico.

2.1.3. Dinámica mitocondrial y recambio en el daño renal

La mitocondria es un organelo altamente dinámico, el cual se encuentra constantemente involucrado en procesos de fisión (fragmentación) o fusión (unión). Así como en procesos de degradación de sus componentes dañados y de síntesis de nuevos componentes (biogénesis). En conjunto, estos procesos determinan su morfología, tamaño y distribución a lo largo de la célula [119,120]. La fusión mitocondrial está regulada por las proteínas implicadas en la fusión de la MOM mitofusinas 1 (Mfn1) y 2 (Mfn2), y por la proteína que participa en la fusión de la MIM, la proteína de atrofia óptica 1 (Opa1) [19]. Por otro lado, el proceso de fisión está regulado por la proteína 1 relacionada a la dinamina (Drp1) y por cuatro proteínas adaptadoras: la proteína de fisión 1 (Fis1), el factor de fisión mitocondrial y los factores de alargamiento mitocondrial 1 y 2 [19,121].

Por otro lado, la bioenergética mitocondrial está estrechamente coordinada con la dinámica, favoreciendo la fisión o la fusión dependiendo de la demanda de energía [107,108]. Así mismo, las ROS mitocondriales pueden regular la morfología y la dinámica mitocondrial, favoreciendo el estrés oxidante en términos generales y la fragmentación de las mitocondrias y su posterior degradación [122]. Por lo tanto, existe una estrecha relación entre los procesos bioenergéticos, redox y dinámicos en las mitocondrias [123].

Por otro lado, el proceso de degradación selectiva de las mitocondrias por autofagia se conoce como mitofagia. Este proceso está regulado por la cinasa putativa inducida por PTEN 1 (Pink1), cuyo aumento en la MOM es causada por la despolarización de las mitocondrias [124]. La proteína Pink1 activa a la E3-ubiquitina ligasa Parkin, que ubiquitina a las proteínas de la MOM permitiendo el reclutamiento de maquinaria de autofagia [122]. La importancia de este proceso radica en eliminar a las mitocondrias dañadas, evitando así la acumulación nociva de mitocondrias dañadas y por tanto el aumento del estrés oxidante [125].

En el caso del riñón, en los modelos de AKI por cisplatino y maleato, se ha descrito un desplazamiento de la dinámica mitocondrial hacia la fisión [19]. Así mismo, se ha descrito la acumulación de proteínas de autofagia y de mitofagia en ratas con

nefrectomía a los 28 días posteriores a la cirugía [74]. Esto en conjunto con estudios de microscopía electrónica que revelan la acumulación de cuerpos autofágicos, podría indicar una mitofagia defectuosa en el daño renal [74,126]. Sin embargo existen discrepancias en los cambios temporales en las proteínas de dinámica [73,74,88,92,127] y biogénesis mitocondriales [74,88] en la AKI y su transición hacia la CKD, mientras que los datos existentes sobre la mitofagia son insuficientes [74]. Por lo tanto, mayores estudios de estos mecanismos permitirían profundizar más acerca de su papel en las alteraciones de la función mitocondrial en la enfermedad renal, esto con el objetivo de desarrollar terapias que permitan prevenir el avance de la CKD.

2.2. La S-glutationilación y la regulación de la homeostasis mitocondrial

Si bien es cierto que un aumento sostenido y descontrolado en la producción de ROS se relaciona con el daño en diversas patologías [111], la noción de que algunas ROS juegan un papel como segundos mensajeros en la señalización celular es también un concepto bien aceptado [128]. Este papel dual ha generado la propuesta de que las ROS poseen un efecto hormético, que consiste en generar un estímulo a bajas concentraciones, pero tienen un efecto perjudicial a niveles superiores [129]. En estudios recientes se ha demostrado que la señalización por ROS juega un papel importante en la regulación de funciones renales como la gluconeogénesis, el transporte de glucosa, la retroalimentación túbulo-glomerular y la reabsorción [111,129–131]. Para que la señalización redox pueda considerarse como tal, se requiere de la existencia de una serie de sensores sensibles a cambios rápidos en el microambiente redox [128,129]. Los grupos tiol (SH) de las cisteínas, parecen ser los candidatos ideales, ya que pueden ser modificados postraduccionalmente dependiendo de los cambios redox [97] y del microambiente [97,132]. Estas modificaciones postraduccionales (PTMs) son conocidas como S-oxidaciones.

Recientemente una PTM, la S-glutationilación (la adición reversible de una molécula de glutatión, GSH) se ha comenzado a considerar como un mecanismo de señalización redox [96,97]. En el caso de la S-glutationilación enzimática, esta es de carácter reversible y es inducida por aumentos leves en las concentraciones de ROS o glutatión oxidado (GSSG). Además esta modificación compite por los residuos de cisteína con otras modificaciones post-traduccionales de carácter irreversible [133]. Sin embargo, el aumento excesivo en la S-glutationilación de carácter no enzimático se ha considerado tradicionalmente como un marcador de estrés oxidante [134]. Diversos autores han sugerido de manera reciente que la S-glutationilación enzimática ejerce efectos protectores de la homeostasis celular [96,97]. Lo que confirma el concepto de que los mecanismos de la homeostasis redox celular son muy complejos y aún no se entienden totalmente [130].

En el caso de las mitocondrias, estas poseen una gran cantidad de proteínas cuya actividad es regulada por la S-glutationilación enzimática, involucradas en procesos como el ciclo de Krebs, la β-oxidación, el ETS, la OXPHOS, el transporte de solutos y la apoptosis [96,97,128,129]. En el caso del ETS, esta PTM se ha asociado con la regulación de la actividad de los complejos mitocondriales y disminución en la producción de ROS por los mismos, previniendo así en contextos de mayor estrés oxidante un aumento posterior en la producción de ROS mitocondriales [96,135] y

protegiendo a las cisteínas contra PTMs irreversibles [130]. Por tal motivo, se ha comenzado a considerar a la S-glutationilación como un mecanismo protector de la homeostasis mitocondrial que permite ligar el metabolismo energético con el estado redox mitocondrial [96,97].

Finalmente, aunque que la S-glutationilación está implicada en la regulación del estado redox, el estado energético y la homeostasis mitocondrial, su papel en los trastornos mitocondriales en el riñón no se ha evaluado [130]. Por lo que los estudios que nos permitan comprender su papel en la disfunción mitocondrial en las distintas enfermedades renales podrían ser de gran relevancia para el desarrollo de terapias destinadas a preservar la función renal y mitocondrial en estas patologías.

2.3. El modelo de daño renal por ácido fólico (FA) y la N-acetilcisteína (NAC)

Una sobredosis de ácido fólico (FA) en roedores o en humanos induce la rápida disminución de la función renal, la muerte celular en el epitelio tubular, anomalías morfológicas en el parénquima renal y la aparición de cristales de FA en los segmentos tubulares. Por lo tanto, el daño renal inducido por FA es un modelo experimental ampliamente utilizado para estudiar la AKI, el cual recrea en gran medida la patología observada en la clínica [15] y es altamente reproducible [136,137]. Aunado a esto, altas dosis de FA o bajas dosis administradas en repetidas ocasiones son capaces de inducir la inflamación y fibrosis crónica, lo que promueve la transición AKI-CKD en menos de 28 días, haciéndolo un modelo valioso para explorar los mecanismos involucrados en dicha transición [136,138,139].

Aunque la necrosis tubular aguda, la obstrucción tubular, la liberación de citocinas, el estrés oxidante y los procesos necróticos y apoptóticos se han implicado en este modelo, características que también son encontradas en la AKI en humanos, los mecanismos moleculares por los cuales la FA induce AKI siguen siendo poco conocidos [136,137,140,141]. De igual manera, se ha descrito que la administración de FA induce en homogeneizados renales una caída drástica en los niveles de GSH y un aumento en los marcadores de estrés oxidante, lo que sugiere que cambios en la S-glutationilación podrían estar presentes en este modelo. Así mismo, en la AKI inducida por FA, se ha reportado una disminución en los niveles de mRNA de las subunidades de los complejos mitocondriales, así como de la proteína 1α coactivadora del receptor activado por el proliferador de peroxisomas (PGC-1α), factor maestro de la biogénesis mitocondrial, así como del factor de transcripción mitocondrial A (TFAM) [142,143]. En conjunto estos resultados sugieren una reducción en la biogénesis mitocondrial. Sin embargo, la bioenergética mitocondrial, así como las alteraciones redox y su contribución al desarrollo de AKI en este modelo no han sido evaluadas. Curiosamente, los procesos inflamatorios y fibróticos han sido relacionados en otros modelos con el deterioro mitocondrial [44–46], lo que sugiere que, en el modelo de FA, la bioenergética mitocondrial y el deterioro del estado redox son persistentes en la transición de AKI-CKD. Sin embargo, dicha hipótesis tampoco ha sido evaluada aún [30,118,127].

Por último, la N-acetilcisteína (NAC) es un donador de grupos sulfhídrilo, permeable a la membrana celular, precursor intracelular del GSH, la cual ejerce actividad selectiva como antioxidante con ciertas ROS [144,145]. Debido a que el estrés oxidante juega un papel fundamental en la AKI, diversos grupos han investigado a la NAC como potencial agente protector [146]. En la clínica se ha demostrado que la administración oral de NAC disminuye el aumento en los marcadores de daño renal e inflamación en las nefropatías inducida por contraste o por cirugía cardiaca [145,147]. Así mismo, en los modelos animales de hiperoxaluria e isquemia/reperfusión, la NAC previene la pérdida del potencial mitocondrial, el estrés oxidante y los cambios en el metabolismo energético [148,149].

Por tales motivos, la NAC se perfila como un poderoso agente capaz de prevenir la disfunción mitocondrial y renal en la AKI inducida por FA. Aunado a esto, dada su capacidad de aumentar el cociente GSH/GSSG, se propone que la administración de NAC inducirá el aumento en la S-glutationilación mitocondrial, preservando así la bioenergética y el estado redox en dicho organelo y, por tanto, evitando la pérdida de la función renal inducida por FA. Sin embargo, hasta el momento dicha hipótesis no se ha explorado.

3. Justificación

La relevancia de este proyecto se basa en que actualmente, los mecanismos moleculares, en especial los relacionados con las mitocondrias, por los cuales se induce la AKI y su progresión hacia la CKD siguen siendo poco conocidos. Debido a que la función renal depende ampliamente de la homeostasis mitocondrial, estudios que nos permitan comprender el papel de las alteraciones mitocondriales dentro las enfermedades renales podrían ser de gran relevancia dado que la información existente en la literatura es escasa, fragmentaria, en algunos casos contradictoria, y que hasta el momento no se han realizado estudios temporales de las alteraciones mitocondriales. Este estudio nos permitirá entender no sólo el papel de la disfunción mitocondrial en la AKI, sino también su avance temporal y su participación en el establecimiento de la CKD. Para poder responder estas preguntas se evaluarán cambios en la función (alteraciones en la bioenergética, dinámica y estado redox), en la ultraestructura y en la S-glutationilación mitocondrial durante la AKI, además de la progresión de estos cambios en la transición hacia la CKD. Entender estos mecanismos mitocondriales abrirá la posibilidad de plantear estrategias que permitan prevenir o retrasar su avance, aminorando así el impacto de esta enfermedad en la salud pública nacional. En este sentido la realización de este proyecto también pretende evaluar la administración de NAC como un posible pretratamiento que permita prevenir la disfunción mitocondrial, la AKI y por tanto el desarrollo de la CKD.

4. Hipótesis

El desarrollo de la AKI inducida por FA estará asociada a la pérdida de la homeostasis bioenergética y redox mitocondrial, generadas por la disminución en la S-glutationilación, favoreciendo además alteraciones en la ultraestructura y dinámica de este organelo. Dichas alteraciones persistirán después de la AKI, permitiendo así la disminución progresiva de la OXPHOS y el aumento del estrés oxidante, lo cual favorecerá el desarrollo de la CKD en este modelo. Por su parte la NAC prevendrá dichas alteraciones mitocondriales al modular el estado redox mitocondrial, previniéndose el desarrollo de la AKI y, por tanto, su transición hacia la CKD.

5. Objetivos

5.1. Objetivo general

Primera parte del proyecto, la AKI:

Determinar si en la AKI inducida por FA existen alteraciones en la bioenergética, ultraestructura, dinámica y estado redox mitocondrial y si estas se relacionan a cambios en la S-glutationilación de las proteínas mitocondriales.

Segunda parte del proyecto, la transición hacia la CKD:

Determinar si en la transición hacia la CKD inducida por FA hay una persistencia del daño mitocondrial observado en la AKI, para caracterizar su posible papel en la progresión del daño renal.

5.2. Objetivos particulares

- Caracterizar las alteraciones en el consumo de oxígeno mitocondrial, la capacidad de la OXPHOS y los cambios en el ΔΨm en los distintos estados respiratorios.
- Identificar los cambios en la actividad de los complejos mitocondriales.
- Evaluar el estado redox mitocondrial y la actividad de las enzimas involucradas en el sistema de S-glutationilación.
- Analizar los cambios en la ultraestructura, morfología y dinámica mitocondriales.
- En cuanto al tratamiento con NAC previo a la inducción de daño por FA:
    - Investigar si tiene algún efecto sobre los posibles cambios mencionados en cada uno de los objetivos previos.
    - Evaluar si es capaz de prevenir el desarrollo de la AKI.
    - Evaluar si al prevenir el daño mitocondrial este es capaz de evitar el desarrollo de la CKD.

6. Materiales y métodos

6.1. Reactivos

Los siguientes reactivos se adquirieron de Sigma-Aldrich (St. Louis, MO, EUA): adenosina 5´-difosfato de sodio (ADP), ADN de testículo de salmón, acetato de

uranilo, Amplex-red, antimicina A, anti-conejo conjugado a partículas de oro, albumina sérica bovina (BSA) libre de ácidos grasos, anticuerpos primarios contra p62 y actina, azida de sodio (NaN_3), azul de bromofenol, cacodilato de sodio, carnitina (C), L-arginina, m-clorocarbonilcianuro fenilhidrazona (CCCP), 1-cloro-2,4 dinitrobenceno (CDNB), colagenasa de *Clostridum histolyticum* (tipo II), citrato de plomo, citocromo c de corazón equino, desoxicolato de sodio, D-glucosa, cloruro de difeniliodonio (DPI), cloruro de sodio (NaCl), cloruro de potasio (KCl), cloruro de cobre II ($CuCl_2$), dihidroetidio (DHE), D-manitol, acido 5,5-Dithiobis-2-nitrobenzoico (DTNB), decilubiquinona (DuB), la sal de sodio de hidrato de 2,6-diclorofenol (DCPIP), ácido etilenglicol-bis(β-aminoetiléter)-N,N,N',N-tetraacético (EGTA), FA, glicerol, GSH, GSSG, glucosa-6-fosfato deshidrogenasa (G6PDH), glutatión reductasa (GR), glutatión-S-transferasa (GST), glutamato de sodio, hexocinasa, peroxidasa de rábano picante (HRP), acido 4-(2-hidroxietil)-1-piperazinetanosulfónico (HEPES), K-lactobionato, cianuro de potasio (KCN), cloruro de manganesio ($MgCl_2$), L-ascorbato, N^G-nitro-L-arginina metil éster (L-NAME), malato de sodio, NAC, fosfato dibásico de sodio (Na_2HPO_4), fosfato monobásico de sodio (NaH_2PO4), nitroazul de tetrazolio (NBT), sal de potasio de nicotinamida dinucleótido fosfato oxidado y reducido (NADPH y $NADP^+$), nicotinamida adenina dinucleótido (NADH), N-etilmaleimida (NEM), floruro de sodio (NaF), ortovanadato de sodio (Na_3VO_4), oligomicina A, palmitoil-carnitina, resina epon, fluoruro de fenilmetilsulfonilo (PMSF), Percoll®, rotenona, safranina O, succinato de sodio, dodecilsulfato de sodio (SDS), sulfato de magnesio ($MgSO_4$), taurina, tetróxido de osmio, tetrametil-p-fenilendiamina (TMPD), tioredoxina, tioredoxina reductasa, Tris-HCl, Tween 20, sacarosa, 3-bensoxazol-2-il-3-bensil-3H-[1,2,3]triazolo[4,5-d]pirimidin-7-il sulfuro (VAS2870), xantina, xantina oxidasa (XO), 2-vinilpiridina (2-VP) y β-mercaptoetanol. El alcohol etílico, cloruro de calcio ($CaCl_2$), bicarbonato de sodio ($NAHCO_3$), formaldehido, glutaraldehído, paraformaldehido, peróxido de hidrogeno (H_2O_2), sulfato de amonio (NH_4SO_2) y la sal disódica del ácido etilendiaminotetraacético (EDTA) dihidratada se obtuvieron de JT Baker México (Edo. México, México). Los anticuerpos contra malondialdehído (MDA) y 4-hidroxinonenal (HNE) y el cóctel de anticuerpos OXPHOS, fueron adquiridos de Abcam (Cambridge, MA, EUA). Mientras que los anticuerpos contra Drp1, Fis1, Opa1, Mfn1, Mfn2 y el canal aniónico dependiente del voltaje (VDAC) a fueron adquiridos de Santa Cruz Biotecnology (Dallas, TX, USA). El cóctel de inhibidores de proteasas libre de EDTA se adquirió de Roche Applied Science (Mannheim, Alemania). El polifructosán se adquirió de Fresenius Kabi-Austria GmbH (Graz, Austria) y el pentobarbital sódico se compró de Salud y Bienestar Animal S.A. (Ciudad de México, México). Estuches comerciales de Spinreact (Girona, España) se utilizaron para medir el BUN y la creatinina plasmática. El estuche del ensayo de actividad de la glutaredoxina (Grx) se adquirió de Cayman Chemical (Ann Arbor, MI, EUA). La línea celular de túbulo proximal derivada de riñón porcino (LLCPK1, ATTC CL-101), se adquirió de American Type Culture Collection (ATCC, Rockville, MD, EUA). El medio de cultivo *Dulbecco's Modified Eagle's* (DMEM), suero fetal bovino (FBS) y la penicilina y estreptomicina se compraron de Biowest (Riverside, MO, EUA).

6.2. Modelo experimental

Los protocolos experimentales fueron aprobados por el comité de Bioética e Investigación de la Facultad de Química (FQ/CICUAL/171/16 y FQ/CICUAL/260/18) y se realizaron de acuerdo con las pautas de la Norma Oficial Mexicana Guías para el uso y cuidado de animales de laboratorio (NOM-062-ZOO-1999) y para la eliminación de residuos biológicos (NOM-087-SEMARNAT-SSA1–2002). El modelo experimental consistió en 4 grupos de ratas Wistar macho (n=5), de 250 a 300 g de peso:

I. **Vehículo (V).** Administrado únicamente con solución de $NaHCO_3$ 300 mM vía intraperitoneal.
II. **FA.** Tratados con una sola inyección intraperitoneal de FA (300 mg/kg) para inducir la AKI [140,142].
III. **NAC+FA.** Tratados con dos dosis de NAC (300 mg/kg) vía intragástrica 24 y 2 h antes de la inyección de FA (pretratamiento) [145,150].
IV. **NAC**. Administrado únicamente con NAC 24 y 2 h antes de la inyección del vehículo.

En el primer protocolo experimental (Fig. 3) después de la administración de los correspondientes tratamientos, las ratas se colocaron en cajas metabólicas por un período de 24 h para la recolección de la orina. Los animales se sacrificaron después de 24 h de la inducción del daño, para esto se anestesiaron vía intraperitoneal con pentobarbital sódico (90 mg/kg) y se colocaron en una mesa homeotérmica (37°C). Una vez comprobada la ausencia de reflejos se procedió a extraer la sangre y ambos riñones, el riñón izquierdo se utilizó para el análisis ultraestructural y el riñón derecho para el aislamiento de las mitocondrias.

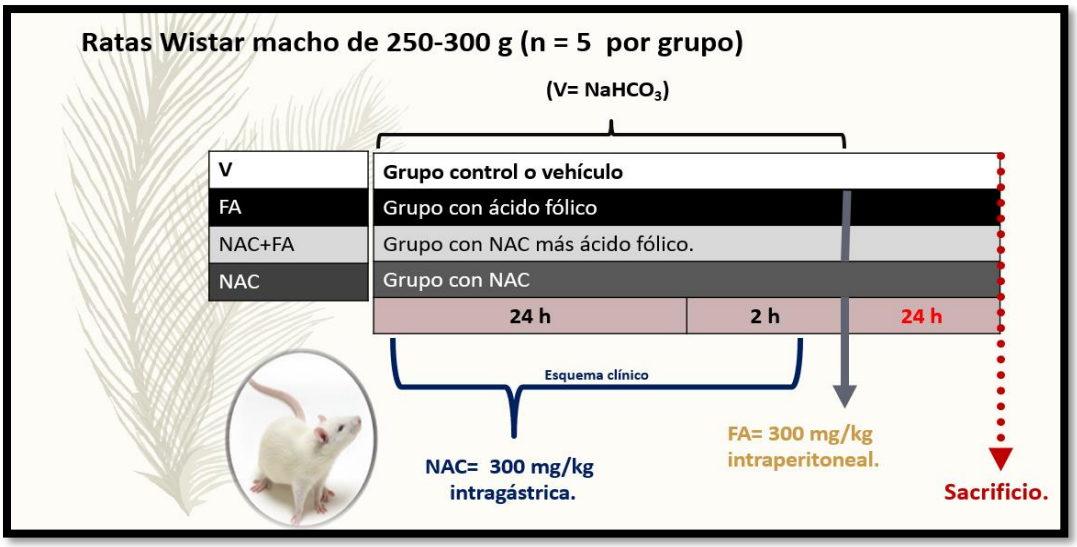

Figura 3. Esquema del primer modelo experimental *in vivo* correspondiente a la fase aguda a las 24 h. Los animales de los cuatro grupos experimentales se sacrificaron 24 h después de administración del FA o V. FA= Ácido fólico, NAC= N-Acetilcisteína, V= Vehículo.

Por su parte en el segundo modelo experimental, para estudiar los fenómenos asociados a la transición entre la AKI hacia la CKD, se conservaron los mismos cuatro grupos experimentales del primer modelo (ver Fig. 3). Sin embargó, se dejó progresar el daño renal. Por lo que el análisis experimental se realizó los días 2, 4, 7, 14 y 28 después de la administración de FA, manteniéndose una n= 5 por grupo y para cada período de tiempo (Fig. 4). Las ratas se alojaron en un cuarto asignado con temperatura controlada con un ciclo de luz-oscuridad de 12-12 h, se mantuvieron con agua y alimentos *ad libitum*.

Figura 4. Esquema del segundo modelo experimental correspondiente a la evolución temporal de los 4 grupos experimentales. Se presentan los días de sacrificio posteriores a la administración del FA o el V, en los cuales se evaluaron los diferentes parámetros. d= días posteriores a la administración de FA; FA= Ácido fólico, NAC= N-Acetilcisteína, V= Vehículo.

6.3. Marcadores de daño renal y parámetros hemodinámicos

La determinación de los marcadores de daño renal de BUN y creatinina en plasma se realizó mediante el uso de estuches comerciales (Spinreact, Girona, España). Brevemente, el ensayo de la creatinina se basó en la reacción de la creatinina con el picrato en medio alcalino, la cual forma un complejo rojizo cuya intensidad puede ser seguida a 495 nm y es proporcional a la concentración de creatinina en la muestra. Por su parte la determinación de BUN se basó en la disminución de la absorbancia a 340 nm del NADH por acción coordinada de la enzima glutamato deshidrogenasa y la ureasa, la cual es proporcional a la concentración de la urea total en la muestra [73].

Con el objetivo de determinar las alteraciones hemodinámicas, las ratas se anestesiaron vía intraperitoneal con pentobarbital sódico (60 mg/kg) y se colocaron en una mesa homeotérmica (37°C). Una vez comprobada la ausencia de reflejos se cateterizaron la tráquea, ambas venas yugulares, ambas arterias femorales y la vejiga con catéteres de polietileno PE-240, PE-50 y PE-90, respectivamente. Para el mantenimiento del equilibrio de hidratación, las ratas se mantuvieron bajo una infusión de BSA isotónica (6 g/dL) durante la cirugía, seguida de una infusión fisiológica de solución salina isotónica (0.9%) a 2.2 mL/h [73].

La presión arterial media (MAP) se monitoreó por medio de un transductor de presión (Modelo MLT844, AD Instruments, Colorado Springs, CO, EUA) colocado en la arteria femoral y los datos se registraron por el sistema de adquisición de datos Power Lab (Advanced Instruments Inc., Needham Heights, MA, EUA). El riñón izquierdo se expuso y se colocó en una capsula de lucita. Para impedir la

deshidratación de la superficie del riñón, este se cubrió con un algodón empapado con solución salina. La medición del flujo sanguíneo renal (RBF) se realizó con una sonda de flujo ultrasónico con tránsito de 2 mm (TS420, Transonic System, NY, NY, USA) colocada alrededor de la arteria renal izquierda, la cual se cubrió con gel de acoplamiento de ultrasonidos Realizocon para registrar. La resistencia vascular renal (RVR) se calculó con la fórmula RVR= MAP/RBF. Se tomó una muestra de sangre en microcapilares y se centrifugó en una centrífuga para micro hematocrito (MICRO-MB, Thermo IEC, Thermo Fisher Scientific Inc, Waltham, MA, USA) y se leyó con un lector de microcapilares (Damon IEC Division, Needham Heights, MA, USA).

Para evaluar la tasa GFR las ratas se infundieron con polifructosán al 5% en solución salina isotónica a una velocidad de 2.2 mL/h. La infusión se dejó un período de 60 minutos para alcanzar el equilibrio y se obtuvieron muestras de plasma y orina, posteriormente, se recolectó la orina por un período de 30 minutos y se obtuvieron nuevamente muestras de plasma. El contenido de polifructosán se midió espectrofotométricamente a 450 nm en plasma y orina, para el cálculo de la GFR [73]. El flujo plasmático renal (RPF) se calculó con la fórmula RPF= RBF*(1-hematocrito); mientras que la fracción de filtración (FF) se definió como FF= GFR/RPF.

6.4. Estudios histológicos y de microscopia electrónica de trasmisión

Para los estudios histológicos, los riñones se retiraron inmediatamente y se seccionaron después del sacrificio. Una porción del tejido se fijó inmediatamente por inmersión en una solución de formaldehído al 10% disuelta en solución salina amortiguada con fosfatos (PBS), a pH 7.4. Después de 1 día de fijación, las secciones de riñón se deshidrataron con soluciones de concentración progresiva de alcohol y se incrustaron en parafina. Se obtuvieron secciones de 5 µm de ancho, las cuales se tiñeron con hematoxilina y eosina (H&E) o tricrómica de Masson, respectivamente, para su evaluación histológica.

Para los estudios ultraestructurales de microscopia electrónica se fijaron pequeños fragmentos de tejido renal con glutaraldehído al 2.5% en amortiguador de cacodilato 0.15 M. Posteriormente se fijaron con tetraóxido de osmio al 1%, se deshidrataron con concentraciones crecientes de alcohol etílico y se infiltraron en resina EPON™ (London Resin Company, London, Reino Unido). Las secciones ultrafinas se colocaron secciones de 70 a 90 nm en rejillas de cobre y se contrastaron con sales de acetato de uranilo y citrato de plomo. Posteriormente se observaron con un microscopio electrónico (Tecnai Spirit BioTwin, FEI, Hillsboro, OR, EUA), para la captura de las micrografías correspondientes.

Para los estudios de inmunomicroscopía electrónica, fragmentos pequeños de la corteza renal se fijaron por inmersión de 2 h a 4 °C en paraformaldehído al 4% en amortiguador Sörensen pH 7.4 y se embebieron en resina hidrosoluble LR-White. Secciones delgadas de 70-90 nm se montaron en rejillas de níquel y se incubaron durante toda la noche a temperatura ambiente con el anticuerpo respectivo. Después de un lavado exhaustivo, se incubaron a temperatura ambiente durante 2 horas con IgG de cabra anti-conejo conjugado a partículas de oro de 5 nm. Las

rejillas se contrastaron con sales de uranio y se analizaron con el mismo microscopio electrónico mencionado anteriormente.

6.5. Aislamiento de mitocondrias

El aislamiento de las mitocondrias del tejido renal se realizó a partir de un protocolo de centrifugación diferencial con gradientes de Percoll previamente descrito [73]. Brevemente, de manera inmediata después del sacrificio, el riñón decapsulado se enfrió inmediatamente por inmersión en solución de medio de aislamiento “A” (D-manitol 225 mM, sacarosa 75 mM, EDTA 1 mM, HEPES 5 mM, BSA al 0,1% pH = 7.4) a 4°C. El tejido se lavó para eliminar la sangre y se cortó un tercio del riñón en pequeños trozos, los cuales se suspendieron en 2 mL de medio de aislamiento “A” en un homogeneizador de vidrio Potter–Elvehjem. Dichos fragmentos se homogeneizaron por 4 pulso con un mortero de TeflonVR acoplado a un taladro.

El homogeneizado se centrifugó durante 5 minutos a 2,500 x g a 4°C y el sobrenadante se volvió a centrifugar 10 minutos a 12,000 x g a 4°C. El botón resultante se resuspendió en una solución de 12% de Percoll con medio de aislamiento “A”. Dicha solución se colocó cuidadosamente sobre una cama de 1.5 mL de Percoll al 24% en medio de aislamiento “A”, generándose 2 fases. Las muestras se centrifugaron a 15,000 x g durante 15 min a 4°C. Finalmente la fracción enriquecida en mitocondrias que corresponde a la parte inferior del tubo se resuspendió en medio de aislamiento sin BSA (medio “B”) y se centrifugó de nuevo a 12,000 x g durante 5 min como lavado. El botón resultante se resuspendió en 180 µL de medio de aislamiento B. La proteína total se cuantificó por el método de Lowry.

6.6. Consumo de O_2 y β-oxidación mitocondriales

La evaluación del consumo mitocondrial de O_2 se realizó utilizando un equipo de respirometría de alta resolución (Oxygraph O2k, OROBOROS, Innsbruck, Austria) a 37 °C. Brevemente, 200 µg de mitocondrias recién aisladas se adicionaron a una celda con un volumen total de 2 mL de medio de respiración MiR05: EGTA 0.5 mM, $MgCl_2$ 3 mM, lactobionato de potasio 60 mM, taurina 20 mM, KH_2PO_4 10 mM, HEPES 20 mM, sacarosa 110 mM y BSA libre de ácidos grasos 1 g/L.

El transporte de electrones se inició mediante la adición de los sustratos ligados al complejo I (CI) [piruvato 5 mM, malato 2 mM y glutamato 10 mM] o por la adición del sustrato ligado al complejo II (CII) [succinato 10 mM más inhibidor del CI, rotenona 0.5 µM]. La respiración asociada aI CI más el CII (CI + CII) se determinó mediante la adición de los sustratos ligados al CI y al CII, pero sin la presencia de rotenona. La respiración en el estado 3 respiratorio (S3) se estimuló a partir de la adición de ADP 2.5 mM. Mientras que para el estado 4 respiratorio inducido por oligomicina (S4o), se adicionó oligomicina 2.5 µM. Por su parte, para la determinación de los parámetros respiratorios asociados a la β-oxidación mitocondrial, se utilizaron los sustratos aptos para el riñón: L-carnitina 2 mM, palmitoil-L-carnitina 2 µM más malato 2 mM [151].

Todos los parámetros anteriormente mencionados se corrigieron por respiración residual (ROX), obtenida tras la adición de rotenona 0.5 µM más antimicina A 2.5 µM (inhibidor del CIII). El índice de control respiratorio (RCI) se definió a partir de la relación S3/S4o y la respiración asociada a la OXPHOS (P) se definió como S3-S4o

[152]. Todos los valores se normalizaron sobre el contenido total de proteína determinado por el método de Lowry [152].

6.7. Potencial de membrana mitocondrial (ΔΨm)

Los cambios en el ΔΨm en los diferentes estados respiratorios se determinaron utilizando un fluorómetro de O2k (OROBOROS, Innsbruck, Austria) a partir de los cambios en la fluorescencia del colorante catiónico Safranina O (2 a 5 µM) en medio MiR05 [28]. Para estimular la respiración CI, CII o CI + CII, se agregaron los sustratos respectivos (ver sección 6.6). El ΔΨm mitocondrial en S3 se obtuvo mediante la adición de ADP saturado 2.5 mM y en S4o por la adición de oligomicina 2.5 µM. Para disipar completamente el ΔΨm y corregir por las interacciones no específicas de la safranina, se añadió CCCP 5 µM. Se emplearon curvas de calibración de safranina para garantizar la linealidad del ensayo. Los resultados se expresaron como los cambios en la concentración medible de safranina O (ΔµM de S) en S3 o S4o con respecto al desacoplamiento de CCCP y los resultados se normalizaron por miligramo de proteína utilizados (ΔµM de S/mg de proteína).

6.8. Actividad de los complejos mitocondriales

Las actividades de los complejos mitocondriales se determinaron utilizando el protocolo antes descrito [73]. Brevemente: la actividad de CI y del CII se determinaron a partir de la desaparición de la absorbancia del decilubiquinol a 600 nm. Mientras que la actividad del CIII se evaluó por el aumento en la absorbancia del citocromo *c* a 550 nm. Finalmente, la actividad del complejo IV (CIV) se evaluó por el consumo de oxígeno en presencia de TMPD más ascorbato. La actividad de cada complejo se determinó en experimentos por separado. Las técnicas se describen a continuación:

6.8.1. Actividad del complejo I (CI)

La medición se realizó utilizando placas de 96 pozos. Las mediciones de absorbancia se realizaron utilizando un lector de microplacas Synergy-Biotek (Biotek Instruments, Winooski, VT, EUA). En cada pozo se colocó la mezcla de reacción, la cual contenía: BSA 3.5 mg/mL, DCPIP 67 µM, antimicina A 1 µM, NADH 0.2 mM, KCN 0.2 mM PBS 30 mM (pH 7.4), en un volumen total de 300 µL y se adicionaron 5 µg de proteína mitocondrial. Para cada muestra se realizó un duplicado al cual se le adicionó rotenona 13 µM como inhibidor. Ambos pozos se incuban simultáneamente 5 min a 37°C. A continuación, se adicionaron 6 µL de DuB 3.12 mM en cada pozo para dar inicio a la reacción, la placa se agitó por 5 s y se realizó una cinética con lecturas cada 20 s por 3 min. La actividad total de la enzima se calculó como la actividad sin inhibidor menos la actividad enzimática con inhibidor presente. La activad (A) se calcula como:

$$A = \frac{(\Delta Abs/\min)(1000)}{(mg\ prot * \varepsilon_{DCPIP})}$$

Siendo ε_{DCPIP} el coeficiente de extinción molar del DCPIP= 19.1 $mM^{-1}cm^{-1}$.

6.8.2. Actividad del CII.

La técnica se realizó en placas de 96 pozos, utilizando un lector de microplacas Synergy-Biotek (Biotek Instruments). En cada pozo se colocó la mezcla de reacción

la cual contenía: BSA 5 mg/mL, DCPIP 67 µM, antimicina A 1 µM, succinato 15 mM, KCN 0.2 mM, PBS 30 mM (pH 7.4), en un volumen total de 300 µL y se adicionaron 5 µg de proteína mitocondrial. Para cada muestra se efectuó un duplicado al cual se le adicionó malonato 10 mM como inhibidor, ambos pozos se incubaron simultáneamente durante 5 min a 37°C. La reacción se inició por adición de 6 µL DuB 3.12 mM, la placa se agitó por 5 s y se realizó una cinética de 3 min con lecturas cada 20 s. La actividad de la enzima total se calculó como la actividad sin inhibidor menos la actividad con inhibidor. La activad (A) se calcula como:

$$A = \frac{(\Delta Abs/\min)(1000)}{(mg\ prot * \varepsilon_{DCPIP})}$$

Siendo ε_{DCPIP} el coeficiente de extinción molar del DCPIP= 19.1 $mM^{-1}cm^{-1}$.

6.8.3. Actividad del CIII.

La técnica se realizó en placas de 96 pozos, utilizando un lector de microplacas Synergy-Biotek (Biotek Instruments). En cada pozo se colocó la mezcla de reacción la cual contenía: BSA a 0.4 mg/mL, Tween 220 µM, rotenona 1 µM, KCN 0.4 mM, $MgCl_2$ 0.6 mM, EDTA 0.1 mM, citocromo C oxidado 17 µM, PBS 30 mM (pH 7.4), en un volumen total de 300 µL y se adicionaron 2.5 µg de muestra mitocondrial. A cada muestra se le realizó un duplicado al cuál se le adicionó antimicina A 30 µM como inhibidor, ambos pozos se incuban simultáneamente 8 min a 37°C. Se adicionaron 5 µL DuB reducida 3.12 mM para iniciar la reacción, la placa se agitó por 5 s y se realizó una cinética de 3 min cada 15 s. La actividad total de la enzima se calculó como la actividad sin inhibidor menos la actividad enzimática con inhibidor presente, donde la actividad de la enzima se calculó como:

$$A = \frac{(\Delta Abs/\min)(1000)}{(mg\ prot * \varepsilon_{cit\ c\ red})}$$

Siendo $\varepsilon_{cit\ c\ red}$ el coeficiente de extinción molar del citocromo c reducido= 18.5 $mM^{-1}cm^{-1}$.

6.8.4. Actividad del CV.

La actividad del CIV se determinó en medio de respiración MiR05 suplementado con rotenona 0.5 µM más antimicina A 2.5 µM. La evaluación del consumo mitocondrial de O_2 se realizó utilizando un equipo de respirometría de alta resolución (Oxygraph O2k, OROBOROS) a 37 °C. Para iniciar la rección se estimuló el consumo de oxígeno mediante la adición de TMPD 0.5 mM más ascorbato 2 mM, posteriormente se adicionó NaN_3 como inhibidor especifico. La actividad total de la enzima se calculó como el consumo de oxígeno sin inhibidor menos el consumo de oxígeno con presencia del inhibidor.

6.9. Actividad de la ATP sintasa.

La actividad de la ATP sintasa se determinó de manera indirecta a partir de la tasa de síntesis del NADPH a 340 nm, al acoplar la reacción de la ATP sintasa a la de la hexocinasa y a la de la glucosa 6-fosfato deshidrogenasa [153] (Fig. 5).

La técnica se realizó en placas de 96 pozos, utilizando un lector de microplacas Synergy-Biotek (Biotek Instruments). En cada pozo se colocaron: hexocinasa 4

U/mL, G6PDH 2 U/mL, glucosa 20 mM, $NADP^+$ 1.4 mM, los sustratos ligados al CI o al CII (ver sección 6.6), PBS 40 mM (pH = 7.4), en un volumen total de 300 µL y se adicionaron 30 µg de mitocondrias frescas. La reacción se inició con 200 mM de ADP y se siguió por 3 min cada 30 s. Se utilizó oligomicina 10 µM como inhibidor especifico, la cual se preincubó por 3 min y se siguió la cinética con oligomicina por 3 min cada 30 s. La actividad enzimatica total se calculó como la actividad sin inhibidor menos la actividad con inhibidor presente, en el que la actividad (A) corresponde a:

$$A = \frac{(\Delta Abs/\min)(1000)}{(mg\ prot * \varepsilon_{NADPH})}$$

Siendo ε_{NADPH} el coeficiente de extinción molar del NADPH= 6.22 $mM^{-1}cm^{-1}$.

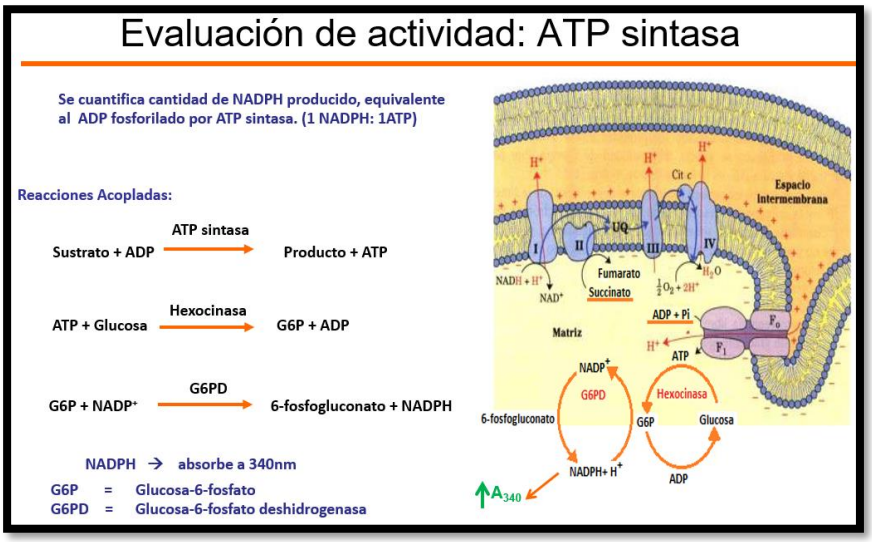

Figura 5. Reacciones acopladas utilizadas para determinar de manera indirecta la actividad de la ATP sintasa. El aumento de la absorbancia a 340nm es directamente proporcional a la actividad de la ATP sintasa.

6.10. Producción de H_2O_2 mitocondrial

La velocidad de producción de H_2O_2 mitocondrial se midió utilizando un fluorómetro de O2k (OROBOROS, Innsbruck, Austria) y usando Amplex Red (10 µM) como sonda. Brevemente, mitocondrias recién aisladas se resuspendieron en 2.0 mL de medio de respiración MiR05 suplementado con HRP 0.5 U/mL. Para obtener la velocidad de producción de H_2O_2 en los diferentes estados respiratorios, se emplearon adiciones secuenciales como se describió previamente (sección 6.6) y se emplearon curvas de calibración de concentraciones de H_2O_2 para asegurar la linealidad del ensayo, una vez realizada la misma la velocidad de producción de peróxido de hidrogeno corresponde a la primara derivada del cambio en la concentración de H2O2 en función del tiempo, determinada por el equipo [154]. La producción basal de H_2O_2 se obtuvo mediante la adición de mitocondrias, la producción alimentando al CI en S4 (S4 ligado a CI) se midió mediante la adición de sustratos ligados a CI. La producción alimentando al CI S3 (S3 ligado a CI) se

determinó mediante la adición de ADP 2.5 mM. Para determinar la producción alimentando al CI más CII en S3 (S3 ligado a CI+CII) se añadió succinato de sodio 10 mM. Finalmente, se añadió oligomicina 2,5 µM para determinar la producción en S4o (S4o ligado a CI+CII).

6.11. Marcadores de estrés oxidante

Los cambios en los niveles de los marcadores de estrés oxidante MDA y 4HNE se evaluaron a partir de la evaluación de dichas modificaciones en las proteínas por Western Blot (WB; ver sección 6.16). Por su parte la inactivación de la actividad de aconitasa mitocondrial se midió como un marcador de estrés oxidante mitocondrial. Para esto se determinó la velocidad de formación del producto intermedio *cis*-aconitato a 240 nm [155]. La actividad mitocondrial de la aconitasa se normalizó sobre la actividad de la citrato sintasa. Brevemente, la actividad del citrato sintasa se determinó a partir del aumento en la absorbancia a 412 nm del aducto ácido 5-tio-2-nitrobenzoico [156]. Ambas técnicas se realizaron en placas de 96 pozos, utilizando un lector de microplacas Synergy-Biotek (Biotek Instruments) y las actividades se expresaron como nanomol por minuto por miligramo de proteína (nmol/min/mg de proteína).

6.12. Actividad de las enzimas antioxidantes

Las actividades de las enzimas antioxidantes en las muestras correspondientes se realizaron de acuerdo a la siguiente metodología:

6.12.1. Superóxido dismutasa (SOD)

La actividad de la SOD se determinó espectrofotométricamente a 560 nm utilizando nitroazul de tetrazolio (NBT) como indicador [156] (ver Fig. 6). Las mediciones realizaron en placas de 96 pozos, utilizando un lector de microplacas Synergy-Biotek (Biotek Instruments). Para esto se preparó una mezcla de reacción con: xantina 0.3 mM, de NBT 150 µM, EDTA 0.6 mM y Na_2CO_3 400 mM, en un volumen total de 332 µL por pozo y la cinética se inició por adición de 30 µL de XO (5 mg/mL en NH_4SO_2 2M). La reacción se dejó avanzar por 15 minutos y se adicionó 0.8 mM de $CuCl_2$ para parar la reacción. La absorbancia se determinó a 560 nm en cada una de las muestras y en un control positivo sin muestra. Se definió una unidad (U) de la SOD como la cantidad de enzima que evita la oxidación de 1 mol de NBT por minuto (en comparación con el control positivo), los resultados se expresaron como U/mg proteína usados.

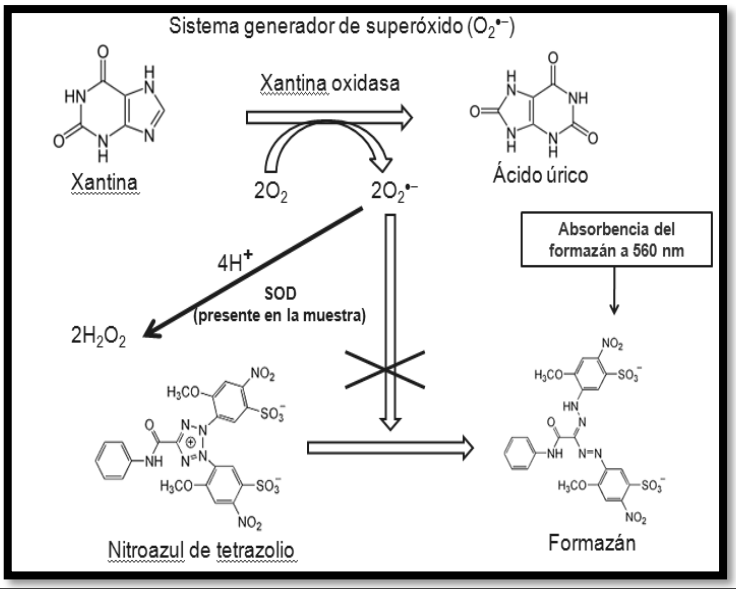

Figura 6. Sistema utilizado para determinar la actividad de la superóxido dismutasa (SOD). La xantina oxidasa (XO) utiliza xantina para producir anión superóxido ($O_2^{\cdot-}$) el cual a su vez oxida al nitroazul de tetrazolio (NBT) para producir formazán, compuesto que absorbe a 560 nm. La actividad de la SOD en la muestra previene la producción de formazán al abatir los niveles de $O_2^{\cdot-}$, por lo que disminuye los incrementos en la absorbancia a 560 nm con respecto al control positivo, lo que se considera como una medida directa de la actividad de la SOD.

6.12.2. Glutatión peroxidasa (Gpx)

La actividad de la Gpx se determinó a partir la desaparición del NADPH en una reacción acoplada a la GR (ver Fig. 7). Las mediciones se realizaron en placas de 96 pozos, utilizando un lector de microplacas Synergy-Biotek (Biotek Instruments). Para esto se preparó una mezcla de reacción con: EDTA 1 mM, NaN_3 1 mM, GSH 1 mM, NADPH 0.2 mM y GR 1 U/mL en PBS 50 mM pH 7.4. La muestra se adicionó a 300 µL de mezcla de reacción y el ensayo se inició por la adición 30 µL de una solución 1.25 mM de H_2O_2. Las lecturas se realizaron cada 30 s por 3 minutos. Una

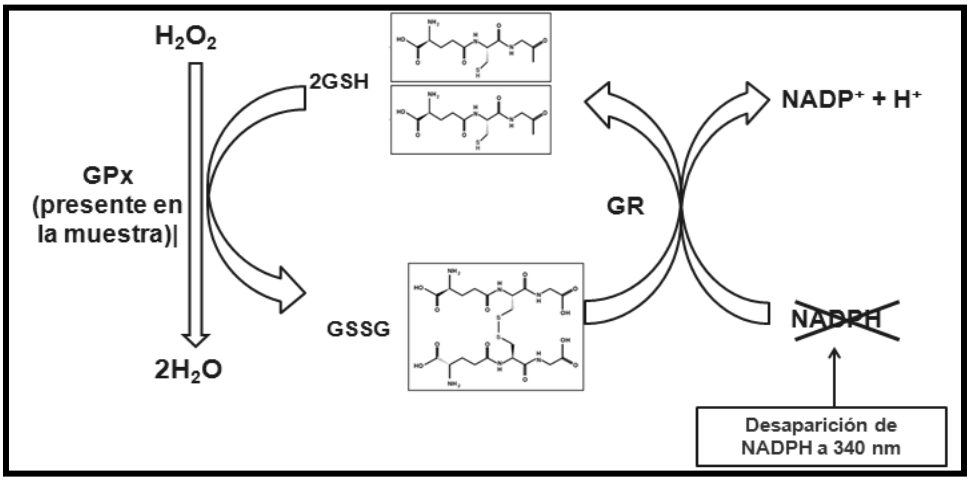

Figura 7. Sistema utilizado para determinar la actividad de la enzima glutatión peroxidasa (GPx) en homogeneizados. La GPx reduce al H_2O_2 al oxidar el glutatión (GSH) a glutatión oxidado o disulfuro (GSSG), mientras que la glutatión reductasa (GR) en una reacción acoplada utiliza el NADPH para volver a reducir el GSSG a GSH. Por tanto, la desaparición de la absorbancia a 340 nm del NADPH se considera como una medida indirecta de la actividad de la GPx en la muestra.

unidad (U) de GPx se definió como la cantidad de enzima que oxida 1 mol de NADPH en un minuto, los datos se expresaron como U/mg de proteína utilizados.

6.12.3. Peroxiredoxina (Prx)

La actividad de la Prx se determinó a partir de la oxidación de NADPH en una reacción acoplada a la tioredoxina reductasa y a la tioredoxina [157] (ver Fig. 8). Las mediciones realizaron en placas de 96 pozos, utilizando un lector de microplacas Synergy-Biotek (Biotek Instruments). Se preparó una mezcla de reacción con: tioredoxina 500 µM, tioredoxina reductasa 50 µM, H_2O_2 1 µM, EDTA 1 mM, sulfato de amonio 100 mM, PBS 25 mM pH 7.0. La muestra se adicionó a 200 µL de mezcla de reacción y el ensayo se inició por la adición de NADPH 150 µM. Las lecturas se realizaron cada 15 s por 3 minutos. Una unidad (U) de Prx se definió como la cantidad de enzima que oxida 1 mol de NADPH en un minuto, los datos se expresaron como U/mg de proteína utilizados.

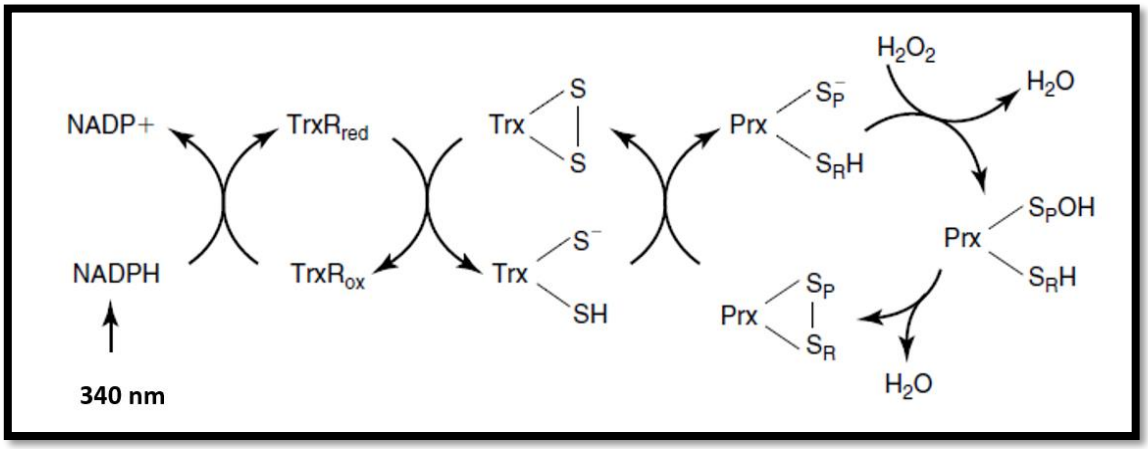

Figura 8. Sistema utilizado para determinar la actividad de la enzima peroxiredoxina (Prx). La Prx reduce al peróxido de hidrogeno (H_2O_2) al oxidar a sus grupos tiol (S), formando un puente disulfuro. Dicho puente es reducido por la tioredoxina (Trx) al oxidar a sus propios grupos tiol, formando un nuevo puente disulfuro en la Trx. Finalmente, la tioredoxina reductasa (TrxR), reduce a la Trx de manera dependiente del NADPH. Por tanto, la desaparición de la absorbancia a 340 nm del NADPH se considera como una medida indirecta de la actividad de la Prx en la muestra. Esquema modificado de *Nelson et al, 2013,* [157].

6.12.4. Catalasa

La determinación de la actividad de la catalasa se realizó por medio del método basado en el seguimiento de la desaparición de H_2O_2 30 mM por absorbancia de dicha molécula a 240 nm al adicionar la muestra (ver Fig. 9). Los datos se expresaron como la constante de primer orden (k) sobre los mg de proteína

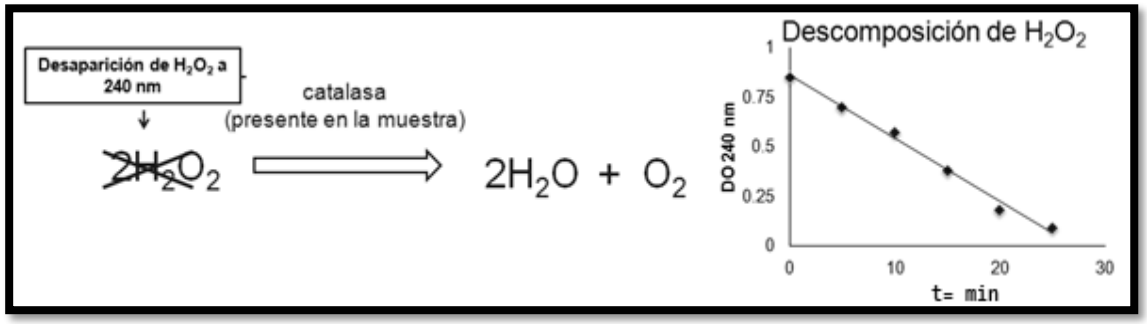

Figura 9. Esquema utilizado para determinar la actividad de la enzima catalasa en homogeneizados. Se considera la desaparición de la absorbancia (DO) a 240 nm al adicionar la muestra como una medida directa de la actividad de esta enzima.

utilizados.

6.13. Niveles de GSH y actividad de las enzimas del sistema de S-glutationilación

6.13.1. Contenido total de glutatión, GSH y GSSG

El contenido total de glutatión (GSH + GSSG) y los niveles de GSSG se midieron en homogeneizados frescos utilizando el método descrito previamente [158]. El ensayo de glutatión total se basa en la reacción del GSH con el DTNB para producir el aducto GS-STNB, el cual es medido a 412 nm. Para tal ensayo se adicionó previamente GR y NADPH a los homogeneizados, quedando únicamente el GSH, el cual luego reacciona libremente con el DTNB. La tasa de cambio en la absorbancia se comparó con estándares de concentración conocida de GSH.

Por otro lado, la medición de los niveles de GSSG se realizó de igual manera, pero las muestras se incubaron previamente con 2-vinil piridina (2-VP), la cual reacciona específicamente con el GSH de manera irreversible. De esta manera la formación del aducto GS-STNB es atribuible únicamente al GSH formado a partir de la reducción del GSSG por la GR. Finalmente, los niveles de GSH se determinaron restando el contenido de GSSG en las muestras tratadas con 2-VP al contenido total de glutatión de las muestras sin 2-VP. Todas las mediciones fueron normalizadas por el contenido de proteínas determinada por el método de Lowry.

6.13.2. Actividad de la Grx

La actividad de eliminación de S-glutatión de Grx se determinó utilizando un estuche comercial de Cayman Chemical (Ann Arbor, MI, EUA). Brevemente, la actividad determinada con el estuche se basa en la reacción de eliminación de S-glutatión de una proteína prediseñada, lo cual genera un producto fluorescente. Así mismo se

utilizó una curva estándar de calibración con concentraciones conocidas de Grx para determinar la actividad en la muestra. Las mediciones se realizaron en placas de 96 pozos, utilizando un lector de microplacas Synergy-Biotek (Biotek Instruments).

6.13.3. Actividad de la GST

La actividad de la GST se determinó a partir del aumento en la absorbancia a 340 nm del aducto formado por el GSH y el CDNB (ver Fig. 10). La reacción se inició con la adición de la muestra a 330 µL de mezcla de reacción (GSH 5 mM, CDNB 1mM en PBS 50 mM pH 7.2) y se realizaron lecturas cada minuto por 3 minutos. Se definió una unidad de GST (U) como la cantidad de enzima que conjuga 1 mol de CDNB con GSH en 1 minuto, los datos se expresaron como U/mg de proteína usados.

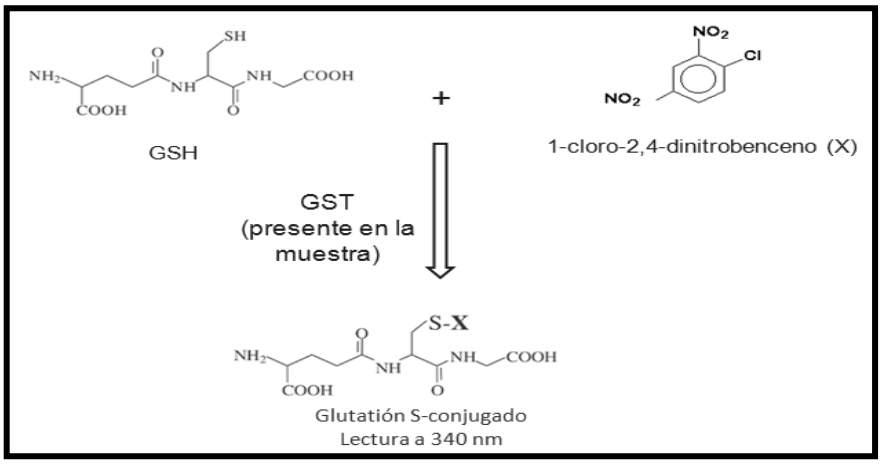

Figura 10. Sistema utilizado para determinar la actividad de la enzima glutatión S-tranferasa (GST). La GST cataliza la reacción de conjugación entre el glutatión (GSH) y el 1-cloro-2,4 dinitrobenceno (CDNB). El aducto resultante absorbe a 340 nm, por lo que se considera al aumento de la absorbancia a esta λ como una medida de la actividad de la GST en la muestra.

6.13.4. Actividad de la GR

La actividad de la GR se determinó a partir la medición de la desaparición de NADPH a 340 nM usando GSSG como sustrato (ver Fig. 11). Las mediciones se realizaron en placas de 96 pozos, utilizando un lector de microplacas Synergy-Biotek (Biotek Instruments, Winooski, VT, EUA). Para esto se preparó una mezcla de reacción con EDTA 1 mM, NADPH 1 mM y GSSG 1 mM, en amortiguador de fosfatos 100 mM pH 7.4. El ensayo se inició por la adición de la muestra a 313 µL de mezcla reacción, con lecturas cada minuto durante 3 min. La unidad de GR se definió como la cantidad de enzima que oxida 1 mol de NADPH/min, los datos se expresaron como U/mg de proteína utilizados.

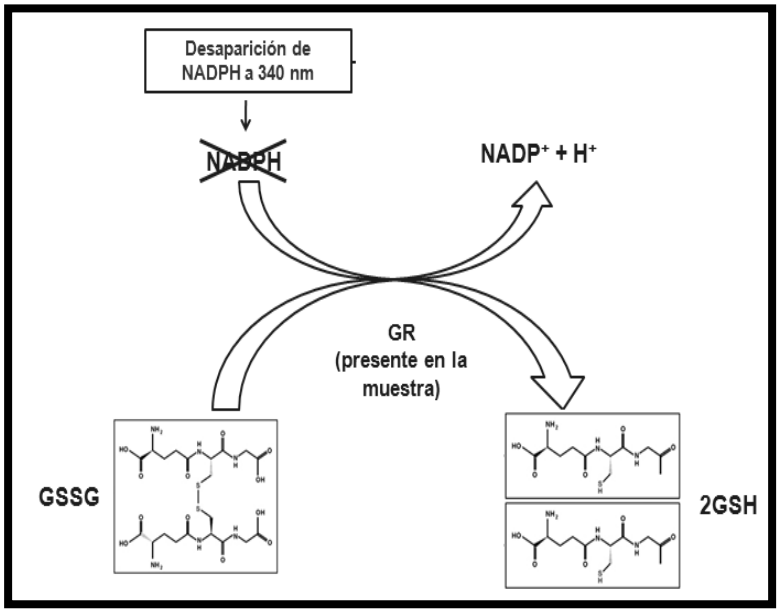

Figura 11. Sistema utilizado para determinar la actividad de la enzima glutatión reductasa (GR). La GR utiliza el NADPH para reducir al glutatión oxidado (GSSG) a glutatión reducido (GSH). Por tanto, la desaparición de la absorbancia a 340 nm del NADPH se considera como una medida de la actividad de la GR en la muestra.

6.14. Aislamiento de PT y DT

El aislamiento de los segmentos de la nefrona se realizó por el método previamente descrito [159]. Brevemente, los riñones se extrajeron, lavaron y picaron sobre una caja Petri enfriada con hielo. Los fragmentos resultantes se colocaron en 15 mL de amortiguador KBS a 4 °C: NaCl 110 mM, $NaHCO_3$ 25 mM, KCl 3 mM, $CaCl_2$ 1.2 mM, $MgSO_4$ 0.7 mM, KH_2PO_4 2 mM, acetato de sodio 10 mM, glucosa 5.5 mM, alanina 5 mM y 0.5 g/L de BSA pH 7.4. Los tejidos se cortaron y se lavaron tres veces, se resuspendieron en 10 mL de KBS que contenía 15 mg de colagenasa y 0.5 mL de BSA al 10% m/v. Posteriormente, se incubaron en un baño de agua durante 20 minutos a 37 °C, a continuación, la suspensión tisular se agitó suavemente para dispersar fragmentos de tejido y se filtró para eliminar las fibras de colágeno. Luego se centrifugó suavemente para remover la colagenasa y el botón se resuspendió en 10 mL de KBS a 4 °C, este procedimiento de lavado se repitió tres veces. Finalmente,

el botón se resuspendió en 30 mL de una mezcla recién preparada de Percoll y KBS fría (1:1, v/v). La suspensión se centrifugó a 1,071 x g por 30 min, lo que resultó en la formación de 3 bandas, la segunda de las cuales está enriquecida con túbulos distales y la tercera con proximales. El contenido de cada fracción se confirmó por la observación en microscopía de luz.

6.15. Determinación de la producción de ROS por la NADPH oxidasa (Nox) y la sintasa de óxido nítrico (Nos)

La determinación de la producción del anión $O2^{\bullet-}$ se realizó por el método fluorescente para homogeneizados de riñón descrito por Satoh *et al.* (2005). Dicha prueba utiliza la oxidación fluorogénica del dihidroetidio a etidio (Eth) como una medida indirecta de ROS. Los homogeneizados respectivos se incubaron con 0.02 mM de DHE, 0.5 mg/mL de ADN de esperma de salmón y los sustratos correspondientes: NADPH 0.1 mM para Nox y L-arginina 1 mM para Nos. Por separado se realizó un duplicado con inhibidores respectivos: 10 µM de DPI y 10 µM de VAS2870 para inhibir a la Nox, y L-NAME 1 mM para la Nos. Las mediciones realizaron en placas de 96 pozos, utilizando un lector de microplacas Synergy-Biotek (Biotek Instruments). El ensayo se realizó a 37 °C durante 25 minutos y la fluorescencia del complejo Eth-DNA se midió a longitudes de onda de excitación/emisión de 480/610 nm. Los datos se expresaron como unidades arbitrarias de fluorescencia (AUF). Para normalizar la intensidad de fluorescencia de cada muestra se dividió sobre el promedio del control respectivo y por la cantidad total de proteína determinada por Lowry.

6.16. Extracción de proteína y Western Blot

Para la extracción total de proteínas, las respectivas muestras se resuspendieron en amortiguador de radioinmunoprecipitación (RIPA): Tris-HCl 40 mM, NaCl 150 mM, EDTA 2 mM, EGTA 1 mM, NaF 5 mM, Na_3VO_4 1 mM, PMSF 1 mM, desoxicolato de sodio al 0.5%, SDS al 0.1% pH 7.6, complementado con el cóctel de inhibidor de proteasas. Las muestras se homogeneizaron usando un homogeneizador Potter-Elvehjem y se centrifugaron a 15,000 x g durante 10 minutos a 4 °C. Se recogieron los sobrenadantes y la proteína total se cuantificó mediante el método de Lowry.

Las cantidades de proteína correspondientes se desnaturalizaron hirviéndolas durante 10 minutos y luego se diluyeron 1:5 en amortiguador Laemmli (Tris-HCl 60 mM, SDS al 2%, glicerol al 10%, β-mercaptoetanol al 5%, azul de bromofenol al 0.01% pH 6.8) [153]. Las muestras (20 µg) y los estándares de peso molecular se cargaron en geles de SDS-poliacrilamida y se realizó la electroforesis. Posteriormente, las proteínas se transfirieron a membranas de fluoruro de polivinilideno (PVDF). La unión a proteínas no específicas se bloqueó por incubación con leche en polvo sin grasa al 5% en amortiguador TBS (Tween 20 al 0.4%) durante 1:30 h a temperatura ambiente. Posteriormente, las membranas se incubaron durante toda la noche a 4 °C con el anticuerpo primario apropiado y posteriormente durante 1:30 h en la oscuridad con el anticuerpo secundario fluorescente correspondiente (1:10,000). Las bandas de proteínas se detectaron por fluorescencia en un equipo Odyssey (LI-COR Biosciences, Lincoln, NE, EUA). Las

bandas de proteínas se analizaron con el software Image Studio™ Lite LI-COR Odyssey (LI-COR Biosciences).

6.17. Cultivo celular

Las células epiteliales del PT LLC-PK1 se cultivaron en medio DMEM suplementadas con FBS al 10% y penicilina/estreptomicina (100/50 U/mL) en una incubadora con atmósfera humidificada y CO_2 al 5% a 37 ºC. Los experimentos se realizaron a una densidad celular de 44,000 células/cm^2 [53]. Después de 24 h de crecimiento, las células se expusieron a NAC 10 mM [56] durante 22 h. Posteriormente, se reemplazó por NAC 10 mM fresco durante 2 h antes de exponer a las células a las diferentes concentraciones de FA (2.5-30 mM) durante 24 h. Una vez terminada la incubación, se tomaron micrografías con un lector Cytation 5 (BioTek Instruments). Las imágenes en campo claro se capturaron por triplicado con un objetivo 20X.

6.18. Consumo de oxígeno en células completas

El consumo de oxígeno en las células intactas se determinó en un equipo de respirometría de alta resolución (Oxygraph O2k, OROBOROS). Después de los tratamientos con FA, FA+NAC o NAC correspondientes, las células se lavaron con PBS 1X y se cosecharon. Las determinaciones se realizaron utilizando 2 mL de medio de cultivo con 10% de FBS a 37 °C. El experimento se inició mediante la adición de las células (2.4 millones como número inicial). Los parámetros respiratorios se definieron de la siguiente manera: 1) Respiración de rutina (*routine respiration*): consumo de oxígeno en presencia de las células únicamente. 2) Respiración de fuga (*Leak respiration*): correspondiente al consumo celular de oxígeno en presencia de oligomicina 5 µM. 3) Respiración desacoplada (*uncoupled respiration*): se determinó mediante valoraciones con 8 µL de DNP 20 µM. 4) P: se determinó mediante la fórmula: Routine-Leak. Todos los parámetros anteriores se corrigieron restando la respiración no mitocondrial, obtenida mediante la adición de rotenona 1 µM más antimicina 5 µM y se normalizaron por el número inicial de células.

6.18. Análisis estadístico

Los datos se presentan como la media ± error estándar de la media (SEM) y se analizaron mediante el software Graph Pad Prism 8 (San Diego, CA, EUA). Las pruebas estadísticas correspondientes se aclaran en cada uno de los pies de figura.

7. Resultados

7.1. La AKI inducida por FA

7.1.1. El pretratamiento con NAC evita la AKI inducida por FA

Para validar el modelo y determinar el efecto del pretratamiento con NAC sobre la AKI inducida por FA, se determinaron 24 h después de la administración de FA, los niveles de los marcadores BUN y creatinina en plasma, así como el volumen urinario y el peso del riñón. Se observó que el FA indujo un aumento notable en la creatinina (Fig. 12A) y BUN (Fig. 12B) en plasma, así como un mayor volumen urinario (Fig. 12C) con respecto al grupo control. Sin embargo, no se observaron cambios significativos en el peso del riñón (Fig. 12 D). Por su parte, el análisis histológico del grupo tratado con FA reveló que abundantes células de PT hinchadas se alternan con células necróticas que contienen múltiples vacuolas en el citoplasma. Así mismo, los múltiples túbulos dañados exhibieron cilindros hialinos en su luz y atrofia epitelial acentuada (Fig. 13C).

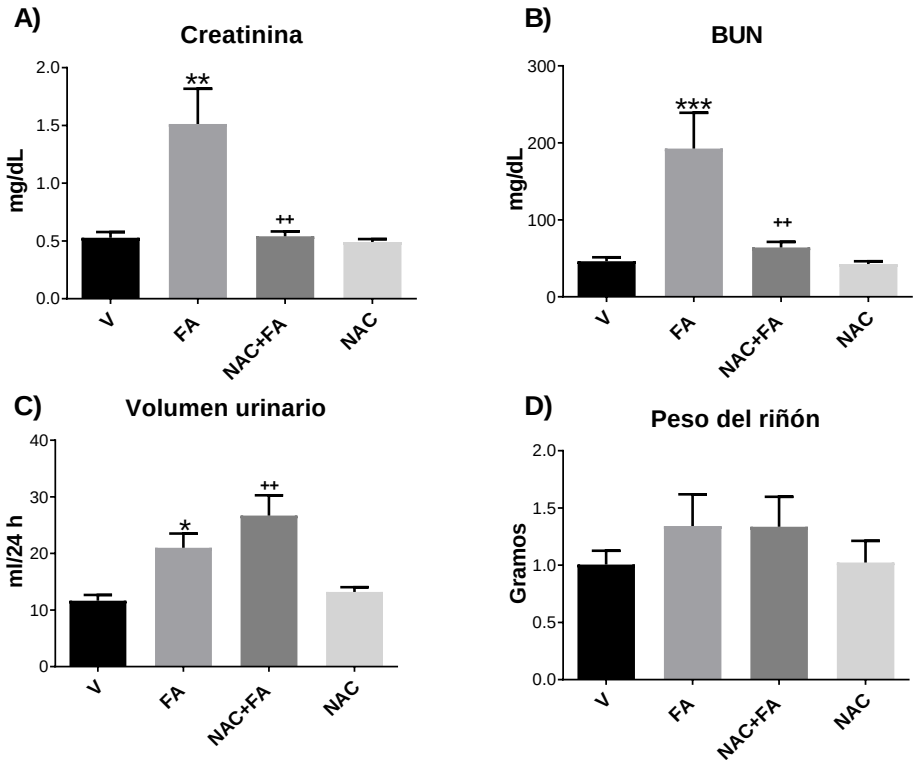

Figura 12. El pretratamiento con NAC evita la AKI inducida por FA. Marcadores de daño renal y el peso del riñón a las 24 h posteriores a la administración de FA **(A)** Creatinina y **(B)** nitrógeno de urea en sangre (BUN) en plasma, **(C)** volumen urinario y **(D)** peso del riñón. V= vehículo FA= ácido fólico, NAC= N-acetilcisteína. Los datos se presentan como la media ± SEM, n= 5-6. *p<0.05, **p<0.01, ***p<0.001 *vs.* V. ⁺⁺p<0.01 *vs.* FA. ANOVA de una vía más una prueba de Tukey subsecuente.

Por su parte, el pretratamiento con NAC previno el aumento en los niveles de creatinina (Fig. 12A) y de BUN (Fig. 12B) en plasma, además de evitar ampliamente

el daño histológico, ya que sólo se observaron áreas focales con túbulos corticales atróficos y segmentos con epitelio regenerativo (Fig. 13D). De manera interesante, el grupo NAC+FA presentó un aumento del volumen urinario con respecto a los grupos V y FA. Sin embargo, el grupo NAC no presentó este aumento (Fig. 12C). No se observaron cambios significativos en el peso del riñón entre los diferentes grupos (Fig. 12D), ni daño histológico renal en el grupo V (Fig. 13A) o en el grupo

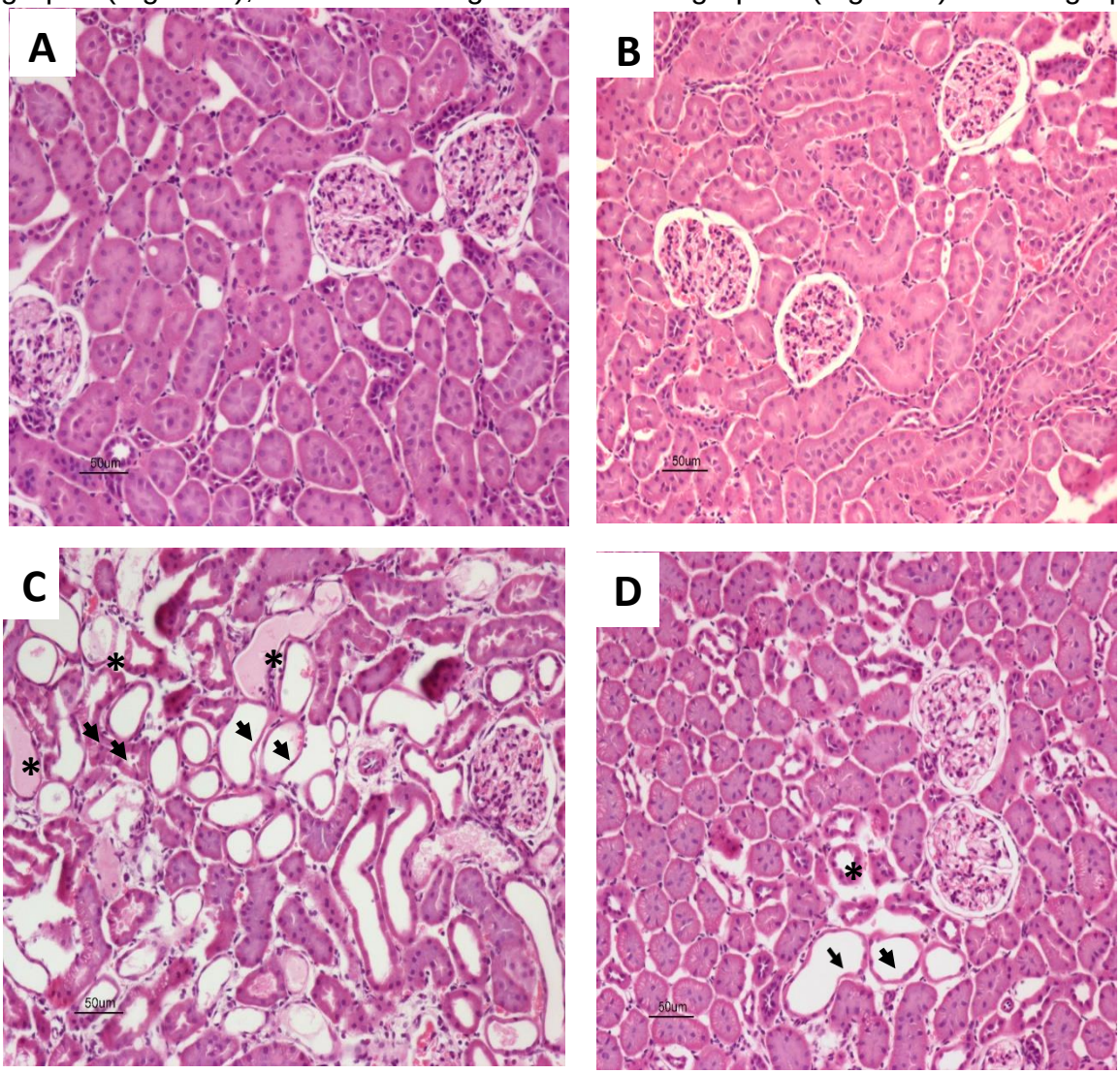

Figura 13. Micrografías representativas de tinción H&E de los riñones de los 4 grupos experimentales a las 24 h posteriores a la administración de FA. (A) Histología de un riñón normal de un animal tratado únicamente con el vehículo. **(B)** Riñón de un animal tratado con N-acetilcisteína (NAC), el cual no muestra ninguna anormalidad histológica. **(C)** En contraste, el riñón del animal tratado con ácido fólico (FA) muestra extenso daño tubular con numerosos túbulos proximales con necrosis y atrofia (flechas), así mismo numerosos túbulos exhiben cilindros hialinos en la luz tubular (asteriscos). **(D)** El riñón del grupo pretratado (NAC+FA) exhibe un tubular mucho menor, donde sólo se observan ocasionalmente túbulos proximales con atrofia (flechas) o actividad regenerativa (asterisco). Todas las micrografías se tomaron a un aumento de 200x, tinción con hematoxilina y eosina (H&E).

NAC (Fig. 13B). En conjunto estos resultados confirman la presencia de AKI a las 24 h posteriores a la administración de FA y el efecto protector del pretratamiento con NAC sobre la AKI.

7.1.2. LA NAC previene las alteraciones en la bioenergética mitocondrial relacionadas con la disfunción del CI en la AKI inducida por FA

Para determinar si la AKI a las 24 h después de la administración de FA se relacionaba con alteraciones en la bioenergética mitocondrial, se procedió a evaluar los parámetros respiratorios en la respiración asociada al CI, al CII y al CI+CII (Fig. 14), así como a los cambios en el ΔΨm en S3 y S4o (Fig. 15). Cabe resaltar que como se observa en la Fig. 15A, tras la adición de las mitocondrias al medio MiR05, se observó un decremento en la florescencia de la safranina. Indicando la que las mitocondrias aisladas presentan un potencial de membrana incluso antes de la adición de sustratos exógenos como el PMG (Fig. 15A). Dicho fenómeno ha sido reportado con anterioridad para colorantes catiónicos como la safranina O, los cuales se un acumulan en la mitocondria dada la existencia de potencial de membrana endógeno, generado por la presencia de sustratos endógenos residuales del aislamiento [160,161]. Lo que, es más, dicho potencial se mantiene solo por periodos cortos tras la adición de las mitocondrias y es susceptible a la despolarización por adición de inhibidores respiratorios como la rotenona o la antimicina A, confirmando que es generado por metabolitos endógenos residuales del aislamiento [160,161].

A las 24 h posteriores a su administración, el FA disminuyó significativamente los parámetros respiratorios S3, P y RCI en la respiración ligada al CI. Así mismo, el FA disminuyó el S3 y P en la respiración ligada al CI+CII (Fig. 14B). Sin embargo, no se observaron cambios significativos en ninguno de los parámetros respiratorios en la respiración ligada al CII (Anexo 1). De igual manera, el FA disminuyó el ΔΨm en S3, sin cambiar el ΔΨm en S4o (Fig. 15B). Estas alteraciones bioenergéticas sugieren que el desacoplamiento mitocondrial inducido por FA y la reducción de la capacidad de la OXPHOS podrían estar relacionados principalmente a problemas en la función del CI. Por lo tanto, se evaluó la actividad de cada uno de los complejos del ETS por separado y de la ATP sintasa alimentando al ETS por CI y por CII en experimentos por separado. El FA disminuyó la actividad de la ATP sintasa cuando ETS se alimentó vía CI (Fig. 16A) o vía CII (Fig. 16B) con respecto al control. De igual manera, en el grupo tratado con FA, se observó una disminución en la actividad del CI (Fig. 16C). Sin observarse cambios en la actividad del CII (Fig. 16D), del CIII o del CIV (Anexo 2).

Por otro lado, el pretratamiento con NAC previno significativamente la disminución en los parámetros S3, P y RCI en la respiración ligada al CI y en los parámetros S3 y P en la respiración ligada al CI+CII (Fig. 14), así como la reducción del ΔΨm en S3 (Fig. 15B) y la disminución en la actividad de la ATP sintasa (Fig. 16A-B) y del CI (Fig. 16C). En conjunto los datos muestran que la NAC previene el desacoplamiento mitocondrial y la reducción en la capacidad de la OXPHOS en la AKI inducida por FA. Para respaldar estos resultados, se evaluaron los parámetros respiratorios en células epiteliales del túbulo proximal LLC-PK1 tratadas con FA. El FA (12.5 mM) a las 24 h redujo significativamente, en las células LLCP-K1, los

parámetros respiratorios: reparación de rutina y P (Anexo 3). Lo cual es consistente con los resultados obtenidos con las mitocondrias aisladas de riñón (Fig. 3), confirmando que el FA por sí solo reduce la capacidad de producción de ATP mitocondrial en el PT. Por su parte, el pretratamiento con NAC 10 mM en las células LLC-PK1 previno la disminución de los parámetros respiratorios: respiración de rutina y P (Anexo 3), confirmando su capacidad de preservar la OXPHOS en el PT.

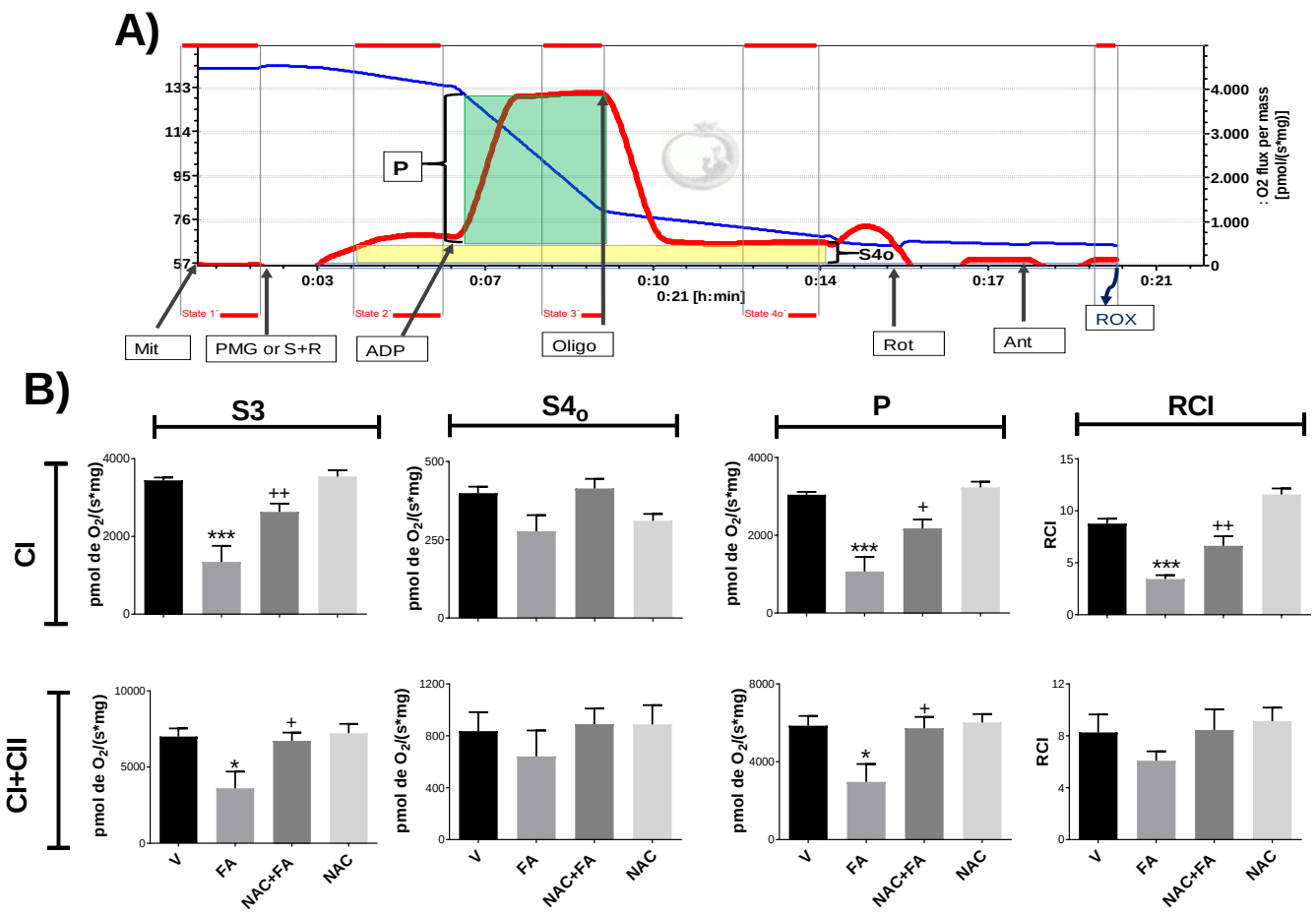

Figura 14. LA NAC previene las alteraciones en los parámetros respiratorios mitocondriales a las 24 h posteriores a la administración de FA. (A) Esquema del método utilizado para determinar cada estado respiratorio. La línea azul corresponde a la concentración de O_2, mientras que la línea roja corresponde a la velocidad de consumo de O_2. Las adiciones están representadas por flechas grises. **(B)** Parámetros respiratorios: estado 3 (S3), estado 4 inducido por oligomicina (S4o), índice de control respiratorio (RCI) y respiración asociada a la OXPHOS (P) en la respiración ligadas a CI y CI+CII. V= vehículo FA= ácido fólico, NAC= N-acetilcisteína. CI= complejo I, CII= complejo II, Mit= mitocondrias, PMG= piruvato-malato-glutamato, S= succinato, S+R= succinato+rotenona, Oligo=oligomicina, Rot= rotenona, Ant= antimicina A, ROX= respiración residual. Media ±SEM, n= 5-6. *p<0.05, ***p<0.001 *vs.* V. ⁺p<0.05, ⁺⁺p<0.01 *vs.* FA. ANOVA de una vía prueba de Tukey.

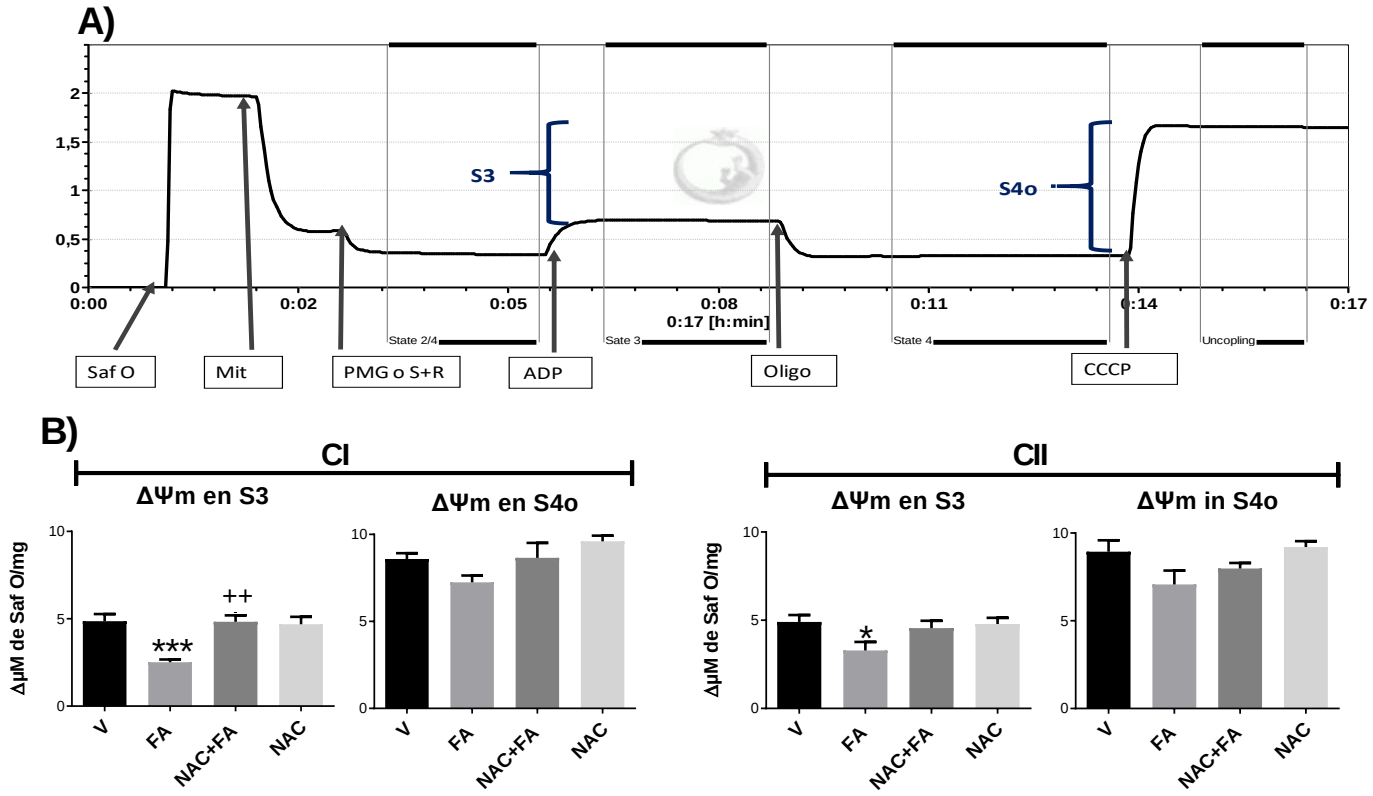

Figura 15. LA NAC previene la disminución en el potencial de membrana mitocondrial (Δψm) a las 24 h posteriores a la administración de FA. **(A)** Esquema del método utilizado para determinar los cambios en el Δψm, la línea negra corresponde a la concentración de safranina O determinada por fluorescencia. **(B)** Δψm en estado 3 (S3) y en estado 4 respiratorio inducido por oligomicina (S4o) en la respiración ligada a CI y CII. V= vehículo, FA= ácido fólico, NAC= N-acetilcisteína. CI= complejo I, CII= complejo II, Saf O= safranina O, Mit= mitocondrias, PMG= piruvato-malato-glutamato, S+R= succinato+rotenona, Oligo= oligomicina, CCCP= cianuro de carbonilo m-clorofenil hidrazona. Los datos se presentan como la media ± SEM, n= 5-6. *p<0.05, ***p<0.001 *vs.* V. $^{++}$p<0.01 *vs.* FA. ANOVA de una vía más Tukey.

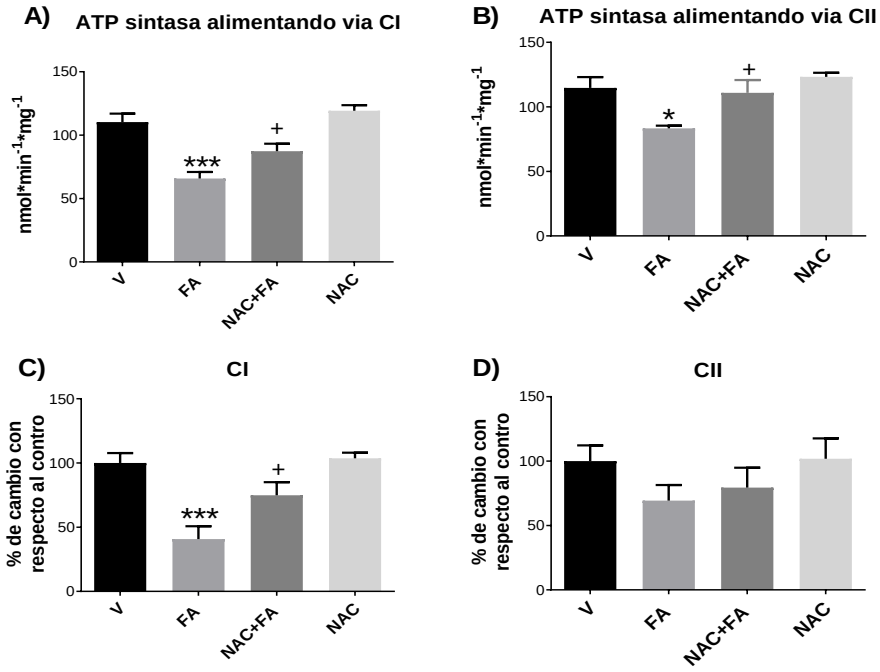

Figura 16. LA NAC previene la disminución en la actividad de los complejos respiratorios y ATP sintasa a las 24 h posteriores a la administración de FA. Actividad de ATP sintasa y complejos respiratorios I (CI) y II (CII) en mitocondrias aisladas. La actividad de la ATP sintasa se determinó alimentando vía **(A)** CI y vía **(B)** CII. Actividad de los complejos mitocondriales **(C)** CI y **(D)** CII. V= vehículo FA= ácido fólico, NAC = N-acetilcisteína. Los datos se presentan como la media ± SEM, n= 5-7. *p<0.05, ***p<0.001 *vs.* V. $^{+}$p<0.05 *vs.* FA. ANOVA de una vía más prueba de Tukey.

7.1.3. La NAC previene el estrés oxidante mitocondrial en la AKI inducida por FA

Para determinar si las alteraciones en la bioenergética mitocondrial inducen el aumento del estrés oxidante en este organelo, se evaluó la producción de H_2O_2 mitocondrial en los diferentes estados respiratorios. El FA indujo el aumento en velocidad de producción de H_2O_2 en todos los estados respiratorios (Fig. 17). Así mismo, la actividad de las enzimas antioxidantes MnSOD, GPx y Prx en la mitocondria renal disminuyó en el grupo tratado con FA (Fig. 18). De manera concordante, el FA indujo el incremento en los niveles de los marcadores de estrés oxidante mitocondrial MDA (Fig. 19A) y 4HNE (Fig. 19B) y la disminución en la actividad de la aconitasa (enzima mitocondrial sensible al estrés oxidante; Fig. 19C). La actividad de esta última se normalizó sobre la actividad de la citrato sintasa (donde no se observaron cambios) para confirmar que la disminución de actividad de la aconitasa se debiera al aumento en el estrés oxidante (Fig. 19C). En conjunto, estos resultados confirman que el FA induce a las 24 h de su administración un estado pro-oxidante en las mitocondrias renales.

Por su parte, el pretratamiento con NAC evitó el aumento en la producción mitocondrial de H_2O_2 inducido por FA en todos los casos (Fig. 17), el aumento en los marcadores de daño oxidante MDA (Fig. 19A) y 4HNE (Fig. 19B), la disminución en el cociente de actividades aconitasa/citrato sintasa (Fig. 19C) y

en las actividades de la MnSOD y la GPx (Fig. 18). Dichos resultados confirman que la NAC es capaz de evitar el estrés oxidante mitocondrial inducido por el FA.

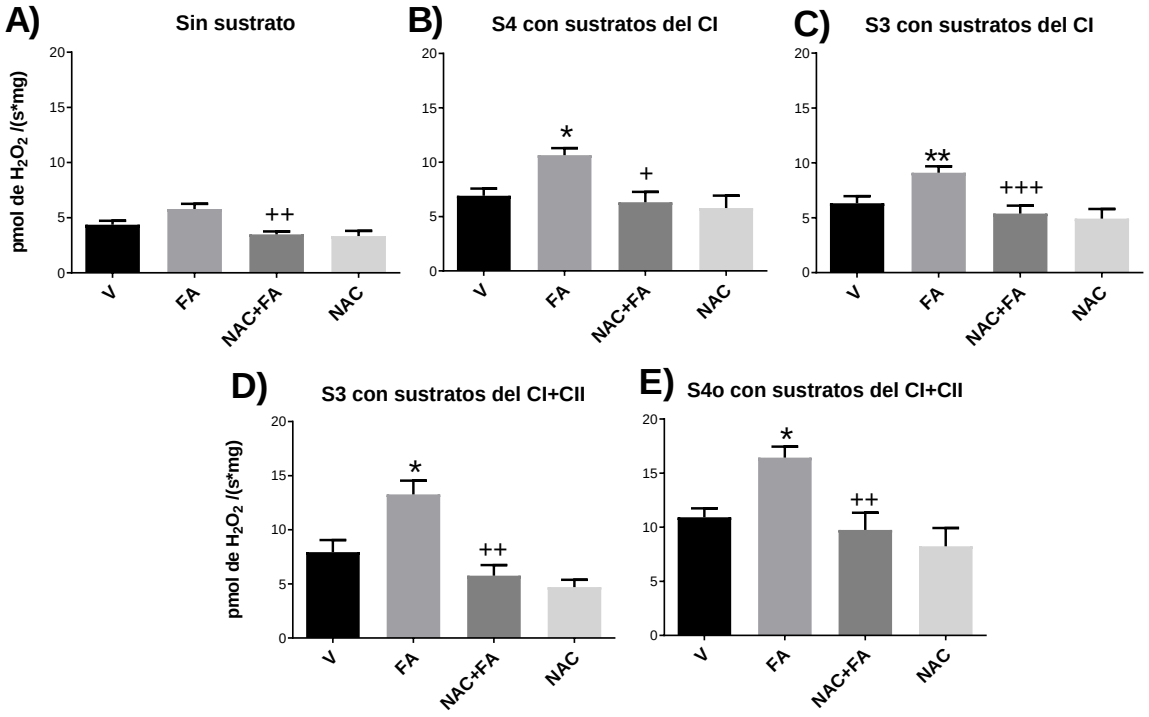

Figura 17. LA NAC previene el aumento en la velocidad de producción de peróxido de hidrógeno (H_2O_2) mitocondrial en los diferentes estados respiratorios. Se evaluaron los siguientes estados: **(A)** mitocondrias sin sustratos exógenos, **(B)** S4 respiratorio alimentando vía CI, **(C)** S3 respiratorio alimentando vía CI, **(D)** S3 respiratorio alimentando vía CI+CII, **(E)** S4o alimentando vía CI+CII. V= vehículo FA= ácido fólico, NAC= N-acetilcisteína. CI= complejo I, CII= complejo II, S3= estado 3, S4= estado 4. Los datos se presentan como la media ± SEM, n= 5-6. *p<0.05, **p<0.01 *vs.* V. $^{++}$p<0.01, $^{+++}$p<0.001 *vs.* FA. ANOVA de una vía más prueba de Tukey.

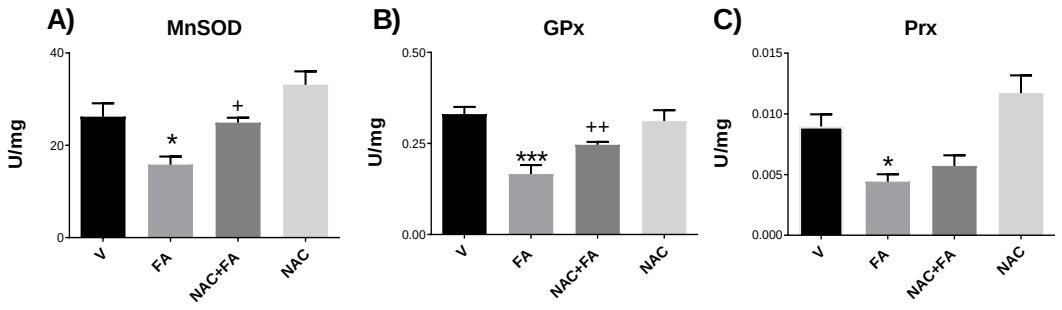

Figura 18. LA NAC previene la disminución en la actividad de enzimas antioxidantes en mitocondrias aisladas. (A) Superóxido dismutasa dependiente de Mn (MnSOD), **(B)** glutatión peroxidasa (GPx) y **(C)** peroxiredoxina (Prx). V= vehículo FA= ácido fólico, NAC= N-acetilcisteína. Los datos se presentan como la media ± SEM, n= 5-6. *p<0.05, ***p<0.001 *vs.* V. $^{+}$p<0.05, $^{++}$p<0.01 *vs.* FA. ANOVA de una vía más una prueba de Tukey.

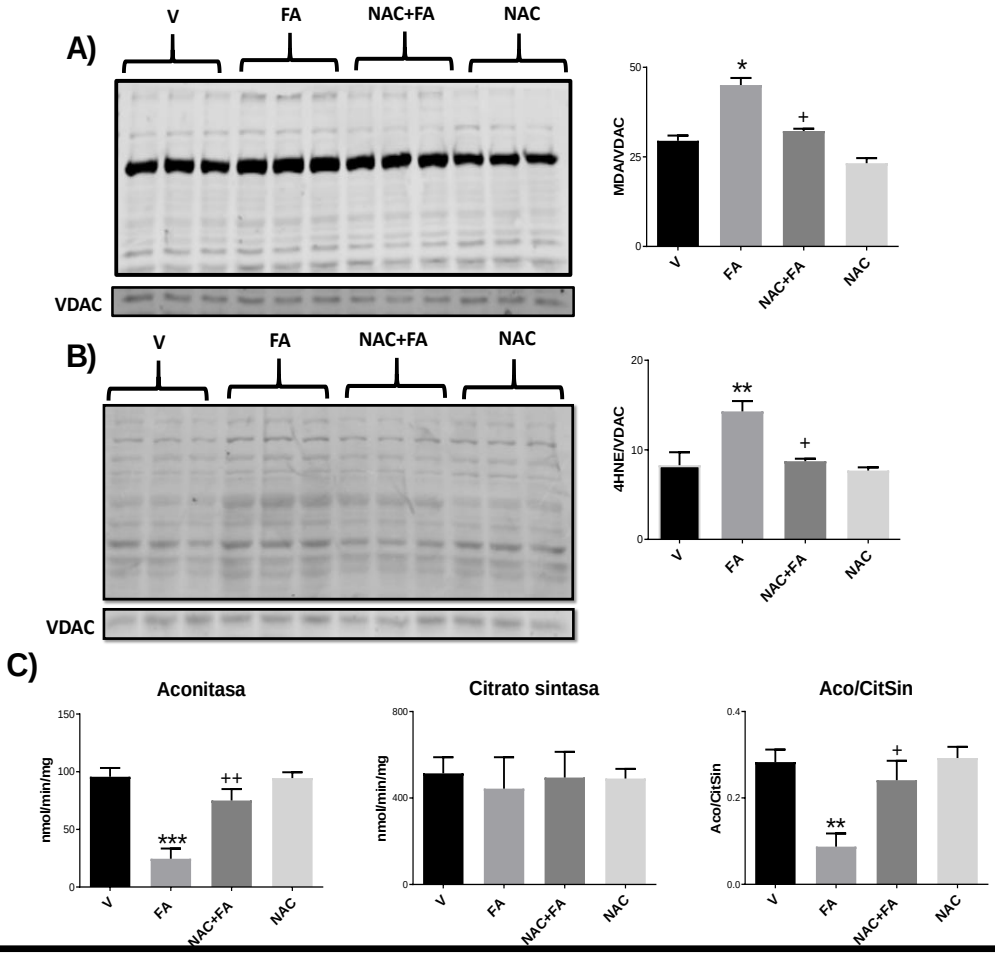

Figura 19. LA NAC previene el aumento en los marcadores de estrés oxidante en mitocondrias aisladas. Marcadores de lipoperoxidación **(A)** malondialdehído (MDA) y **(B)** 4-hidroxinenal (4HNE) determinados por Western Blot y su cuantificación por densitometría. Se utilizó al canal aniónico dependiente de voltaje (VDAC) como control de carga. Los datos se presentan como la media ± SEM, n =3. **(C)** Actividades de las enzimas aconitasa y citrato sintasa, así como el cociente de ambas actividades (Aco/CitSin). V= vehículo FA= ácido fólico, NAC= N-acetilcisteína. Los datos se presentan como la media ± SEM, n=5-6. *p<0.05, **p<0.01, ***p<0.001 *vs.* V. $^{+}$p<0.05, $^{++}$p<0.01 *vs.* FA. ANOVA de una vía más prueba de Tukey.

7.1.4. La NAC inhibe el aumento de la producción de ROS en los segmentos tubulares en la AKI inducida por FA

El aumento en la producción mitocondrial de ROS se ha relacionado ampliamente con la sobre-activación de la Nox y la Nos en modelos de daño renal como la nefrectomía [159,162,163], desencadenando la sobreproducción de superóxido ($O_2^{\bullet -}$) y contribuyendo a la pérdida de la función renal [111,113,164,165]. Para evaluar si la producción de H_2O_2 mitocondrial inducida por el FA se relacionaba con la sobre activación de estas enzimas, se evaluó la producción de ROS ligadas al NADPH y a la L-arginina (sustratos de la Nox y la Nos respectivamente) en los segmentos de la nefrona más ricos en mitocondrias, es decir, el PT y el DT [8,166], así como en la corteza renal.

A las 24 h, en el grupo tratado con FA se observó un aumento en la producción de ROS ligada al NADPH y a la L-arginina en el PT, el DT y la corteza renal (Fig. 20), el cual fue especialmente marcado en la corteza renal. Además, se observó una disminución en la actividad de la catalasa en el grupo con FA (Fig. 21A) y un aumento en el marcador de estrés oxidante 4HNE (Fig. 21B). Por otro lado, en el grupo NAC+FA se observaron niveles menores de ROS ligadas al NADPH y a la L-arginina en ambos segmentos tubulares y en la corteza, con respecto al grupo FA (Fig. 20). Así mismo, la NAC evitó la disminución en la actividad de catalasa y el aumento en los niveles de 4HNE en la corteza (Fig. 21). En conjunto estos resultados confirman que la NAC previene la sobreproducción de ROS y el estrés oxidante inducidos por FA en los segmentos ricos en mitocondrias.

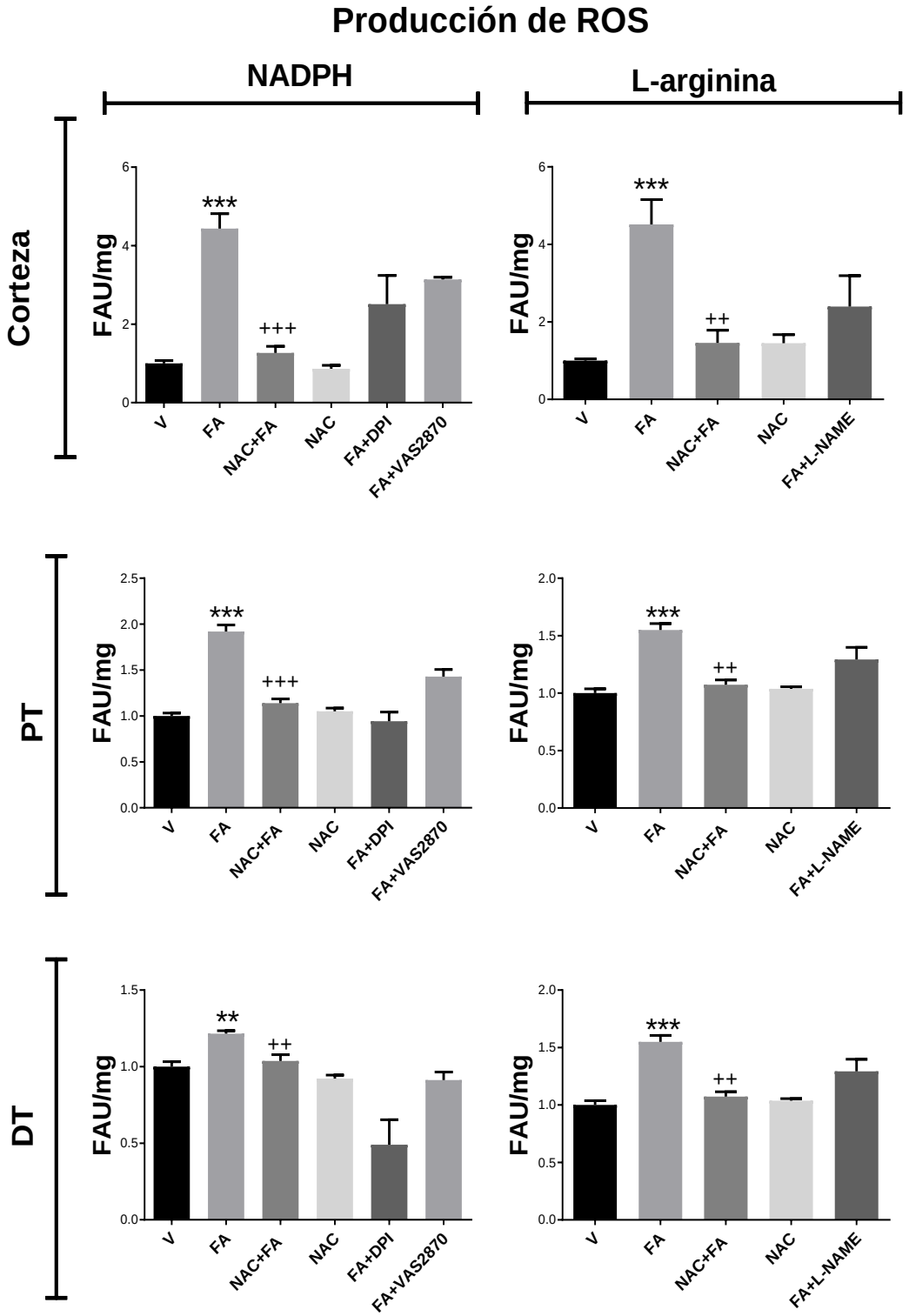

Figura 20. LA NAC previene el aumento en la producción de ROS ligadas al NADPH y a la L-arginina. La N-acetilcisteína (NAC) inhibe la producción el aumento en la producción de ROS inducido por FA en la corteza rena, el túbulo de proximal (PT) y el túbulo distal (DT). La producción de ROS se evaluó mediante la adición de los sustratos correspondientes (NADPH o L-arginina) y se usaron como inhibidores el difenil-iodonio (DPI), el éster metílico de L-NG-nitroarginina (L-NAME) y el VAS2870, inhibidor de Nox. V= vehículo FA= ácido fólico, NAC= N-acetilcisteína. Media ± SEM, n= 5-6. **p<0.01, ***p<0.001 *vs.* V. $^{++}$p<0.01, $^{+++}$p<0.001 *vs.* FA. ANOVA de una vía más prueba de Tukey.

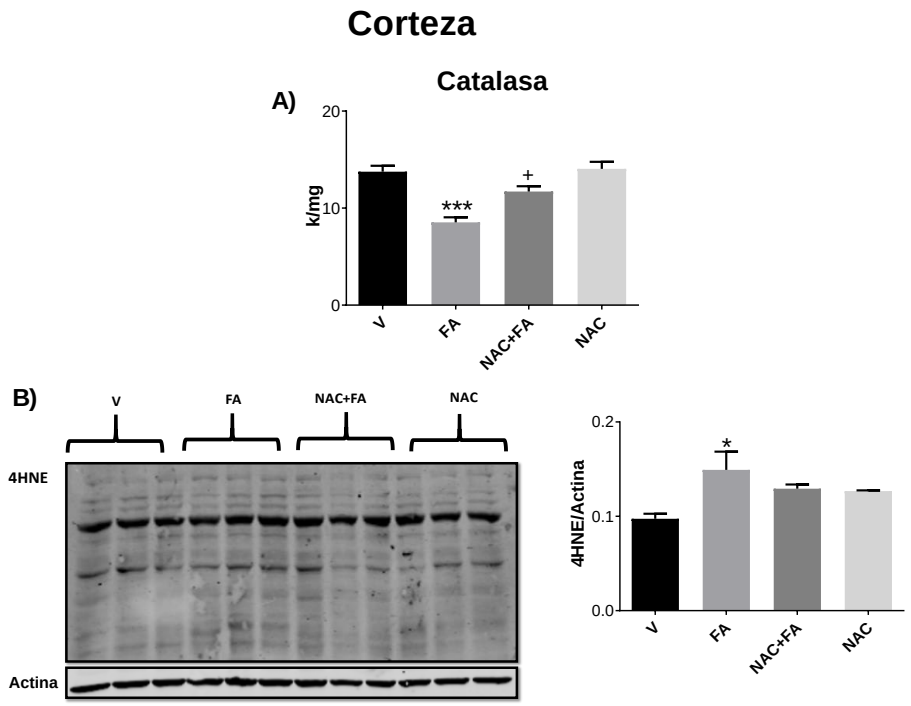

Figura 21. LA NAC previene el estrés oxidante en corteza renal. (A) Actividad de catalasa en la corteza renal, la actividad enzimática se expresó como k/mg de proteína (k = constante de primer orden). **(B)** Marcador de daño oxidante 4 hidroxinonenal (4HNE) en la corteza renal determinados por Western Blot y su cuantificación por densitometría. V= vehículo, FA= ácido fólico, NAC= N-acetilcisteína. Los datos se presentan como la media ± SEM, n= 5-6. *P<0.05, ***P<0.001 *vs.* V. ⁺P<0.05 *vs.* FA. ANOVA de una vía más prueba de Tukey.

7.1.5. La NAC previene la pérdida de la S-glutationilación en el proteoma mitocondrial en la AKI inducida por FA

Se señaló recientemente a la S-glutationilación como un mecanismo molecular capaz de ligar de manera directa los cambios en el metabolismo energético con la homeostasis redox y la dinámica mitocondrial [96,97,135]. Por lo tanto, para evaluar si la disfunción biogénica y el estrés oxidante mitocondrial observados se relacionan con variaciones en dicha modificación, los cambios en la cantidad total de proteínas mitocondriales S-glutationiladas se determinaron por WB. Para evitar la interferencia de la S-glutationilación no enzimática e inespecífica, un grupo específico de mitocondrias se aisló y homogeneizó con amortiguador de aislamiento mitocondrial adicionado con NEM 50 mM [96,167].

En el grupo tratado con FA se observaron niveles menores de proteínas mitocondriales S-glutationiladas (Fig. 22A). De manera concordante, se observó una disminución significativa en los niveles de GSH, en la relación GSH/GSSG y en el contenido total de glutatión (GSH + GSSG), así como un aumento en los niveles de GSSG (Fig. 22B) en la mitocondria. La medición de la actividad de las enzimas relacionadas con la S-glutationilación enzimática mitocondrial reveló una mayor actividad de remoción de la S-glutationilación por parte de la Grx y una menor actividad de la GST en las mitocondrias del grupo tratado con FA (Fig.

22C), explicando así la disminución observada en los niveles de la S-glutationilación (Fig. 22A).

Por el contrario, los grupos FA+NAC y NAC presentaron mayores niveles proteínas mitocondriales S-glutationiladas (Fig. 22A), con respecto al grupo tratado con FA. La administración previa de NAC también preservó los niveles mitocondriales de GSH, la relación GSH/GSSG, el contenido de glutatión total y evitó el aumento de los niveles de GSSG (Fig. 22B) en las mitocondrias renales. De igual manera, la NAC preservó parcialmente la disminución en la actividad de la GST y evitó el aumento de la actividad de remoción de S-glutatión por parte de la Grx (Fig. 22C).

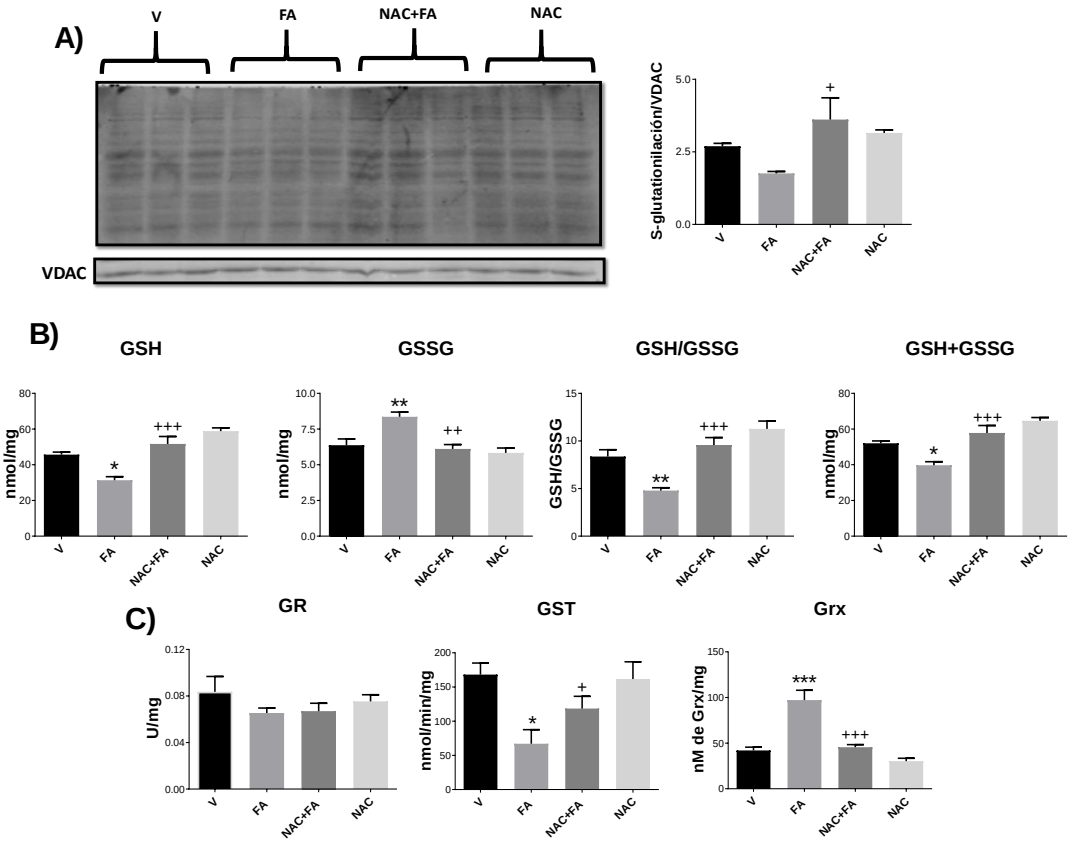

Figura 22. LA NAC previene la perdida de la S-glutationilación mitocondrial. (A) Niveles totales de S-glutatión de las proteínas mitocondriales medidas por Western Blot y su cuantificación por densitometría.Las bandas observadas corresponden a las distintas proteínas S-glutationiladas, se utilizó un anticuerpo contra residuos de glutatión modificados. Media ± SEM, n= 3. **(B)** Niveles mitocondriales de glutatión reducido (GSH), glutatión oxidado (GSSG), la relación GSH/GSSG y el glutatión total (GSH+GSSG). Media ± SEM, n= 5-6. **(C)** Actividad de las enzimas involucradas en el sistema enzimático de S-glutatión: glutatión reductasa (GR), glutatión S-transferasa (GST) y glutaredoxina (Grx). V= vehículo, FA= ácido fólico, NAC= N-acetilcisteína, VDAC= canal aniónico dependiente de voltaje. Los datos se presentan como la media ± SEM, n= 5-6. *p<0.05, **p<0.01, ***p<0.001 *vs.* V. $^{+}$p<0.05, $^{++}$p<0.01, $^{+++}$p<0.001 *vs.* FA. ANOVA de una vía más prueba de Tukey.

7.1.6. La NAC evita el desplazamiento de la dinámica mitocondrial hacia la fisión en la AKI inducida por FA

Como se discutió anteriormente, se ha sugerido que en diversos modelos experimentales de AKI, las alteraciones bioenergéticas y el estrés oxidante mitocondrial inducen el desequilibrio en los procesos que regulan la dinámica mitocondrial (fusión por fisión) y el recambio (biogénesis y mitofagia) [19,166,168]. Sin embargo, no se tenía conocimiento hasta el momento de los cambios en dichos procesos en el modelo de daño renal por FA. Para iniciar se realizó el análisis por microscopía electrónica de transmisión del PT. Dicho análisis reveló que en las células epiteliales del grupo tratado con FA se observan mitocondrias fragmentadas y de menor tamaño, con respecto al control, con las crestas mitocondriales poco definidas, además de una abundancia de cuerpos autofágicos (Fig. 23B). Por lo que se procedió a evaluar los niveles de los marcadores de dinámica mitocondrial por WB.

En el grupo tratado con FA se observó un aumento los niveles de Drp1 mediante inmunomicroscopía electrónica y se observó un mayor inmunomarcaje en la membrana externa mitocondrial en las células epiteliales del PT del grupo tratado con FA (Fig. 23E) en comparación con el grupo control (Fig. 23D), implicando un desplazamiento de la dinámica mitocondrial hacia el proceso de fisión. Para confirmar dichos resultados, los niveles de las proteínas de fisión Drp1 y Fis1 se evaluaron por WB en mitocondrias aisladas, donde se observó un aumento en las mismas (Fig. 24A) y una disminución en los niveles de las proteínas de fusión Opa1 y Mfn1 (Fig. 24B). En conjunto, estos datos confirman que el tratamiento con FA induce fisión mitocondrial en el PT.

Por otro lado, el pretratamiento con NAC previno la fragmentación de la mitocondria inducida por FA y preservó la ultraestructura de la mitocondria en el PT (Fig. 23C). La NAC evitó el aumento en niveles menores de Drp1 en la mitocondria observado por microscopia electrónica en comparación con el grupo tratado con FA (Fig. 23F). De manera concordante el tratamiento con NAC también previno el aumento en los niveles de proteínas Fis1 y Drp1 (Fig. 24A) en la mitocondria evaluado por WB, sugiriendo que la NAC previene, al menos parcialmente, el desbalance en la dinámica mitocondrial inducido por el FA.

Micrografías representativas de microscopía electrónica e inmunomicroscopía electrónica

Figura 23. Micrografías representativas de microscopía electrónica a las 24 h posteriores a la administración de FA. (A) Las células epiteliales del túbulo proximal contorneado del grupo control muestra mitocondrias y lisosomas (flechas) bien conservados en el citoplasma. **(B)** En contraste, el citoplasma de las células epiteliales del grupo con ácido fólico (FA) muestra mitocondrias fragmentadas, con borrado de crestas y abundantes autofagosomas (asteriscos). **(C)** En el grupo con N-acetilcisteína (NAC)+FA se observa un daño mitocondrial menor y pequeños lisosomas aislados. **(D)** Inmunomicroscopía electrónica de Drp1, se observa muestra un marcado (flechas) ocasional en las mitocondrias del túbulo contorneado proximal en el grupo control. **(E)** En comparación, se muestra un marcaje abundante de Drp1 en la membrana externa de las mitocondrias del grupo tratado con FA. **(F)** Se observa un marcaje menor de Drp1 en las mitocondrias del grupo NAC + FA.

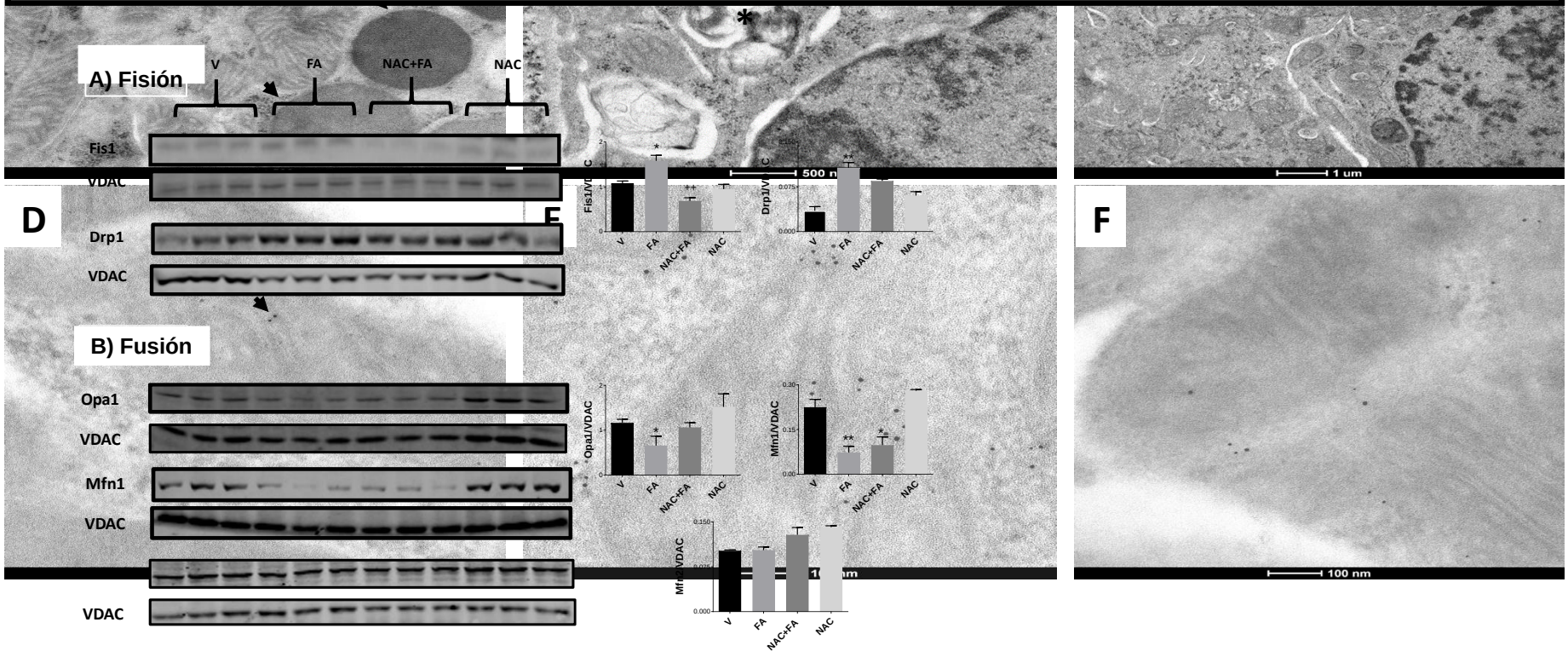

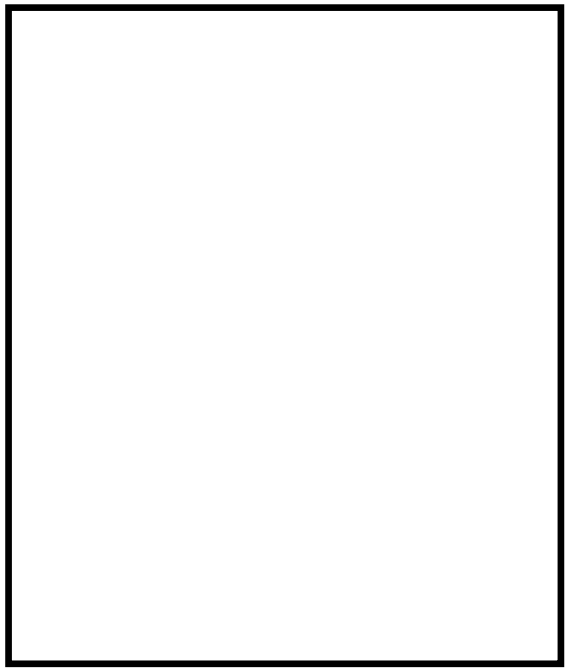

7.1.7. El FA induce en la AKI una disminución en la biogénesis mitocondrial y una mitofagia alterada

Como se discutió anteriormente, la fisión mitocondrial es un mecanismo implicado en la eliminación de las mitocondrias disfuncionales a través del proceso de autofagia selectiva conocido como mitofagia [120,124], la cual se ha sugerido en las alteraciones mitocondriales en los modelos AKI inducidos por isquemia/reperfusión [169] y cisplatino [170]. Para determinar si el desplazamiento observado hacia fisión mitocondrial (Fig. 23-24) se relaciona con alteraciones de la mitofagia, se evaluaron los niveles de la proteína de mitofagia Pink1 en las mitocondrias y de las proteínas autofágicas: LC3-I, LC3-II y p62 en los PT. El grupo tratado con FA mostró a las 24 h posteriores a su administración, un aumento significativo en los niveles mitocondriales de Pink1 y una disminución en los niveles de LC3-I y II, sin embargo, los niveles de p62 no sufrieron cambios con respecto al grupo control (Fig. 25).

Por otro lado, se ha reportado que la administración de FA causa una disminución en el mRNA de algunas proteínas mitocondriales en el riñón [142,143]. Por lo cual, se procedió a evaluar los niveles de las proteínas relacionadas con la biogénesis mitocondrial: coactivador 1-alfa del receptor gamma activado por proliferador de peroxisomas (PGC-1α), factor respiratorio nuclear 1 (NRF1) y 2 (NRF2) en PT, y el TFAM en mitocondrias aisladas. En el grupo FA se observó a las 24 h posteriores a su administración, una disminución en los niveles de todas las proteínas evaluadas con respecto al control (Fig. 26), confirmando que en la AKI inducida por FA, la biogénesis mitocondrial está reducida.

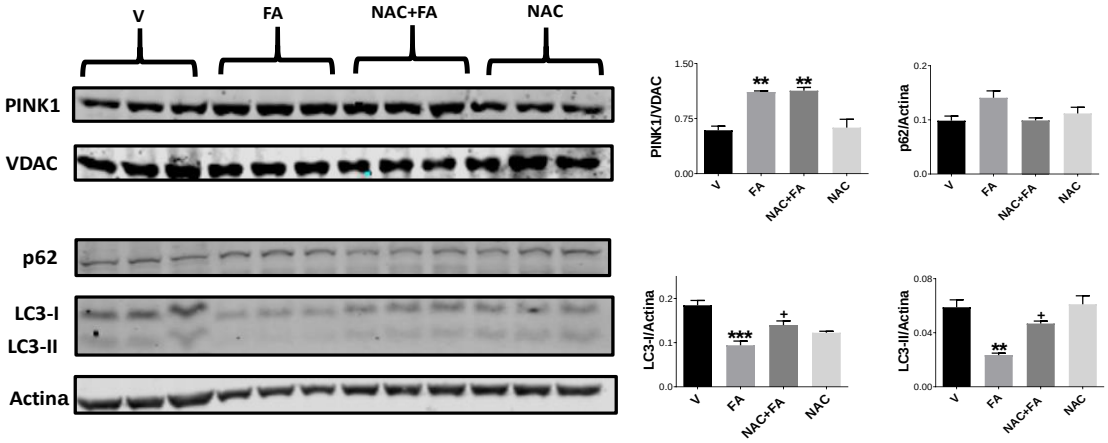

Figura 25. LA NAC previene las alteraciones en la mitofagia y autofagia 24 h después de la administración de FA. Niveles de la proteína de mitofagia cinasa putativa inducida por PTEN 1 (PINK1) en mitocondrias aisladas y de las proteínas autofágicas: proteína 1A/1B de cadena ligera asociadas a microtúbulos 3 I/II (LC3-I / II) y p62 en el túbulo proximal. Las proteínas actina y el canal aniónico dependiente del voltaje (VDAC) se utilizaron como controles de carga, respectivamente. V= vehículo, FA= ácido fólico, NAC= N-acetilcisteína. Los datos se presentan como la media ± SEM, n= 3. **p<0.01, ***P<0.001 *vs.* V. ⁺p<0.05 *vs.* FA. ANOVA de una vía más prueba de Tukey.

Por su parte, la administración de NAC evitó parcialmente la disminución de los niveles LC3-I y II (Fig. 25). Aunque se observaron menos autofagosomas por microscopia electrónica (Fig. 23C), no tuvo un efecto significativo en los niveles de Pink1 y p62 (Fig. 25) y en las proteínas relacionadas a la biogénesis mitocondrial (con la excepción de PGC-1α, Fig. 26), a las 24 h posteriores a la administración del FA. Dichos resultados sugieren que el efecto protector de la NAC no estaría directamente vinculados a estos dos mecanismos, al menos en este tiempo.

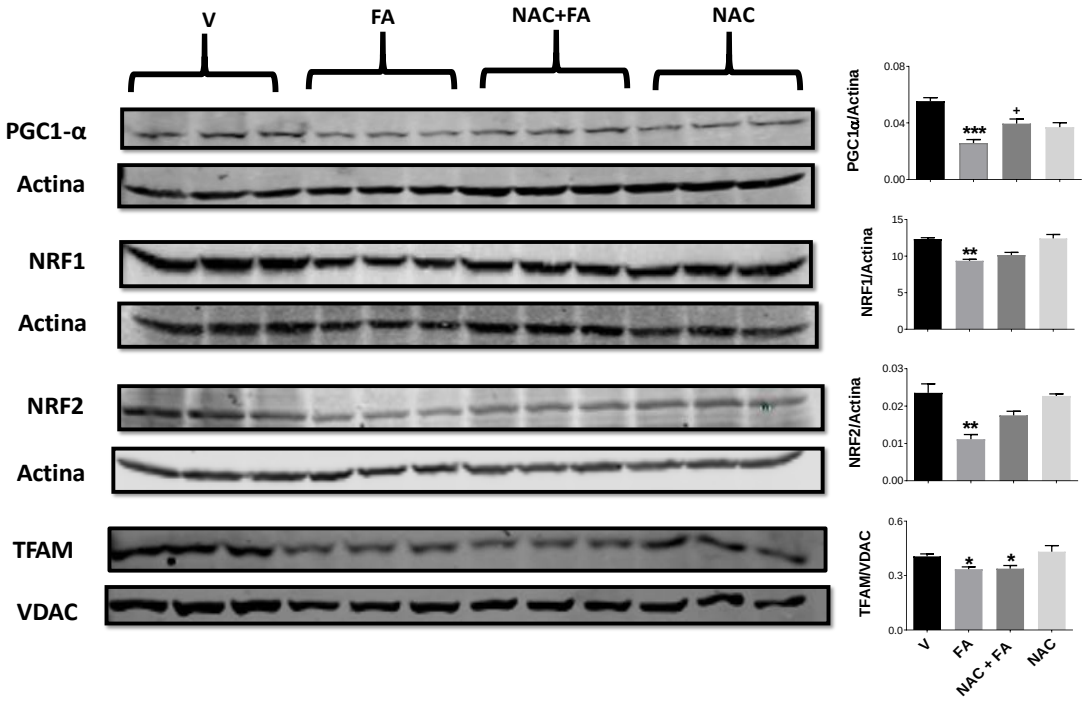

Figura 26. El FA induce la disminución en la biogénesis mitocondrial 24 h después de la administración de FA. Niveles de las proteínas de biogénesis mitocondrial en homogeneizados de túbulos proximales: coactivador 1-alfa del receptor gamma activado por proliferador de peroxisomas (PGC-1α), factor respiratorio nuclear 1 (NRF1) y 2 (NRF2). Niveles del factor de transcripción mitocondrial A (TFAM), en mitocondrias aisladas. La proteína actina y el canal aniónico dependiente del voltaje (VDAC) se utilizaron como controles de carga, respectivamente. V= vehículo, FA= ácido fólico, NAC= N-acetilcisteína. Los datos se presentan como la media ± SEM, n= 3. *p<0.05, **p<0.01, ***P<0.001 *vs.* V. $^{+}$p<0.05 *vs.* FA. ANOVA de una vía más prueba de Tukey.

7.1.8. Anexos primera parte.

7.1.8.1. Respiración ligada al complejo II a las 24 h posteriores a la administración de FA

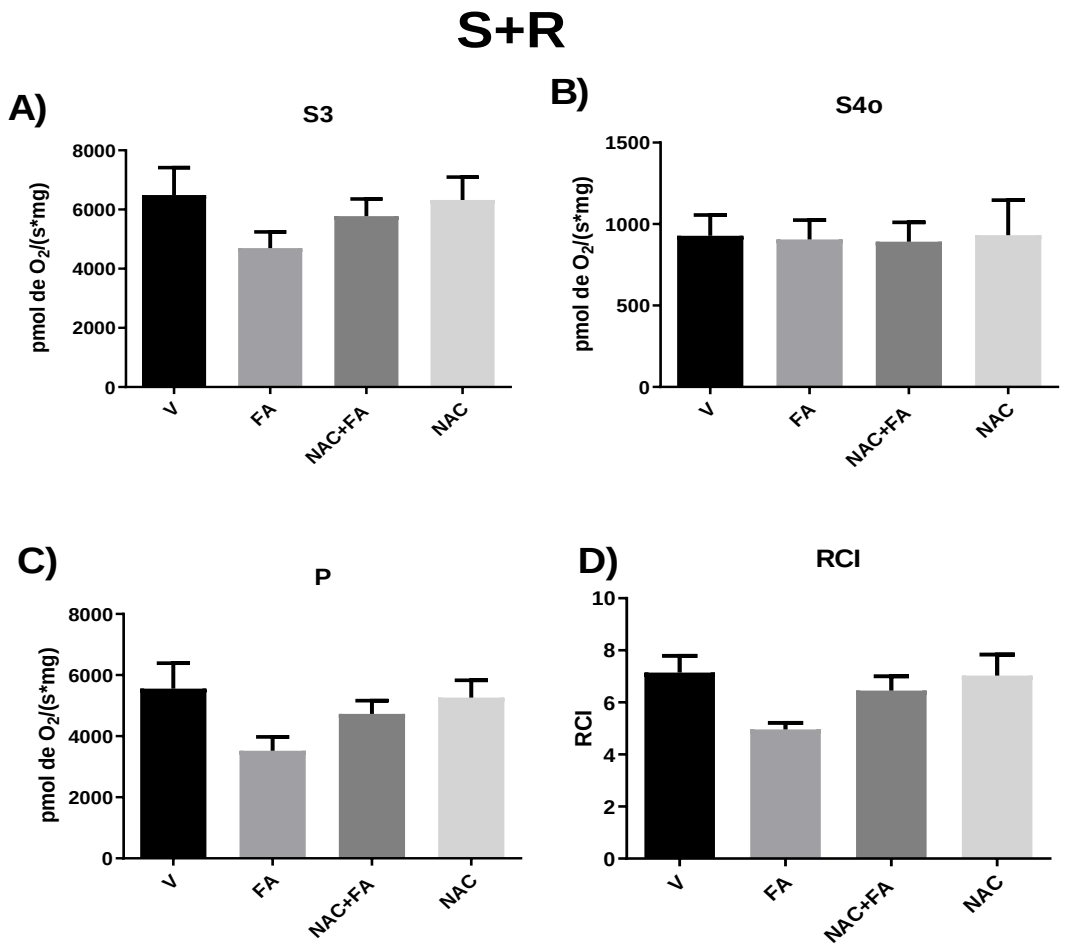

Anexo 1. Parámetros respiratorios de la respiración ligada al CII: **(A)** estado 3 (S3), **(B)** estado 4 inducido por oligomicina (S4o), índice de **(C)** respiración asociada a la OXPHOS (P) e **(D)** índice de control respiratorio (RCI). V= vehículo FA= ácido fólico, NAC= N-acetilcisteína. CII= complejo II, Mit= mitocondrias, S= succinato, S+R= succinato+rotenona. Media ± SEM, n= 5-6. ANOVA de una vía prueba de Tukey. No se observaron cambios significativos entre los diferentes grupos.

7.1.8.2. Actividad de los complejos mitocondriales a las 24 h posteriores a la administración de FA

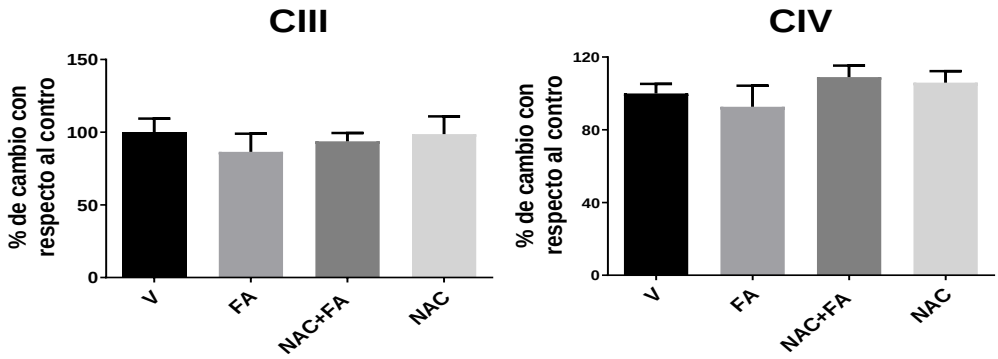

Anexo 2. Actividad del complejo III (CII) y del complejo IV (CIV) 24 h posteriores a la administración de FA. V= vehículo FA= ácido fólico, NAC= N-acetilcisteína. Media ± SEM, n= 5-6. ANOVA de una vía prueba de Tukey. No se observaron cambios significativos entre los diferentes grupos.

7.1.8.3. Parámetros en células LLC-PK1

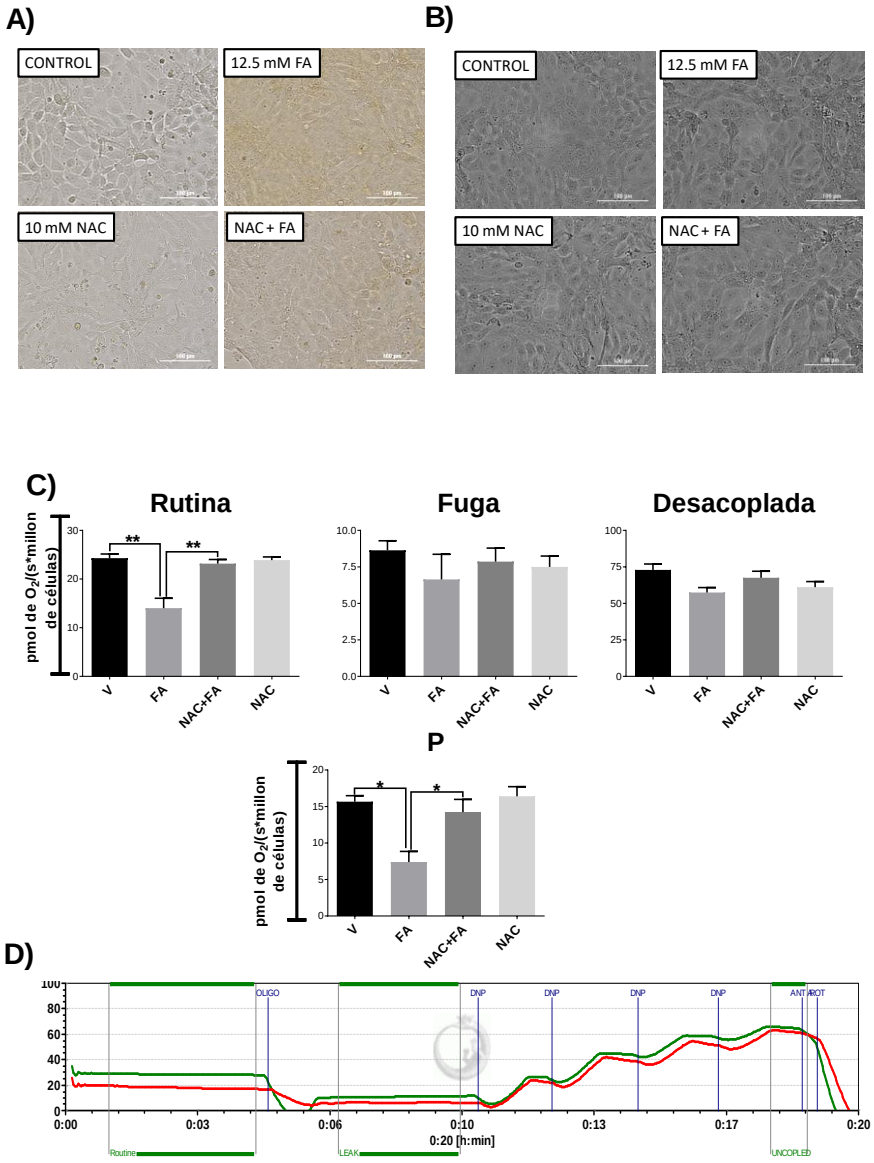

Anexo 3. (A) Imágenes representativas en color de la microscopía de campo claro de los diferentes grupos, se observa una gran cantidad de precipitados cristalinos en el grupo tratado con FA. **(B)** Imágenes representativas en escala de grises de la microscopía de campo claro de los diferentes grupos, se observan alteraciones morfológicas modestas en las células del grupo FA. **(C)** Parámetros respiratorios en células epiteliales del túbulo proximal intactas LLC-PK1: Respiración de rutina (*Rutine)*. Consumo de oxígeno en presencia únicamente de las células en su medio. Respiración de fuga (*Leak)*. Correspondiente al consumo celular de oxígeno en presencia de oligomicina 5 µM. Respiración desacoplada (*Uncoupling*). La respiración desacoplada se logró mediante titulaciones de 8 µL de dinitrofenol (DNP) 20 µM. *P*. Respiración atribuible a la OXPHOS: *Rutin- Leak*. **(D)** Trazo representativo de los experimentos de respirometría. La línea verde corresponde a las células de control y la línea roja representa las células tratadas con FA. La figura es representativa de tres experimentos diferentes. Los datos representan la media ± SEM, n= 3. *p<0.05 y **p <0.01. V= vehículo FA= ácido fólico, NAC= N-acetilcisteína.

7.2. La transición AKI-CKD inducida por el FA

Si bien se han reportado alteraciones en la bioenergética mitocondrial en el corazón [171] y el músculo esquelético [172–174] en estadios crónicos, en otros modelos de daño renal progresivo como la nefrectomía, nuestro conocimiento sobre el avance de las alteraciones mitocondriales en el riñón y su papel en la transición AKI-CKD aún es muy limitado. Sin embargo, se ha postulado que el desajuste en la bioenergética [175] y el desbalance redox mitocondrial [95,115] contribuye a dicha progresión. Por tal motivo y dada la naturaleza progresiva del daño renal inducido por la administración de altas dosis de FA [137,140,142], para la segunda fase del proyecto se planteó la realización de estudios temporales bioenergética y estado redox mitocondrial para determinar su relación con la transición AKI-CKD.

7.2.1. El efecto de la NAC en la transición AKI-CKD inducida por el FA

Para caracterizar la progresión del daño renal inducido por el FA, se evaluaron los niveles de los marcadores clásicos de daño renal BUN y creatinina en plasma. Después de dos días de su administración, el FA indujo el aumento en los niveles plasmáticos de BUN y creatinina, así como en la relación de peso de riñón/peso total, en comparación con el grupo control (Fig. 27A-C). Aunado a esto, el análisis histológico por H&E reveló en el grupo FA, a los 2 días posteriores a su administración, una gran cantidad de células hinchadas que se alternan con células necróticas, así como PT con cilindros hialinos en su luz (Fig. 27D). Dichas alteraciones son prevenidas al día 2 (Fig. 27A-D). Estos resultados son consistentes con lo observado a las 24 h (Fig. 12-13). De manera interesante, el BUN y la creatinina muestran una tendencia a disminuir después de los 4 días (Fig. 27A-B). En conjunto dichos resultados indican que el pico del daño agudo se encuentra entre los días 1-2 posteriores a la administración de FA. Esto es concordante con estudios previos en ratones, en los que los niveles de BUN y creatinina volvieron a los niveles de control después de 4 días de administración de FA [140,142].

Si bien el FA induce la AKI en los primeros días posteriores a su administración, se ha reportado que también induce un aumento en los marcadores de inflamación y fibrosis entre los 6 a 14 días después su administración [140,142], sugiriendo la progresión del daño renal. Por lo que para determinar la transición hacia la CKD procedimos a evaluar la GFR y los parámetros hemodinámicos 28 días después de la administración de FA, observando una disminución en la GFR y un aumento en la RVR, lo que desencadenó la disminución del RBF y del RPF (Fig. 28A). A nivel estructural, a los 28 días posteriores a la administración del FA, se observó la acumulación leve de tejido fibrótico en el parénquima renal (Fig. 28B), confirmando así la transición AKI-CKD en este modelo.

Por su parte, el pretratamiento con NAC al evitar el desarrollo de la AKI (Fig. 12-13, 27), previene la disminución de la GFR y RBF, el aumento de RVR (Fig. 28A) y evitó la acumulación de tejido fibrótico en el parénquima renal (Fig. 28B). Dichos datos en conjunto sugieren que la NAC previene la transición de AKI-CKD inducida por FA.

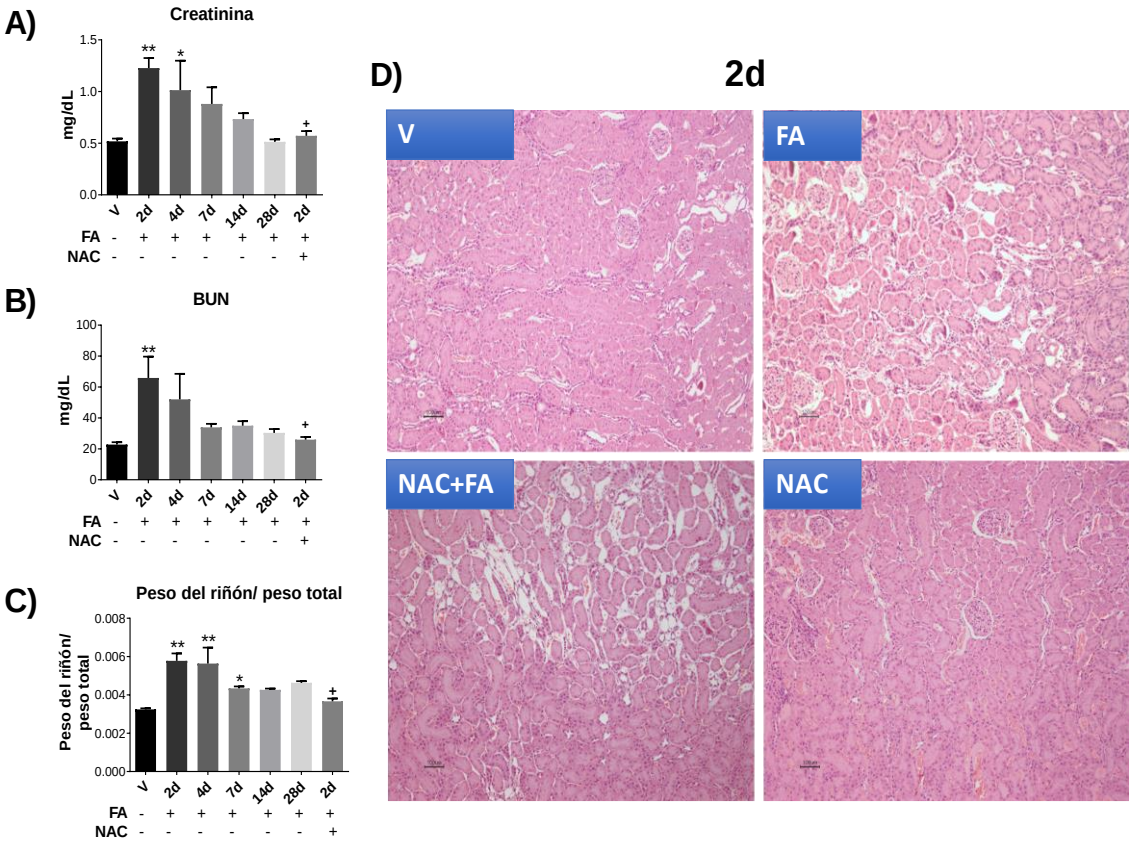

Figura 27. La NAC previene AKI inducida por el FA y su avance hacia la CKD. Curso temporal de los marcadores clásicos de daño renal **(A)** creatinina y **(B)** nitrógeno de urea en sangre (BUN) en plasma, así como **(C)** la relación peso de riñón/peso total. Medias ± SEM, n= 5-6. *p <0.05 y ** p<0.01. ANOVA de una vía más Dunnet *vs.* V; $^{+}$p<0.05 T de Student *vs.* FA 2d. **(D)** Micrografías representativas de riñón de los 4 grupos experimentales a los 2d. Todas las micrografías se tomaron a un aumento de 200x, las barras negras corresponden a una distancia de 100 µm, tinción con hematoxilina/eosina. V= vehículo, FA= ácido fólico, NAC= N-acetilcisteína, d= días después de la administración de FA.

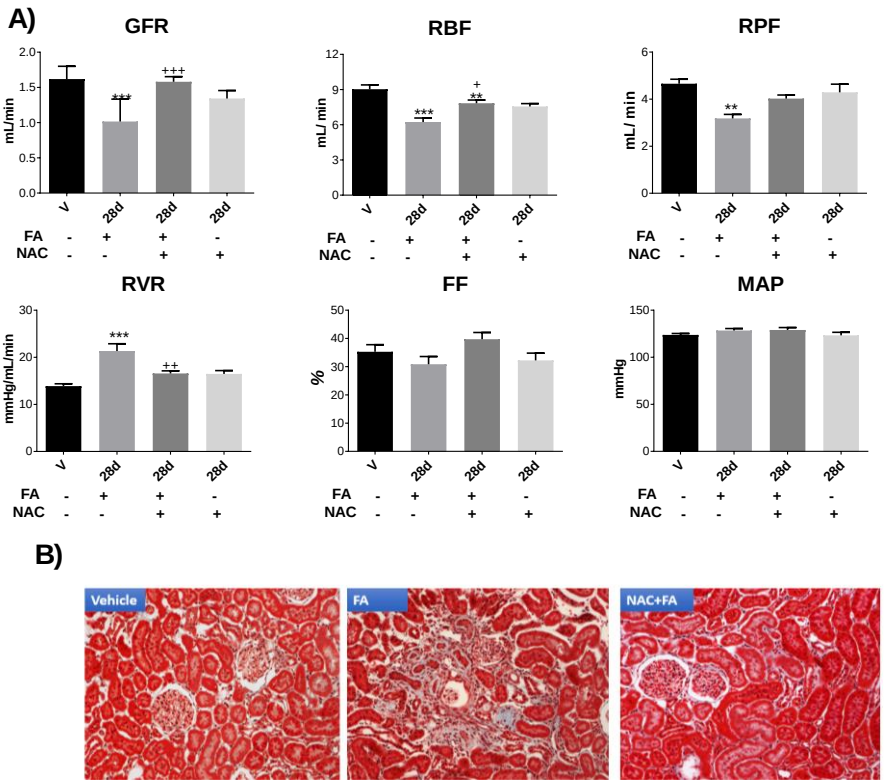

Figura 28. La NAC previene el daño renal crónico a los 28 d después de la administración de FA. (A) Parámetros hemodinámicos: tasa de filtración glomerular (GFR), flujo sanguíneo renal (RBF), flujo plasmático renal (RPF), resistencia vascular renal (RVR), fracción de filtración (FF) y presión arterial media (MAP). Media ± SEM, n= 4-5. **p<0.01 y ***p<0.001 vs. V; $^{+}$p<0,05 y $^{++}$p<0,01 vs FA 28d; ANOVA de una vía más prueba de Tukey. **(B)** Micrografías renales representativas de la tinción tricrómica de Masson de los cuatro grupos experimentales 28 días después de la administración de FA. V= Vehículo, FA= Ácido fólico, NAC= N-acetilcisteína, d= días después de la administración de FA.

7.2.2. El FA induce la persistencia de la disfunción en la bioenergética mitocondrial durante la transición AKI-CKD

Para determinar si la transición de AKI-CKD se relaciona con la persistencia de la disfunción mitocondrial, evaluamos los parámetros respiratorios en la respiración ligada a CI en mitocondrias renales. El FA indujo la disminución de los parámetros S3 y P en la etapa aguda, los cuales volvieron a valores similares a los del control después de 7 y 14 días, respectivamente (Fig. 29A, C). Estos datos indican que la reducción de la capacidad de la OXPHOS en la respiración relacionada con CI persistió hasta el día 7. Curiosamente, FA indujo un aumento gradual de la respiración S4o (Fig. 29B), lo cual explica el desacoplamiento mitocondrial observado en todos los tiempos estudiados (Fig. 29D). Aunado a esto el FA indujo la disminución en el ΔΨm en el S3 durante todo en el intervalo de tiempo evaluado (Fig. 29E). Dicho resultado concuerda con la reducción en la capacidad de la OXPHOS (Fig. 29) y con la pérdida de las crestas mitocndriales observada a 28 días (Anexo 5). Sin embargo, no se encontraron cambios en el ΔΨm en S4o entre los diferentes tiempos (Fig. 29F).

Por su parte, el pretratamiento con NAC mantuvo la protección mitocondrial 2 días después de la administración de FA, evitando la disminución de la respiración en el S3 y en P, la caída en el ΔΨm en S3 y el desacoplamiento mitocondrial (Fig. 29). De igual manera la NAC también preservó parcialmente los parámetros respiratorios y el ΔΨm 28 días después de la administración de FA (Fig. 29), así como la ultraestructura mitocondrial (Anexo 5). Dichos resultados sugieren que la NAC preserva la capacidad de la OXPHOS en la transición AKI-CKD inducida por el FA.

Dado que las alteraciones respiratorias observadas sugerían que la reducción en la actividad de los complejos del ETS persistía hasta el día 28. Evaluamos por separado la actividad de CI y de los otros elementos ETS involucrados en la respiración ligada al CI. A los 2 días posteriores a su administración, el FA induce la persistencia en la disminución de la actividad del CI (Fig. 30A). La cual, si bien tendió a recuperarse con el tiempo, no regresó a los niveles del control (Fig. 30A). De manera concordante, la NAC previno al día 2 la disminución en la actividad del CI (Fig. 30A), lo que es consistente con nuestros resultados previamente reportados en el día 1 [13]. De manera interesante, el FA indujo la reducción a partir del día 2 hasta el día 28 en la actividad de CIII, la cual también fue revertida por la administración previa de NAC (Fig. 30B). Finalmente, no se observaron cambios entre los diferentes grupos en la actividad del CIV (Fig. 30C). Dichos resultados sugieren que en tiempos posteriores al día 1, la disfunción mitocondrial se debe también a la disminución en la actividad del CIII.

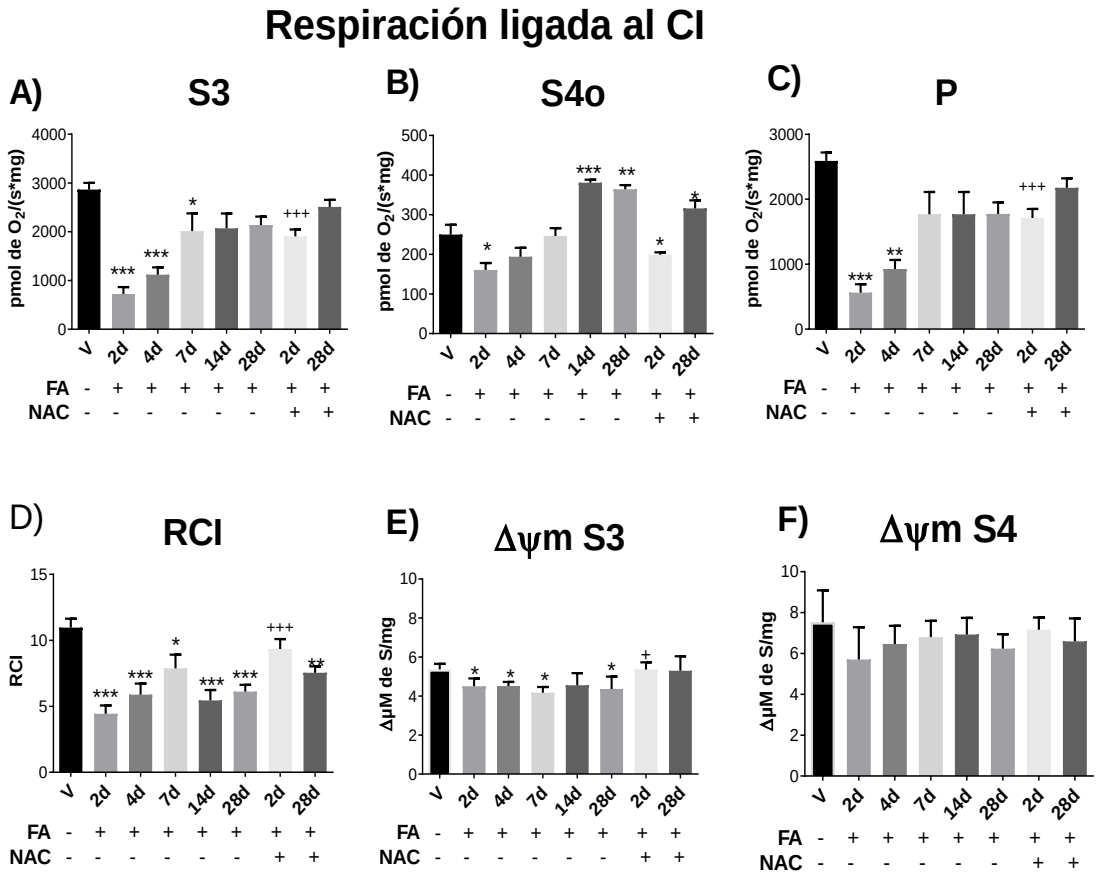

Figura 29. La NAC preserva los parámetros respiratorios y el potencial de membrana mitocondrial (ΔΨm) en la transición AKI-CKD inducida por FA. Evaluación temporal de los parámetros respiratorios mitocondriales en la respiración ligada al complejo I(CI): **(A)** estado 3 (S3), **(B)** estado 4 inducido por oligomicina (S4o), **(C)** respiración asociada a la OXPHOS (P) y **(D)** índice de control respiratorio (RC). Evaluación temporal de los cambios en Δψm en los estados respiratorios **(E)** S3 y **(F)** S4o. V= vehículo, FA= ácido fólico, NAC= N-acetilcisteína, d= días después de la administración de FA. Medias ± SEM, n= 6-7. *p<0.05, **p<0.01, ***p<0.001. ANOVA más Dunnet vs V; ⁺p<0.05 y ⁺⁺⁺p<0.001 t de Student vs FA 2d.

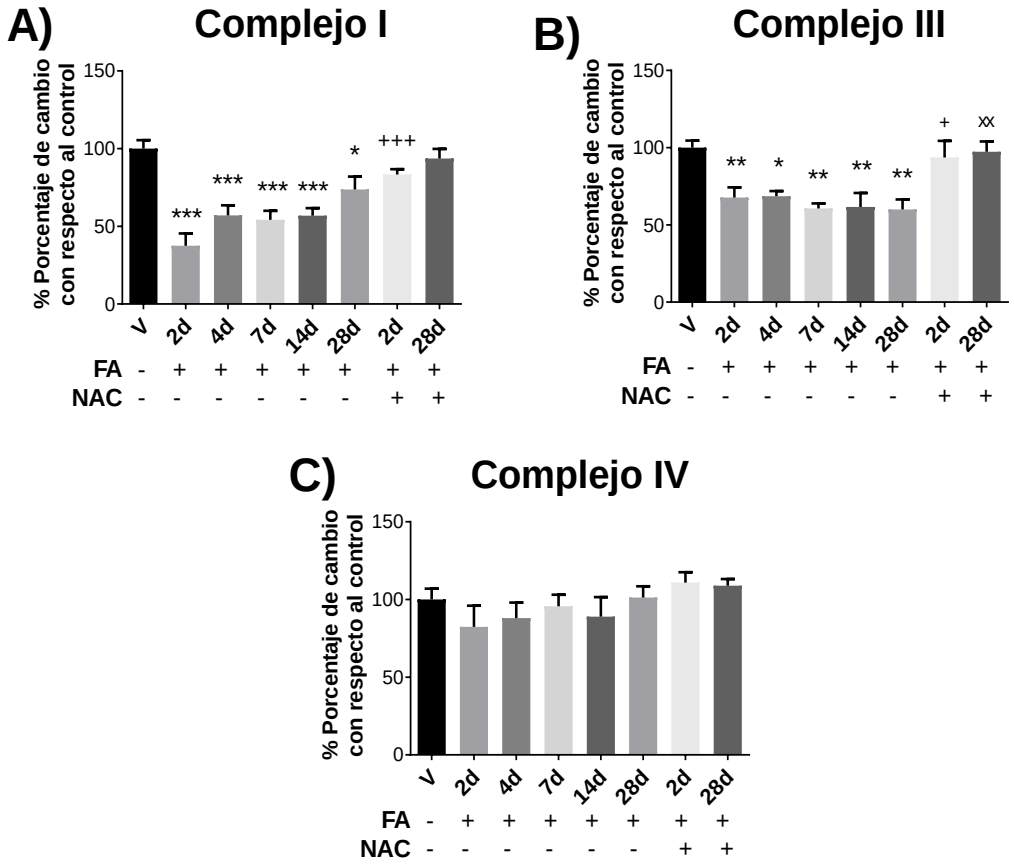

Figura 30. La NAC preserva la actividad de los complejos mitocondriales en la transición AKI-CKD inducida por FA. Evaluación temporal de la actividad de los complejos mitocondriales implicados en la respiración ligada a CI: **(A)** complejo I, **(B)** complejo III y **(C)** complejo IV. V= vehículo, FA= ácido fólico, NAC= N-acetilcisteína, d= días después de la administración de FA. Medias ± SEM, n= 5-6. *p<0.05, **p<0.01, ***p<0.001. ANOVA más Dunnet *vs.* V; ⁺p<0.05 y ⁺⁺⁺p<0.001 T de Student *vs.* FA 2d. ˣˣp<0.01 T de Student *vs.* FA 28d.

7.2.3. El FA induce una disfunción persistente en la β-oxidación durante la transición de AKI a CKD

Como se mencionó anteriormente, aunque en el riñón la producción de ATP es sostenida por la oxidación de diversos sustratos, el aporte mayoritario está dado por la β-oxidación de los ácidos grasos [8,176]. Aunado a esto, se ha reportado que los mRNA de las proteínas de β-oxidación se encuentran desregulados en modelos animales [74,177,178] y en pacientes con CKD [178,179], por lo que se

procedió a evaluar si la disfunción mitocondrial observada también estaba relacionada a la disfunción de β-oxidación.

La administración de FA redujo en todos los tiempos los parámetros S3 (Fig. 31A) y P (Fig. 31C). De igual manera el FA redujo la RCI desde el día 2, el cual se mantuvo hasta el día 28 (Fig. 31D). Sin embargo, el FA no tuvo ningún efecto significativo en la respiración S4o en los tiempos evaluados (Fig. 31B). Estos resultados sugieren que la administración de FA afectó la β-oxidación en la transición AKI a CKD principalmente vía la disminución en la producción de ATP y el desacoplamiento mitocondrial.

Por otro lado, la NAC previno la disminución en S3 y en P inducida por FA, a 2 días después de la administración de este último (Fig. 31A, C). Además, estos efectos protectores también estuvieron presentes a los 28 días, cuando también se previno el desacoplamiento mitocondrial (Fig. 31D).

Figura 31. La NAC previene la disfunción en la β-oxidación mitocondrial en la transición AKI-CKD inducida por FA. Evaluación temporal de los parámetros respiratorios asociados a la β-oxidación mitocondrial: **(A)** estado 3 (S), **(B)** estado 4 inducido por oligomicina (S4o), **(C)** respiración asociada a la OXPHOS (P) y **(D)** índice de control respiratorio (RCI). Se utilizaron L-carnitina 2 mM, palmitoil-L-carnitina 2 µM más malato 2 mM como sustratos para la β-oxidación. V= vehículo, FA= ácido fólico, NAC= N-acetilcisteína, d= días después de la administración de FA. Medias ± SEM, n= 5-6. *p<0.05, **p<0.01, *** p<0.001 ANOVA más Dunnet *vs.* V; $^{+}$p<0.05 y $^{++}$p<0.01 T de Student *vs.* FA 2d. ^{xx}p<0.01 T de Student *vs.* FA 28d.

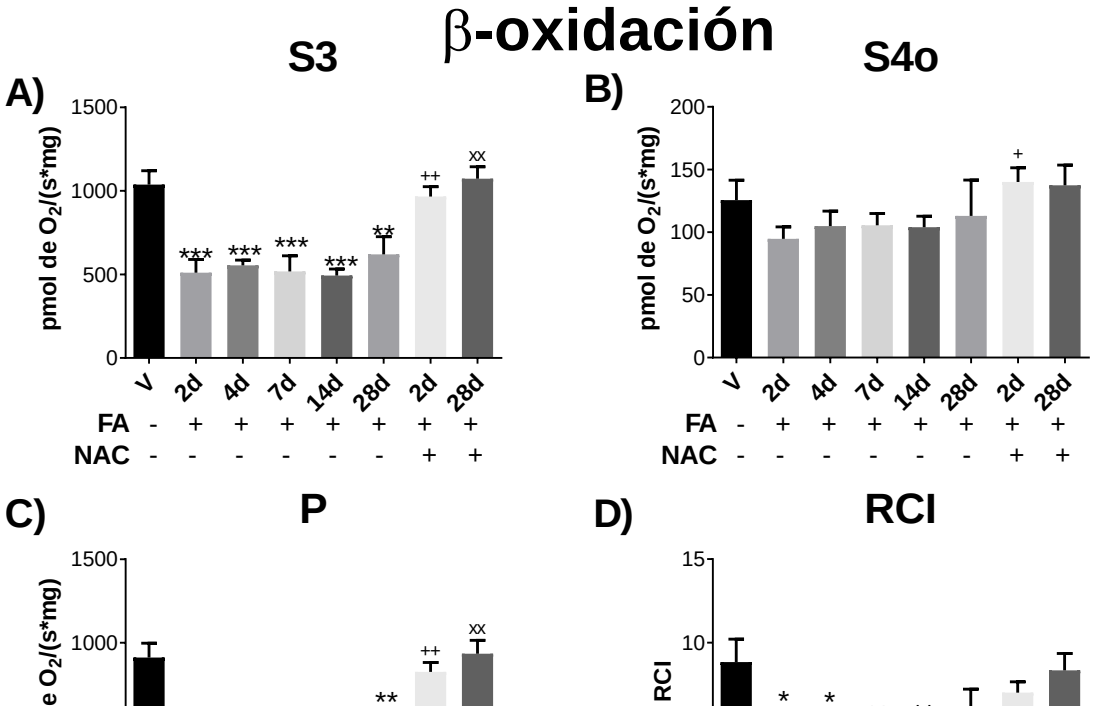

7.2.4. El FA induce un estado pro-oxidante permanente en las mitocondrias durante la transición de AKI-CKD

Para evaluar si la persistencia en el desacoplamiento mitocondrial y el aumento de S4o (Fig. 29) están vinculados a la persistencia del estrés oxidante en las mitocondrias, determinamos la actividad de aconitasa como marcador de estrés oxidante, así como la actividad de las enzimas GR y GPx en mitocondrias aisladas. Dos días después de la administración de FA, la actividad de la aconitasa se mantuvo disminuida y permaneció por debajo del control incluso 28 días después (Fig. 32A). Asimismo, las mitocondrias del grupo FA mostraron una reducción en todo el intervalo de tiempo evaluado en las actividades de la GPx (Fig. 32B) y la GR (Fig. 32C). Estos datos concuerdan con la elevación de la producción de H_2O_2 mitocondrial a los 28 días posteriores a la administración de FA (Fig. 32D) y con los niveles aumentados del marcador de estrés oxidante 4-HNE en mitocondrias (Fig. 32E). Lo que en conjunto confirma la persistencia de un estado pro-oxidante en las mitocondrias durante la progresión del daño renal.

Por otro lado, la NAC evitó, desde el día 2, la disminución en la actividad de la aconitasa (Fig. 32A) y de las enzimas antioxidantes (Fig. 32B, C), protección que se mantuvo hasta el día 28 posterior a la administración de FA. De igual manera previno el aumento en la producción de H_2O_2 mitocondrial (Fig. 32D) y en los niveles de 4-HNE en la mitocondria (Fig. 32E). Estos resultados confirman que la NAC previene el estrés oxidante mitocondrial inducido por FA en la transición AKI-CKD.

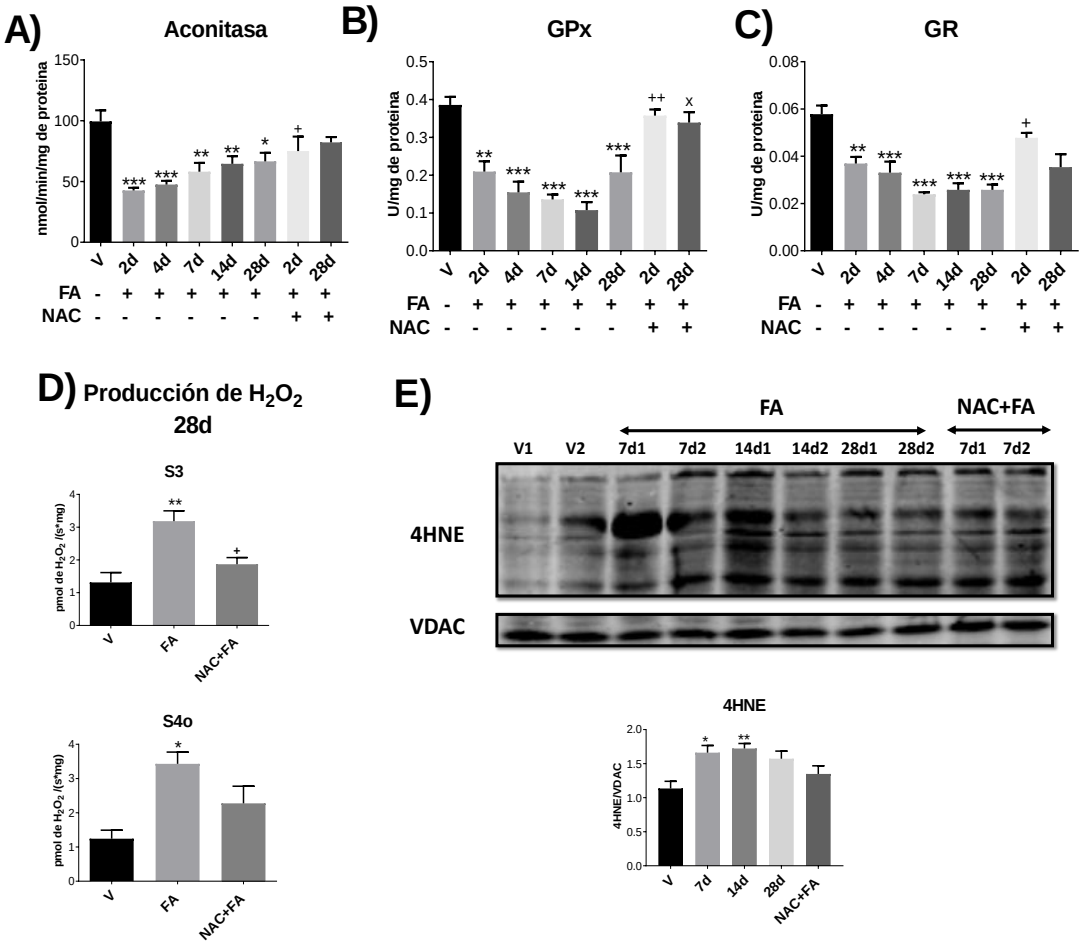

Figura 32. La NAC previene la persistencia del estrés oxidante mitocondrial en la transición AKI-CKD. Evaluación temporal de la actividad enzimática de la **(A)** aconitasa, **(B)** glutatión peroxidasa (GPx) y **(C)** glutatión reductasa (GR) en mitocondrias aisladas. V= vehículo, FA= ácido fólico, NAC= N-acetilcisteína, d= días después de la administración de FA. Los datos son medias ± SEM, n= 5-6. *p<0.05, **p<0.01, ***p<0.001 ANOVA más Dunnet *vs.* V; $^{+}$p<0.05 y $^{++}$p<0.01 T de Student *vs.* FA 2d. ^{xx}p<0.01 T de Student *vs.* FA 28d. **(D)** Evaluación de la producción de peróxido de hidrógeno (H_2O_2) mitocondrial en mitocondrias aisladas, 28 días después de la administración de FA en el estado respiratorio 3 (S3) y el estado 4 inducido por oligomicina (S4o). Media ± SEM, n= 5-6. *p<0.05 y **p <0.01 *vs.* V; $^{+}$p<0,05 *vs.* FA 28d; ANOVA más Tukey. **(E)** Marcador de estrés oxidante 4-hydroxynonenal (4-HNE) en mitocondrias aisladas por Western Blot y su cuantificación por densitometría. VDAC= canal de aniónico dependiente del voltaje. Media ± SEM, n= 4. *p<0.05, **p<0.01 ANOVA más Dunnet *vs.* V.

7.2.5. Anexo segunda parte. Transicion de AKI-CKD

7.2.5.1 Curso temporal de los cambios en la masa y biogénesis mitocondrial

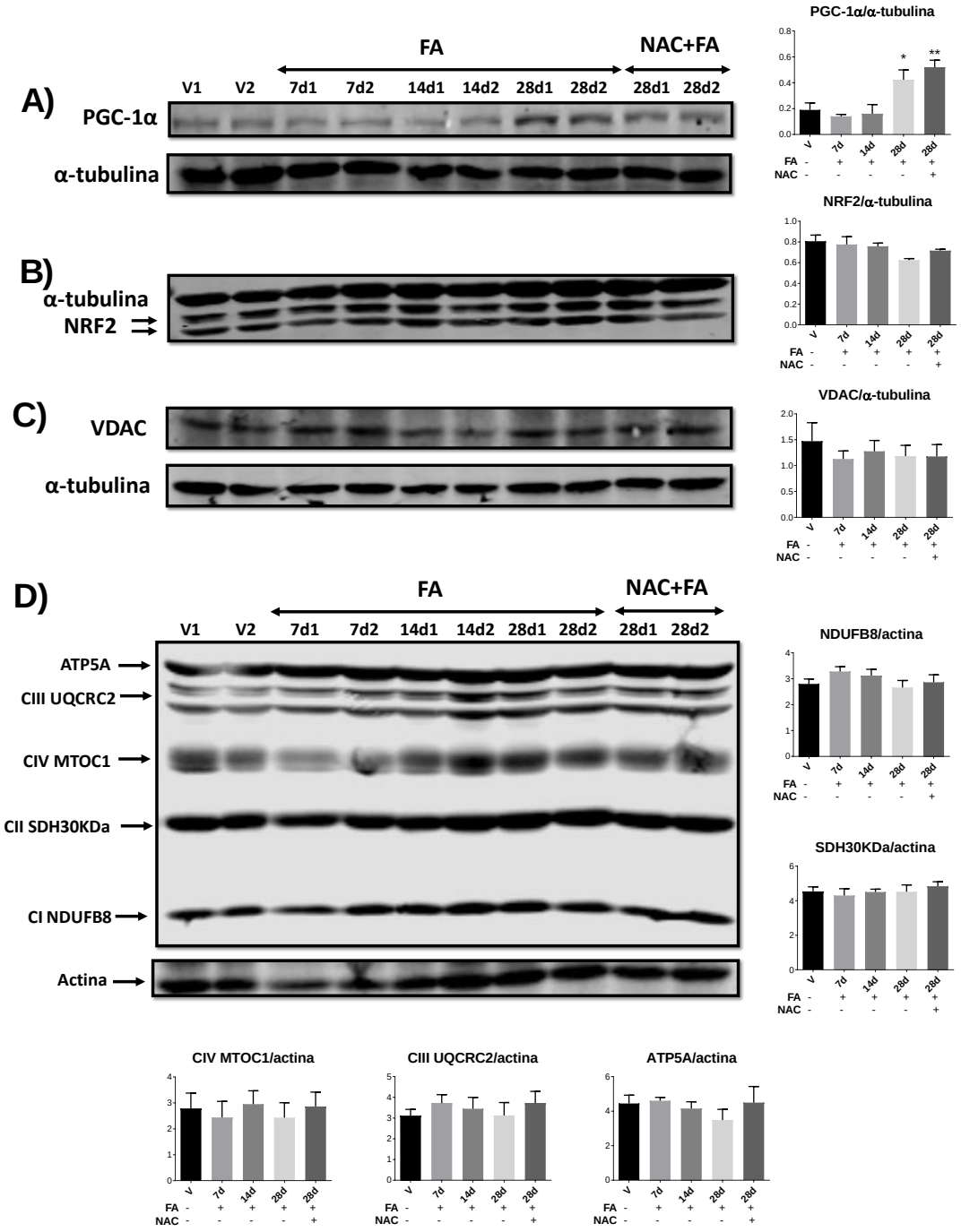

Anexo 4. Masa mitocondrial y biogénesis. Evaluación temporal por Western Blot y su densitometría de los marcadores de biogénesis mitocondrial: **(A)** coactivador 1-alfa del receptor gamma activado por proliferador de peroxisomas (PGC-1α), **(B)** factor respiratorio nuclear 2 (NRF2), así como del **(C)** canal aniónico dependiente de voltaje (VDAC) y **(D)** una subunidad de cada uno de los complejos mitocondriales. Los datos se expresan como la media ± SEM, n= 4. *p<0.05, **p<0.01 ANOVA más Dunnet *vs.* V. V= vehículo, FA= ácido fólico,

NAC= N-acetilcisteína, d= días después de la administración de FA. Subunidad del complejo I: CI-NDUFB8; subunidad del complejo II: CII-SDHB30KDa; subunidad del complejo III: CIII-UQCRC2, subunidad del complejo IV: CIV-MTCO1; subunidad alfa de la ATP sintasa (ATP5A).

7.2.5.2. Microscopia electrónica 28 días posteriores a la administración de FA

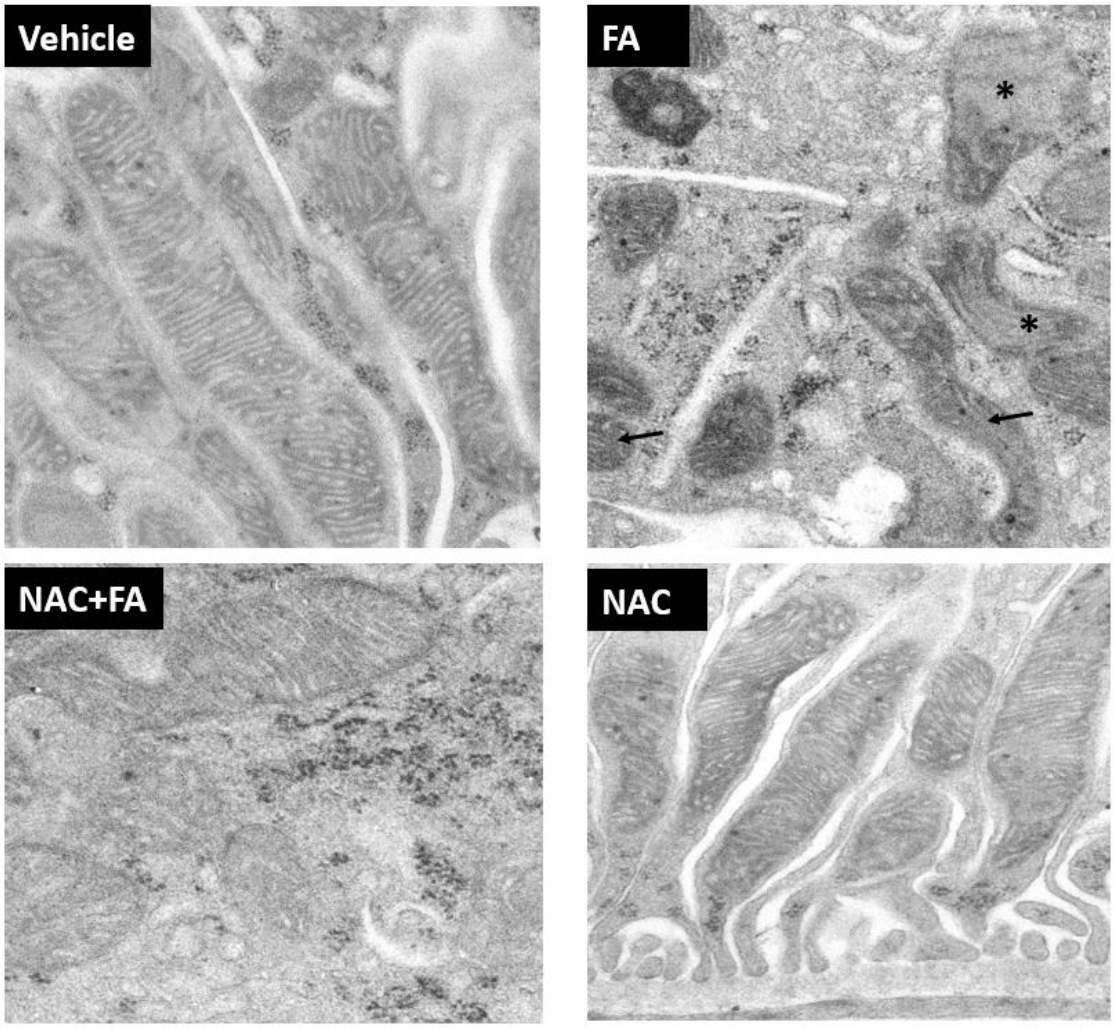

Anexo 5. Micrografías representativas de microscopía electrónica de las mitocondrias de las células epiteliales del túbulo contorneado proximal a los 28 días. Se observa una ultraestructural normal en las mitocondrias del grupo control que sólo recibieron el vehículo. En contraste, las mitocondrias de ratas tratadas con FA mostraron un tamaño y forma irregulares con disrupción de las crestas (flecha) y perdida de la definición de estas (asterisco). El pretratamiento con NAC previno parcialmente el daño mitocondrial inducido por FA, mientras que el tratamiento sólo con NAC no indujo ningún cambio en la morfología mitocondrial. FA= ácido fólico, NAC= N-acetilcisteína, d= días después de la administración de FA.

8. Discusión

8.1. La NAC previene las alteraciones mitocondriales asociadas a la pérdida de la S-glutationilación en la AKI inducida por AF

Si bien en el caso de la AKI inducida por diversos citotóxicos, se ha descrito una correlación entre el daño tubular y las alteraciones mitocondriales [180][181][98][168], los mecanismos moleculares relacionados con la mitocondria por los cuales se induce la AKI siguen siendo poco conocidos. En este sentido el modelo de FA no sólo es ampliamente usado para estudiar los mecanismos involucrados en la AKI, ya que reproduce las alteraciones patológicas observadas en clínica y es altamente reproducible [136,137,182]; sino que en este modelo también se inducen una serie de procesos mal adaptativos que conducen a la transición a la CKD, en menos de 28 días [136,138,139], lo cual lo convierte en un modelo útil para estudiar el papel de la mitocondria tanto en la AKI como en la transición AKI-CKD.

En el metabolismo normal el FA está presente en su forma reducida, el tetrahidrofolato (THF), el cual se produce intracelularmente en la reducción dependiente de NADPH por el complejo enzimático de la dihidrofolato reductasa (DHFR) [183,184]. Los metabolitos del folato en plasma contienen un solo residuo de glutamato y son transportados al interior celular por el intercambiador de folatos reducido y por el receptor de folato de alta afinidad [184–187]. Sin embargo, la administración farmacológica de altos niveles de FA conduce a un aumento súbito en los niveles plasmáticos de THF [184,187]. En el caso del riñón, los metabolitos de folato se acumulan en concentraciones más altas que en otros tejidos debido a los altos niveles de expresión del receptor de folato de alta afinidad en este órgano, especialmente en las células PT [187], donde son almacenados como derivados de poliglutamato impermeables a la membrana celular [185,186]. Aunque los folatos en la célula se distribuyen entre las mitocondrias, el núcleo y el citosol, las mitocondrias almacenan el 40% del folato celular total [185,187], consumiendo altos niveles de NADPH [183,184] y disminuyendo así la defensa antioxidante [140]. Por lo cual, este organelo es especialmente vulnerable a altas dosis de FA [142].

En el caso de la AKI inducida por FA, se había especulado que el desajuste en las mitocondrias podría estar involucrado en el desarrollo de alteraciones como el estrés oxidante, la apoptosis de las células tubulares y el aumento en los procesos inflamatorios característicos de este modelo [47,48]. Sin embargo, hasta de este trabajo, no se habían realizado estudios de bioenergética y estado redox mitocondrial, que confirmaran dicha suposición. En este trabajo demostramos por primera vez que el FA indujo a las 24 h posteriores a su administración un desequilibrio en la bioenergética mitocondrial, caracterizado por la disminución en los parámetros respiratorios S3, P y RCI en la respiración ligada al CI y en la respiración ligada al CI+CII (Fig. 14). Así como la disminución en el $\Delta\Psi m$ en S3 (Fig. 15) y la pérdida en la definición de las crestas mitocondriales observada por microscopia electrónica (Fig. 23). En conjunto dichos datos implican que el FA, 24 h después de su administración, genera una crisis energética, a partir del desacoplamiento mitocondrial y la disminución en la capacidad de la OXPHOS. El desacoplamiento mitocondrial y la reducción de la capacidad de la OXPHOS a las 24 h posteriores a la administración de este compuesto pueden ser explicadas a partir de la disminución en la actividad del

CI y de la ATP sintasa (Fig. 16). Dado que el CI es el más afectado de los elementos del ETS (Fig. 16, S2), esto también explica el mayor grado de alteraciones observado en la respiración ligada al CI (Fig. 14).

Si bien las altas dosis de FA, junto con su baja solubilidad en agua, favorecen la precipitación de cristales de folato en la luz tubular, generando oclusión, inflamación y el aumento en la muerte de las células tubulares [140,188]. Los experimentos de respirometría en las células LLC-PK1 revelaron que el pretratamiento con FA también reduce el valor de P (Anexo 3), demostrando que incluso en ausencia de fenómenos de oclusión en el parénquima renal, las dosis altas de FA reducen la OXPHOS en el PT. Dado que en el riñón la producción de ATP se mantiene principalmente por la OXPHOS [20,21,64,65], la reducción observada en la OXPHOS (Fig. 14-15) estaría comprometiendo la función tubular y la supervivencia celular en segmentos con altas tasas de reabsorción como el PT. Aunado a esto, la pérdida del $\Delta\Psi m$ (Fig. 15) es capaz de favorecer la muerte celular apoptótica, ampliamente observada en las células epiteliales tubulares diversos modelos de AKI [189,190].

De igual manera, el desacoplamiento mitocondrial (Fig. 14), desencadena una mayor fuga de electrones del ETS, favoreciendo la producción de ROS. Lo que explica de manera directa el aumento observado en la producción de H_2O_2 mitocondrial a las 24 h posteriores a la administración del FA (Fig. 17). Dicha información es de particular importancia, ya que junto con la disminución en la actividad del sistema antioxidante enzimático mitocondrial (Fig. 18), demuestra por primera vez que la administración de altas dosis de FA induce un estado pro-oxidante en las mitocondrias, como lo confirman los marcadores de estrés (Fig. 19A-C). Aún más, dicho estado pro-oxidante en la mitocondria va de la mano con niveles mitocondriales menores de GSH, el aumento en GSSG y un contenido menor de glutatión total (Fig. 22). Este estado pro-oxidante mitocondrial está siendo generado en principio por la alta capacidad de internalización de folato en el riñón, especialmente en el PT [18,72,75], el cual una vez dentro de la célula es reducido y almacenado como derivados de THF, implicando de esta manera un enorme gasto de NADPH [184–186] y disminuyendo así los equivalentes reductores, especialmente en GSH. Dicha disminución afecta principalmente a las mitocondrias (Fig. 22), dada la alta dependencia del sistema enzimático antioxidante mitocondrial del GSH [96] y a que dicho organelo almacena el 40% de los folatos en la célula [185,187].

De igual manera, el aumento del estrés oxidante mitocondrial (Fig. 19) observado a las 24 h posteriores a la administración del FA, concuerda con trabajos previos que informan una menor actividad de las SOD, de la catalasa y de la GPx, así como un menor contenido de GSH y un aumento en los niveles de MDA en homogeneizados de riñón total de animales tratados con FA [140,189,190]. Sin embargo, este trabajo es el primero en describir que dichas alteraciones se relacionan directamente con la disfunción en la bioenergética mitocondrial (Figs. 14-15) en la AKI. En este contexto es importante resaltar que se ha descrito que, bajo condiciones de estrés oxidante, el CI mitocondrial puede sufrir modificaciones post-traduccionales irreversibles en residuos específicos de cisteína, las cuales disminuyen su actividad y aumentan la producción de ROS mitocondriales [191,192]. De manera más específica, dichos residuos pueden sufrir la S-sulfenilación (R-SOH) bajo condiciones leves de estrés oxidante, pero

si el mismo persiste o es mayor, las cisteínas sufren la S-sulfinilación (R-SO_2H) e incluso la S-sulfonilación (R-SO_3H), la cual inactiva irreversiblemente al CI [40]. Por su parte, la S-glutationilación no solo compite por los residuos de cisteínas con estas modificaciones, sino que también al ser reversible enzimáticamente, es capaz de restaurar totalmente la actividad del CI, una vez disminuido el estrés oxidante [96,97]. Aunado a esto, se ha descrito que la S-glutationilación de la ATP sintasa previene la R-SOH de los residuos Cys294 y Cys103, los cuales favorecen la formación de un puente disulfuro disminuyendo irreversiblemente la producción de ATP [193,194]. Esto es de particular importancia, ya que 24 h después de la administración del FA, se observó un aumento en el estrés oxidante mitocondrial (Figs. 18-19), el aumento en la producción de H_2O_2 mitocondrial (Fig. 17) así como la disminución de las actividades del CI y de la ATP sintasa (Fig. 16), lo que sugiere la disminución en la S-glutationilación de dichas proteínas mitocondriales. Lo cual concuerda con la reducción en los niveles totales de proteínas mitocondriales S-glutationiladas y con el aumento en la actividad de remoción de la S-glutationilación de la Grx mitocondrial (Fig. 22).

Por su parte, a las 24 h posteriores a la administración de FA, el pretratamiento con NAC evitó el aumento en los marcadores de estrés oxidante mitocondrial (Fig. 19), la disminución en las actividades de las enzimas antioxidantes (Fig. 18) y el aumento de la producción mitocondrial de H_2O_2 (Fig. 17). Dicha preservación del balance redox está vinculada con su capacidad observada para preservar los parámetros respiratorios y el acoplamiento mitocondrial (Fig. 14), a partir de la protección en las actividades de CI y de la ATP sintasa (Fig. 16). De manera interesante, el pretratamiento con NAC también evitó la disminución en los niveles de GSH, en los niveles de glutatión total (GSH+GSSG), en la S-glutationilación de las proteínas mitocondriales y el aumento en la actividad de remoción de la S-glutationilación de la Grx (Fig. 22). Lo que en conjunto sugiere que los efectos protectores de NAC en las mitocondrias están asociados a su capacidad para preservar la S-glutationilación mitocondrial. Esto concuerda con la idea sugerida recientemente por otros autores de que la S-glutationilación enzimática, bajo ciertas condiciones, actúa como un mecanismo protector que vincula los cambios en el metabolismo energético con el estado redox mitocondrial, preservando la homeostasis en dicho organelo [96,97,135]. Sin embargo, aún son necesarios estudios más profundos de proteómica para evaluar la S-glutationilación especifica en estas proteínas y comprobar dicha hipótesis.

Por otro lado, el aumento en la producción de ROS mitocondriales se ha asociado ampliamente con la sobre-activación patológica de la Nox y Nos desacoplada [159,162,163], aumentando así el estrés oxidante en el riñón, la expresión de citocinas proinflamatorias y de factores profibróticos, los cuales favorecen la progresión del daño renal [111,113,164,165]. En el caso del daño renal inducido por FA, a las 24 h posteriores a su administración, este induce el aumento en la producción de ROS ligada a NADPH y L-arginina (sustratos de la Nox y Nos, respectivamente) en los segmentos con mayor contenido mitocondrial y la corteza renal (Fig. 20). Como se observa en la Fig. 20, el grupo tratado con FA reveló una mayor producción de ROS ligada a NADPH, la cual es inhibida mayormente por el VAS2870, sugiriendo que dichas ROS son principalmente atribuibles a la Nox. De hecho, en varios estudios se ha asociado la sobre-activación de la Nox y en especial de la Nox4, con el aumento en la

expresión de citocinas proinflamatorias y factores profibróticos [111,112,195–198], por lo que la hiperactivación patológica de Nos y especialmente de Nox favorecidas por el aumento en la producción de ROS mitocondriales (Fig. 17), sería un mecanismo por el cuál la disfunción mitocondrial contribuye al daño renal. Aún más, la prevención de alteraciones mitocondriales por la NAC también evita la sobreproducción de ROS en los segmentos ricos en mitocondrias (Fig. 20) y por lo tanto el estrés oxidante (Fig. 21) y el desarrollo de la AKI (Figs. 12-13).

Como se describe en la introducción, existe una diferencia no solo entre el tamaño y la abundancia mitocondrial en los distintos segmentos de la nefrona, siendo los segmentos corticales como el PT, DT y el TAL los segmentos con mayor cantidad de mitocondrias [10]. De igual manera, el potencial de membrana mitocondrial ($\Delta\Psi m$) y la preferencia de sustratos respiratorios por este organelo nefrona también cambia a lo largo de los segmentos de la nefrona [12,14,15,17,18]. Si bien, las mitocondrias de estos segmentos pueden responder de manera diferencial a los distintos tipos de daño, se ha observado que las mitocondrias de los segmentos corticales son particularmente más susceptibles al daño [18,82–84]. Esto es concordante con la mayor producción de ROS encontrada en los segmentos del PT y el DT en este trabajo (Fig. 20).

Por otra parte, la bioenergética está estrechamente coordinada con la dinámica y el recambio mitocondrial, favoreciendo la fisión y la mitofagia o la fusión y la biogénesis dependiendo de las demandas de energía de la célula [122,169,199]. De igual manera, el equilibrio redox mitocondrial es capaz de regular de manera directa los procesos de mitofagia y dinámica mitocondrial [121–123]. En el caso de la AKI, específicamente la inducida por cisplatino [170] y por maleato [154,168], se demostró reciente que el desacoplamiento mitocondrial junto con la pérdida del $\Delta\Psi m$ y el aumento del estrés oxidante, conducen al aumento en la fisión mitocondrial y su posterior degradación por mitofagia. De hecho, se ha postulado que en la AKI inducida por citotóxicos existe un aumento en la fisión mitocondrial en las primeras etapas de la lesión renal [19,122,123]. En este trabajo, demostramos por primera vez que, a las 24 h posteriores a su administración, el FA induce la fragmentación mitocondrial y el aumento del proceso de fisión (Figs. 23-24). Dichos cambios se estarían desencadenando por la pérdida del $\Delta\Psi m$ (Fig. 15), el desacoplamiento mitocondrial (Fig. 14B) y el aumento del estrés oxidante (Fig. 19). Estas evidencias sugieren que las alteraciones en la dinámica mitocondrial serían el resultado de un deterioro en la bioenergética y el estado redox mitocondrial. Por su parte, los efectos protectores del pretratamiento con NAC en la bioenergética y el estado redox mitocondrial (Figs. 14-19), explican la preservación observada por microscopia electrónica en la morfología mitocondrial (Fig. 23), así como la prevención de las alteraciones en la dinámica mitocondrial (Figs. 23-24) a las 24 h posteriores a la administración del FA.

La pérdida del $\Delta\Psi m$, el aumento del estrés oxidante y el desplazamiento de la dinámica mitocondrial hacia la fisión son inductores conocidos de la remoción de este organelo por el proceso de mitofagia [200–203]. Por lo que en nuestro modelo esperábamos un aumento en este proceso. Efectivamente, a las 24 posteriores a su administración, el FA aumentó los niveles mitocondriales de la proteína de autofagia Pink1 y disminuyó los niveles de las proteínas de autofagia

LC3-I y LC3-II (Fig. 25), implicando la inducción de la mitofagia en el PT. Sin embargo, también se observó un aumento en los niveles de p62 (Fig. 25) y la microscopía electrónica en el PT reveló la acumulación de cuerpos vesiculares con mitocondrias fragmentadas (Fig. 23), lo que sugiere un proceso de mitofagia interrumpido. Por su parte, el pretratamiento con NAC no previno significativamente las alteraciones en los niveles de proteínas de autofagia con respecto al grupo FA (Fig. 25), aunque sí disminuyó el número de cuerpos vesiculares observados por microscopía electrónica en el PT (Fig. 23).

Por último, a las 24 h posteriores a su administración, el FA disminuyó en el PT los niveles de las proteínas de biogénesis mitocondrial PGC-1α, NRF1, NRF2 y TFAM en las mitocondrias (Fig. 26). Esto concuerda con lo descrito por trabajos anteriores, en los que se observó en los homogeneizados de riñón completo una disminución en los niveles de mRNA de PGC-1α, TFAM, junto con la disminución en el número de copias de mtDNA entre 2 y 14 días posteriores a la administración de FA [142,143]. Estos estudios también reportaron una fuerte correlación entre el deterioro de la biogénesis mitocondrial y el desarrollo de los procesos que conducen a la transición AKI-CKD en este modelo [142,143]. Por su parte el pretratamiento con NAC no previno significativamente la caída de los marcadores de biogénesis mitocondrial (Fig. 26). Esto sugiere que los mecanismos de protección de NAC no estarían directamente relacionados con dicho proceso.

Finalmente, para integrar los resultados obtenidos en esta primera parte, proponemos el esquema presentado en la Figura 33, donde en conjunto, nuestros resultados sugieren que la prevención, por parte de la NAC, de las alteraciones en la bioenergética, el estado redox y dinámica mitocondrial es capaz de prevenir el desarrollo de la AKI inducida por FA a las 24 h posteriores a la administración de este.

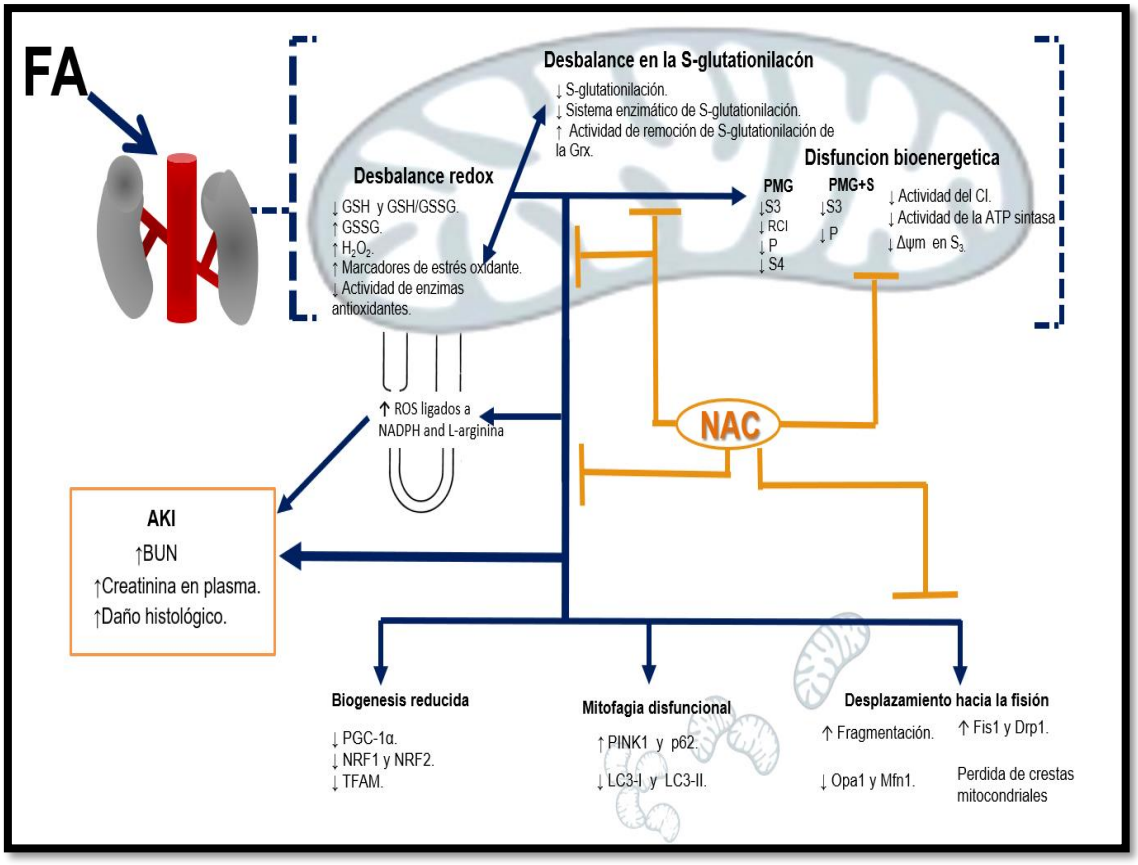

Figura 33. Esquema integrativo en la AKI. Veinticuatro horas después de la administración de ácido fólico (AF), el pretratamiento con N-acetilcisteína (NAC) previene el desbalance redox y en la S-glutationilación mitocondrial, previniendo así las alteraciones bioenergéticas y por tanto también el desplazamiento de la dinámica mitocondrial hacia la fisión. Los efectos protectores mitocondriales de NAC también evitan el aumento en la producción de especies reactivas de oxígeno (ROS) ligadas al NADPH y a la L-arginina en los segmentos ricos en mitocondrias como el túbulo proximal (PT). Con lo que la NAC previene el desarrollo de la AKI inducida por FA. Aunado a esto, el FA también induce la disminución de la biogénesis mitocondrial y la mitofagia disfuncional. Aunque a las 24 h el pretratamiento con NAC no reduce de manera significativa las alteraciones en los niveles de las proteínas involucradas en estos procesos, la NAC sí disminuye efectivamente la acumulación de cuerpos vacuolares en el PT. BUN= nitrógeno ureico en sangre; CI= complejo I mitocondrial; Drp1= proteína 1 relacionada con la dinamina; Fis1= proteína de fisión 1; GSH= glutatión reducido; GSSG= glutatión disulfuro u oxidado; Grx= glutaredoxina; LC3 (I / II) = proteína 1A / 1B asociada a microtúbulos de la cadena ligera 3 (I / II); Mfn1= mitofusina 1; Opa1= proteína de atrofia óptica 1; NRF (1/2)= factor respiratorio nuclear (1/2); P= respiración asociada a la OXPHOS; S3= estado respiratorio 3; S4= estado respiratorio 4; PGC-1α= coactivador alfa del receptor activado por proliferador de peroxisoma 1-alfa; PINK1= quinasa putativa inducida por PTEN 1; PMG= respiración ligada al CI alimentada con piruvato-malato-glutamato; PMG+S= respiración ligada al CI+CII alimentada con piruvato-malato-glutamato más con succinato; RCI= índice de control respiratorio; TFAM= factor de transcripción mitocondrial A; ΔΨm= potencial de membrana mitocondrial.

8.2. La evolución temporal del deterioro en la bioenergética y estado redox inducida por el FA favorece la transición AKI-CKD

Como se mencionó anteriormente, se sabe bien que episodios graves de AKI son capaces de desencadenar el desarrollo de la CKD [5,49–51]. Aún más, la gravedad de la lesión durante el evento AKI es un buen indicador de la rapidez con que progresará la CKD [62]. Dada la naturaleza progresiva del daño renal inducido por FA [137,140,142] y las alteraciones mitocondriales observadas en la fase aguda (Figs. 14-26), esto lo hace un modelo ideal para evaluar el papel de la mitocondria en la transición AKI-CKD.

En cuanto a la función renal, la evaluación temporal reveló que el aumento de BUN y de creatinina en plasma alcanzaron un máximo a los 2 días después de la administración de FA y disminuye posteriormente a lo largo del tiempo (Fig. 27A, B). Además, las alteraciones histológicas asociadas con la AKI, como la muerte celular, la pérdida de la definición del borde en cepillo y el hinchamiento celular en el PT se mantienen en el día 2 (Fig. 27D). Estos resultados confirman que la AKI está presente entre los días 1 y 2 después de la administración de FA. Por su parte la disminución progresiva del BUN y la creatinina en plasma en los días posteriores (Fig. 27A, B), concuerda con lo descrito por estudios previos en ratones administrados con FA, en donde este fenómeno marca el final de la etapa aguda y el inicio de la transición hacia la CKD [140,142]. Dicha transición se caracteriza por el deterioro renal progresivo, como lo demuestran estudios previos, en los que entre los días 2 a 14 después de la administración de FA, se observa el aumento temporal de procesos patológicos como: estrés oxidante, muerte celular apoptótica, inflamación, fibrosis, transición epitelio-mesénquima y reparación mal adaptativa de la parénquima renal [142,143,178,195]. En el presente trabajo, la pérdida progresiva de la función renal es confirmada por la disminución a los 28 días de la GFR (el principal parámetro de evaluación de la función renal), así como por la disminución en el RBF y en el RPF y el aumento en la RVR (Fig. 28A). Estos resultados, junto con el aumento observado del proceso fibrótico en el riñón a los 28 días (Fig. 28B) confirman la progresión a CKD. Lo cual es congruente con los estudios previos en ratones en los que se observa la transición AKI-CKD desde los 14 días posteriores a la administración de FA [142,143,178].

Si bien se había especulado que la disfunción en la bioenergética mitocondrial estaba presente a lo largo la progresión hacia la CKD y favorecía la misma [142,178], la falta de estudios temporales de la bioenergética mitocondrial durante la transición AKI-CKD dificultaba la comprobación de dicha hipótesis. En este trabajo, caracterizamos por primera vez las alteraciones temporales en la bioenergética mitocondrial en el modelo de daño renal inducido por FA. Específicamente, observamos que a los 2 días en AKI, se mantiene la reducción en la capacidad de la OXPHOS (Fig. 29A, C), la reducción en el $\Delta\Psi m$ (Fig. 29E) y desacoplamiento mitocondrial (Fig. 29D) en la respiración ligada al CI, sugiriendo que la producción mitocondrial de ATP se ve fuertemente afectada en la AKI. Estos cambios están asociados principalmente a la reducción de la actividad del CI y del CIII (Fig. 30A, B). Curiosamente, a las 24 h posteriores a la administración de FA, no se observó ningún cambio en la actividad del CIII (Anexo 2), lo que implica que el deterioro en el CI precede al deterioro en el CIII. Dicho efecto puede ser explicado dada la mayor susceptibilidad del CI a modificaciones post-traduccionales irreversibles inducidas por el estrés oxidante

[191,192]. En este contexto, un estudio reciente reveló que a los 3 días posteriores a la administración de FA, la inhibición del CI por la administración de rotenona exacerba el daño renal [204], destacando que la disfunción mitocondrial en el CI favorece la progresión del daño renal.

En el caso de la etapa avanzada, se observó la recuperación progresiva en el S3 y en la P (Fig. 29A, C), lo cual es consistente con la recuperación temporal en la actividad el CI (Fig. 30A). Sin embargo, el aumento progresivo de S4o a lo largo del tiempo (Fig. 29 B), explica por qué incluso en la etapa avanzada el RCI se mantuvo reducido con respecto al control (Fig. 29D). Estos resultados implican que, aunque la producción de ATP mitocondrial se recupera a lo largo del tiempo, dicha recuperación se acompaña por un desacoplamiento mitocondrial permanente. El desacoplamiento mitocondrial que permanece a lo largo del curso temporal es de particular interés, ya que favorece el aumento permanente del estrés oxidante mitocondrial, como lo confirman la reducción en la actividad aconitasa (Fig. 32A), en la actividad de las enzimas antioxidantes mitocondriales (Fig. 32B, C) y el aumento en los niveles mitocondriales de 4-HNE (Fig. 32E). De igual manera se ha descrito que la disfunción del CI y el desacoplamiento generan el aumento en la producción mitocondrial de ROS [159,162,163], lo que explica el aumento en la producción de H_2O_2 mitocondrial observada a los 28 días posteriores a la administración de FA (Fig. 32D). De hecho el aumento en los niveles de ROS favorece la expresión de citocinas proinflamatorias y factores profibróticos, desencadenando la progresión del daño renal [111,113,164,165].

Por otro lado, en este trabajo también describimos por primera vez las alteraciones temporales en la β-oxidación mitocondrial. Observamos que desde la fase aguda hay una reducción en el S3, en el RCI y en la capacidad de la OXPHOS asociada a la β-oxidación de ácidos grasos (Fig. 31A, C, D), lo cual sugiere que la producción de ATP a partir de la β-oxidación de ácidos grasos disminuye permanentemente después de la administración de FA. Esto es particularmente importante en el riñón, donde la mayor producción de ATP se atribuye a la β-oxidación de ácidos grasos [8,176]. De manera concordante, se ha descrito tanto en modelos animales [74,177,178] como en pacientes con CKD [178,179], una disminución en los niveles de mRNA de las proteínas asociadas a la β-oxidación en riñón. En el caso de animales administrados con FA, dichos niveles son menores a los del control, pero sin diferencia en el número de copias de mtDNA [178]. Por lo que, en conjunto con nuestros resultados, estos datos sugieren un estado permanente de estrés bioenergético a lo largo de la progresión del daño renal. En este contexto, existe un consenso en la literatura de que las mitocondrias en estadios avanzados de CKD no son capaces de mantener la demanda energética [73,76,77], como lo demuestra la acumulación de fosfato inorgánico, el aumento en el consumo de oxígeno y disminución del transporte de sodio en el riñón. Dichos cambios se han descrito también en pacientes con CKD [78–80].

La disminución en los niveles de las proteínas de la β-oxidación mitocondrial parece ser una alteración común en diversos modelos de CKD [74,79,205]. De hecho, en el modelo de FA, se ha descrito que la disminución en los mensajeros de las proteínas de la β-oxidación mitocondrial precede al proceso de fibrosis renal [178]. Esto es congruente con la reducción observada en los parámetros

respiratorios de la β-oxidación desde la fase aguda (Fig. 31) en días anteriores a la fibrosis renal (Fig. 28B). Además, recientemente se demostró que tan sólo la inhibición de la β-oxidación es suficiente para reprogramar a las células epiteliales tubulares hacia un fenotipo profibrótico [178]. De hecho, dichos autores sugirieron que los niveles de las proteínas de la β-oxidación en la CKD podría ser una manifestación de una disfunción mitocondrial más amplia [178]. Esto es congruente con nuestros resultados, en los que se demuestra que el deterioro en la β-oxidación (Fig. 31) está acompañado por la reducción en los parámetros respiratorios mitocondriales en la respiración ligada al CI (Fig. 29), por una reducción en la actividad del CI y CIII (Fig. 30) y por un aumento en la producción de H_2O_2 mitocondrial (Fig. 32D). En particular, se sabe que las ROS mitocondriales activan mecanismos patológicos relacionados a la fibrosis [30,117,118], por tanto la disfunción mitocondrial temprana desencadena la disminución de la β-oxidación y el aumento en la producción de ROS, promoviendo la fibrosis renal en este modelo.

Por otro lado, si bien la administración de FA conduce durante la fase de AKI a la disminución en el mRNA de las proteínas de biogénesis mitocondrial en el riñón [142,143], lo que se traduce en la disminución observada en los niveles de proteína de las mismas a las 24 h (Fig. 26). Curiosamente las proteínas de biogénesis junto con los marcadores de masa mitocondrial no mostraron cambios significativos entre los días 7-28 posteriores a la administración de FA en comparación con el grupo control (Anexo 4), lo que sugiere que la disminución inducida por FA en la biogénesis mitocondrial está presente solamente en la fase aguda de la enfermedad.

Por su parte, el pretratamiento con NAC previno, incluso a los 2 días posteriores a la administración del FA, el desarrollo de la AKI (Fig. 27). De igual manera, la NAC previno desde el día 2 y hasta el día 28, la disminución inducida por el FA en la OXPHOS (Fig. 29A, C) y en el ΔΨm (Fig. 29E), así como el desacoplamiento mitocondrial (Fig. 29D) en la respiración ligada al CI. Lo cual indica que la NAC conservó la producción de ATP mitocondrial a lo largo del curso temporal evaluado. Esta protección está asociada a la preservación de las actividades del CI y del CIII tanto en la fase aguda como en la crónica (Fig. 30A, B). De manera congruente, la NAC también evitó la reducción inducida por FA en S3, RCI y en la capacidad de la OXPHOS asociada a la β-oxidación de ácidos grasos (Fig. 29A, C, D) en la transición AKI-CKD, confirmando la preservación general en la producción mitocondrial de ATP mitocondrial. La preservación de la función mitocondrial por la NAC estaría relacionada con la prevención del estrés oxidante en las mitocondrias tanto en la fase aguda como en la crónica (Fig. 32A-D) y por lo tanto evitaría la evolución hacia la CKD (Fig. 28A-B). De hecho, la NAC evitó a los 28 días la disminución inducida por el FA en la GFR y en el RBF y el aumento de RVR (Fig. 28A), así como el proceso fibrótico (Fig. 28B).

Finalmente, como se propone en el diagrama integrativo de esta segunda parte (Fig. 34), la AKI inducida por FA está relacionada al deterioro en la bioenergética mitocondrial, a partir de la reducción de la actividad del CI y CIII, lo que genera la reducción en el S3, el S4o, la P, el RCI y en el ΔΨm en la respiración asociada al CI. Así como la reducción en los parámetros respiratorios vinculados a la β-oxidación. Si bien hay una recuperación progresiva de S3 y de la P en la

respiración ligada a CI, las alteraciones en los parámetros respiratorios vinculados a la β-oxidación y el desacoplamiento mitocondrial persisten a lo largo del tiempo. Juntos, estos generan la permanencia de un estado pro-oxidante en las mitocondrias incluso en etapas avanzadas. Esto favorece las alteraciones hemodinámicas y el proceso de fibrosis, desencadenando el desarrollo de la transición hacia la CKD. Por otro lado, la preadministración de NAC previene las alteraciones en la bioenergética mitocondrial en AKI inducidas por FA, evitando su persistencia en el tiempo y el aumento del estrés oxidante mitocondrial. Por lo que NAC es capaz de prevenir al menos parcialmente la fibrosis y las alteraciones hemodinámicas. En conjunto, nuestros resultados sugirieren que la preservación de la mitocondria en la AKI es capaz de prevenir la progresión del daño renal hacia la CKD el modelo de daño renal inducido por FA. De hecho, el uso de compuestos capaces de preservar la función mitocondrial ha demostrado atenuar la progresión del daño renal como la nefrectomía [21,73,76,206]. De igual manera, más recientemente se sugirió que restaurar la β-oxidación mitocondrial podría ser beneficioso para el tratamiento de la CKD [178]. Sin embargo, aún se necesitan más estudios para confirmar esta hipótesis.

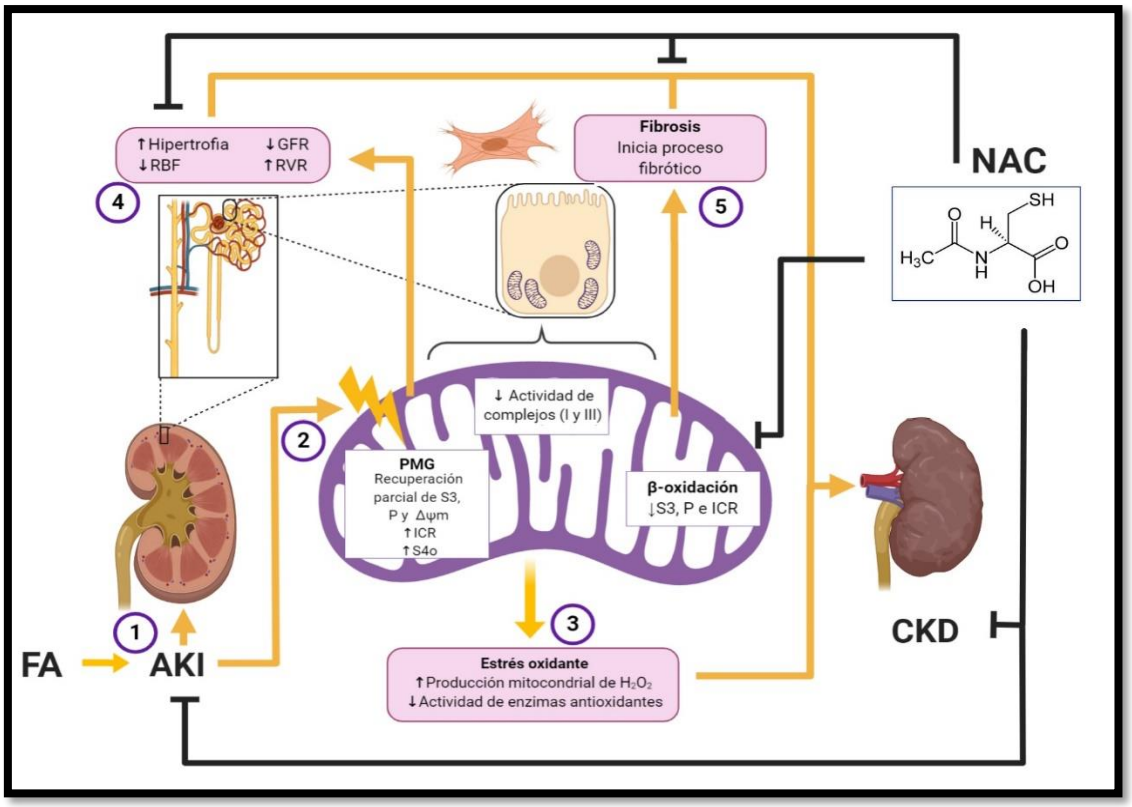

Figura 34. Esquema integrativo de la transición AKI-CKD. (1) El FA induce AKI temprana, lo cual está relacionado con el deterioro de la bioenergética mitocondrial. **(2)** En la etapa aguda, hay una reducción en la actividad del CI y del CIII, lo que conduce a una disminución en el S3, el S4o, la P, el RCI y el ΔΨm en la respiración vinculada al CI. Pero también a una reducción en el S3, la P y el RCI en la β-oxidación de los ácidos grasos. Si bien hay una recuperación parcial en el S3, en la P y en ΔΨm en la respiración ligada al CI, el S4o y el RCI y los parámetros respiratorios vinculados a la β-oxidación se ven afectados de manera permanente. Lo cual indica una reducción permanente en la producción de ATP, así como el desacoplamiento mitocondrial. **(3)** Así mismo el FA favorece un estrés oxidante permanente en las mitocondrias, reduciendo la actividad de las enzimas antioxidantes y aumentando la producción mitocondrial de peróxido de hidrogeno (H_2O_2). Finalmente, las alteraciones mitocondriales en su conjunto favorecen procesos como **(4)** las alteraciones hemodinámicas y **(5)** la fibrosis, implicadas en la transición AKI-CKD. Por su parte, el pretratamiento con NAC, previne el deterioro mitocondrial en la AKI inducida por FA, evitando así la progresión de la disfunción mitocondrial con el tiempo y por tanto los procesos de fibrosis y las alteraciones hemodinámicas que favorecen el avance a la CKD. AKI= insuficiencia renal aguda, CKD= enfermedad renal crónica, CI= complejo I, CIII= complejo III, FA= ácido fólico, GFR= tasa de filtración glomerular, NAC= N-acetilcisteína, P= respiración atribuible a la fosforilación oxidativa, PMG= piruvato-malato-glutamato, sustratos del CI, RBF= flujo sanguíneo renal, RCI= índice de control respiratorio, RVR= resistencia vascular renal, S3= estado respiratorio 3, S4o= estado respiratorio 4 inducido por oligomicina, ΔΨm= potencial de membrana mitocondrial.

9. Conclusiones

- El pretratamiento con FA induce a las 24 h la disfunción en la bioenergética mitocondrial, generando así alteraciones en la dinámica y la mitofagia.

- Las alteraciones bioenergéticas son provocadas por la disminución en la S-glutationilación y un estado pro-oxidante mitocondrial

- La disfunción mitocondrial a las 24h favorece el desarrollo de la AKI.

- Los efectos protectores de la NAC sobre la AKI se relacionan la prevención de la función mitocondria.

- El NAC previene la disfunción mitocondrial a partir de la preservación de la S-glutationilación y el estado redox en este organelo.

- Las alteraciones bioenergéticas y el estrés oxidante mitocondrial inducidas por el FA persisten después de la AKI.

- La disfunción en la β-oxidación y el desacoplamiento mitocondrial son un fenómeno persisten de durante la transición AKI-CKD.

- La persistencia del daño mitocondria después de la AKI inducida por FA favorece el desarrollo de la CKD.

- Preservar la función mitocondrial durante un evento de AKI previene el desarrollo de la CKD.

10. Perspectivas

- Se plantea realizar estudios de proteómica en mitocondrias, con el objetivo de determinar la identidad de las proteínas que sufren cambios en su S-glutationilación.
- Se plantea realizar estudios temporales de dinámica mitocondrial, para determinar su participación en la progresión hacia la CKD.
- Se plantea realizar estudios temporales de autofagia y mitofagia, para determinar su participación en la progresión hacia la CKD.
- Se plantea realizar esquemas de postratamiento con la NAC, para determinar si estos pueden revertir el daño mitocondrial y por tanto el desarrollo de la CKD.
- Se plantea realizar estudios de los cambios den la S-glutationilación en otros modelos de daño renal asociados a la disfunción mitocondrial como la nefrectomía.

11. Referencias

[1] B.M. Koeppen, B.A. Stanton, 2 - Structure and Function of the Kidneys, in: B.M. Koeppen, B.A. Stanton (Eds.), Ren. Physiol. (Fifth Ed., Fifth Edit, Mosby, Philadelphia, 2013: pp. 15–26. doi:https://doi.org/10.1016/B978-0-323-08691-2.00002-8.

[2] BrennerRector, Anatomy of the Kidney, Taal Brenner Rector's Kidney, 9th Ed. (2011) 1–111. doi:10.1016/B978-1-4160-6193-9.10002-8.

[3] D.U. Silverthorn, Fisiología humana : Un enfoque integrado, 4th ed., Buenos Aires, 2009.

[4] C. Lote, Principles of renal physiology, 4th ed., Springer New York, 2014.

[5] A.B. Fogo, A.H. Cohen, R.B. Colvin, J.C. Jennette, C.E. Alpers, Fundamentals of renal pathology, First edit, Springer Berlin Heidelberg, Berlin, Heidelberg, 2014. doi:10.1007/978-3-642-39080-7.

[6] A.S.L.Y. Jianghui Hou, Madhumitha Rajagopal, NIH Public Access, (2013) 479–501. doi:10.1146/annurev-physiol-030212-183705.Claudins.

[7] A. Doucet, A.I. Katz, High-affinity Ca-Mg-ATPase along the rabbit nephron, Am. J. Physiol. 242 (1982) F346–F352.

[8] T. Sekine, H. Endou, Solute Transport, Energy Consumption, and Production in the Kidney, in: Seldin and Geibisch's The Kidney, Fifth Edit, Elsevier, 2013: pp. 143–175. doi:10.1016/B978-0-12-381462-3.00006-9.

[9] F. Kiil, K. Aukland, H. Refsum, Renal sodium transport and oxygen consumption., Am. J. Physiol. 201 (1961) 511–6.

[10] W. Pfaller, M. Rittinger, Quantitative morphology of the rat kidney, Int. J. Biochem. 12 (1980) 17–22.

[11] K. Klein, W. Maw-Song, S. Torikai, D.D. Warren, K. Kurakawa, Substrate oxidation by isolated single nephron segments of the rat, Kidney Int. 20 (1981) 29–35.

[12] R.L.S. Goncalves, C.L. Quinlan, I. V Perevoshchikova, M. Hey-Mogensen, M.D. Brand, Sites of superoxide and hydrogen peroxide production by muscle mitochondria assessed ex vivo under conditions mimicking rest and exercise., J. Biol. Chem. 290 (2015) 209–27. doi:10.1074/jbc.M114.619072.

[13] M. Lehir, U. Dubach, Peroxisomal and Mitochondrial Beta-Oxidation in the Rat Kidney: Distribution of Fatty Acyl-Coenzyme A Oxidase and 3-Hydroxyacyl-Coenzyme A Dehydrogenase Activities along the Nephron, J. Histochem. Cytochem. (1982).

[14] S.I. Harris, R.S. Balaban, L. Barrett, L.J. Mandel, Mitochondrial respiratory capacity and Na+- and K+-dependent adenosine triphosphatase-mediated ion transport in the intact renal cell, J. Biol. Chem. 256 (1981) 10319–10328.

[15] W.G. Guder, S. Wagner, G. Wirthensohn, Metabolic fuels along the nephron : Pathways and intracellular mechanisms of interaction GlutamineW, 29 (1986).

[16] V. Affairs, N. Orleans, Metabolic support of collecting duct transport, 53 (1998) 408–415.

[17] A.M. Hall, G.J. Rhodes, R.M. Sandoval, P.R. Corridon, B.A. Molitoris, In vivo multiphoton imaging of mitochondrial structure and function during acute kidney injury, Kidney Int. 83 (2014) 72–83. doi:10.1038/ki.2012.328.In.

[18] A.M. Hall, R.J. Unwin, N. Parker, M.R. Duchen, Multiphoton imaging reveals differences in mitochondrial function between nephron segments., J. Am. Soc. Nephrol. 20 (2009) 1293–302. doi:10.1681/ASN.2008070759.

[19] M. Zhan, C. Brooks, F. Liu, L. Sun, Z. Dong, Mitochondrial dynamics: regulatory mechanisms and emerging role in renal pathophysiology, Kidney Int. 83 (2013) 568–581. doi:10.1038/ki.2012.441.

[20] Y. Ishimoto, R. Inagi, Mitochondria: a therapeutic target in acute kidney injury., Nephrol. Dial. Transplant. 31 (2015) 1062–1069. doi:10.1093/ndt/gfv317.

[21] S. Granata, A. Dalla Gassa, P. Tomei, A. Lupo, G. Zaza, Mitochondria: a new therapeutic target in chronic kidney disease., Nutr. Metab. (Lond). 12 (2015) 1–21. doi:10.1186/s12986-015-0044-z.

[22] R. Che, Y. Yuan, S. Huang, A. Zhang, Mitochondrial dysfunction in the pathophysiology of renal diseases, Am. J. Physiol. Physiol. 306 (2014) F367–F378. doi:10.1152/ajprenal.00571.2013.

[23] A. Mather, C. Pollock, Glucose handling by the kidney., Kidney Int. Suppl. 79 (2011) S1–S6. doi:10.1038/ki.2010.509.

[24] A. Maleque, H. Endou, C. Koseki, F. Sakai, Nephron heterogeneity: gluconeogenesis from pyruvate in rabbit nephron, FEBS Lett. 116 (1980) 154–156. doi:10.1016/0014-5793(80)80631-4.

[25] E. Cersosimo, P.E. Molina, N.N. Abumrad, Renal lactate metabolism and gluconeogenesis during insulin-induced hypoglycemia, Diabetes. 47 (1998) 1101–1106. doi:10.2337/diabetes.47.7.1101.
[26] A.A. McDonough, S.C. Thomson, Metabolic Basis of Solute Transport, in: Brenner and Rector's The Kidney, Ninth Edit, Elsevier, 2012: pp. 138–157. doi:10.1016/b978-1-4160-6193-9.10004-1.
[27] R.J. Mailloux, W.G. Willmore, S-glutathionylation reactions in mitochondrial function and disease., Front. Cell Dev. Biol. 68 (2014) 1–17. doi:10.3389/fcell.2014.00068.
[28] C.L. Quinlan, I. V. Perevoshchikova, M. Hey-Mogensen, A.L. Orr, M.D. Brand, Sites of reactive oxygen species generation by mitochondria oxidizing different substrates, Redox Biol. 1 (2013) 304–312. doi:10.1016/j.redox.2013.04.005.
[29] C.L. Quinlan, J.R. Treberg, I. V. Perevoshchikova, A.L. Orr, M.D. Brand, Native rates of superoxide production from multiple sites in isolated mitochondria measured using endogenous reporters, Free Radic. Biol. Med. 53 (2012) 1807–1817. doi:10.1016/j.freeradbiomed.2012.08.015.
[30] B.-Z. Shao, Z.-Q. Xu, B.-Z. Han, D.-F. Su, C. Liu, NLRP3 inflammasome and its inhibitors: a review., Front. Pharmacol. 6 (2015) 262. doi:10.3389/fphar.2015.00262.
[31] S. Granata, V. Masola, E. Zoratti, M.T. Scupoli, A. Baruzzi, M. Messa, F. Sallustio, L. Gesualdo, A. Lupo, G. Zaza, NLRP3 inflammasome activation in dialyzed chronic kidney disease patients, PLoS One. 10 (2015) 1–16. doi:10.1371/journal.pone.0122272.
[32] J.F. Chen, H. Liu, H.F. Ni, L.L. Lv, M.H. Zhang, A.H. Zhang, R.N. Tang, P.S. Chen, B.C. Liu, Improved mitochondrial function underlies the protective effect of pirfenidone against tubulointerstitial fibrosis in 5/6 nephrectomized rats, PLoS One. 8 (2013) 1–15. doi:10.1371/journal.pone.0083593.
[33] Y. Yuan, Y. Chen, P. Zhang, S. Huang, C. Zhu, G. Ding, B. Liu, T. Yang, A. Zhang, Mitochondrial dysfunction accounts for aldosterone-induced epithelial-to-mesenchymal transition of renal proximal tubular epithelial cells, Free Radic. Biol. Med. 53 (2012) 30–43. doi:10.1016/j.freeradbiomed.2012.03.015.
[34] J. Blaine, M. Chonchol, M. Levi, Renal control of calcium, phosphate, and magnesium homeostasis, Clin. J. Am. Soc. Nephrol. 10 (2015) 1257–1272. doi:10.2215/CJN.09750913.
[35] C. Giorgi, A. Danese, S. Missiroli, S. Patergnani, P. Pinton, Calcium Dynamics as a Machine for Decoding Signals, Trends Cell Biol. 28 (2018) 258–273. doi:10.1016/j.tcb.2018.01.002.
[36] C. Giorgi, S. Marchi, P. Pinton, The machineries, regulation and cellular functions of mitochondrial calcium, Nat. Rev. Mol. Cell Biol. (2018). doi:10.1038/s41580-018-0052-8.
[37] G. Csordás, D. Weaver, G. Hajnóczky, Endoplasmic Reticulum–Mitochondrial Contactology: Structure and Signaling Functions, Trends Cell Biol. 28 (2018) 523–540. doi:10.1016/j.tcb.2018.02.009.
[38] J. Prudent, H.M. McBride, The mitochondria–endoplasmic reticulum contact sites: a signalling platform for cell death, Curr. Opin. Cell Biol. 47 (2017) 52–63. doi:10.1016/j.ceb.2017.03.007.
[39] H. Nishi, T. Higashihara, R. Inagi, Lipotoxicity in kidney, heart, and skeletal muscle dysfunction, Nutrients. 11 (2019) 1–17. doi:10.3390/nu11071664.
[40] A.A. Sharfuddin, S.D. Weisbord, P.M. Palevsky, B.A. Molitoris, Acute Kidney Injury, in: K. Skorecki, G.M. Chertow, P.A. Marsden, M.W. Taal, A.S.L. Yu (Eds.), Brenner and Rector's The Kidney, Ninth Edit, Elsevier, Philadelphia, 2012: pp. 1044–1099. doi:10.1016/B978-1-4160-6193-9.10030-2.
[41] M.E. Thomas, C. Blaine, A. Dawnay, M. a J. Devonald, S. Ftouh, C. Laing, S. Latchem, A. Lewington, D. V Milford, M. Ostermann, The definition of acute kidney injury and its use in practice., Kidney Int. 87 (2014) 1–12. doi:10.1038/ki.2014.328.
[42] E.D. Siew, A. Davenport, The growth of acute kidney injury: a rising tide or just closer attention to detail? GROWTH IN THE INCIDENCE OF AKI: IS IT REAL? Changes in the incidence of AKI using administrative codes, Kidney Int. 87 (2014) 46–61. doi:10.1038/ki.2014.293.
[43] M. Morigi, L. Perico, C. Rota, L. Longaretti, S. Conti, D. Rottoli, R. Novelli, G. Remuzzi, A. Benigni, Sirtuin 3–dependent mitochondrial dynamic improvements protect against acute kidney injury, J. Clin. Invest. 125 (2015) 715–726. doi:10.1172/JCI77632.
[44] P.K.T. Li, E.A. Burdmann, R.L. Mehta, Acute kidney injury: Global health alert, Hong Kong J. Nephrol. 15 (2013) 1–5. doi:10.1016/j.hkjn.2013.03.001.

[45] M. Negrette-Guzmán, S. Huerta-Yepez, O.N. Medina-Campos, Z.L. Zatarain-Barrón, R. Hernández-Pando, I. Torres, E. Tapia, J. Pedraza-Chaverri, Sulforaphane Attenuates Gentamicin-Induced Nephrotoxicity: Role of Mitochondrial Protection, Evidence-Based Complement. Altern. Med. 2013 (2013) 1–17. doi:10.1155/2013/135314.
[46] M. Ostermann, K. Liu, Pathophysiology of AKI, Best Pract. Res. Clin. Anaesthesiol. 31 (2017) 305–314. doi:10.1016/j.bpa.2017.09.001.
[47] M.N. Rana, J. Tangpong, M.M. Rahman, Toxicodynamics of Lead, Cadmium, Mercury and Arsenic- induced kidney toxicity and treatment strategy: A mini review., Toxicol. Reports. 5 (2018) 704–713. doi:10.1016/j.toxrep.2018.05.012.
[48] A.A. Sharfuddin, B.A. Molitoris, Pathophysiology of ischemic acute kidney injury, Nat. Rev. Nephrol. 7 (2011) 189–200. doi:10.1038/nrneph.2011.16.
[49] A.M. El Nahas, K.B. Aminu, Chronic kidney disease: the global challenge, Lancet. 365 (2005) 331–340. doi:10.1016/S0140-6736(05)70199-9.
[50] M.W. Taal, B.M. Brenner, Adaptation to Nephron Loss and Mechanisms of Progression in Chronic Kidney Disease, in: K. Skorecki, G.M. Chertow, P.A. Marsden, M.W. Taal, A.S.L. Yu (Eds.), Brenner & Rector's The Kidney, Ninth Edit, Elsevier, 2012: pp. 1918–1971. doi:10.1016/B978-1-4160-6193-9.10051-X.
[51] T. Shafi, J. Coresh, Chronic Kidney Disease: Definition, Epidemiology, Cost, and Outcomes, in: J. Himmelfarb, M.H. Sayegh (Eds.), Chronic Kidney Dis. Dial. Transplant., 3rd ed., Elsevier Inc., 2010: pp. 3–21. doi:10.1016/B978-1-4377-0987-2.00001-7.
[52] J.-J. Carrero, M. Hecking, I. Ulasi, L. Sola, B. Thomas, Chronic Kidney Disease, Gender, and Access to Care: A Global Perspective, Semin. Nephrol. 37 (2017) 296–308. doi:10.1016/j.semnephrol.2017.02.009.
[53] A. Khwaja, M. El Kossi, J. Floege, M. El Nahas, The management of CKD: A look into the future, Kidney Int. 72 (2007) 1316–1323. doi:10.1038/sj.ki.5002489.
[54] L.S. Gallardo Vidal, A.J. Rodríguez Méndez, M. Burgos Ochoa, M.L. Martínez Martínez, P. García Solís, M.E. Villagrán Herrera, A.M. Pérez Baza, Utilidad de un modelo de predicción para la enfermedad renal crónica en una unidad de primer nivel de atención, Nefrología. (2015) 3–5. doi:10.1016/j.nefro.2015.10.010.
[55] A. Méndez-Durán, G. Pérez-Aguilar, F. Ayala-Ayala, R.A. Ruiz-Rosas, J.D.J. González-Izquierdo, J. Dávila-Torres, Panorama epidemiológico de la insuficiencia renal crónica en el segundo nivel de atención del Instituto Mexicano del Seguro Social, Diálisis y Traspl. 35 (2014) 148–156. doi:10.1016/j.dialis.2014.08.001.
[56] A. Méndez-Durán, J. Francisco Méndez-Bueno, T. Tapia-Yañez, A.M. Montes, L. Aguilar-Sánchez, Epidemiologia de la insuficiencia renal cronica en México, Dial. y Traspl. 31 (2010) 7–11. doi:10.1016/S1886-2845(10)70004-7.
[57] D. Amato, C. Alvarez-Agular, R. Limones-Castañeda, E. Rodriguez, M. Avila-Diaz, F. Arreola, A. Gomez, R. Panigua, Prevalence of chronic kidney disease in an urban Mexican population, Kidney Int. 68 (2005) 11–17.
[58] M. Morlans, J.R. Laporte, X. Vidal, D. Cabeza, P.D. Stolley, End-stage renal disease and non-narcotic analgesics: a case-control study., Br. J. Clin. Pharmacol. 30 (1990) 717–23.
[59] E.D. Siew, A. Davenport, The growth of acute kidney injury: A rising tide or just closer attention to detail?, Kidney Int. 87 (2015) 46–61. doi:10.1038/ki.2014.293.
[60] A.C. Webster, E. V. Nagler, R.L. Morton, P. Masson, Chronic Kidney Disease, Lancet. 389 (2017) 1238–1252. doi:10.1016/S0140-6736(16)32064-5.
[61] O. Akinlolu, Addressing the global burden of chronic kidney disease through clinical and translational research., Trans. Am. Clin. Climatol. Assoc. 125 (2014) 229–43; discussion 243-6.
[62] V. Jha, G. Garcia-Garcia, K. Iseki, Z. Li, S. Naicker, B. Plattner, R. Saran, A.Y.M. Wang, C.W. Yang, Chronic kidney disease: Global dimension and perspectives, Lancet. 382 (2013) 260–272. doi:10.1016/S0140-6736(13)60687-X.
[63] K. Doi, H. Rabb, Impact of acute kidney injury on distant organ function: Recent findings and potential therapeutic targets, Kidney Int. 89 (2016) 555–564. doi:10.1016/j.kint.2015.11.019.
[64] P.S. Brookes, Y.S. Yoon, J.L. Robotham, M.W. Anders, S.S. Sheu, Calcium, ATP, and ROS: a mitochondrial love-hate triangle, Am. J. Physiol. Physiol. 287 (2004) C817–C833. doi:10.1152/ajpcell.00139.2004.
[65] P. Mukhopadhyay, B. Horváth, Z. Zsengellér, J. Zielonka, G. Tanchian, E. Holovac, M. Kechrid, V. Patel, I.E. Stillman, S.M. Parikh, J. Joseph, B. Kalyanaraman, P. Pacher, Mitochondrial-targeted antioxidants represent a promising approach for prevention of

cisplatin-induced nephropathy., Free Radic. Biol. Med. 52 (2012) 497–506. doi:10.1016/j.freeradbiomed.2011.11.001.
[66] Y. Ishimoto, R. Inagi, Mitochondria: A therapeutic target in acute kidney injury, Nephrol. Dial. Transplant. 31 (2016) 1062–1069. doi:10.1093/ndt/gfv317.
[67] C. Brooks, Q. Wei, S. Cho, Z. Dong, Regulation of mitochondrial dynamics in acute kidney injury in cell culture and rodent models, 119 (2009) 1275–1285. doi:10.1172/JCI37829DS1.
[68] S. Granata, G. Zaza, S. Simone, G. Villani, D. Latorre, P. Pontrelli, M. Carella, F.P. Schena, G. Grandaliano, G. Pertosa, Mitochondrial dysregulation and oxidative stress in patients with chronic kidney disease, BMC Genomics. 10 (2009) 1–13. doi:10.1186/1471-2164-10-388.
[69] E. Molina-Jijón, O.E. Aparicio-Trejo, R. Rodríguez-Muñoz, J.C. León-Contreras, M. del Carmen Cárdenas-Aguayo, O.N. Medina-Campos, E. Tapia, L.G. Sánchez-Lozada, R. Hernández-Pando, J.L. Reyes, L. Arreola-Mendoza, J. Pedraza-Chaverri, The nephroprotection exerted by curcumin in maleate-induced renal damage is associated with decreased mitochondrial fission and autophagy, BioFactors. (2016). doi:10.1002/biof.1313.
[70] G. Zaza, S. Granata, V. Masola, C. Rugiu, F. Fantin, L. Gesualdo, F.P. Schena, A. Lupo, Downregulation of Nuclear-Encoded Genes of Oxidative Metabolism in Dialyzed Chronic Kidney Disease Patients, PLoS One. 8 (2013) 1–9. doi:10.1371/journal.pone.0077847.
[71] J.P. Hayslett, M. Kashgarian, F.H. Epstein, Functional correlates of compensatory renal hypertrophy., J. Clin. Invest. 47 (1968) 774–799. doi:10.1172/JCI105772.
[72] K. Tabei, D.J. Levenson, B.M. Brenner, Early enhancement of fluid transport in rabbit proximal straight tubules after loss of contralateral renal excretory function, J. Clin. Invest. 72 (1983) 871–881. doi:10.1172/JCI111058.
[73] O.E. Aparicio-Trejo, E. Tapia, E. Molina-Jijón, O.N. Medina-Campos, N.A. Macías-Ruvalcaba, J.C. León-Contreras, R. Hernández-Pando, F.E. García-Arroyo, M. Crist??bal, L.G. Sánchez-Lozada, J. Pedraza-Chaverri, Curcumin prevents mitochondrial dynamics disturbances in early 5/6 nephrectomy: Relation to oxidative stress and mitochondrial bioenergetics, BioFactors. 43 (2017) 293–310. doi:10.1002/biof.1338.
[74] L. V Fedorova, A. Tamirisa, D.J. Kennedy, S.T. Haller, G. Budnyy, J.I. Shapiro, D. Malhotra, Mitochondrial impairment in the five-sixth nephrectomy model of chronic renal failure: proteomic approach., BMC Nephrol. 14 (2013) 209–230. http://www.pubmedcentral.nih.gov/articlerender.fcgi?artid=3851543&tool=pmcentrez&rendertype=abstract.
[75] W. DIng, T. Liu, X. Bi, Z. Zhang, Mitochondria-Targeted Antioxidant Mito-Tempo Protects Against Aldosterone-Induced Renal Injury in Vivo, Cell. Physiol. Biochem. 44 (2017) 741–750. doi:10.1159/000485287.
[76] J.M. Forbes, D.R. Thorburn, Mitochondrial dysfunction in diabetic kidney disease, Nat. Rev. Nephrol. 14 (2018) 291–312. doi:10.1038/nrneph.2018.9.
[77] S. Hwang, R. Bohman, P. Navas, J.T. Norman, T. Bradley, L.G. Fine, Hypertrophy of renal mitochondria., J. Am. Soc. Nephrol. 1 (1990) 822–7.
[78] S. Kume, T. Uzu, S. Araki, T. Sugimoto, K. Isshiki, M. Chin-Kanasaki, M. Sakaguchi, N. Kubota, Y. Terauchi, T. Kadowaki, M. Haneda, A. Kashiwagi, D. Koya, Role of altered renal lipid metabolism in the development of renal injury induced by a high-fat diet., J. Am. Soc. Nephrol. 18 (2007) 2715–2723. doi:10.1681/ASN.2007010089.
[79] H.H. Szeto, S. Liu, Y. Soong, N. Alam, G.T. Prusky, S. V. Seshan, Protection of mitochondria prevents high-fat diet induced glomerulopathy and proximal tubular injury, Kidney Int. 90 (2016) 997–1011. doi:10.1016/j.kint.2016.06.013.
[80] S. Hallan, M. Afkarian, L.R. Zelnick, B. Kestenbaum, S. Sharma, R. Saito, M. Darshi, G. Barding, D. Raftery, W. Ju, M. Kretzler, K. Sharma, I.H. de Boer, Metabolomics and Gene Expression Analysis Reveal Down-regulation of the Citric Acid (TCA) Cycle in Non-diabetic CKD Patients, EBioMedicine. 26 (2017) 68–77. doi:10.1016/j.ebiom.2017.10.027.
[81] M.T. Coughlan, T.-V. Nguyen, S.A. Penfold, G.C. Higgins, V. Thallas-Bonke, S.M. Tan, N.J. Van Bergen, K.C. Sourris, B.E. Harcourt, D.R. Thorburn, I.A. Trounce, M.E. Cooper, J.M. Forbes, Mapping time-course mitochondrial adaptations in the kidney in experimental diabetes, Clin. Sci. 130 (2016) 711–720. doi:10.1042/cs20150838.
[82] Mackenzie Walser, Progression of chronic renal failure in man, Kidney Int. 37 (1990)

1195–1210.
[83] A. Priyadarshi, S. Periyasamy, T.J. Burke, S.L. Britton, D. Malhotra, J.I. Shapiro, Effects of reduction of renal mass on renal oxygen tension and erythropoietin production in the rat, Kidney Int. 61 (2002) 542–546. doi:10.1046/j.1523-1755.2002.00140.x.
[84] B.M. Brenner, Nephron adaptation to renal injury or ablation., Am. J. Physiol. 249 (1985) F324–F337. doi:10.1152/ajprenal.1985.249.3.F324.
[85] L. Sun, Q. Yuan, T. Xu, L. Yao, J. Feng, J. Ma, L. Wang, C. Lu, D. Wang, Pioglitazone Improves Mitochondrial Function in the Remnant Kidney and Protects against Renal Fibrosis in 5/6 Nephrectomized Rats, Front. Pharmacol. 8 (2017) 1–10. doi:10.3389/fphar.2017.00545.
[86] H. Zhao, Y. jun Liu, Z. rui Liu, D. dong Tang, X. wen Chen, Y. hua Chen, R. ning Zhou, S. qi Chen, H. xin Niu, Role of mitochondrial dysfunction in renal fibrosis promoted by hypochlorite-modified albumin in a remnant kidney model and protective effects of antioxidant peptide SS-31, Eur. J. Pharmacol. 804 (2017) 57–67. doi:10.1016/j.ejphar.2017.03.037.
[87] O.E. Aparicio-Trejo, E. Tapia, L.G. Sánchez-Lozada, J. Pedraza-Chaverri, Mitochondrial bioenergetics, redox state, dynamics and turnover alterations in renal mass reduction models of chronic kidney diseases and their possible implications in the progression of this illness, Pharmacol. Res. 135 (2018) 1–11. doi:10.1016/j.phrs.2018.07.015.
[88] Y. Hui, M. Lu, Y. Han, H. Zhou, W. Liu, L. Li, R. Jin, Resveratrol improves mitochondrial function in the remnant kidney from 5/6 nephrectomized rats, Acta Histochem. 119 (2017) 392–399. doi:10.1016/j.acthis.2017.04.002.
[89] H.H. Szeto, S. Liu, Y. Soong, S. V. Seshan, L. Cohen-Gould, V. Manichev, L.C. Feldman, T. Gustafsson, Mitochondria Protection after Acute Ischemia Prevents Prolonged Upregulation of IL-1β and IL-18 and Arrests CKD., J. Am. Soc. Nephrol. 28 (2017) 1437–1449. doi:10.1681/ASN.2016070761.
[90] M.T. Sweetwyne, J.W. Pippin, D.G. Eng, K.L. Hudkins, Y.A. Chiao, M.D. Campbell, D.J. Marcinek, C.E. Alpers, H.H. Szeto, P.S. Rabinovitch, S.J. Shankland, The mitochondrial-targeted peptide, SS-31, improves glomerular architecture in mice of advanced age, Kidney Int. 91 (2017) 1126–1145. doi:10.1016/j.kint.2016.10.036.
[91] L.H. Lash, D.A. Putt, S.J. Horky, R.K. Zalups, Functional and toxicological characteristics of isolated renal mitochondria: Impact of compensatory renal growth, Biochem. Pharmacol. 62 (2001) 383–395. doi:10.1016/S0006-2952(01)00673-6.
[92] J.L. Thomas, H. Pham, Y. Li, E. Hall, G.A. Perkins, S.S. Ali, H.H. Patel, P. Singh, Hypoxia-inducible factor-1α activation improves renal oxygenation and mitochondrial function in early chronic kidney disease, Am. J. Physiol. - Ren. Physiol. 313 (2017) F282 LP-F290. doi:10.1152/ajprenal.00579.2016.
[93] E. Tapia, V. Soto, K.M. Ortiz-Vega, G. Zarco-Márquez, E. Molina-Jijón, M. Cristóbal-García, J. Santamaría, W.R. García-Niño, F. Correa, C. Zazueta, J. Pedraza-Chaverri, Curcumin induces Nrf2 nuclear translocation and prevents glomerular hypertension, hyperfiltration, oxidant stress, and the decrease in antioxidant enzymes in 5/6 nephrectomized rats, Oxid. Med. Cell. Longev. 2013 (2012) 1–14. doi:10.1155/2012/269039.
[94] J. Trujillo, Y.I. Chirino, E. Molina-Jijón, A.C. Andérica-Romero, E. Tapia, J. Pedraza-Chaverrí, Renoprotective effect of the antioxidant curcumin: Recent findings., Redox Biol. 1 (2013) 448–456. doi:10.1016/j.redox.2013.09.003.
[95] B. Benipal, L.H. Lash, Influence of renal compensatory hypertrophy on mitochondrial energetics and redox status, Biochem. Pharmacol. 81 (2011) 295–303. doi:10.1016/j.bcp.2010.10.010.
[96] R.J. Mailloux, J.R. Treberg, Protein S-glutathionlyation links energy metabolism to redox signaling in mitochondria, Redox Biol. 8 (2016) 110–118. doi:10.1016/j.redox.2015.12.010.
[97] R.J. Mailloux, X. Jin, W.G. Willmore, Redox regulation of mitochondrial function with emphasis on cysteine oxidation reactions, Redox Biol. 2 (2014) 123–139. doi:10.1016/j.redox.2013.12.011.
[98] E. Molina-Jijón, E. Tapia, C. Zazueta, M. El Hafidi, Z.L. Zatarain-Barrón, R. Hernández-Pando, O.N. Medina-Campos, G. Zarco-Márquez, I. Torres, J. Pedraza-Chaverri, Curcumin prevents Cr(VI)-induced renal oxidant damage by a mitochondrial pathway, Free Radic. Biol. Med. 51 (2011) 1543–1557. doi:10.1016/j.freeradbiomed.2011.07.018.
[99] E. Tapia, L.G. Sánchez-Lozada, W.R. García-Niño, E. García, a Cerecedo, F.E. García-

Arroyo, H. Osorio, a Arellano, M. Cristóbal-García, M.L. Loredo, E. Molina-Jijón, J. Hernández-Damián, M. Negrette-Guzmán, C. Zazueta, S. Huerta-Yepez, J.L. Reyes, M. Madero, J. Pedraza-Chaverrí, Curcumin prevents maleate-induced nephrotoxicity: Relation to hemodynamic alterations, oxidative stress, mitochondrial oxygen consumption and activity of respiratory complex I., Free Radic. Res. 48 (2014) 1342–54. doi:10.3109/10715762.2014.954109.

[100] J. Trujillo, L.F. Granados-Castro, C. Zazueta, A.C. Andérica-Romero, Y.I. Chirino, J. Pedraza-Chaverrí, Mitochondria as a target in the therapeutic properties of curcumin, Arch. Pharm. (Weinheim). 347 (2014) 873–884. doi:10.1002/ardp.201400266.

[101] L.M. Reyes-Fermín, S.H. Avila-Rojas, O.E. Aparicio-Trejo, E. Tapia, I. Rivero, J. Pedraza-Chaverri, The Protective Effect of Alpha-Mangostin against Cisplatin-Induced Cell Death in LLC-PK1 Cells is Associated to Mitochondrial Function Preservation, Antioxidants. 8 (2019) 133. doi:10.3390/antiox8050133.

[102] S.H. Avila-Rojas, E. Tapia, A. Briones-Herrera, O.E. Aparicio-Trejo, J.C. León-Contreras, R. Hernández-Pando, J. Pedraza-Chaverri, Curcumin prevents potassium dichromate (K2Cr2O7)-induced renal hypoxia, Food Chem. Toxicol. 121 (2018) 472–482. doi:10.1016/j.fct.2018.09.046.

[103] W. Ding, H. Guo, C. Xu, B. Wang, M. Zhang, F. Ding, Mitochondrial reactive oxygen species-mediated NLRP3 inflammasome activation contributes to aldosterone-induced renal tubular cells injury, Oncotarget. 7 (2016). doi:10.18632/oncotarget.8243.

[104] E. Molina-Jijón, O.E. Aparicio-Trejo, R. Rodríguez-Muñoz, J.C. León-Contreras, M. del Carmen Cárdenas-Aguayo, O.N. Medina-Campos, E. Tapia, L.G. Sánchez-Lozada, R. Hernández-Pando, J.L. Reyes, L. Arreola-Mendoza, J. Pedraza-Chaverri, The nephroprotection exerted by curcumin in maleate-induced renal damage is associated with decreased mitochondrial fission and autophagy, BioFactors. 42 (2016) 686–702. doi:10.1002/biof.1313.

[105] K.A. Nath, A.J. Croatt, T.H. Hostetter, Oxygen consumption and oxidant stress in surviving nephrons., Am. J. Physiol. 258 (1990) F1354-62.

[106] P. Wenzel, H. Mollnau, M. Oelze, E. Schulz, J.M.D. Wickramanayake, J. Müller, S. Schuhmacher, M. Hortmann, S. Baldus, T. Gori, R.P. Brandes, T. Münzel, A. Daiber, First evidence for a crosstalk between mitochondrial and NADPH oxidase-derived reactive oxygen species in nitroglycerin-triggered vascular dysfunction., Antioxid. Redox Signal. 10 (2008) 1435–47. doi:10.1089/ars.2007.1969.

[107] A. Daiber, Redox signaling (cross-talk) from and to mitochondria involves mitochondrial pores and reactive oxygen species., Biochim. Biophys. Acta. 1797 (2010) 897–906. doi:10.1016/j.bbabio.2010.01.032.

[108] Y. Liu, Y. Wang, W. Ding, Y. Wang, Mito-TEMPO Alleviates Renal Fibrosis by Reducing Inflammation, Mitochondrial Dysfunction, and Endoplasmic Reticulum Stress, Oxid. Med. Cell. Longev. 2018 (2018) 1–13. doi:10.1155/2018/5828120.

[109] R. Kozieł, H. Pircher, M. Kratochwil, B. Lener, M. Hermann, N. a Dencher, P. Jansen-Dürr, Mitochondrial respiratory chain complex I is inactivated by NADPH oxidase Nox4., Biochem. J. 452 (2013) 231–9. doi:10.1042/BJ20121778.

[110] H. Wang, X. Chen, Y. Su, P. Paueksakon, W. Hu, M.-Z. Zhang, R.C. Harris, T.S. Blackwell, R. Zent, A. Pozzi, P47(Phox) Contributes To Albuminuria and Kidney Fibrosis in Mice., Kidney Int. 87 (2015) 948–962. doi:10.1038/ki.2014.386.

[111] M. Sedeek, R. Nasrallah, R.M. Touyz, R.L. Hébert, NADPH oxidases, reactive oxygen species, and the kidney: friend and foe., J. Am. Soc. Nephrol. 24 (2013) 1512–8. doi:10.1681/ASN.2012111112.

[112] H. Watanabe, Y. Miyamoto, D. Honda, H. Tanaka, Q. Wu, M. Endo, T. Noguchi, D. Kadowaki, Y. Ishima, S. Kotani, M. Nakajima, K. Kataoka, S. Kim-Mitsuyama, M. Tanaka, M. Fukagawa, M. Otagiri, T. Maruyama, p-Cresyl sulfate causes renal tubular cell damage by inducing oxidative stress by activation of NADPH oxidase., Kidney Int. 83 (2013) 582–92. doi:10.1038/ki.2012.448.

[113] A.M. Garrido, K.K. Griendling, NADPH oxidases and angiotensin II receptor signaling., Mol. Cell. Endocrinol. 302 (2009) 148–58. doi:10.1016/j.mce.2008.11.003.

[114] H.J. Kim, N.D. Vaziri, Contribution of impaired Nrf2-Keap1 pathway to oxidative stress and inflammation in chronic renal failure., Am. J. Physiol. Renal Physiol. 298 (2010) F662-71. doi:10.1152/ajprenal.00421.2009.

[115] N.D. Vaziri, Y. Bai, Z. Ni, Y. Quiroz, R. Pandian, B. Rodriguez-Iturbe, Intra-renal angiotensin II/AT1 receptor, oxidative stress, inflammation, and progressive injury in

renal mass reduction., J. Pharmacol. Exp. Ther. 323 (2007) 85–93. doi:10.1124/jpet.107.123638.
[116] A. Görlach, E.Y. Dimova, A. Petry, A. Martínez-Ruiz, P. Hernansanz-Agustín, A.P. Rolo, C.M. Palmeira, T. Kietzmann, Reactive oxygen species, nutrition, hypoxia and diseases: Problems solved?, Redox Biol. 6 (2015) 372–385. doi:10.1016/j.redox.2015.08.016.
[117] A. Voulgaris, O. Marrone, M.R. Bonsignore, P. Steiropoulos, Chronic kidney disease in patients with obstructive sleep apnea. A narrative review., Sleep Med. Rev. 47 (2019) 74–89. doi:10.1016/j.smrv.2019.07.001.
[118] Y. Yuan, Y. Chen, P. Zhang, S. Huang, C. Zhu, G. Ding, B. Liu, T. Yang, A. Zhang, Mitochondrial dysfunction accounts for aldosterone-induced epithelial-to-mesenchymal transition of renal proximal tubular epithelial cells, Free Radic. Biol. Med. 53 (2012) 30–43. doi:10.1016/j.freeradbiomed.2012.03.015.
[119] P.H.G.M. Willems, R. Rossignol, C.E.J. Dieteren, M.P. Murphy, W.J.H. Koopman, Redox Homeostasis and Mitochondrial Dynamics, Cell Metab. 22 (2015) 207–218. doi:10.1016/j.cmet.2015.06.006.
[120] H.M. Ni, J.A. Williams, W.X. Ding, Mitochondrial dynamics and mitochondrial quality control, Redox Biol. 4 (2015) 6–13. doi:10.1016/j.redox.2014.11.006.
[121] B. Westermann, Mitochondrial fusion and fission in cell life and death, Nat. Rev. Mol. Cell Biol. 11 (2010) 872–884. doi:10.1038/nrm3013.
[122] T.M. Durcan, E.A. Fon, The three ‘ P ’ s of mitophagy : PARKIN , modifications, Genes Dev. 29 (2015) 989–999. doi:10.1101/gad.262758.115.GENES.
[123] G. Nowak, D. Bakajsova, A.M. Samarel, Protein kinase C-epsilon activation induces mitochondrial dysfunction and fragmentation in renal proximal tubules., Am. J. Physiol. Renal Physiol. 301 (2011) F197-208. doi:10.1152/ajprenal.00364.2010.
[124] R.J. Youle, D.P. Narendra, Mechanisms of mitophagy, Nat. Rev. Mol. Cell Biol. 12 (2011) 9–14. doi:10.1038/nrm3028.
[125] S. Rovira-Llopis, C. Bañuls, N. Diaz-Morales, A. Hernandez-Mijares, M. Rocha, V.M. Victor, Mitochondrial dynamics in type 2 diabetes: Pathophysiological implications, Redox Biol. 11 (2017) 637–645. doi:10.1016/j.redox.2017.01.013.
[126] J.T. Norman, S. Hwang, L.G. Fine, D. Nephrology, T. Bradley, J. Am, Hypertrophy of renal mitochondria, J. Am. Soc. Nephrol. I (1990) 822–827.
[127] H. Zhao, Y. jun Liu, Z. rui Liu, D. dong Tang, X. wen Chen, Y. hua Chen, R. ning Zhou, S. qi Chen, H. xin Niu, Role of mitochondrial dysfunction in renal fibrosis promoted by hypochlorite-modified albumin in a remnant kidney model and protective effects of antioxidant peptide SS-31, Eur. J. Pharmacol. 804 (2017) 57–67. doi:10.1016/j.ejphar.2017.03.037.
[128] F. Ursini, M. Maiorino, H.J. Forman, Redox homeostasis: The Golden Mean of healthy living, Redox Biol. 8 (2016) 205–215. doi:10.1016/j.redox.2016.01.010.
[129] M.S. Goligorsky, Oxidative Stress and the Kidney: Riding on the Curve of Hormesis, Antioxid. Redox Signal. 25 (2016) 117–118. doi:10.1089/ars.2016.6794.
[130] G. Tamma, G. Valenti, Evaluating the Oxidative stress in Renal diseases: What is the role for S-glutathionylation?, Antioxid. Redox Signal. 25 (2016) 1–48. doi:10.1089/ars.2016.6794.
[131] C.N. White, C.C. Liu, A. Garcia, E.J. Hamilton, K.K.M. Chia, G.A. Figtree, H.H. Rasmussen, Activation of cAMP-dependent signaling induces oxidative modification of the cardiac Na+-K+ pump and inhibits its activity, J. Biol. Chem. 285 (2010) 13712–13720. doi:10.1074/jbc.M109.090225.
[132] V.-M. Bui, S.-L. Weng, C.-T. Lu, T.-H. Chang, J.T.-Y. Weng, T.-Y. Lee, SOHSite: incorporating evolutionary information and physicochemical properties to identify protein S-sulfenylation sites., BMC Genomics. 17 Suppl 1 (2016) 9. doi:10.1186/s12864-015-2299-1.
[133] M.M. Gallogly, J.J. Mieyal, Mechanisms of reversible protein glutathionylation in redox signaling and oxidative stress, Curr. Opin. Pharmacol. 7 (2007) 381–391. doi:10.1016/j.coph.2007.06.003.
[134] J.J. Mieyal, P.B. Chock, Posttranslational modification of cysteine in redox signaling and oxidative stress: Focus on s-glutathionylation., Antioxid. Redox Signal. 16 (2012) 471–5. doi:10.1089/ars.2011.4454.
[135] P.T. Kang, C.L. Chen, Y.R. Chen, Increased mitochondrial prooxidant activity mediates up-regulation of Complex i S-glutathionylation via protein thiyl radical in the murine heart of eNOS-/-, Free Radic. Biol. Med. 79 (2015) 56–68.

doi:10.1016/j.freeradbiomed.2014.11.016.
[136] A. Ortiz, M.D. Sanchez-Niño, M.C. Izquierdo, C. Martin-Cleary, L. Garcia-Bermejo, J.A. Moreno, M. Ruiz-Ortega, J. Draibe, J.M. Cruzado, M.A. Garcia-Gonzalez, J.M. Lopez-Novoa, M.J. Soler, A.B. Sanz, Translational value of animal models of kidney failure, Eur. J. Pharmacol. 759 (2015) 205–220. doi:10.1016/j.ejphar.2015.03.026.
[137] D. Chunsun, P.K. Lawrence, L. Youhua, Animal Models of Kidney Diseases, Model. Biomed. Res. (2008) 657–664.
[138] S. He, N. Liu, G. Bayliss, S. Zhuang, EGFR activity is required for renal tubular cell dedifferentiation and proliferation in a murine model of folic acid-induced acute kidney injury, AJP Ren. Physiol. 304 (2013) F356–F366. doi:10.1152/ajprenal.00553.2012.
[139] T.-C. Fang, Proliferation of Bone Marrow-Derived Cells Contributes to Regeneration after Folic Acid-Induced Acute Tubular Injury, J. Am. Soc. Nephrol. 16 (2005) 1723–1732. doi:10.1681/ASN.2004121089.
[140] A. Gupta, V. Puri, R. Sharma, S. Puri, Folic acid induces acute renal failure (ARF) by enhancing renal prooxidant state, Exp. Toxicol. Pathol. 64 (2012) 225–232. doi:10.1016/j.etp.2010.08.010.
[141] A.P. Singh, A. Muthuraman, A.S. Jaggi, N. Singh, K. Grover, R. Dhawan, Animal models of acute renal failure, Pharmacol. Reports. 64 (2012) 31–44. doi:10.1016/S1734-1140(12)70728-4.
[142] L.J. Stallons, R.M. Whitaker, R.G. Schnellmann, Suppressed mitochondrial biogenesis in folic acid-induced acute kidney injury and early fibrosis, Toxicol. Lett. 224 (2014) 326–332. doi:10.1016/j.toxlet.2013.11.014.
[143] O. Ruiz-Andres, B. Suarez-Alvarez, C. Sánchez-Ramos, M. Monsalve, M.D. Sanchez-Niño, M. Ruiz-Ortega, J. Egido, A. Ortiz, A.B. Sanz, The inflammatory cytokine TWEAK decreases PGC-1α expression and mitochondrial function in acute kidney injury, Kidney Int. 89 (2016) 399–410. doi:10.1038/ki.2015.332.
[144] M. Sharma, A. Sud, T. Kaur, C. Tandon, S.K. Singla, M. Sharma, A. Sud, T. Kaur, C. Tandon, N-acetylcysteine with apocynin prevents hyperoxaluria-induced mitochondrial protein perturbations in nephrolithiasis, 5762 (2016). doi:10.1080/10715762.2016.1221507.
[145] A. Amini, S. Masoumi-Moghaddam, D.L. Morris, Utility of bromelain and N-acetylcysteine in treatment of peritoneal dissemination of gastrointestinal mucin-producing malignancies, First eddi, Springer International, Switzerland, 2016. doi:10.1007/978-3-319-28570-2.
[146] G. Marenzi, E. Sisillo, A.L. Bartorelli, Studies on Renal Disorders, 2011. doi:10.1007/978-1-60761-857-7.
[147] G. Marenzi, E. Sisillo, A.L. Bartorelli, N -Acetylcysteine in Kidney Disease, (n.d.) 367–388. doi:10.1007/978-1-60761-857-7.
[148] X.L. Shen, Y. Zhang, W. Xu, R. Liang, J. Zheng, Y. Luo, Y. Wang, K. Huang, An iTRAQ-based mitoproteomics approach for profiling the nephrotoxicity mechanisms of ochratoxin A in HEK 293 cells, J. Proteomics. 78 (2013) 398–415. doi:10.1016/j.jprot.2012.10.010.
[149] M. Sharma, A. Sud, T. Kaur, C. Tandon, S.K. Singla, N-acetylcysteine with apocynin prevents hyperoxaluria-induced mitochondrial protein perturbations in nephrolithiasis, Free Radic. Res. 50 (2016) 1032–1044. doi:10.1080/10715762.2016.1221507.
[150] H.Z. Wang, Z.Y. Peng, X.Y. Wen, T. Rimmelé, J. V. Bishop, J.A. Kellum, N-acetylcysteine is effective for prevention but not for treatment of folic acid-induced acute kidney injury in mice, Crit. Care Med. 39 (2011) 2487–2494. doi:10.1097/CCM.0b013e31822575fc.
[151] E. Ojuka, B. Andrew, N. Bezuidenhout, S. George, G. Maarman, H.P. Madlala, A. Mendham, P.O. Osiki, Measurement of β-oxidation capacity of biological samples by respirometry: a review of principles and substrates, Am. J. Physiol. Metab. 310 (2016) E715–E723. doi:10.1152/ajpendo.00475.2015.
[152] C.M. Palmeira, A.J. Moreno, Mitochondrial Bioenergetics. Methods an Protocol, First, London, 2012.
[153] D. Cano-Ramírez, C.E. Torres-Vargas, S. Guerrero-Castillo, S. Uribe-Carvajal, R. Hernández-Pando, J. Pedraza-Chaverri, M. Orozco-Ibarra, Effect of glycolysis inhibition on mitochondrial function in rat brain, J. Biochem. Mol. Toxicol. 26 (2012) 206–211. doi:10.1002/jbt.21404.
[154] A. Briones-Herrera, S.H. Avila-Rojas, O.E. Aparicio-Trejo, M. Cristóbal, J.C. León-

Contreras, R. Hernández-Pando, E. Pinzón, J. Pedraza-Chaverri, L.G. Sánchez-Lozada, E. Tapia, Sulforaphane prevents maleic acid-induced nephropathy by modulating renal hemodynamics, mitochondrial bioenergetics and oxidative stress, Food Chem. Toxicol. 115 (2018) 185–197. doi:10.1016/j.fct.2018.03.016.
[155] M. Negrette-Guzmán, W.R. García-Niño, E. Tapia, C. Zazueta, S. Huerta-Yepez, J.C. León-Contreras, R. Hernández-Pando, O.E. Aparicio-Trejo, M. Madero, J. Pedraza-Chaverri, Curcumin Attenuates Gentamicin-Induced Kidney Mitochondrial Alterations: Possible Role of a Mitochondrial Biogenesis Mechanism, Evidence-Based Complement. Altern. Med. 2015 (2015) 1–16. doi:10.1155/2015/917435.
[156] E.T. Chouchani, L. Kazak, M.P. Jedrychowski, G.Z. Lu, B.K. Erickson, J. Szpyt, K.A. Pierce, D. Laznik-Bogoslavski, R. Vetrivelan, C.B. Clish, A.J. Robinson, S.P. Gygi, B.M. Spiegelman, Mitochondrial ROS regulate thermogenic energy expenditure and sulfenylation of UCP1, Nature. 532 (2016) 112–116. doi:10.1038/nature17399.
[157] K.J. Nelson, D. Parsonage, Measurement of peroxiredoxin activity, Curr. Protoc. Toxicol. (2011) 1–28. doi:10.1002/0471140856.tx0710s49.
[158] S. González-Reyes, S. Guzmán-Beltrán, O.N. Medina-Campos, J. Pedraza-Chaverri, Curcumin pretreatment induces Nrf2 and an antioxidant response and prevents hemin-induced toxicity in primary cultures of cerebellar granule neurons of rats, Oxid. Med. Cell. Longev. 2013 (2013). doi:10.1155/2013/801418.
[159] O.E. Aparicio-Trejo, E. Tapia, E. Molina-Jijón, O.N. Medina-Campos, N.A. Macías-Ruvalcaba, J.C. León-Contreras, R. Hernández-Pando, F.E. García-Arroyo, M. Cristóbal, L.G. Sánchez-Lozada, J. Pedraza-Chaverri, Curcumin prevents mitochondrial dynamics disturbances in early 5/6 nephrectomy: Relation to oxidative stress and mitochondrial bioenergetics, BioFactors. 43 (2017) 293–310. doi:10.1002/biof.1338.
[160] S.R. Chowdhury, J. Djordjevic, B.C. Albensi, P. Fernyhough, Simultaneous evaluation of substrate-dependent oxygen consumption rates and mitochondrial membrane potential by TMRM and safranin in cortical mitochondria, Biosci. Rep. 36 (2016) 1–12. doi:10.1042/BSR20150244.
[161] G. Krumschnabel, A. Eigentler, M. Fasching, E. Gnaiger, Use of safranin for the assessment of mitochondrial membrane potential by high-resolution respirometry and fluorometry, 1st ed., Elsevier Inc., 2014. doi:10.1016/B978-0-12-416618-9.00009-1.
[162] S. Kröller-Schön, S. Steven, S. Kossmann, A. Scholz, S. Daub, M. Oelze, N. Xia, M. Hausding, Y. Mikhed, E. Zinßius, M. Mader, P. Stamm, N. Treiber, K. Scharffetter-Kochanek, H. Li, E. Schulz, P. Wenzel, T. Münzel, A. Daiber, Molecular Mechanisms of the Crosstalk Between Mitochondria and NADPH Oxidase Through Reactive Oxygen Species—Studies in White Blood Cells and in Animal Models, Antioxid. Redox Signal. 20 (2013) 247–266. doi:10.1089/ars.2012.4953.
[163] R.P. Brandes, N. Weissmann, K. Schröder, Nox family NADPH oxidases: Molecular mechanisms of activation., Free Radic. Biol. Med. 76 (2014) 208–26. doi:10.1016/j.freeradbiomed.2014.07.046.
[164] F. Jiang, G.-S. Liu, G.J. Dusting, E.C. Chan, NADPH oxidase-dependent redox signaling in TGF-β-mediated fibrotic responses., Redox Biol. 2 (2014) 267–72. doi:10.1016/j.redox.2014.01.012.
[165] P. Gill, C. Wilcox, NADPH oxidases in the kidney, Antioxid. Redox Signal. 8 (2006) 1597–1607.
[166] P. Bhargava, R.G. Schnellmann, Mitochondrial energetics in the kidney, Nat. Rev. Nephrol. 13 (2017) 629–646. doi:10.1038/nrneph.2017.107.
[167] J. Guo, M.J. Gaffrey, D. Su, T. Liu, D.G. Camp, R.D. Smith, W.J. Qian, Resin-Assisted enrichment of thiols as a general strategy for proteomic profiling of cysteine-based reversible modifications, Nat. Protoc. 9 (2014) 64–75. doi:10.1038/nprot.2013.161.
[168] E. Molina-Jijón, O.E. Aparicio-Trejo, R. Rodríguez-Muñoz, J.C. León-Contreras, M. del Carmen Cárdenas-Aguayo, O.N. Medina-Campos, E. Tapia, L.G. Sánchez-Lozada, R. Hernández-Pando, J.L. Reyes, L. Arreola-Mendoza, J. Pedraza-Chaverri, The nephroprotection exerted by curcumin in maleate-induced renal damage is associated with decreased mitochondrial fission and autophagy, BioFactors. 42 (2016) 686–702. doi:10.1002/biof.1313.
[169] A.R. Anzell, R. Maizy, K. Przyklenk, T.H. Sanderson, Mitochondrial Quality Control and Disease: Insights into Ischemia-Reperfusion Injury, Mol. Neurobiol. 55 (2018) 2547–2564. doi:10.1007/s12035-017-0503-9.
[170] B. Ortega-Domínguez, O.E. Aparicio-Trejo, F.E. García-Arroyo, J.C. León-Contreras, E.

Tapia, E. Molina-Jijón, R. Hernández-Pando, L.G. Sánchez-Lozada, D. Barrera-Oviedo, J. Pedraza-Chaverri, Curcumin prevents cisplatin-induced renal alterations in mitochondrial bioenergetics and dynamic, Food Chem. Toxicol. 107 (2017) 373–385. doi:10.1016/j.fct.2017.07.018.
[171] F. Correa, M. Buelna-Chontal, S. Hernández-Reséndiz, W. R García-Niño, F. J Roldán, V. Soto, A. Silva-Palacios, A. Amador, J. Pedraza-Chaverrí, E. Tapia, C. Zazueta, Curcumin maintains cardiac and mitochondrial function in chronic kidney disease., Free Radic. Biol. Med. 61 (2013) 119–29. doi:10.1016/j.freeradbiomed.2013.03.017.
[172] R. Barazzoni, X. Zhu, M. Deboer, R. Datta, M.D. Culler, M. Zanetti, G. Guarnieri, D.L. Marks, Combined effects of ghrelin and higher food intake enhance skeletal muscle mitochondrial oxidative capacity and AKT phosphorylation in rats with chronic kidney disease., Kidney Int. 77 (2010) 23–8. doi:10.1038/ki.2009.411.
[173] P.G. Yazdi, H. Moradi, J.-Y. Yang, P.H. Wang, N.D. Vaziri, Skeletal muscle mitochondrial depletion and dysfunction in chronic kidney disease., Int. J. Clin. Exp. Med. 6 (2013) 532–9.
[174] M. Tamaki, K. Miyashita, S. Wakino, M. Mitsuishi, K. Hayashi, H. Itoh, Chronic kidney disease reduces muscle mitochondria and exercise endurance and its exacerbation by dietary protein through inactivation of pyruvate dehydrogenase., Kidney Int. 85 (2014) 1330–9. doi:10.1038/ki.2013.473.
[175] B. Benipal, L.H. Lash, Modulation of mitochondrial glutathione status and cellular energetics in primary cultures of proximal tubular cells from remnant kidney of uninephrectomized rats, Biochem. Pharmacol. 85 (2013) 1379–1388. doi:10.1016/j.bcp.2013.02.013.
[176] O.E. Aparicio-Trejo, E. Tapia, L.G. Sánchez-Lozada, J. Pedraza-Chaverri, Mitochondrial bioenergetics, redox state, dynamics and turnover alterations in renal mass reduction models of chronic kidney diseases and their possible implications in the progression of this illness, Pharmacol. Res. 135 (2018) 1–11. doi:10.1016/j.phrs.2018.07.015.
[177] K. Stadler, I.J. Goldberg, K. Susztak, The Evolving Understanding of the Contribution of Lipid Metabolism to Diabetic Kidney Disease, Curr. Diab. Rep. 15 (2015). doi:10.1007/s11892-015-0611-8.
[178] H.M. Kang, S.H. Ahn, P. Choi, Y.A. Ko, S.H. Han, F. Chinga, A.S.D. Park, J. Tao, K. Sharma, J. Pullman, E.P. Bottinger, I.J. Goldberg, K. Susztak, Defective fatty acid oxidation in renal tubular epithelial cells has a key role in kidney fibrosis development, Nat. Med. 21 (2015) 37–46. doi:10.1038/nm.3762.
[179] F. Afshinnia, T.M. Rajendiran, T. Soni, J. Byun, S. Wernisch, K.M. Sas, J. Hawkins, K. Bellovich, D. Gipson, G. Michailidis, S. Pennathur, Impaired β -Oxidation and Altered Complex Lipid Fatty Acid Partitioning with Advancing CKD , J. Am. Soc. Nephrol. 29 (2018) 295–306. doi:10.1681/asn.2017030350.
[180] B. Ortega-Domínguez, O.E. Aparicio-Trejo, F.E. García-Arroyo, J.C. León-Contreras, E. Tapia, E. Molina-Jijón, R. Hernández-Pando, L.G. Sánchez-Lozada, D. Barrera-Oviedo, J. Pedraza-Chaverri, Curcumin prevents cisplatin-induced renal alterations in mitochondrial bioenergetics and dynamic, Food Chem. Toxicol. 107 (2017) 373–385. doi:10.1016/j.fct.2017.07.018.
[181] M. Negrette-Guzmán, W.R. García-Niño, E. Tapia, C. Zazueta, S. Huerta-Yepez, J.C. León-Contreras, R. Hernández-Pando, O.E. Aparicio-Trejo, M. Madero, J. Pedraza-Chaverri, Curcumin Attenuates Gentamicin-Induced Kidney Mitochondrial Alterations: Possible Role of a Mitochondrial Biogenesis Mechanism, Evidence-Based Complement. Altern. Med. 2015 (2015) 1–16. doi:10.1155/2015/917435.
[182] M.S. Szczypka, A.J. Westover, S.G. Clouthier, J.L.M. Ferrara, H.D. Humes, Rare Incorporation of Bone Marrow-Derived Cells Into Kidney After Folic Acid-Induced Injury, Stem Cells. 23 (2005) 44–54. doi:10.1634/stemcells.2004–0111.
[183] G.S. Ducker, J.D. Rabinowitz, One-Carbon Metabolism in Health and Disease, Cell Metab. 25 (2017) 27–42. doi:10.1016/j.cmet.2016.08.009.
[184] F.H. Nazki, A.S. Sameer, B.A. Ganaie, Folate: Metabolism, genes, polymorphisms and the associated diseases, Gene. 533 (2014) 11–20. doi:10.1016/j.gene.2013.09.063.
[185] J.T. Fox, P.J. Stover, Folate-Mediated One-Carbon Metabolism, Vitam. Horm. 79 (2008) 1–44. doi:10.1016/S0083-6729(08)00401-9.
[186] C.D. Chancy, R. Kekuda, W. Huang, P.D. Prasad, J.M. Kuhnel, F.M. Sirotnak, P. Roon, V. Ganapathy, S.B. Smith, Expression and differential polarization of the reduced-folate transporter-1 and the folate receptor α in mammalian retinal pigment epithelium, J. Biol.

Chem. 275 (2000) 20676–20684. doi:10.1074/jbc.M002328200.
[187] L.B. Bailey, Folate in Health and Disease, 2nd ed., Taylor & Francis, Washington, D.C., 2009.
[188] M.E. Huguenin, A. Birbaumer, F.P. Brunner, J. Thorhorst, U. Schmidt, U.C. Dubach, G. Thiel, An evaluation of the role of tubular obstruction in Folic Acid-Induced Acute renal failure in the rat, Nephron. 22 (1978) 41–45.
[189] E.Y. Plotnikov, A. V. Kazachenko, M.Y. Vyssokikh, A.K. Vasileva, D. V. Tcvirkun, N.K. Isaev, V.I. Kirpatovsky, D.B. Zorov, The role of mitochondria in oxidative and nitrosative stress during ischemia/reperfusion in the rat kidney, Kidney Int. 72 (2007) 1493–1502. doi:10.1038/sj.ki.5002568.
[190] H.H. Szeto, S. Liu, Y. Soong, D. Wu, S.F. Darrah, F.-Y. Cheng, Z. Zhao, M. Ganger, C.Y. Tow, S. V. Seshan, Mitochondria-Targeted Peptide Accelerates ATP Recovery and Reduces Ischemic Kidney Injury, J. Am. Soc. Nephrol. 22 (2011) 1041–1052. doi:10.1681/ASN.2010080808.
[191] P.T. Kang, L. Zhang, C.L. Chen, J. Chen, K.B. Green, Y.R. Chen, Protein thiyl radical mediates S-glutathionylation of complex i, Free Radic. Biol. Med. 53 (2012) 962–973. doi:10.1016/j.freeradbiomed.2012.05.025.
[192] M. Forkink, F. Basit, J. Teixeira, H.G. Swarts, W.J.H. Koopman, P.H.G.M. Willems, Complex I and complex III inhibition specifically increase cytosolic hydrogen peroxide levels without inducing oxidative stress in HEK293 cells, Redox Biol. 6 (2015) 607–616. doi:10.1016/j.redox.2015.09.003.
[193] J. Garcia, D. Han, H. Sancheti, L.P. Yap, N. Kaplowitz, E. Cadenas, Regulation of mitochondrial glutathione redox status and protein glutathionylation by respiratory substrates, J. Biol. Chem. 285 (2010) 39646–39654. doi:10.1074/jbc.M110.164160.
[194] S.-B. Wang, C.I. Murray, H.S. Chung, J.E. Van Eyk, Redox regulation of mitochondrial ATP synthase., Trends Cardiovasc. Med. 23 (2013) 14–8. doi:10.1016/j.tcm.2012.08.005.
[195] A. Ortiz, C. Lorz, M.P. Catalan, T.M. Danoff, Y. Yamasaki, J. Egido, E.G. Neilson, Expression of apoptosis regulatory proteins in tubular epithelium stressed in culture or following acute renal failure, Kidney Int. 57 (2000) 969–981. doi:10.1046/j.1523-1755.2000.00925.x.
[196] C. Dai, J. Yang, Y. Liu, Single Injection of Naked Plasmid Encoding Hepatocyte Growth Factor Prevents Cell Death and Ameliorates Acute Renal Failure in Mice, J. Am. Soc. Nephrol. 13 (2002) 411–422. http://jasn.asnjournals.org/content/13/2/411%5Cnhttp://jasn.asnjournals.org/content/13/2/411.full.pdf%5Cnhttp://jasn.asnjournals.org/content/13/2/411.short%5Cnhttp://www.ncbi.nlm.nih.gov/pubmed/11805170.
[197] K. Doi, K. Okamoto, K. Negishi, Y. Suzuki, A. Nakao, T. Fujita, A. Toda, T. Yokomizo, Y. Kita, Y. Kihara, S. Ishii, T. Shimizu, E. Noiri, Attenuation of folic acid-induced renal inflammatory injury in platelet-activating factor receptor-deficient mice, Am. J. Pathol. 168 (2006) 1413–1424. doi:10.2353/ajpath.2006.050634.
[198] A. Ortega, D. Rámila, A. Izquierdo, L. González, A. Barat, R. Gazapo, R.J. Bosch, P. Esbrit, Role of the renin-angiotensin system on the parathyroid hormone-related protein overexpression induced by nephrotoxic acute renal failure in the rat., J. Am. Soc. Nephrol. 16 (2005) 939–949. doi:10.1681/ASN.2004040328.
[199] T. Wai, T. Langer, Mitochondrial Dynamics and Metabolic Regulation, Trends Endocrinol. Metab. 27 (2016) 105–117. doi:10.1016/j.tem.2015.12.001.
[200] L. Xiao, X. Xu, F. Zhang, M. Wang, Y. Xu, D. Tang, J. Wang, Y. Qin, Y. Liu, C. Tang, L. He, A. Greka, Z. Zhou, F. Liu, Z. Dong, L. Sun, The mitochondria-targeted antioxidant MitoQ ameliorated tubular injury mediated by mitophagy in diabetic kidney disease via Nrf2/PINK1, Redox Biol. 11 (2017) 297–311. doi:10.1016/j.redox.2016.12.022.
[201] Y. Zhao, Y. Guo, Y. Jiang, X. Zhu, Y. Liu, X. Zhang, Mitophagy regulates macrophage phenotype in diabetic nephropathy rats, Biochem. Biophys. Res. Commun. 494 (2017) 42–50. doi:10.1016/j.bbrc.2017.10.088.
[202] S. Hallan, K. Sharma, The Role of Mitochondria in Diabetic Kidney Disease, Curr. Diab. Rep. 16 (2016) 1–9. doi:10.1007/s11892-016-0748-0.
[203] O.E. Aparicio-Trejo, E. Tapia, L.G. Sánchez-Lozada, J. Pedraza-Chaverri, Mitochondrial bioenergetics, redox state, dynamics and turnover alterations in renal mass reduction models of chronic kidney diseases and their possible implications in the progression of this illness, Pharmacol. Res. 135 (2018) 1–11. doi:10.1016/j.phrs.2018.07.015.

[204] W. Zhang, Y. Yang, H. Gao, Y. Zhang, Z. Jia, S. Huang, Inhibition of Mitochondrial Complex I Aggravates Folic Acid-Induced Acute Kidney Injury, 210008 (2019) 1002–1013. doi:10.1159/000501934.
[205] B. Feng, R. Meng, B. Huang, Y. Bi, S. Shen, D. Zhu, Silymarin protects against renal injury through normalization of lipid metabolism and mitochondrial biogenesis in high fat-fed mice, Free Radic. Biol. Med. 110 (2017) 240–249. doi:10.1016/j.freeradbiomed.2017.06.009.
[206] L. Xiao, X. Xu, F. Zhang, M. Wang, Y. Xu, D. Tang, J. Wang, Y. Qin, Y. Liu, C. Tang, L. He, A. Greka, Z. Zhou, F. Liu, Z. Dong, L. Sun, The mitochondria-targeted antioxidant MitoQ ameliorated tubular injury mediated by mitophagy in diabetic kidney disease via Nrf2/PINK1, Redox Biol. 11 (2017) 297–311. doi:10.1016/j.redox.2016.12.022.

12.Indice de figuras.

Figura	Pagina
Figura 1. Estructura de la nefrona	12
Figura 2. Mecanismo Nox/mitocondria de aumento de la producción de ROS	19
Figura 3. Esquema del primer modelo experimental in vivo correspondiente a la fase aguda a las 24 h	28
Figura 4. Esquema del segundo modelo experimental correspondiente a la evolución temporal de los 4 grupos experimentales	29
Figura 5. Reacciones acopladas utilizadas para determinar de manera indirecta la actividad de la ATP sintasa	34
Figura 6. Sistema utilizado para determinar la actividad de la superóxido dismutasa (SOD)	36
Figura 7. Sistema utilizado para determinar la actividad de la enzima glutatión peroxidasa (GPx) en homogeneizados**.**	36
Figura 8. Sistema utilizado para determinar la actividad de la enzima peroxiredoxina (Prx)	37
Figura 9. Esquema utilizado para determinar la actividad de la enzima catalasa en homogeneizados	38
Figura 10. Sistema utilizado para determinar la actividad de la enzima glutatión S-tranferasa (GST)	39
Figura 11. Sistema utilizado para determinar la actividad de la enzima glutatión reductasa (GR)	40
Figura 12. El pretratamiento con NAC evita la AKI inducida por FA	43
Figura 13. Micrografías representativas de tinción H&E de los riñones de los 4 grupos experimentales a las 24 h posteriores a la administración de FA	44
Figura 14. LA NAC previene las alteraciones en los parámetros respiratorios mitocondriales a las 24 h posteriores a la administración de FA**.**	47
Figura 15. LA NAC previene la disminución en el potencial de membrana mitocondrial (Δψm) a las 24 h posteriores a la administración de FA	48
Figura 16. LA NAC previene la disminución en la actividad de los complejos respiratorios y ATP sintasa a las 24 h posteriores a la administración de FA	49
Figura 17. LA NAC previene el aumento en la velocidad de producción de peróxido de hidrógeno (H_2O_2) mitocondrial en los diferentes estados respiratorios	50
Figura 18. LA NAC previene la disminución en la actividad de enzimas antioxidantes en mitocondrias aisladas	51
Figura 19. LA NAC previene el aumento en los marcadores de estrés oxidante en mitocondrias aisladas	51
Figura 20. LA NAC previene el aumento en la producción de ROS ligadas al NADPH y a la L-arginina	53
Figura 21. LA NAC previene el estrés oxidante en corteza renal	54
Figura 22. LA NAC previene la perdida de la S-glutationilación mitocondrial	55
Figura 23. Micrografías representativas de microscopía electrónica a las 24 h posteriores a la administración de FA	57
Figura 24. LA NAC previene las alteraciones en el desplazamiento de la dinámica mitocondrial hacia la fisión 24 h después de la administración de FA.	58

Figura 25. LA NAC previene las alteraciones en la mitofagia y autofagia 24 h después de la administración de FA 59
Figura 26. El FA induce la disminución en la biogénesis mitocondrial 24 h después de la administración de FA 60
Figura 27. La NAC previene AKI inducida por el FA y su avance hacia la CKD 65
Figura 28. La NAC previene el daño renal crónico a los 28 d después de la administración de FA 66
Figura 29. La NAC preserva los parámetros respiratorios y el potencial de membrana mitocondrial (ΔΨm) en la transición AKI-CKD inducida por FA 67
Figura 30. La NAC preserva la actividad de los complejos mitocondriales en la transición AKI-CKD inducida por FA 68
Figura 31. La NAC previene la disfunción en la β-oxidación mitocondrial en la transición AKI-CKD inducida por FA 69
Figura 32. La NAC previene la persistencia del estrés oxidante mitocondrial en la transición AKI-CKD 70
Figura 33. Esquema integrativo en la AKI 79
Figura 34. Esquema integrativo de la transición AKI-CKD 84

Free Radical Biology and Medicine 130 (2019) 379–396

Contents lists available at ScienceDirect

Free Radical Biology and Medicine

journal homepage: www.elsevier.com/locate/freeradbiomed

Original article

Protective effects of N-acetyl-cysteine in mitochondria bioenergetics, oxidative stress, dynamics and S-glutathionylation alterations in acute kidney damage induced by folic acid

Omar Emiliano Aparicio-Trejo[a], Laura María Reyes-Fermín[a], Alfredo Briones-Herrera[a], Edilia Tapia[b], Juan Carlos León-Contreras[c], Rogelio Hernández-Pando[c], Laura Gabriela Sánchez-Lozada[b], José Pedraza-Chaverri[a,*]

[a] Department of Biology, Faculty of Chemistry, National Autonomous University of Mexico (UNAM), Mexico City 04510, Mexico
[b] Department of Nephrology and Laboratory of Renal Pathophysiology, National Institute of Cardiology "Ignacio Chávez", Mexico City 14080, Mexico
[c] Experimental Pathology Section, National Institute of Medical Sciences and Nutrition "Salvador Zubirán", 14000 Mexico City, Mexico

ARTICLE INFO

Keywords:
Acute kidney damage
Folic acid
N-acetyl-cysteine
Mitochondrial bioenergetics
Mitochondrial dynamics and S-glutathionylation

ABSTRACT

Folic acid (FA)-induced acute kidney injury (AKI) is a widely used model for studies of the renal damage and its progression to chronic state. However, the molecular mechanisms by which FA induces AKI remain poorly understood. Since renal function depends on mitochondrial homeostasis, it has been suggested that mitochondrial alterations contribute to AKI development. Additionally, N-acetyl-cysteine (NAC) can be a protective agent to prevent mitochondrial and renal dysfunction in this model, given its ability to increase mitochondrial glutathione (GSH) and to control the S-glutathionylation levels, a reversible post-translational modification that has emerged as a mechanism able to link mitochondrial energy metabolism and redox homeostasis. However, this hypothesis has not been explored. The present study demonstrates for the first time that, at 24 h, FA induced mitochondrial bioenergetics, redox state, dynamics and mitophagy alterations, which are involved in the mechanisms responsible for the AKI development. On the other hand, NAC preadministration was able to prevent mitochondrial bioenergetics, redox state and dynamics alterations as well as renal damage. The protective effects of NAC on mitochondria and renal function could be related to its observed capacity to preserve the S-glutathionylation process and GSH levels in mitochondria. Taken together, our results support the idea that these mitochondrial processes can be targets for the prevention of the renal damage and its progression in FA-induced AKI model.

1. Introduction

Acute kidney injury (AKI) is characterized by a sudden deterioration of the renal functions within a relatively short time interval [1,2]. It has recently been demonstrated, in animal models and in patients, that one strong episode of AKI or a series of them may result in the development of chronic kidney disease (CKD) [3–6]. Both diseases are growing worldwide public health problems [7–11], which have high mortality rates [12]. Additionally, concerning CKD, clinical approaches are insufficient to prevent the advance of the disease [4,6,13]. This highlights the necessity of exploring the mechanisms involved in AKI development as well as its progression to CKD [1,14].

Folic acid (FA)-induced renal damage is a widely used experimental model to study AKI, because it recreates the pathology reported in the clinic [15] and is highly reproducible [16,17]. Although acute tubular necrosis, tubular obstruction, cytokines release, oxidative stress and necrotic and apoptotic processes have been implicated in this model, the molecular mechanisms by which FA induces AKI remain poorly understood [16–19]. Additionally, one high dose of FA or repeated low doses of it can induce chronic processes, such inflammation and fibrosis, making this model a valuable tool to explore the mechanisms involved in AKI to CKD transition [16,20,21].

Furthermore, in the kidney the renal reabsorption is maintained principally by mitochondrial oxidative phosphorylation (OXPHOS). Mitochondria regulate functions related to energetic homeostasis and cell signaling [22–25] and is considered one of the main sites of reactive oxygen species (ROS) production in the cell [26]. In the case of AKI *in vivo* models, the segments with high dependence on mitochondrial ATP

* Corresponding author.
E-mail address: pedraza@unam.mx (J. Pedraza-Chaverri).

https://doi.org/10.1016/j.freeradbiomed.2018.11.005
Received 17 July 2018; Received in revised form 6 October 2018; Accepted 6 November 2018
Available online 12 November 2018
0891-5849/

production, such as the proximal tubule (PT), are more prone to damage [27]. Actually, in AKI models induced by cisplatin [28], ischemia/reperfusion [29] and maleate [30], there is a correlation between tubular damage and mitochondrial bioenergetics and dynamics alterations. Nonetheless, in the case of CKD the existing information is still limited, most of the information comes from the 5/6 nephrectomy model, where impairment of mitochondrial bioenergetics and dynamics have been reported in advanced stages of chronic disease [31–34]. So, it has been hypothesized that mitochondrial bioenergetics alterations, oxidative stress and dynamics imbalance contributes to the transition from AKI to CKD [27,35,36].

It has recently been shown that the function of the many mitochondrial proteins involved in energy metabolism is regulated by post-translational modifications induced by an increase in ROS levels, such as S-glutathionylation, the reversible addition of glutathione (GSH) to cysteine residues [37–40]. In contrast with the non-enzymatic process, the enzymatic S-glutathionylation has been associated with a reduction of oxidative stress [39,41] and with processes that regulate the mitochondrial dynamics (fission-fusion) and turnover (biogenesis and mitophagy) [39,40]. Therefore, the enzymatic S-glutathionylation is a mechanism that links changes in the redox state with regulation of the energy metabolism and with mitochondrial dynamics [39–41]. In this regard, N-acetyl-cysteine (NAC), a sulfhydryl groups donor and GSH precursor [42,43], has been proposed as a possible modulator of S-glutathionylation given its ability to regulate intracellular GSH levels [39,44]. NAC has also been employed to prevent mitochondrial potential loss, oxidative stress and changes in energy metabolism in models of AKI induced by hyperoxaluria and ochratoxin A [42,45]. Furthermore, oral NAC administration in patients prevents the increase in renal damage markers in cardiac surgery and in contrast-induced nephropathy [43,46]. Hence, NAC may be a powerful agent able to prevent mitochondrial and renal dysfunction in AKI.

In FA-induced AKI model, decreases have been observed in the mRNA levels of peroxisome proliferator gamma coactivator 1α (PGC-1α), mitochondrial transcription factor A (TFAM), NADH dehydrogenase- [ubiquinone] 1 beta subcomplex subunit 8 (NDUFβ8), ATP synthase subunit β (ATPS-β), succinate dehydrogenase subunit A (Sdha) and cytochrome C oxidase subunit I (COXI), suggesting a reduction in mitochondrial biogenesis [47,48]. However, the mitochondrial bioenergetics and redox alterations and their contribution to the AKI development are still unknown. In the present study, we explored, for the first time, the mitochondrial bioenergetics, turnover and redox alterations involved in mitochondrial dysfunction in the FA-induced AKI model, and also their possible association with changes in mitochondrial S-glutathionylation and activity of the enzymes involved in the regulation of this post-translational modification. The effects of NAC on mitochondrial and renal function were also assessed. Further, we evaluated if these effects were related to the capacity of this compound to regulate the GSH/glutathione disulfide (GSSG) ratio in mitochondria.

2. Material and methods

2.1. Chemicals

Adenosine 5′-diphosphate sodium salt (ADP), amplex red, antimycin A, L-arginine, carbonyl cyanide m-chlorophenylhydrazone, fat free bovine serum albumin (BSA), carbonyl cyanide m-chlorophenylhydrazone (CCCP), collagenase from *Clostridum histolyticum* (type II), cytochrome c from equine heart, D-(+)-glucose, diphenylene iodonium (DPI), dihydroethidium (DHE), D-mannitol, decylubiquinone (DUB), 2,6-dichlorophenolindophenol sodium salt hydrate (DCPIP), 5,5′-dithio-bis (2 nitrobenzoic) acid (DTNB), ethylene glycol-bis(2-aminoethylether)-N,N,N′,N′-tetraacetic acid (EGTA), FA, GSH, glucose, glucose-6-phosphate dehydrogenase, glutathione reductase (GR), glutathione-S-transferase (GST), glutamic acid, hexokinase, 4-(2-hydroxyethyl)-1-piperazineethanesulfonic acid (HEPES), horseradish peroxidase (HRP), K-lactobionate, manganese (II) chloride ($MgCl_2$) tetrahydrate, malic acid, monochlorobimane, N-ethylmaleimide (NEM), nitroblue tetrazolium (NBT), NADPH, $NADP^+$, NADH, NAC, Percoll®, potassium cyanide (KCN), primary antibodies against p62 and β-actin, rotenone, safranin O, salmon testes deoxyribonucleic acid (DNA), sodium succinate dibasic, sodium phosphate dibasic (Na_2HPO_4), sodium phosphate monobasic (NaH_2PO_4), sodium glutamate, sodium L-ascorbate, sodium malate, sodium dodecyl sulfate (SDS), sucrose, 2,4 dinitrochlorobenzene (CDNB), dinitrophenol (DNP), taurine, tetramethyl-p-phenylene diamine (TMPD), L-N^G-nitroarginine methyl ester (L-NAME), 3-benzoxazol-2-yl-3-benzyl-3H-[1,2,3]triazolo[4,5-*d*]pyrimidin-7-yl sulfide (VAS2870), xanthine, xanthine oxidase, 2-vinylpyridine (2-VP) and 5-nm gold particles were purchased from Sigma-Aldrich (St. Louis, MO, USA). Calcium chloride ($CaCl_2$), sodium bicarbonate ($NaHCO_3$) and ethylenediaminetetraacetic acid disodium salt dihydrate (EDTA) were obtained from JT Baker (Xalostoc, Edo. Mexico, Mexico). Protease inhibitor cocktail was purchased from Roche Applied Science (Mannheim, Germany). Commercial kits from Spinreact (Girona, Spain) were used to measure blood urea nitrogen (BUN) and plasma creatinine. The sedative sodium pentobarbital (Sedalphorte^{MR}) was purchased from Salud y Bienestar Animal S.A. de C.V. (Mexico City, Mexico). Antibodies against voltage dependence anion channel (VDAC), GSH, microtubule-associated protein 1A/1B-light chain 3 I (LC3-I), malondialdehyde (MDA), PGC-1α, TFAM and 4-hydroxynonenal (4HNE) were purchased from Abcam (Cambridge, MA, USA). Antibodies against dynamin-related protein 1 (Drp1), mitochondrial fission 1 protein (Fis1), optic atrophy 1 (Opa1) and mitofusin 1 (Mfn1) and 2 (Mfn2), nuclear respiratory factor 1 (NRF1) and 2 (NRF2) and PTEN-induced putative kinase 1 (PINK1) were purchased from Santa Cruz Biotechnology (Dallas, TX, USA). Glutaredoxin (Grx) fluorescent activity assay kit was from Cayman Chemical (Ann Arbor, MI, USA). Proximal tubular cell line derived from porcine kidney (LLC-PK1, ATTC CL-101), were from American Type Culture Collection (ATCC, Rockville, MD, USA). Dulbecco's Modified Eagle's Medium (DMEM), fetal bovine serum (FBS), and penicillin/streptomycin were purchased from Biowest (Riverside, MO, USA).

2.2. Experimental design

The experimental protocol was approved by Bioethics and Research Committees from the Faculty of Chemistry (FQ/CICUAL/171/16) and was conducted according to the guidelines of Mexican Official Norm Guides for the use and care of laboratory animals (NOM-062-ZOO-1999) and for the disposal of biological residues (NOM-087-SEMARNAT-SSA1–2002). Four groups of male Wistar rats with an initial body weight between 230 and 250 g (about 10 weeks old) were employed (n = 5–6/group): (1) Vehicle, animals were injected with 0.5 ml of 300 mM $NaHCO_3$. (2) FA, they were administered with a single intraperitoneal dose of FA (300 mg kg^{-1} body weight) dissolved in 300 mM $NaHCO_3$ [18,47]. (3) NAC + FA, animals were pre-treated with NAC (300 mg/kg) 24 and 2 h before FA administration [43,49]. (4) NAC, rats only received NAC. Rats had free access to water and food and were kept in metabolic cages to collect 24 h urine.

2.3. Renal damage markers

Twenty-four hours after FA administration, animals were anesthetized with sodium pentobarbital (60 mg/kg), blood was obtained from cardiac puncture and plasma was separated and stored at 4 °C to evaluate BUN and creatinine as markers of renal damage.

2.4. Morphological studies

The histological study was performed as previously described [36]. Briefly, three kidneys each one from different animals per group were

perfused, immediately removed and sectioned; one portion of the tissue was immediately fixed by immersion in 10% formaldehyde solution dissolved in phosphate buffered saline (PBS). After one day of fixation, kidney sections were dehydrated with alcohol solutions of progressive concentration and then embedded in paraffin. Sections of 5 μm width were obtained and stained with hematoxylin/eosin for histological evaluation. For the ultrastructural study, small tissue fragments from the kidney cortex were fixed with 2.5% glutaraldehyde in 0.15 M cacodylate buffer, post-fixed with 1% osmium tetroxide, dehydrated with ethyl alcohol in ascending concentrations and infiltrated in epoxy resin. Ultrathin sections were contrasted with uranyl acetate and lead citrate, and subsequently observed with an electron microscope (Tecnai Spirit BioTwin, FEI, Hillsboro, OR, USA), immunoelectron microscopy was employed for the detection of mitochondrial fission protein Drp1. For this procedure small fragments of kidney cortex were immediately fixed by immersion in 4% paraformaldehyde dissolved in Sörensen buffer and embedded in LR-White hydrosoluble resin. Thin sections from 70 to 90 nm were mounted on nickel grids and incubated for 2 h at room temperature with polyclonal specific rabbit immunoglobulins anti-Drp1 protein; after extensive washing, grids were incubated with the secondary antibody goat anti-rabbit IgG conjugated to 5-nm gold particles. The grids were contrasted with uranium salts and analyzed with the electron microscope.

2.5. Isolation of renal mitochondria

After sacrifice, kidneys were cooled by immersion in isolation buffer (225 mM D-mannitol, 75 mM sucrose, 1 mM EDTA, 5 mM HEPES, 0.1% BSA, pH = 7.4) at 4 °C and then cut in small pieces. Mitochondria were isolated from total renal mass, tissues were homogenized in a glass Potter–Elvehjem with a TeflonVR pestle in the same buffer and mitochondria were obtained by differential centrifugation with Percoll gradients [36]. The pellet was resuspended in 100 μL of BSA-free isolation buffer and the mitochondrial total protein was measured by the Lowry method.

2.6. Mitochondrial O_2 consumption

Evaluation of mitochondrial O_2 consumption was performed with a high resolution respirometry (oxygraph O2k, OROBOROS, Innsbruck, Austria) at 37 °C. Isolated mitochondria (200 μg of total protein) were loaded into the chamber that contained 2 ml of MiR05 respiration buffer: 0.5 mM EGTA, 3 mM $MgCl_2$, 60 mM K-lactobionate, 20 mM taurine, 10 mM KH_2PO_4, 20 mM HEPES, 110 mM sucrose and 1 g/L BSA essentially fatty acid free. Electron transport was started by addition of complex I (CI) linked substrates 5 mM sodium pyruvate, 2 mM malate and 10 mM glutamate or complex II (CII) linked substrate 10 mM succinate plus 0.5 μM rotenone (CI inhibitor). Complex I plus complex II (CI + CII) respiration was achieved by addition of CI and CII linked substrates without rotenone. State 3 (S3) respiration was stimulated by the addition of 2.5 mM ADP and 2.5 μM oligomycin induced state 4 (S4o). All the above parameters were corrected by residual respiration (ROX), which was obtained by addition of 0.5 μM rotenone plus 2.5 μM antimycin A (a complex III inhibitor). The respiratory control index (RCI) was defined as the S3/S4o ratio and OXPHOS associated respiration (P) was defined as S3–S4o [50]. All reported values were normalized by total protein content.

2.7. Mitochondrial membrane potential (ΔΨm)

The changes in ΔΨm in the different respiratory states were measured as previously reported [28]. Briefly, the changes in safranin O fluorescence (2 μM) in MiR05 medium were used to monitor the changes in ΔΨm. To stimulate CI, CII or CI + CII respiration, the respective substrates were added (see above). Mitochondrial membrane potential in S3 was obtained by addition of saturant 2.5 mM ADP and in S4o by 2.5 μM oligomycin. Finally, 5 μM CCCP was added to dissipate completely the ΔΨm and to correct by the non-specific interactions. Calibration curves of safranin were employed to ensure the linearity of the assay. Results were expressed as the changes in the measurable concentration of safranin O (ΔμM of Saf O) in S3 or S4o with respect to CCCP decoupling, and the results were normalized per milligram of protein (ΔμM of Saf O/mg of protein).

2.8. ATP synthase and mitochondrial respiratory complexes activities

Mitochondrial complexes activities were assessed as previously described [28,36]. Briefly, CI activity was measured based on CI capacity to oxidize NADH while reducing DUB to $DUBH_2$, which is then oxidized by DCPIP. The CI activity is followed by the disappearance of oxidized DCPIP at 600 nm. CII activity was measured in a separate assay in presence of 2.5 μM rotenone, using the CII capacity of reduce DUB, so the decrease in the absorbance at 600 nm was proportional to the activity of CII. The activity of complex III (CIII) was evaluated using the increase in absorbance at 550 nm (cytochrome c reduction) by addition of $DUBH_2$. The activity of complex IV (CIV) was evaluated in the respiration medium MiR05 supplemented with 0.5 μM rotenone plus 2.5 μM antimycin A, the oxygen consumption was stimulated by the addition of 0.5 mM TMPD plus 2 mM ascorbate, the oxygen consumption rate was proportional to CIV activity. ATP synthase activity was measured following the reduction of $NADP^+$ at 340 nm using an enzyme-linked assay [36]. Absorbance measurements were performed at 37 °C using a Synergy-Biotek microplate reader (Biotek Instruments, Winooski, VT, USA) and the oxygen consumption rate measurements were performed using high resolution respirometry (oxygraph O2k). The specific activity of each complex was determined by the subtraction of the activity in the presence of the appropriate inhibitor from the non-inhibited one, the results were expressed as nmol/min/mg of protein.

2.9. Mitochondrial H_2O_2 production

Mitochondrial H_2O_2 was measured in an O2k-Fluorometer (OROBOROS, Innsbruck, Austria) using Amplex red as a probe. Isolated mitochondria were resuspended in 2.0 ml of MiR05 plus HRP 0.5 U/ml. Calibration curves were employed to ensure the linearity of the assay. Briefly, to obtain the H_2O_2 production rate in the different respiratory states, sequential additions were employed as previously described [51]. Basal H_2O_2 production was obtained by mitochondria addition, the production in S4 feeding CI (State 4 CI linked) was measured by addition of CI linked substrates (see above). The production in S3 feeding CI (State 3 CI linked) was measured by addition of 2.5 mM ADP. To determine CI plus CII feeding production (State 3 CI + CII linked), 10 mM sodium succinate was added. Finally, 2.5 μM oligomycin was added to determine the production in S4o (State 4 CI + CII linked).

2.10. Activity of antioxidant enzymes and oxidative stress markers in mitochondria and renal cortex

Isolated mitochondria were used for the measurements of antioxidant enzymes as previously described [51]. Briefly, Mn superoxide dismutase (MnSOD) activity was evaluated by spectrophotometry at 560 nm using NBT as a probe. Glutathione peroxidase (GPx) activity was measured by the disappearance of NADPH at 340 nm in a coupled reaction with GR. Peroxiredoxin (Prx) activity was measured following NADPH oxidation *via* thioredoxin reductase and thioredoxin-coupled assay [52]. The lipoperoxidation markers protein-MDA adducts and 4HNE were evaluated in mitochondria by Western blot (WB) [36]. The inactivation of aconitase activity was evaluated as a mitochondrial oxidative stress marker by determining the rate of formation of the intermediate product cis-aconitate at 240 nm, as we previously described [53]. Mitochondrial aconitase activity was normalized by the citrate synthase activity. Briefly, the activity of citrate synthase was

determined by recording the increase in the absorbance at 412 nm of 5-thio-2-nitrobenzoic acid (TNB) adduct [54]. Both activities were expressed as nmol per minute per milligram of protein (nmol/min/mg of protein). Additionally, catalase activity and 4HNE levels were measured in renal cortex homogenates. Briefly, the assay of catalase activity was performed based on the disappearance of 30 mM H_2O_2 at 240 nm; data were expressed as k/mg of protein (k = constant of first order).

2.11. Activity of the enzymes involved in the S-glutathionylation system in mitochondria

Isolated mitochondria were employed to determine the activities of the enzymes involved in the S-glutathionylation system: GST, GR and Grx. Briefly, GST activity was evaluated by measuring the increase in absorbance at 340 nm generated by the adduct GSH-CDNB, meanwhile GR activity was evaluated by measuring the disappearance of NADPH at 340 nm [51]. The removal of S-glutathionylation activity of the Grx was evaluated using a commercial kit. In each case, the activities were normalized by protein content. The levels of total mitochondrial protein S-glutathionylation were evaluated by WB.

2.12. Total glutathione content, GSH and GSSG levels

Total glutathione (GSH + GSSG) content and GSSG levels were measured in renal homogenates using a previously described method [55]. The total glutathione assay is based on the reaction of GSH with DTNB to produce TNB, which is detectable at 412 nm, and GSSG-TNB adduct (GS-TNB). The GR added to the assay reduces the GS-TNB to GSH, which then reacts with DTNB. The rate of change in absorbance was compared with GSH standards. The measurement of GSSG was made in a similar way, but the samples were incubated with 2-VP, which scavenges GSH; this allows for GSSG to be reduced to GSH by GR. The levels of GSH were determined by subtraction of GSH content in 2-VP-treated samples to GSH content of samples without 2-VP. All measurements were normalized by protein content.

2.13. Isolation of PT and distal tubules (DT)

PT and DT were isolated by a previously described method [36]. Briefly, the kidneys were dissected and the cortex was separated and put on a cold Petri dish. Renal tubules were isolated by Percoll gradient, the fragments of kidney were placed in 15 ml of Krebs-bicarbonate solution (KBS) buffer at 4 °C: 110 mM NaCl, 25 mM $NaHCO_3$, 3 mM KCl, 1.2 mM $CaCl_2$, 0.7 mM $MgSO_4$, 2 mM KH_2PO_4, 10 mM sodium acetate, 5.5 mM glucose, 5 mM alanine, and 0.5 g/L of BSA, pH 7,4. Tissues were cut to fine pieces and washed three times, resuspended in 10 ml of KBS containing 15 mg of collagenase and 0.5 ml 10% BSA and incubated in a water bath for 20 min at 37 °C. The tissue suspension was gently stirred and centrifuged, the pellet was resuspended in 10 ml cold KBS and this step was repeated three times to remove the collagen fibers. Then the pellet was resuspended in 30 ml of a cold mix of Percoll and KBS buffer 1:1 v/v with protease inhibitors. The suspension was centrifuged at 1071 × g for 30 min, which resulted in the formation of 4 enriched bands: the first with DT and the fourth with PT. Band content was confirmed by light microscopy observation.

2.14. ROS production in tubule segments and cortex

ROS production was performed in isolated PT and DT and kidney cortex by the fluorescent method previously described [36], where fluorogenic oxidation of DHE to ethidium (Eth) was used to measure ROS production. Respective homogenates (20 mg) were incubated with 0.02 mmol/L DHE, 0.5 mg/ml salmon testes DNA and the corresponding substrates: 0.1 mM NADPH for NADPH oxidase (NOX) and 1 mM L-arginine for nitric oxide synthase (NOS), according to previous protocols [30]. A separate test with inhibitors was performed: 10 μM DPI and 10 μM VAS2870 were used to inhibit NADPH linked ROS, and 1 mM L-NAME to inhibit L-arginine linked ROS. The assay was performed at 37 °C for 25 min and the fluorescence of the complex Eth-DNA was measured at excitation/emission wavelengths of 480/610 nm. Data were expressed as arbitrary units of fluorescence (AUF), to normalize the fluorescence intensity, each sample was divided between the respective control average and with the total amount of protein.

2.15. Protein extraction and WB

For total protein extraction, mitochondria or PT pellet were resuspended in radioimmunoprecipitation buffer (RIPA): 40 mM Tris-HCl, 150 mM NaCl, 2 mM EDTA, 10% glycerol, 1% Triton X-100, 0.5% sodium deoxycholate, and 0.2% SDS, pH 7.6. Then, the samples were incubated for 30 min at 48 °C and were sonicated three times for 30 s at low intensity in an ultrasonic processor. Homogenates were centrifuged at 14,000 × g per 40 min at 4 °C and the supernatants were collected. Thirty μg of total protein were denatured by boiling for 10 min and then diluted 1:5 in Laemmli buffer (60 mM Tris-Cl, pH = 6.8, 2% SDS, 10% glycerol, 5% β-mercaptoethanol, 0.01% bromophenol blue). Samples were loaded on 12% SDS-polyacrylamide gels and electrophoresed. Molecular weight standards were run in parallel. Proteins were transferred to polyvinylidene fluoride (PVDF) membranes. Nonspecific protein binding was blocked by incubation with 5% nonfat dry milk in PBS containing 0.4% Tween 20, for 1 h, at room temperature. Membranes were incubated overnight at 4 °C, first with the appropriated primary antibody, and then with the corresponding fluorescent secondary antibody (1:5000) for 1 h in darkness. Protein bands were detected by fluorescence in the Odyssey scanner (LI-COR Biosciences, Lincoln, NE, USA). Protein band density was analyzed by Image Studio™ Lite Software LI-COR Odyssey (LI-COR Biosciences).

2.16. Cell culture and cell viability

Proximal tubule epithelial LLC-PK1 cells were grown in DMEM, supplemented with 10% FBS and penicillin/streptomycin (100/50 U/ml) in a humidified incubator with 5% CO_2 atmosphere at 37 °C. The experiments were at density of 44 000 cell/cm^2, passage within 16–30 [53]. After 24 h of growth, the LLC-PK1 were exposed to 10 mM NAC [56] for 22 h. Subsequently, the medium was replaced by fresh 10 mM NAC for 2 h before being exposed to a different FA concentration (2.5–30 mM) for 24 h. Micrograph images were taken with a Cytation 5 Cell Imaging Multi-Mode Reader (BioTek Instruments, Winooski, VT). One brightfield colorless or brightfield color images were captured by triplicate with a 20x objective. Cells were washed with DMEM without SFB three times and replaced with fresh DMEM for brightfield colorless images and with only PBS twice for brightfield color images, to avoid rinsing off all the extracellular folic acid precipitate.

2.17. Cell respirometry

The oxygen consumption in intact cells was performed using a high resolution respirometry oxygraph O2k meter (Oroboros Instruments). After the corresponding treatment, cells were washed with PBS 1X and harvested. Determinations were made using 2 ml of culture medium with 10% FBS at 37 °C. Each experiment was started by the addition of the cells (2.404 million as a initial number), the respiratory parameters were defined as follows: Oxygen consumption in the presence of cells (Routine), leak of the respiration, corresponding to the cellular oxygen consumption in presence of 5 μM oligomycin (Leak), uncoupled respiration was achieved by titrations of 8 μL of 20 μM DNP (Uncoupled) and P was calculated by the formula: Routine-Leak. All parameters were corrected by subtracting the non-mitochondrial respiration, obtained by the addition of 1 μM rotenone plus 5 μM antimycin A, and normalized by the initial number of cells.

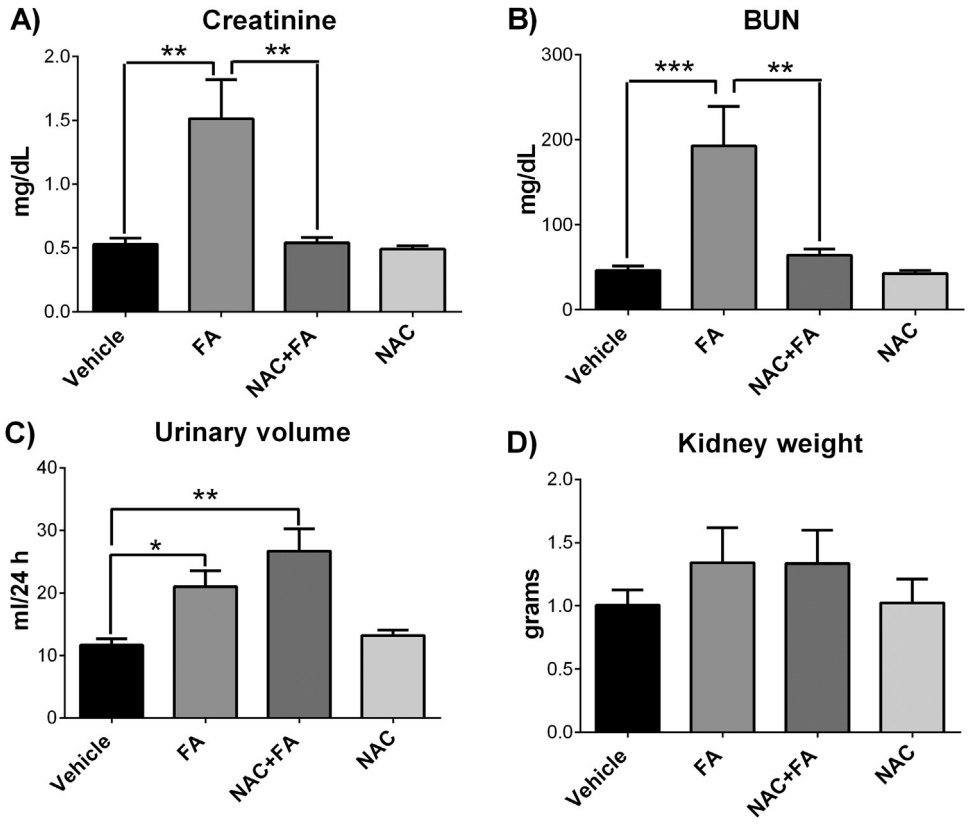

Fig. 1. Markers of renal function and kidney weight of the four experimental groups. **(A)** creatinine and **(B)** blood urea nitrogen (BUN) in plasma, **(C)** urinary volume and **(D)** kidney weight of the four groups. FA = Folic Acid, NAC = N-acetyl-cysteine. Data are mean ± SEM, n = 5–6. *P < 0.05, **P < 0.01, ***P < 0.001.

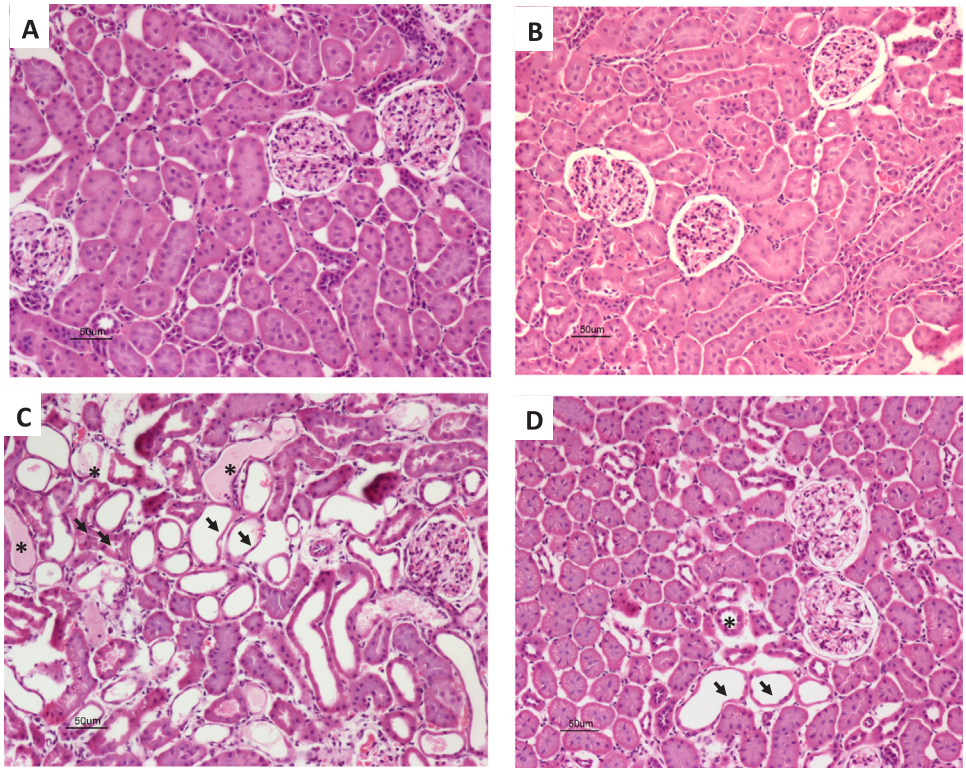

Fig. 2. Representative kidney micrographs of the four experimental groups. **(A)** Normal histology of the kidney from vehicle-treated animal. **(B)** The kidney from animal treated with N-acetyl-cysteine (NAC) does not show any histological abnormality. **(C)** In contrast, the kidney from folic acid (FA)-treated animal show extensive tubular damage, numerous proximal tubules show necrotic and atrophic flat epithelium (arrows) and many tubules exhibit hyaline casts in the tubular lumen (asterisks). **(D)** This tubular damage is lesser in FA + NAC animal; just occasional proximal tubules show atrophy (arrows) or regenerative activity (asterisk). All micrographs 200x magnification, hematoxylin/eosin staining.

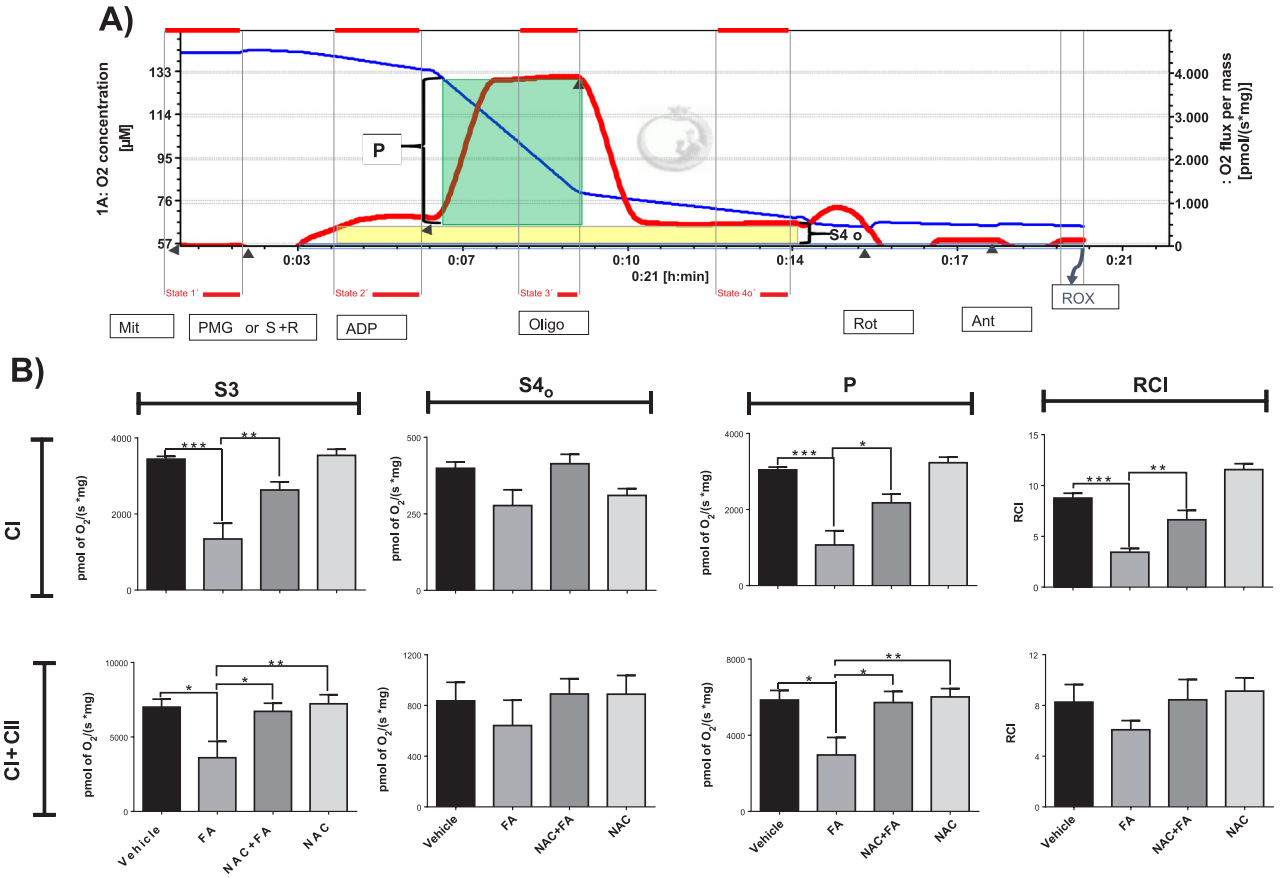

Fig. 3. Respiratory parameters in isolated mitochondria of the four experimental groups. (A) Schematic representations of the method used to determine the oxygen consumption in each respiratory state; blue line corresponds to O_2 concentration, meanwhile red line corresponds to the rate of oxygen consumption. The additions are represented by gray arrows. **(B)** Mitochondrial respiratory parameters: state 3 (S3), state 4 induced by oligomycin (S4o), respiratory control index (RCI) and OXPHOS associated respiration (P) in CI and CI + CII linked respirations. FA = Folic Acid, NAC = N-acetyl-cysteine. CI = complex I, CII = complex II, Mit = mitochondria, PMG = pyruvate–malate-glutamate, S = succinate, S + R = succinate + rotenone, Oligo = Oligomycin, Rot = rotenone, Ant = Antimycin A, ROX = Residual not mitochondrial respiration. Data are mean ± SEM, n = 5–6. *P < 0.05, **P < 0.01, ***P < 0.001. (For interpretation of the references to color in this figure legend, the reader is referred to the web version of this article.)

2.18. Statistical analysis

Data were presented as mean ± standard error of the mean (SEM). They were analyzed by one-way analysis of variance with a subsequent Tukey test using the software Graph- Pad Prism 6 (San Diego, CA, USA). A P-value less than 0.05 was considered significant.

3. Results

3.1. NAC prevents FA induced renal damage

Our first aim was to determine the effect of NAC pretreatment on how FA induced renal damage. It was found, that 24 h after its administration, FA induced a remarkable increase in creatinine (Fig. 1A) and BUN (Fig. 1B) in plasma, as well as a higher urinary volume (Fig. 1C) with respect to the control group. The histological analysis of the FA group revealed copious PT that showed numerous swollen cells with multivacuolar cytoplasm that alternate with necrotic cells, many damaged tubules exhibited hyaline casts in their lumen, and other PT showed accentuated epithelium atrophy (Fig. 2C). NAC pre-administration significantly prevented the increase in creatinine (Fig. 1A) and in BUN (Fig. 1B) levels, with significant improvement of the histological damage, just focal areas of atrophic cortical tubules and regenerative epithelium were seen (Fig. 2D). Interestingly, NAC preadministration (NAC + FA) group tended to show an increase of urinary volume with respect to the control and FA groups. However, NAC did not show this increase (Fig. 1C). No significant changes were observed in the kidney weight between the different groups (Fig. 1D). Renal histological damage was not seen either on vehicle-treated animals (Fig. 2A) nor in animals treated with NAC (Fig. 2B).

3.2. NAC prevented FA-induced mitochondrial bioenergetics alterations attributable to CI and ATP synthase dysfunction

To determine if there were mitochondrial bioenergetics alterations related to kidney dysfunction at 24 h after FA administration, we proceeded to evaluate the mitochondrial respiratory parameters (Fig. 3A) in CI, CII and CI + CII linked respiration as well as ΔΨm in S3 and S4o (Fig. 4A). FA significantly decreased the respiratory parameters S3, P and RCI in CI linked respiration. FA also diminished S3 and P in CI + CII linked respiration (Fig. 3B). However, no significant changes were observed in any of the respiratory parameters in CII linked respiration (Data not shown). FA also reduced ΔΨm in respiratory S3 (principally associated to OXPHOS) in both CI and CII linked respiration, without changes the ΔΨm in S4o (Fig. 4B).

These bioenergetics alterations suggest that FA-induced mitochondrial decoupling and the OXPHOS capacity reduction could be mainly related to CI dysfunctions. Therefore, we evaluated the ATP synthase activity feeding the electron transport system (ETS) by CI and by CII in separate experiments. FA decreased the ATP synthase activity when ETS was fed by CI (Fig. 5A) or by CII (Fig. 5B). Nonetheless, in the FA group, the drop in the activity of mitochondrial complexes was

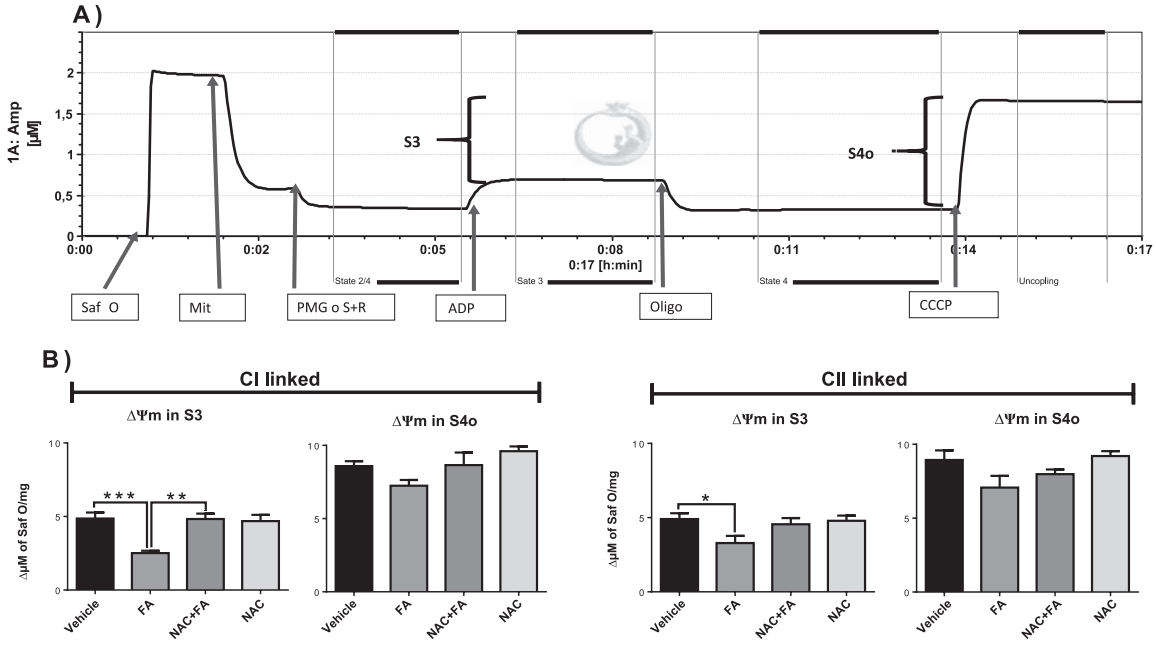

Fig. 4. Mitochondrial membrane potential (Δψm) in isolated mitochondria in the different respiratory states. (A) Schematic representations of the method used to determine Δψm, black line corresponds to safranin O concentration determined by fluorescence. **(B)** Δψm in state 3 (S3) and state 4 induced by oligomycin (S4o) in CI and CII linked respiration. FA = Folic Acid, NAC = N-acetyl-cysteine. CI = complex I, CII = complex II, Saf O = Safranin O, Mit = mitochondria, PMG = pyruvate–malate-glutamate, S + R = succinate + rotenone, Oligo = Oligomycin, CCCP = Carbonyl cyanide m-chlorophenyl hydrazone. Data are mean ± SEM, n = 5–7. *P < 0.05, **P < 0.01, ***P < 0.001.

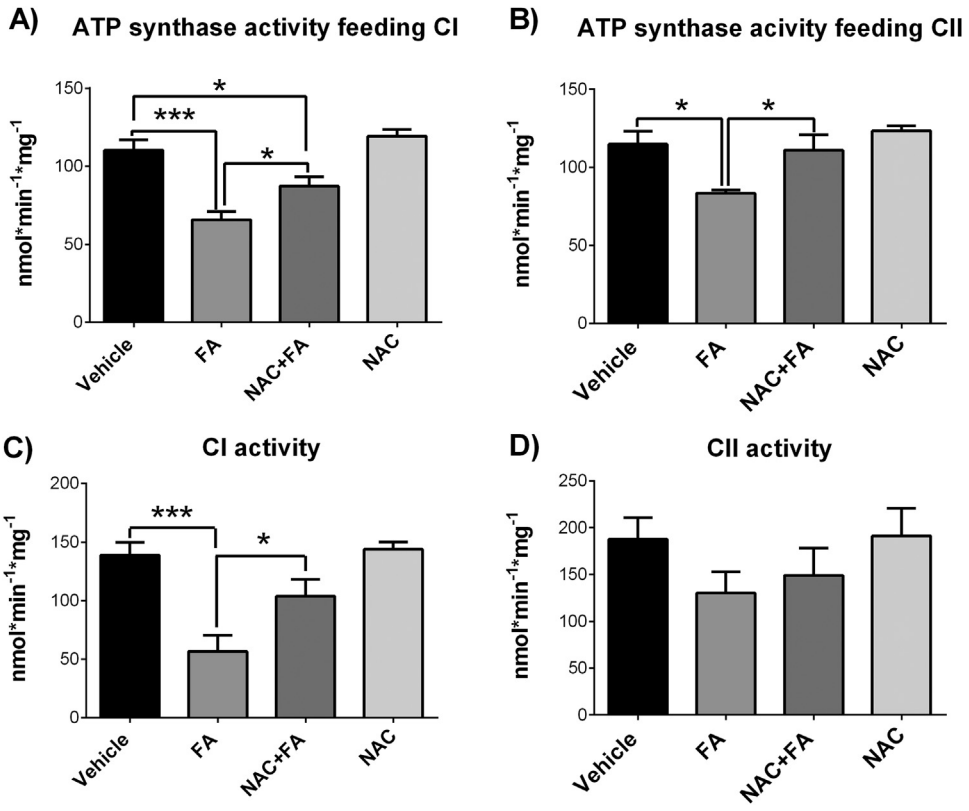

Fig. 5. Activity of ATP synthase and respiratory complexes I (CI) and II (CII) in isolated mitochondria of the four experimental groups. ATP synthase activity was measured feeding by (A) CI and by (B) CII. Activity of mitochondrial (C) CI and (D) CII. FA = Folic Acid, NAC = N-acetyl-cysteine. Data are mean ± SEM, n = 5–7. *P < 0.05, ***P < 0.001.

significant in CI (Fig. 5C), but not CII (Fig. 5D), CIII nor CIV (data not shown).

On the other hand, NAC pre-administration significantly prevented the decrease in S3, in P and in RCI in CI linked respiration and in S3 and in P in CI + CII linked respiration (Fig. 3), as well as the reduction of ΔΨm in S3 in CI and in CII linked respiration (Fig. 4B) and the decrease in ATP synthase (Fig. 5A and B) and CI (Fig. 5C) activity. These data show that at least at 24 h, NAC preserved the mitochondrial coupling and OXPHOS capacity in this AKI model.

To support these results, respiratory parameters were evaluated in intact proximal tubule epithelial LLC-PK1 cells. FA pretreatment (12.5 mM) at 24 h significantly reduced routine respiration and P in

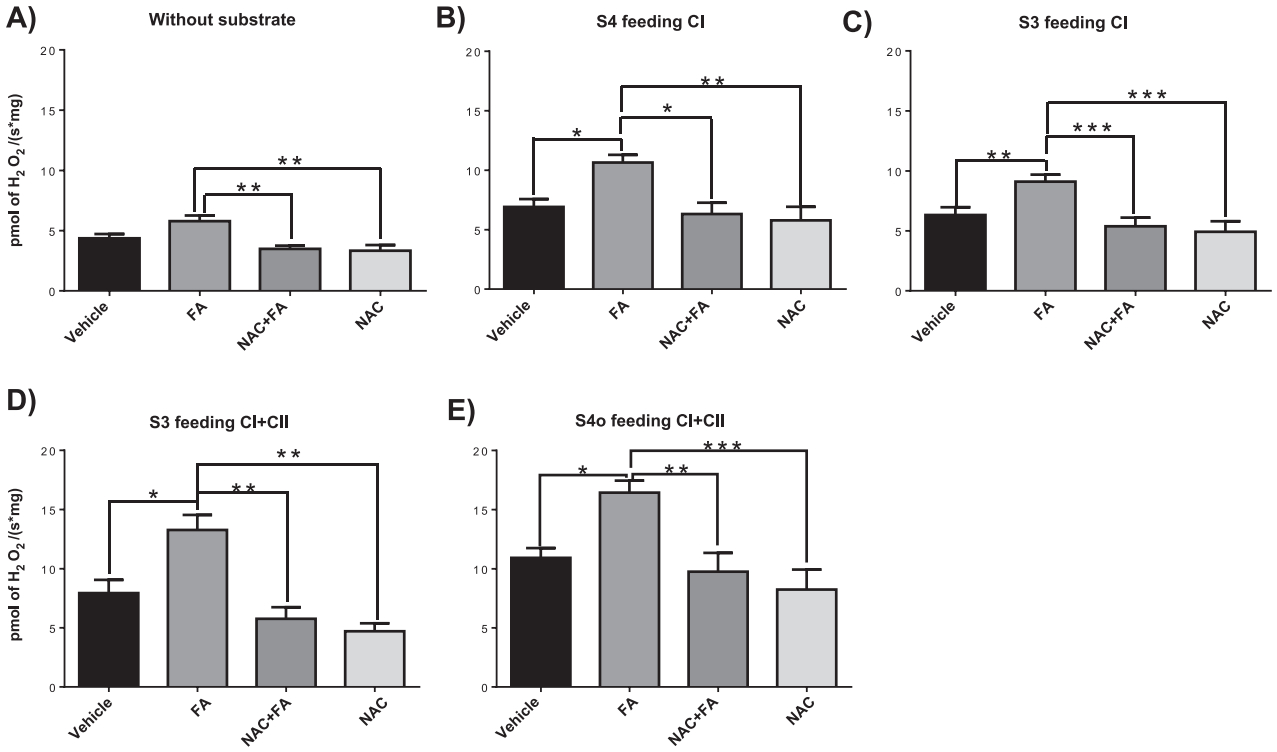

Fig. 6. Hydrogen peroxide (H_2O_2) production rates in isolated mitochondria in the different respiratory states. Sequential addition was employed: **(A)** mitochondria without exogenous substrates; **(B)** S4 feeding CI; **(C)** S3 feeding CI; **(D)** S3 feeding CI + CII; **(E)** S4o feeding CI + CII. FA = Folic Acid, NAC = N-acetylcysteine. CI = complex I, CII = complex II, S3 = state 3, S4 = state 4. Data are mean ± SEM, n = 5–6. *P < 0.05, **P < 0.01, ***P < 0.001.

LLCP-K1 cells (Supplementary Fig. 1). This is consistent with the results obtained in isolated mitochondria (Fig. 3), implying that high doses of FA *per se* reduce the mitochondrial ATP production capacity in the kidney. Interestingly, FA-induced decrease in uncoupled respiration was not significant, which suggests that reserve capacity of ETS in the *in vivo* model was not totally compromised by FA. Additionally, pretreatment with 10 mM NAC prevented the decrease in P and Routine respiration (Supplementary Fig. 1), preserving the OXPHOS capacity in LLC-PK1 cells.

3.3. NAC prevented FA-induced mitochondrial H_2O_2 production and oxidative stress

To evaluate if mitochondrial bioenergetics alterations induce oxidative stress in this organelle, we proceeded to evaluate mitochondrial H_2O_2 production in the different respiratory states. In all respiratory states, FA induced an increase in the rate of H_2O_2 production (Fig. 6). This increase was accompanied by higher levels of mitochondrial oxidative stress markers MDA (Fig. 7A) and 4HNE (Fig. 7B) and by a decrease in aconitase activity (a sensitive mitochondrial target of ROS), the latter was normalized by citrate synthase activity (where no changes were observed) to confirm that the decrease in aconitase activity was specific (Fig. 7C). In addition, the activity of antioxidant enzymes MnSOD, GPx and Prx in mitochondria was diminished in the FA group (Fig. 8). Taken together these results confirm that FA induces at 24 h a prooxidant state in renal mitochondria.

Notably, NAC pre-administration prevented the FA induced increase in mitochondrial H_2O_2 production in all respiratory states (Fig. 6) and in oxidative damage markers MDA (Fig. 7A) and 4HNE (Fig. 7B) as well as the decrease in the aconitase/citrate synthase ratio (Fig. 7C) and in MnSOD and GPx activities but curiously not in Prx activity (Fig. 8). Taken together, these results confirm that NAC prevented FA-induced mitochondrial oxidative stress. No significant changes were observed in all parameters mentioned for the NAC only administered group with respect to the vehicle group.

3.4. NAC inhibits ROS production increase in tubular segment and kidney cortex homogenates induced by FA

In renal damage models, the increase in mitochondrial ROS production has been widely related to the activation of NOX and NOS [36,57,58]. It triggers ROS overproduction, which contributes to renal damage progression [59–62]. In order to evaluate if FA-induced mitochondrial H_2O_2 production was related to the increase in ROS by these enzymes, we proceeded to evaluate the NADPH and L-arginine (substrates of the NOX and the NOS respectively) linked ROS production in mitochondria-rich nephron segments PT and DT, and in renal cortex [63,64].

At 24 h, the FA-treated group showed higher levels of NADPH and L-arginine linked ROS production in isolated homogenates of PT and DT segments and in renal cortex (Fig. 9). This increase was especially marked in the renal cortex. Additionally, in the renal cortex, the FA group showed a decrease in catalase activity (Fig. 10A) and an increase in the oxidative stress marker 4HNE (Fig. 10B), supporting the idea of oxidative stress in this group. On the other hand, the increase in NADPH linked ROS was higher in PT (the richest mitochondria segment) than in the DT segment. On the other hand, the NAC + FA group showed lower levels of NADPH and L-arginine linked ROS production in both tubular segments and in the renal cortex than in the FA group (Fig. 9), and prevented the decrease in catalase activity and the increase in 4HNE levels in cortex (Fig. 10). This confirms that NAC prevented ROS overproduction in homogenates induced by FA.

3.5. NAC preserved the loss of mitochondrial proteome S-glutathionylation and glutathione levels in mitochondria induced by FA

The S-glutathionylation of mitochondrial proteins has recently emerged as a molecular mechanism able to regulate the function of this

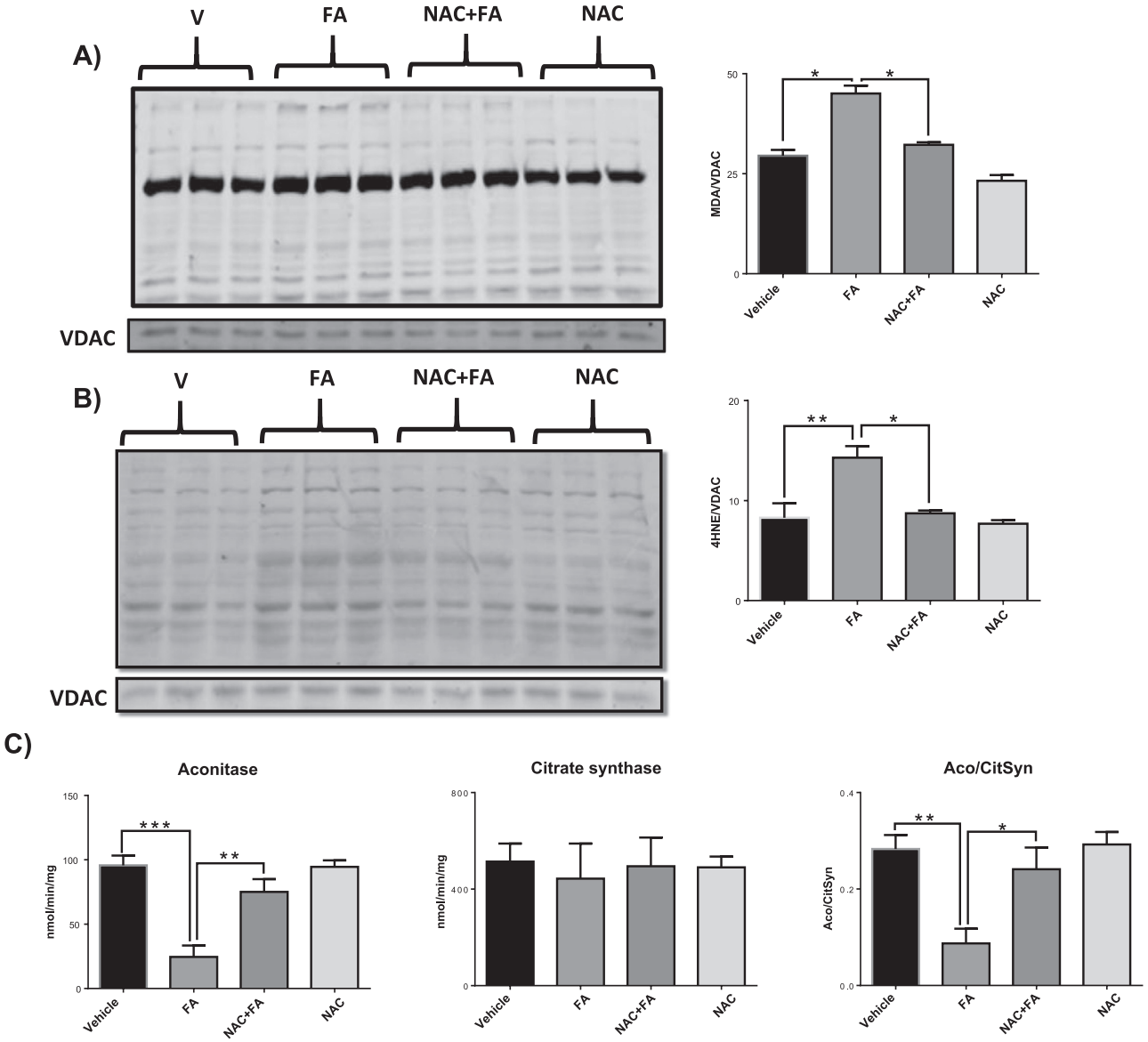

Fig. 7. Oxidative stress markers in isolated mitochondria of the four groups studied. (A) malondialdehyde (MDA) and **(B)** 4 hydroxynonenal (4HNE) determined by western blot and the semiquantitative data obtained by densitometry. Voltage depending anion channel (VDAC) was used as a charge control. Data are mean ± SEM, n = 3. **(C)** Activities of the enzymes aconitase and citrate synthase and the ratio of activities of both enzymes (Aco/CitSyn). V = vehicle, FA = Folic Acid, NAC = N-acetyl-cysteine. Data are mean ± SEM, n = 5–6. *P < 0.05, **P < 0.01, ***P < 0.001.

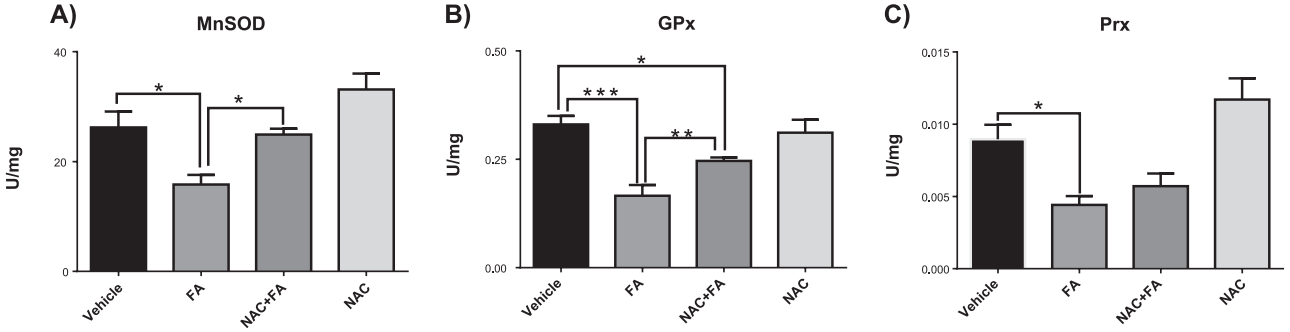

Fig. 8. Activity of antioxidant enzymes in isolated mitochondria of the four experimental groups. (A) Mn superoxide dismutase (MnSOD), **(B)** glutathione peroxidase (GPx) and **(C)** peroxiredoxin (Prx). FA = Folic Acid, NAC = N-acetyl-cysteine. Data are mean ± SEM, n = 5–6. *P < 0.05, **P < 0.01, ***P < 0.001.

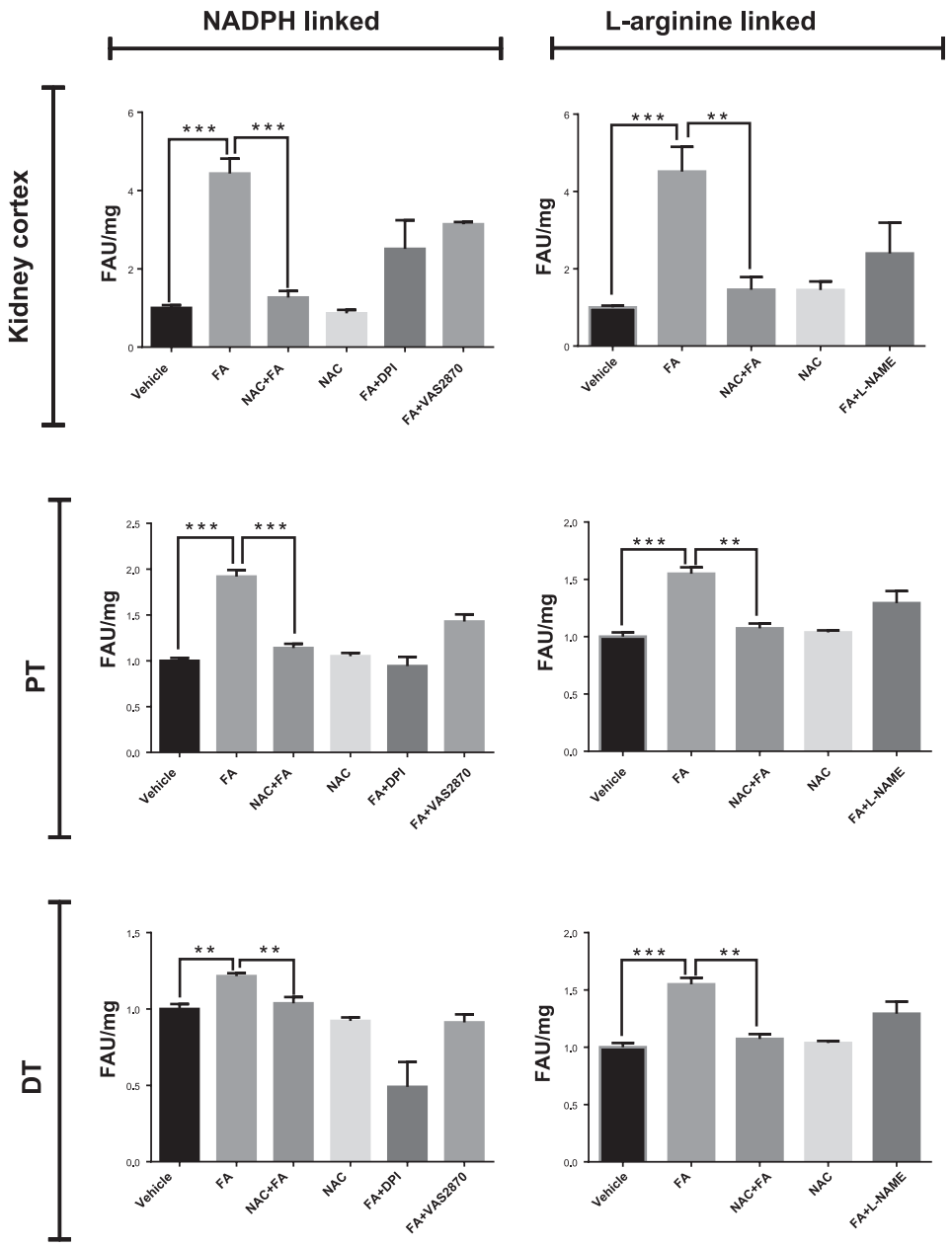

Fig. 9. NADPH linked and L-arginine linked reactive oxygen (ROS) production in the four groups studied. N-acetyl-cysteine (NAC) inhibits the folic acid (FA)-induced over ROS production in renal cortex, proximal (PT) and distal (DT) tubules. NADPH or L-arginine linked ROS was evaluated by adding the corresponding substrates. Diphenyliodonium (DPI), L-N^G-nitroarginine methyl ester (L-NAME) and 3-benzoxazol-2-yl-3-benzyl-3H-[1,2,3]triazolo[4,5-d]pyrimidin-7-yl sulfide (VAS2870) were used as inhibitors. Data are mean ± SEM, n = 5–6. **p < 0.01, ***p < 0.001.

organelle linking energetic metabolism with mitochondrial redox homeostasis and dynamics [39–41]. So, to evaluate if the observed mitochondrial biogenetics dysfunction and the oxidative stress could be related to changes in this modification, the amount of mitochondrial S-glutathionylated proteins was measured by WB. To prevent non-enzymatic and nonspecific S-glutathionylation, 50 mM NEM was added to the mitochondrial isolation buffer [39,65] only in the samples to be determined by WB. The FA group showed low levels of mitochondrial S-glutathionylated proteins (Fig. 11A). Additionally, there was a significant decrease in GSH levels, in GSH/GSSG ratio and in total glutathione content (GSH + GSSG) as well as an increase in GSSG levels (Fig. 11B). The measurement of the activity of the enzymes related to mitochondrial enzymatic S-glutathionylation revealed higher S-glutathionylation removal activity of Grx and lower GST activity in FA rats (Fig. 11C), which agree with previous results.

Conversely, FA + NAC and NAC groups presented higher levels of mitochondrial S-glutathionylated proteins (Fig. 11A). NAC pre-administration also preserved the mitochondrial GSH levels, the GSH/GSSG ratio, the total glutathione content and prevented the increase in GSSG levels (Fig. 11B). Furthermore, NAC partially preserved the activity of GST and prevented the increase in S-glutathionylation removal activity of Grx (Fig. 11C). Interestingly, the NAC-treated group showed an increase in GSH levels, GSH/GSSG ratio and GSH + GSSG with respect to the control group (Fig. 11B).

3.6. NAC prevented the FA-induced mitochondrial dynamics imbalance

Data obtained from AKI experimental models indicate that mitochondrial bioenergetics alterations and oxidative stress induce the imbalance in the processes that regulate mitochondrial dynamics

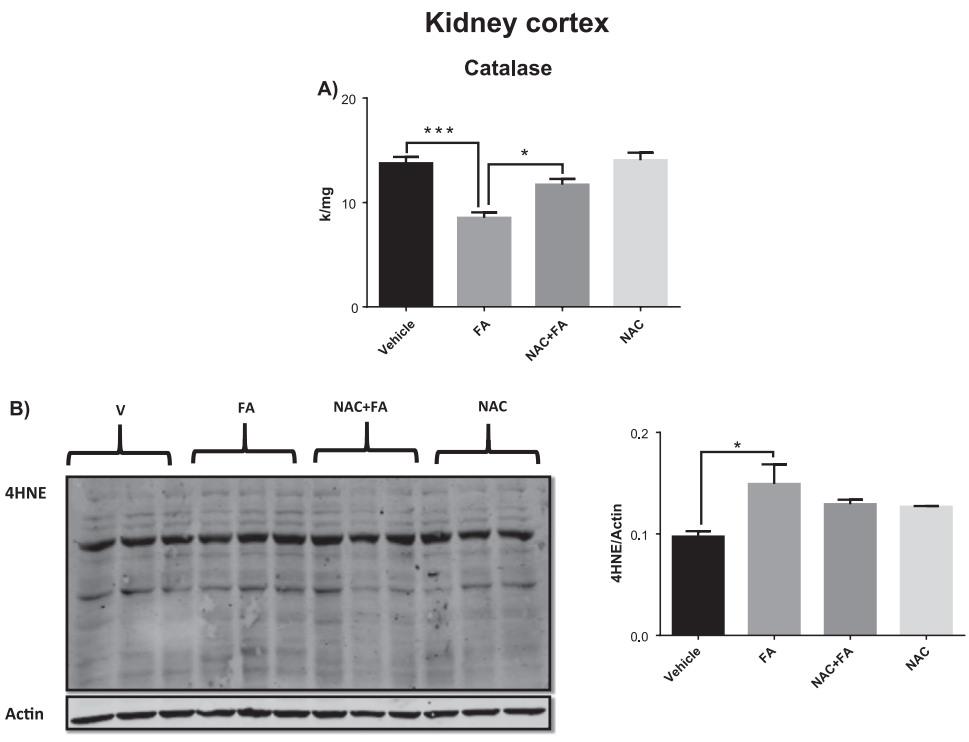

Fig. 10. **(A)** Catalase activity in kidney cortex, the enzyme activity was expressed as k/mg of protein (*k* = first order constant). **(B)** Oxidative damage markers 4 hydroxynonenal (4HNE) in kidney cortex determined by western blot. Semiquantitative data obtained by densitometry are on right. V = vehicle, FA = Folic Acid, NAC = N-acetyl-cysteine. Data are mean ± SEM, n = 5–6. *p < 0.05 and ***p < 0.001.

(fission-fusion) and turnover (biogenesis and mitophagy) [30,64,66]. Electron microscopy analysis revealed, in the epithelial cells of the FA-treated group, numerous small mitochondria with cristae effacement and autophagic bodies (Fig. 12B). Therefore, the FA-induced alterations on mitochondrial dynamics were investigated.

The FA-treated group showed an increase in the mitochondrial levels of the fission proteins Drp1 and Fis1 (Fig. 13A) and a decrease in the levels of the fusion proteins Opa1 and Mfn1 (Fig. 13B), which implies a shift of mitochondrial dynamics to the fission process. To confirm these results, the levels of Drp1 protein were evaluated by immunoelectron microscopy and higher immunolabeling seen in mitochondria located in external membranes from PT epithelial cells of rats treated with FA (Fig. 12E) compared to the control group (Fig. 12D). Taken together these data confirm that FA treatment induces mitochondrial fission in PT segment.

On the other hand, NAC pretreatment prevents the FA-induced mitochondrial fragmentation and preserved mitochondria structure (Fig. 12C). NAC also prevented the increase in the levels of Fis1 and Drp1 proteins (Fig. 13A). Data obtained by immunoelectron microscopy showed lesser levels of Drp1 in comparison to the kidney of animals treated with FA (Fig. 12F). However, the increase in the levels of Opa1 and Mfn1 proteins with respect to FA group was not significant (Fig. 13B).

3.7. FA induced an impaired mitophagy and decreased mitochondrial biogenesis

Mitochondrial fission is a necessary mechanism for the removal of dysfunctional mitochondria through the selective autophagy process known as mitophagy [67,68]. It has been reported that impaired mitophagy may be involved in mitochondrial disturbances in AKI models induced by ischemia/reperfusion [69] and cisplatin [28].

To determine if the shift to mitochondrial fission was related to mitophagy alterations, the levels of the mitophagy protein PINK1 in mitochondria and the subsequent autophagy proteins: microtubule-associated protein 1A/1B-light chain 3 I (LC3-I) and II (LC3-II) and p62 in PT were evaluated. The FA-treated group showed a significant increase in mitochondrial PINK1 levels and a decrease in LC3-I and II levels. However p62 levels were increased (Fig. 14).

On the other hand, the administration of FA caused a decrease in the mRNA of some mitochondrial proteins in the kidney [47,48]. For this reason, we proceeded to evaluate the levels of proteins related to mitochondrial biogenesis, such as PGC-1α, NRF1 and NRF2 in PT, and TFAM, in isolated mitochondria. We found a decrease in the levels of proteins related to biogenesis in the FA group with respect to the control group (Fig. 15), confirming the hypothesis that in the FA-induced AKI model, the mitochondrial biogenesis is restrained.

Finally, the NAC administration only partially prevented the decrease of LC3-I and II (Fig. 14) and showed lesser autophagosomes (Fig. 12C), but had no significant effect on the levels of PINK1 and p62 (Fig. 14), nor on the mitochondrial biogenesis-related proteins (with the exception of PGC-1α, Fig. 15) suggesting that the NAC observed protective effects in mitochondria were not directly linked to these mechanisms.

4. Discussion

Although the model of FA resembles the pathology of clinical cases of AKI [15], the molecular mechanisms by which FA induces AKI and its progression remain poorly understood [16–19]. Under normal conditions, the biologically active FA form is the reduced species tetrahydrofolate (THF) [70], which is produced in a reaction catalyzed by the dihydrofolate reductase (DHFR) multienzymatic complex in a $NADP^+$/NADPH dependent way [71]. However, when pharmacological doses of different folates are given, it appears in blood as 5-methyltetrahydrofolate (5-MTHF) [71,72]. This serum folate form contains a single glutamate residue and is transported inside the cell by the reduced folate carrier exchanger or by an endocytic process mediated by the high affinity folate receptor [71–74] and it is subsequently stored as polyglutamate derivatives impermeable to the cell membrane [73,74]. Due to the high affinity of the folate receptor in the kidney, folate can accumulate in high levels in the kidney [72]. Actually, in the FA-induced AKI, due to folate poor water solubility, it precipitates intratubularly, as a consequence of fluid reabsorption, as a folate crystals that are associated with subsequent acute tubular cell death [18,75]. These folylpolyglutamates are distributed between the cytosol, the

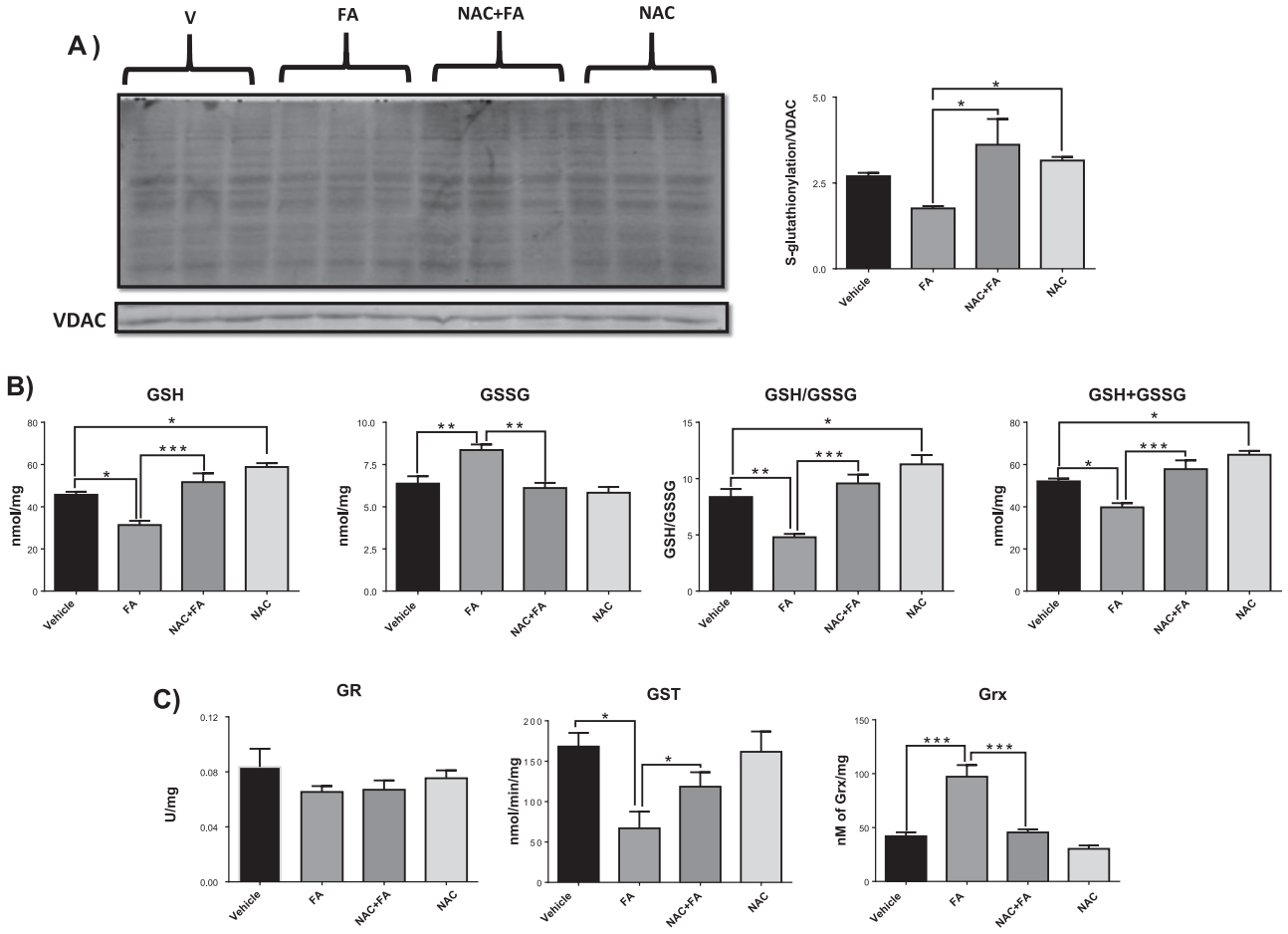

Fig. 11. S-glutathionylation, glutathione levels and activity of enzymes involved in S-glutathionylation in isolated mitochondria. (A) S-glutathionylation levels of total mitochondria proteins measured by western blot and their quantification. Data are mean ± SEM, n = 3. **(B)** Mitochondria levels of glutathione (GSH), glutathione disulfide (GSSG), the ratio GSH/GSSG and total glutathione (GSH + GSSG). Data are mean ± SEM, n = 5–6. **(C)** Activity of the enzymes involved in the S-glutathionylation system: glutathione reductase (GR), glutathione S-transferase (GST) and glutaredoxin (Grx). V = vehicle, FA = Folic Acid, NAC = N-acetylcysteine, VDAC = Voltage depending anion channel. Data are mean ± SEM, n = 6–7. *p < 0.05, **p < 0.01, ***p < 0.001.

nucleus and the mitochondria, the latter storing approximately 40% of the folates in the cell [72,73].

FA-induced AKI is characterized by tubular injury, tubular cell apoptosis, inflammatory processes and fibrosis in the advanced phase [76–79], features that are also found in clinic AKI [18]. Interestingly, mitochondrial dysfunction, especially mitochondrial biogenesis imbalance, has been implicated in the development of these alterations [47,48]. However mitochondrial bioenergetics or redox state studies have not been done. In this work, we demonstrated for the first time, that FA induced at 24 h a mitochondrial bioenergetics imbalance characterized by a decrease in the respiratory parameters S3, P and RCI in CI and in CI + CII linked respiration (Fig. 3). Together with the reduction of ΔΨm in S3 in CI and in CII linked respiration (Fig. 4) and the loss of mitochondrial cristae effacement (Fig. 12), these data implicate that FA causes mitochondrial decoupling and a decrease in the OXPHOS capacity. Additionally, in LLC-PK1 cells, FA pretreatment also reduces the P value (Supplementary Fig. 1), showing that even in the absence of occlusion phenomena in kidney parenchyma, high doses of FA *per se* reduce OXPHOS in PT cells. Considering that in the kidney, the ATP production is maintained principally by the OXPHOS [22–25], the mitochondrial bioenergetics alterations compromise the tubular function and the cell survival in segments with high reabsorption rates, especially the PT [27]. Additionally, the loss of ΔΨm can induce apoptotic cell death associated with tubular epithelial cell injury in AKI [80,81]. In fact, in other AKI models like the one induced by cisplatin [28], ischemia/reperfusion [29] or maleate [30], the mitochondrial bioenergetics alterations correlate with tubular damage and the loss of renal function. In FA-induced AKI, we proved that at 24 h mitochondrial decoupling and OXPHOS capacity reduction can be explained by the decrease in ATP synthase (Fig. 5) and in CI (Fig. 5C) activity, which also explain the highest degree of alterations observed in CI-linked respiration.

Mitochondrial decoupling is also related to the rise in mitochondrial H_2O_2 production observed in the FA group (Fig. 6), since a higher level of electron leak triggers ROS production. Furthermore, we demonstrated for the first time, that FA induced at 24 h a prooxidant state in mitochondria (Fig. 7A-C), characterized by a decrease in the activity of antioxidant enzymes (Fig. 8) and lower levels of GSH and total glutathione content (GSH + GSSG) in mitochondria (Fig. 11). This mitochondrial prooxidant state can be explained by the high internalization rates of folate in the kidney, especially in PT [18,72,75], because inside the cell, the storage as THF derivatives implies a high cost of NADPH [71,73,74]. Therefore the FA generates a depletion in the reducing equivalents, especially in GSH, which mainly affects the mitochondria, since GSH is the main non-enzymatic antioxidant in this organelle [39] and mitochondria store approximately 40% of folates [72,73]. Our data are in agreement with previous works that reported lower activities of SOD, catalase and GPx, lower GSH content and higher MDA levels in total kidney homogenates of FA-treated animals [18,80,81]. Additionally, the mitochondrial redox imbalance can be directly related to the observed mitochondrial bioenergetics alterations. In this context, it has been described that under oxidative stress CI

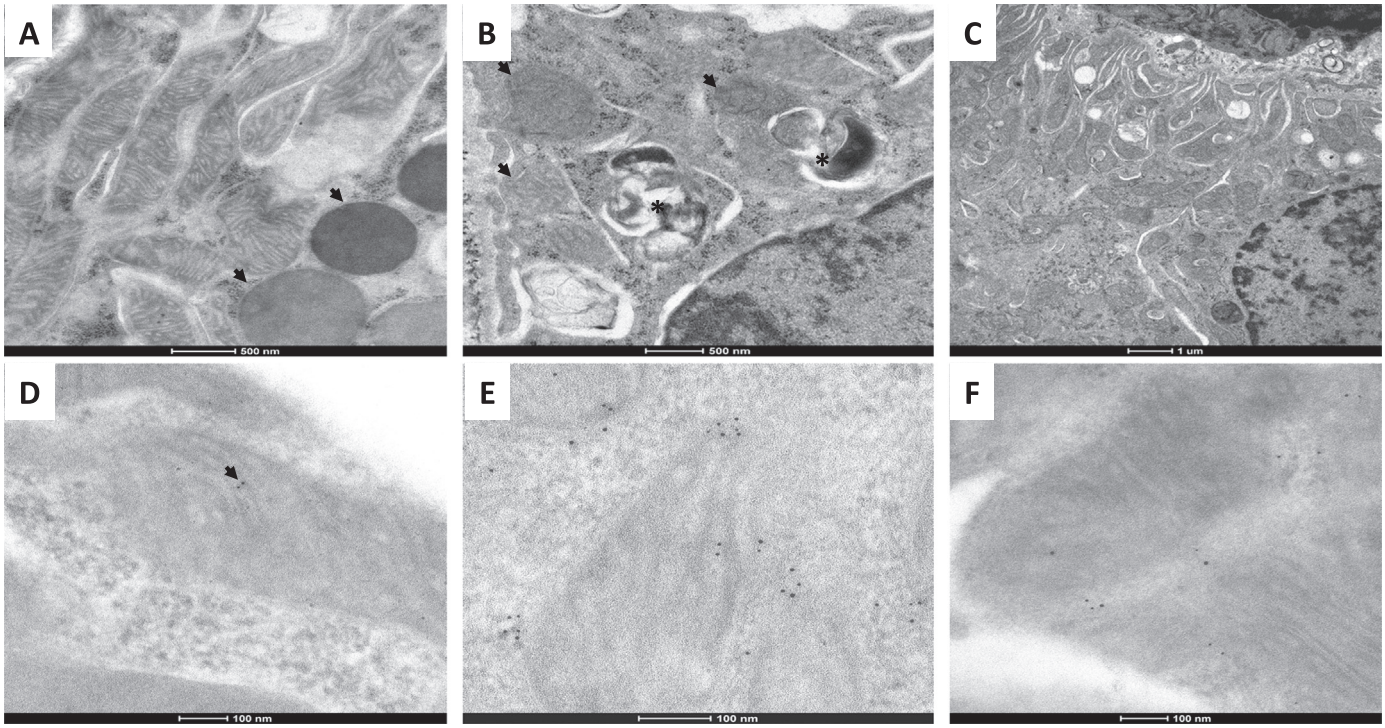

Fig. 12. Representative electron microscopy micrographs of the four experimental groups. (A) Kidney from control rat show well preserved mitochondria and lysosomes (arrows) in the cytoplasm of epithelial cell from convoluted proximal tubule. **(B)** In contrast, the cytoplasm of epithelial cell from folic acid (FA) treated animal show small mitochondria with cristae effacement and autophagosomes (asterisks). **(C)** Proximal convoluted epithelial cell from N-acetyl-cysteine (NAC) + FA rat show lesser mitochondrial damage, isolated small lysosomes and numerous empty vacuoles. **(D)** Immunoelectron microscopy to detect Drp1 show occasional labeling in mitochondria (black dots arrow) from epithelial cell of proximal convoluted tubule. **(E)** In comparison, more Drp1 labeling is show in the external membrane of small mitochondria from tubular epithelial cell of FA treated animal. **(F)** Mild Drp1 labeling is seen in mitochondria from epithelial tubular cell of NAC + FA treated animal.

suffers irreversible post-translational modifications in specific cysteine residues that decrease its activity and increase mitochondrial ROS production [82,83]. In fact, CI cysteine residues can undergo S-sulfenylation (R-SOH), and if oxidative stress persists they can suffer S-sulfinylation ($R\text{-}SO_2H$) and even S-sulfonylation ($R\text{-}SO_3H$), which irreversibly inactivates CI [40]. These modifications compete with S-glutathionylation for the cysteines residues, however only S-glutathionylation can be reversed, restoring totally CI activity [39,40]. Moreover, S-glutathionylation of ATP synthase prevents R-SOH of the Cys294 and Cys103, which triggers a disulfide bond formation and irreversible decrease of ATP production [84,85]. In the present work, an increase in mitochondrial prooxidant state was observed (Figs. 7 and 8) which may be responsible for the decrease in ATP synthase and CI activities (Fig. 5) possibly by the increase in mitochondrial H_2O_2 production (Fig. 6) and by irreversible post-translational modifications. Interestingly, FA also diminished the mitochondrial total levels of S-glutathionylation and raised the S-glutathionylation removal activity of Grx in this organelle (Fig. 11).

NAC preadministration prevented mitochondrial oxidative damage (Fig. 7), the decrease of antioxidant enzymes activities (Fig. 8) and the increase in H_2O_2 production (Fig. 6), which is related to is capacity to preserve the respiratory parameters (Fig. 3) by preventing the loss in CI and ATP synthase activities (Fig. 5). NAC pretreatment also preserved the decrease in GSH, in total glutathione (GSH + GSSG) levels, in the mitochondrial S-glutathionylation and it prevented the increase in S-glutathionylation removal activity of Grx (Fig. 11). This suggests that the NAC protective effects in mitochondria are associated to its capacity to preserve the mitochondrial S-glutathionylation, especially in OXPHOS proteins, which prevents the loss of the activity of these proteins in the posterior oxidative context induced by FA. However, deeper proteomics studies are necessary to sustain this hypothesis. Although some authors recently postulated the idea that enzymatic S-glutathionylation, at certain levels can act as a protective mechanism that links changes in energy metabolism with the redox state to preserve mitochondrial balance [39–41], suggesting that the mechanisms involved in mitochondrial homeostasis are still not fully understood.

Additionally, in AKI and CKD the increase in mitochondrial ROS production has been widely associated with pathological ROS overproduction by NOX and NOS [36,57,58], which enhances oxidative stress in kidney and increases the expression of proinflammatory cytokines and profibrotic factors that triggers the renal damage progression [59–62]. We describe for the first time that FA induces a rise in NADPH and L-arginine-linked ROS production in homogenates of renal cortex and mainly PT, one of the segments with highest mitochondrial content (Fig. 9). Since inflammatory and fibrotic processes are involved in renal damage progression in the FA model [76–79], possibly by the pathological overactivation of NOS and specially of NOX, is a mechanism by which mitochondrial dysfunction contributes to renal damage. The prevention of mitochondrial alterations by NAC decreased both substrates linked ROS production in all segments (Fig. 9) as well as the renal damage (Figs. 1 and 2).

Nephroprotective effects and the inhibition of NOX activity induced by FA supplementation have been documented in hyperhomocysteinemia conditions, where protection may be related to the decrease of homocysteine levels mediated by tetrahydrofolate [86–88], rather than to a direct effect on NOX or on oxidative stress. Additionally, FA doses in these papers (usually < 10 mg/day) are much lower than those used in FA induced AKI models (> 250 mg/day) and the administration route differs. Furthermore, it is well documented that FA-induced AKI triggers a pro-oxidant and proinflammatory state in the kidney [18,48]. This contrasts with the reduction of MDA levels induced by low dose of FA in hyperhomocysteinemia-induced kidney damage [86]. Therefore,

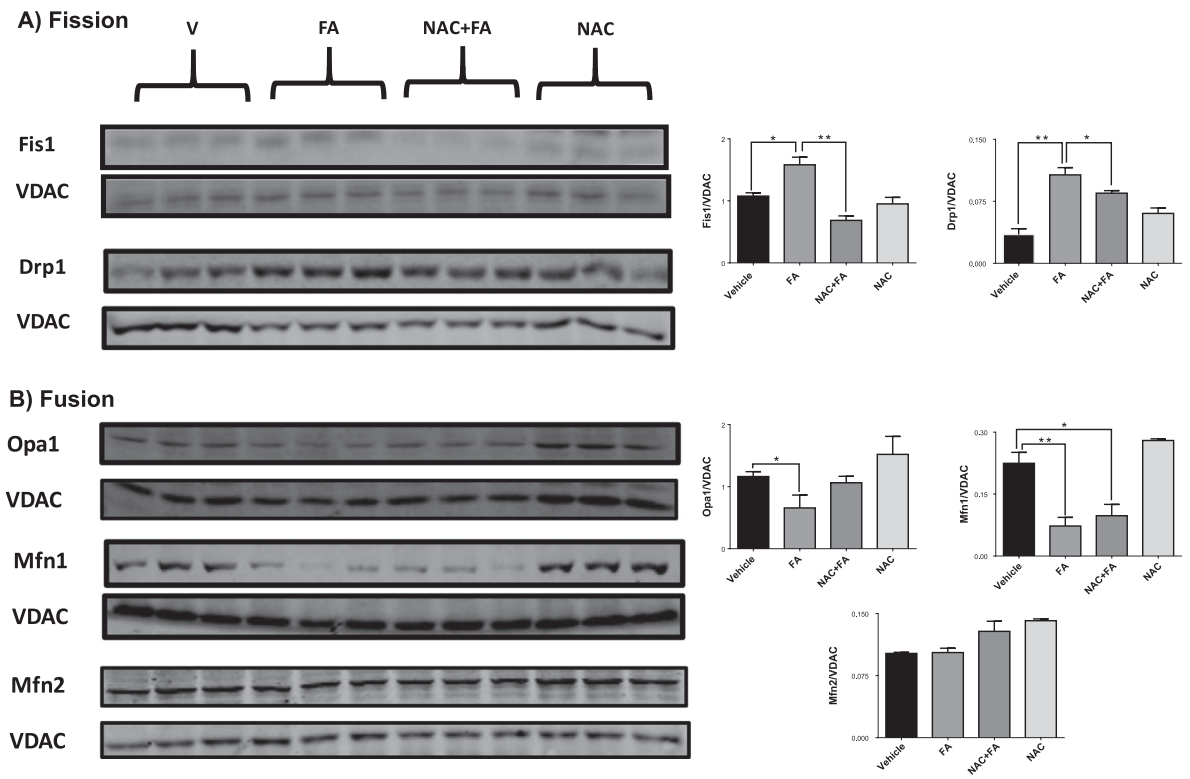

Fig. 13. Dynamics markers in isolated mitochondria of the four groups studied. (A) Levels of mitochondrial fission proteins dynamin-related protein 1 (Drp1) and mitochondrial fission 1 protein (Fis1) and their quantifications. **(B)** Levels of mitochondrial fusion proteins optic atrophy 1 (Opa1), mitofusin 1 (Mfn1) and 2 (Mfn2) evaluated in isolated mitochondria by western blot and their quantifications. Voltage depending anion channel (VDAC) was used as a load control. V = vehicle, FA = Folic Acid, NAC = N-acetyl-cysteine. Data are mean ± SEM, n = 3. *p < 0.05, **p < 0.01.

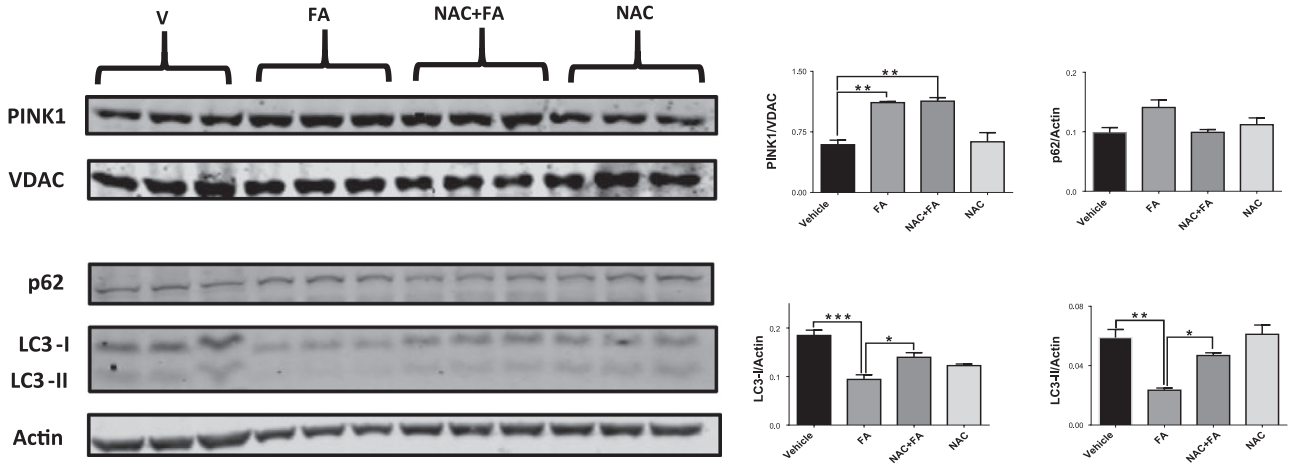

Fig. 14. Mitophagy and autophagy markes in the four groups of rats. Levels of mitophagy protein PTEN-induced putative kinase 1 (PINK1) in isolated mitochondria and autophagy proteins microtubule-associated protein 1A/1B-light chain 3 I/II (LC3-I/II) and p62 in proximal tubule. β-Actin and voltage depending anion channel (VDAC) were used as a load controls for proximal tubules and mitochondria, respectively. V = vehicle, FA = Folic Acid, NAC = N-acetyl-cysteine. Data are mean ± SEM, n = 3. *p < 0.05, **p < 0.01, ***p < 0.001.

protective or prooxidant stress of FA effects could depend on the dose, administration route and preexistent kidney damage conditions.

As seen in Fig. 9, the FA group showed higher NADPH-linked ROS production, which is partially inhibited by VAS2870, suggesting a NOX contribution. Several reports have associated NOX upregulation with renal disease development [59]. In CKD models, NOX4-derived ROS increase the expression of proinflammatory cytokines and profibrotic factors [89], mechanism present in CKD to AKI transition induced by FA [17,48], which supports the idea of an over activation of NOX in this model. However, more experiments are needed to support this hypothesis.

On the other hand, mitochondrial bioenergetics is tightly coordinated with its dynamics and turnover processes, favoring fission and mitophagy or fusion and biogenesis depending on the energy demands [69,90,91]. Furthermore, ROS are also able to regulate at short times mitochondrial mitophagy and dynamics [91–93]. In the case of cisplatin [28] and maleate [30,51] induced AKI, it was demonstrated that mitochondrial decoupling, loss of ΔΨm and oxidative stress in mitochondria lead to mitochondrial fragmentation and a shift of dynamics to fission, favoring its posterior degradation by mitophagy. In fact, AKI has been related to mitochondrial fission increase at early stages after kidney injury [66,91,93]. Additionally, in CKD models, like

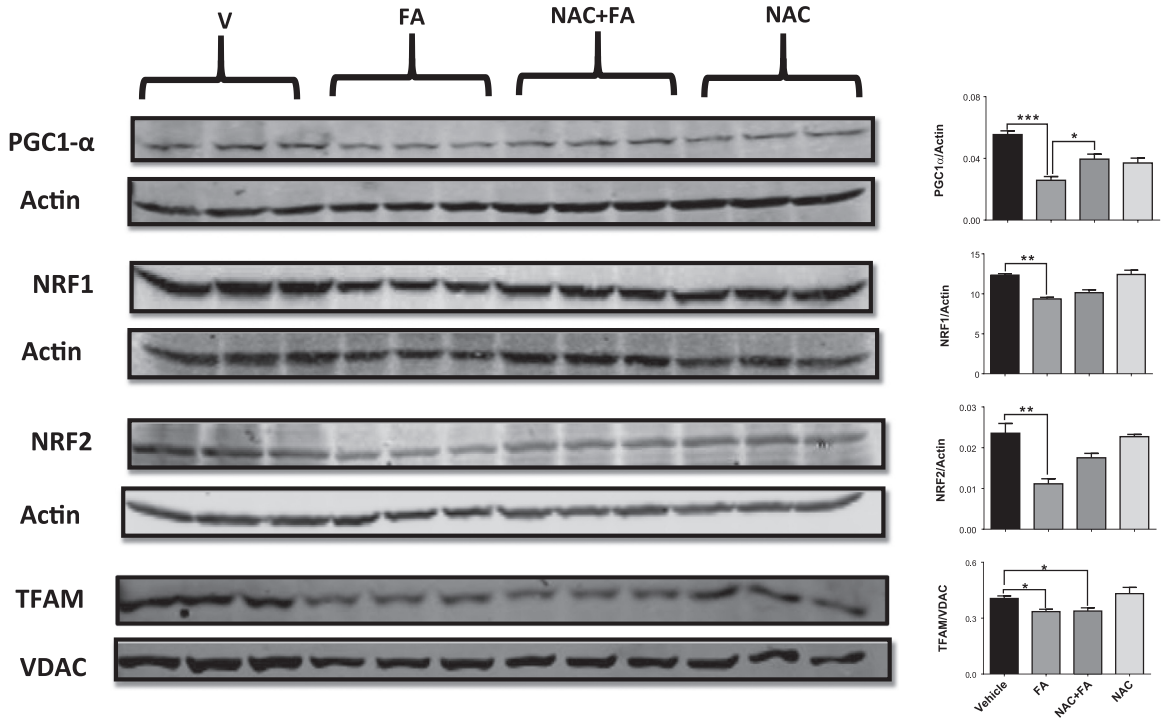

Fig. 15. Levels of mitochondrial biogenesis markers in homogenates from proximal tubules (PGC-1α, NRF1, NRF2) and in isolated mitochondria (TFAM). Peroxisome proliferator-activated receptor gamma coactivator 1-alpha (PGC-1α), nuclear respiratory factor 1 (NRF1) and 2 (NRF2), and mitochondrial transcription factor A (TFAM); and their quantification. β-Actin and voltage depending anion channel (VDAC) were used as a load controls for proximal tubules and mitochondria, respectively. V = vehicle, FA = Folic Acid, NAC = N-acetyl-cysteine. Data are mean ± SEM, n = 3. *p < 0.05, **p < 0.01, ***p < 0.001.

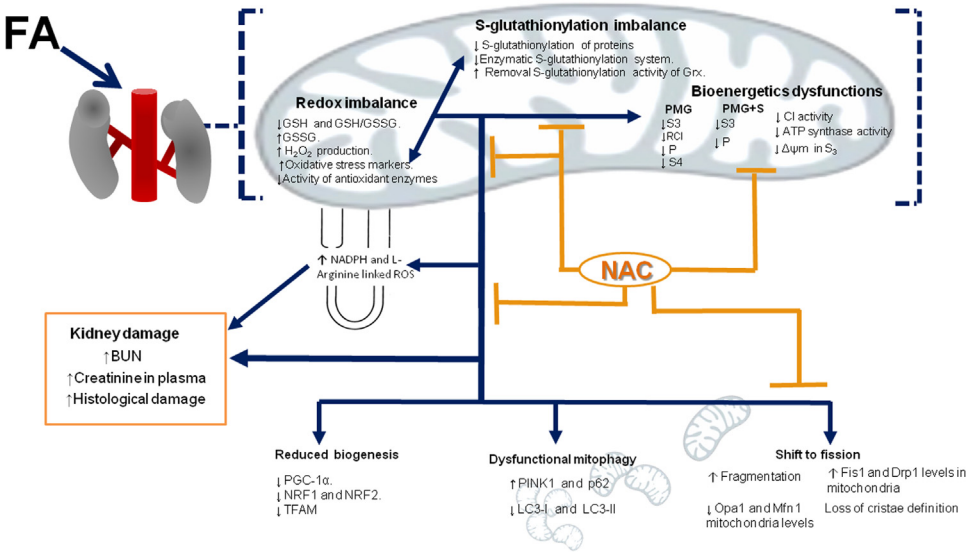

Fig. 16. Integrative scheme. At 24 h N-acetyl-cysteine (NAC) pretreatment is able to prevent the folic (FA) induced mitochondrial redox and S-glutathionylation imbalance, which prevents the bioenergetics alterations and the shift to mitochondrial dynamics to fission. The NAC mitochondrial protective effects also prevent the increase in NADPH and L-arginine linked reactive oxygen species (ROS) production in tissues homogenates especially in mitochondria rich segments like proximal tubules (PT), both effects are responsible of the prevention of the kidney damage induced by FA. Additionally, FA also induces the decrease of mitochondrial biogenesis and dysfunctional mitophagy. Although NAC pretreatment reduces in a non-significant way the alterations in the levels of the proteins involved in these processes at 24 h, NAC effectively decreases the accumulation of vacuolar bodies in PT. BUN = blood urea nitrogen; CI = mitochondrial complex I; Drp1 = dynamin-related protein 1; Fis1 = fission protein 1; GSH = glutathione; GSSG = glutathione disulfide; Grx = glutaredoxin; LC3 (I/II) = Microtubule-associated protein 1A/1B-light chain 3 (I/II); Mfn1 = mitofusin 1; Opa1 = optic atrophy 1 protein; NRF(1/2) = nuclear respiratory factor (1/2); P = OXPHOS associated respiration; S3 = respiratory state 3; S4 = respiratory state 4; PGC-1α = peroxisome proliferator-activated receptor gamma coactivator 1-alpha; PINK1 = PTEN-induced putative kinase 1; PMG = pyruvate-malate-glutamate linked respiration; PMG + S = pyruvate-malate-glutamate plus succinate linked respiration; RCI = respiratory control index; TFAM = mitochondrial transcription factor A; ΔΨm = mitochondrial membrane potential.

5/6 nephrectomy, bioenergetics alterations, oxidative stress, mitochondrial membrane depolarization as well as renal function loss, are observed at early stages, prior to the displacement of dynamics towards fission. These evidences suggest that the alterations in the mitochondrial dynamics would be, in the first place, the result of mitochondrial redox and bioenergetics impairment induced by original damage. However, the subsequent contribution of mitochondrial dynamics alterations to the progression of CKD in more advanced stages must be taken into account. Especially because in chronic stage of diabetic and non-diabetic CKD models, an increase was reported in mitochondrial fragmentation produced by the shift of mitochondrial dynamics to fission and an impairment of mitophagy flux [94–97], which was associated with progressive loss of renal function. Nevertheless, sequential studies are still needed to clarify the correlation between dynamics and the disease progression in these models. In this work, we demonstrated for the first time that FA induces mitochondrial fragmentation and

increase in fission process (Figs. 12 and 13), which would be triggered by loss of ΔΨm (Fig. 4), decoupling of mitochondria (Fig. 3B) and oxidative damage (Fig. 7) observed at 24 h in this organelle. The protective effects of NAC preadministration in mitochondrial bioenergetics and redox state (Figs. 3–11) can explain the observed preservation of mitochondrial morphology (Fig. 12) and the prevention of mitochondrial dynamics alterations (Figs. 12 and 13) at 24 h. Likewise, ΔΨm loss together with oxidative stress and increase of fission are well known inductors of mitophagy [69,91]. Effectively, FA increased mitochondrial PINK1 levels and decreased LC3-I and LC3-II levels (Fig. 14) implying induction of mitophagy in PT. However, an increase in p62 levels was also observed (Fig. 14) and electron microscopy in PT revealed accumulation of vesicular bodies with fragmented mitochondria (Fig. 12), which suggests an interrupted mitophagy process in FA group. Additionally, pretreatment with NAC did not significantly prevent the alterations in autophagy proteins levels with respect to FA group (Fig. 14), although it decreased the number of observed vesicular bodies by electronic microscopy in PT (Fig. 12).

We also observed that FA decreased in PT the levels of mitochondrial biogenesis proteins PGC-1α, NRF1, NRF2 and TFAM (Fig. 15). This is in agreement with previous reports that show in total kidney homogenates, a decrease in mRNA levels of PGC-1α, TFAM, NDUFβ8, ATPS-β, Sdha and COXI and in mtDNA copies between 2 and 14 days after FA administration [47,48]. These studies also reported a strong correlation between mitochondrial biogenesis impairment and fibrosis and inflammation development, processes that lead to AKI-CKD transition in this model [47,48]. Interestingly the administration of TWEAK, a NF-κB inhibitor, not only preserved the PGC-1α levels, but also improved renal function in mice administered with FA [48]. Although NAC preadministration did not significantly prevent the drop in biogenesis markers (Fig. 15), it prevented the bioenergetics (Figs. 3–5), redox (Figs. 6–10), morphologic (Fig. 12) and dynamics alterations (Figs. 12 and 13) and also ameliorated renal damage (Figs. 1 and 2). This suggests that NAC protective mechanisms are not directly linked to mitochondrial biogenesis, however it also implies that NAC improvement of mitochondrial homeostasis may lead to a novel therapeutic approach for AKI treatment.

5. Conclusion

It was shown that NAC pretreatment is able to prevent at 24 h the mitochondrial bioenergetics, redox state and dynamics alterations induced by FA administration. This could be related to the observed NAC capacity to preserve S-glutathionylation and GSH levels in mitochondria. As we summarize in the integrative scheme (Fig. 16), NAC mitochondrial protective effects could be related with the preservation of renal function. Taken together, our results suggest that the prevention of mitochondrial bioenergetics, redox state and dynamics impairment (and even mitochondrial biogenesis as other authors suggested) can be a good approach to prevent the AKI. Moreover, mitochondrial protection can prevent the oxidative stress, tubular injury and death, as well as inflammatory and fibrotic processes that contribute to the AKI to CKD transition in this model. Deeper Mitochondrial proteomic studies of S-glutathionylation are needed to clarify the role of this post-translational modification in mitochondrial balance, as well as temporal studies of mitochondrial bioenergetics, redox state, dynamics and turnover to completely understand the role of mitochondria in this pathology. Nevertheless, the present study supports the idea that these mitochondrial processes are important targets to design novel therapeutic strategies to prevent renal damage and its progression.

Acknowledgement

This work was supported by the by the mexican instituitions: Consejo Nacional de Ciencia y Tecnología (CONACYT) grant number 220046, Programa de Apoyo a Proyectos de Investigación e Innovación Tecnológica (PAPIIT) grant number IN201316, and Programa de Apoyo a la Investigación y al Posgrado (PAIP) grant number 5000-9105. We thank Dr. Ismael Torres and Dr. Enrique Pinzón for the technical support with experimental animals and special thanks to Programa de Apoyo a los Estudios de Posgrado (PAEP) for the support received.

Conflict of interests

The authors report no conflict of interests.

Appendix A. Supporting information

Supplementary data associated with this article can be found in the online version at doi:10.1016/j.freeradbiomed.2018.11.005.

References

[1] A.A. Sharfuddin, S.D. Weisbord, P.M. Palevsky, B.A. Molitoris, Acute kidney injury, in: K. Skorecki, G.M. Chertow, P.A. Marsden, M.W. Taal, A.S.L. Yu (Eds.), Brenner and Rector's the Kidney, ninth ed., Elsevier, Philadelphia, 2012, pp. 1044–1099, , https://doi.org/10.1016/B978-1-4160-6193-9.10030-2.

[2] M.E. Thomas, C. Blaine, A. Dawnay, M.A.J. Devonald, S. Ftouh, C. Laing, S. Latchem, A. Lewington, D.V. Milford, M. Ostermann, The definition of acute kidney injury and its use in practice, Kidney Int. 87 (2014) 1–12, https://doi.org/10.1038/ki.2014.328.

[3] A.B. Fogo, A.H. Cohen, R.B. Colvin, J.C. Jennette, C.E. Alpers, Fundamentals of Renal Pathology, first ed., Springer Berlin Heidelberg, Berlin, Heidelberg, 2014, https://doi.org/10.1007/978-3-642-39080-7.

[4] A.M. El Nahas, K.B. Aminu, Chronic kidney disease: the global challenge, Lancet 365 (2005) 331–340, https://doi.org/10.1016/S0140-6736(05)70199-9.

[5] M.W. Taal, B.M. Brenner, Adaptation to nephron loss and mechanisms of progression in chronic kidney disease, in: K. Skorecki, G.M. Chertow, P.A. Marsden, M.W. Taal, A.S.L. Yu (Eds.), Brenner & Rector's the Kidney, ninth ed., Elsevier, Philadelphia, PA, 2012, pp. 1918–1971, , https://doi.org/10.1016/B978-1-4160-6193-9.10051-X.

[6] T. Shafi, J. Coresh, Chronic kidney disease: definition, epidemiology, cost, and outcomes, in: J. Himmelfarb, M.H. Sayegh (Eds.), Chronic Kidney Dis. Dial. Transplant. 3rd ed., Elsevier Inc, Philadelphia, PA, 2010, pp. 3–21, , https://doi.org/10.1016/B978-1-4377-0987-2.00001-7.

[7] E.D. Siew, A. Davenport, The growth of acute kidney injury: a rising tide or just closer attention to detail? Kidney Int. 87 (2014) 46–61, https://doi.org/10.1038/ki.2014.293.

[8] J.-J. Carrero, M. Hecking, I. Ulasi, L. Sola, B. Thomas, Chronic kidney disease, gender, and access to care: a global perspective, Semin. Nephrol. 37 (2017) 296–308, https://doi.org/10.1016/j.semnephrol.2017.02.009.

[9] A.C. Webster, E.V. Nagler, R.L. Morton, P. Masson, Chronic kidney disease, Lancet 389 (2017) 1238–1252, https://doi.org/10.1016/S0140-6736(16)32064-5.

[10] A. Khwaja, M. El Kossi, J. Floege, M. El Nahas, The management of CKD: a look into the future, Kidney Int. 72 (2007) 1316–1323, https://doi.org/10.1038/sj.ki.5002489.

[11] O. Akinlolu, Addressing the global burden of chronic kidney disease through clinical and translational research, Trans. Am. Clin. Climatol. Assoc. 125 (2014) 229–243 (discussion243–246).

[12] P.K.T. Li, E.A. Burdmann, R.L. Mehta, Acute kidney injury: global health alert, Hong Kong, J. Nephrol. 15 (2013) 1–5, https://doi.org/10.1016/j.hkjn.2013.03.001.

[13] V. Jha, G. Garcia-Garcia, K. Iseki, Z. Li, S. Naicker, B. Plattner, R. Saran, A.Y.M. Wang, C.W. Yang, Chronic kidney disease: global dimension and perspectives, Lancet 382 (2013) 260–272, https://doi.org/10.1016/S0140-6736(13)60687-X.

[14] K. Doi, H. Rabb, Impact of acute kidney injury on distant organ function: recent findings and potential therapeutic targets, Kidney Int. 89 (2016) 555–564, https://doi.org/10.1016/j.kint.2015.11.019.

[15] M.S. Szczypka, A.J. Westover, S.G. Clouthier, J.L.M. Ferrara, H.D. Humes, Rare incorporation of bone marrow-derived cells into kidney after folic acid-induced injury, Stem Cells 23 (2005) 44–54, https://doi.org/10.1634/stemcells.2004-0111.

[16] A. Ortiz, M.D. Sanchez-Niño, M.C. Izquierdo, C. Martin-Cleary, L. Garcia-Bermejo, J.A. Moreno, M. Ruiz-Ortega, J. Draibe, J.M. Cruzado, M.A. Garcia-Gonzalez, J.M. Lopez-Novoa, M.J. Soler, A.B. Sanz, Translational value of animal models of kidney failure, Eur. J. Pharmacol. 759 (2015) 205–220, https://doi.org/10.1016/j.ejphar.2015.03.026.

[17] D. Chunsun, P.K. Lawrence, L. Youhua, Animal models of kidney diseases, Model. Biomed. Res. (2008) 657–664.

[18] A. Gupta, V. Puri, R. Sharma, S. Puri, Folic acid induces acute renal failure (ARF) by enhancing renal prooxidant state, Exp. Toxicol. Pathol. 64 (2012) 225–232, https://doi.org/10.1016/j.etp.2010.08.010.

[19] A.P. Singh, A. Muthuraman, A.S. Jaggi, N. Singh, K. Grover, R. Dhawan, Animal models of acute renal failure, Pharmacol. Rep. 64 (2012) 31–44, https://doi.org/10.1016/S1734-1140(12)70728-4.

[20] S. He, N. Liu, G. Bayliss, S. Zhuang, EGFR activity is required for renal tubular cell dedifferentiation and proliferation in a murine model of folic acid-induced acute

kidney injury, AJP Ren. Physiol. 304 (2013) F356–F366, https://doi.org/10.1152/ajprenal.00553.2012.
[21] T.-C. Fang, Proliferation of bone marrow-derived cells contributes to regeneration after folic acid-induced acute tubular injury, J. Am. Soc. Nephrol. 16 (2005) 1723–1732, https://doi.org/10.1681/ASN.2004121089.
[22] P.S. Brookes, Y.S. Yoon, J.L. Robotham, M.W. Anders, S.S. Sheu, Calcium, ATP, and ROS: a mitochondrial love-hate triangle, Am. J. Physiol. Physiol. 287 (2004) C817–C833, https://doi.org/10.1152/ajpcell.00139.2004.
[23] P. Mukhopadhyay, B. Horváth, Z. Zsengellér, J. Zielonka, G. Tanchian, E. Holovac, M. Kechrid, V. Patel, I.E. Stillman, S.M. Parikh, J. Joseph, B. Kalyanaraman, P. Pacher, Mitochondrial-targeted antioxidants represent a promising approach for prevention of cisplatin-induced nephropathy, Free Radic. Biol. Med. 52 (2012) 497–506, https://doi.org/10.1016/j.freeradbiomed.2011.11.001.
[24] Y. Ishimoto, R. Inagi, Mitochondria: a therapeutic target in acute kidney injury, Nephrol. Dial. Transplant. 31 (2015) 1062–1069, https://doi.org/10.1093/ndt/gfv317.
[25] S. Granata, A. Dalla Gassa, P. Tomei, A. Lupo, G. Zaza, Mitochondria: a new therapeutic target in chronic kidney disease, Nutr. Metab. 12 (2015) 1–21, https://doi.org/10.1186/s12986-015-0044-z.
[26] C.L. Quinlan, I.V. Perevoshchikova, M. Hey-Mogensen, A.L. Orr, M.D. Brand, Sites of reactive oxygen species generation by mitochondria oxidizing different substrates, Redox Biol. 1 (2013) 304–312, https://doi.org/10.1016/j.redox.2013.04.005.
[27] R. Che, Y. Yuan, S. Huang, A. Zhang, Mitochondrial dysfunction in the pathophysiology of renal diseases, Am. J. Physiol. Ren. Physiol. 306 (2014) F367–F378, https://doi.org/10.1152/ajprenal.00571.2013.
[28] B. Ortega-Domínguez, O.E. Aparicio-Trejo, F.E. García-Arroyo, J.C. León-Contreras, E. Tapia, E. Molina-Jijón, R. Hernández-Pando, L.G. Sánchez-Lozada, D. Barrera-Oviedo, J. Pedraza-Chaverri, Curcumin prevents cisplatin-induced renal alterations in mitochondrial bioenergetics and dynamic, Food Chem. Toxicol. 107 (2017) 373–385, https://doi.org/10.1016/j.fct.2017.07.018.
[29] A.M. Hall, G.J. Rhodes, R.M. Sandoval, P.R. Corridon, B.A. Molitoris, In vivo multiphoton imaging of mitochondrial structure and function during acute kidney injury, Kidney Int. 83 (2014) 72–83, https://doi.org/10.1038/ki.2012.328.In.
[30] E. Molina-Jijón, O.E. Aparicio-Trejo, R. Rodríguez-Muñoz, J.C. León-Contreras, M. del Carmen Cárdenas-Aguayo, O.N. Medina-Campos, E. Tapia, L.G. Sánchez-Lozada, R. Hernández-Pando, J.L. Reyes, L. Arreola-Mendoza, J. Pedraza-Chaverri, The nephroprotection exerted by curcumin in maleate-induced renal damage is associated with decreased mitochondrial fission and autophagy, BioFactors 42 (2016) 686–702, https://doi.org/10.1002/biof.1313.
[31] L. Sun, Q. Yuan, T. Xu, L. Yao, J. Feng, J. Ma, L. Wang, C. Lu, D. Wang, Pioglitazone improves mitochondrial function in the remnant kidney and protects against renal fibrosis in 5/6 nephrectomized rats, Front. Pharmacol. 8 (2017) 1–10, https://doi.org/10.3389/fphar.2017.00545.
[32] J.F. Chen, H. Liu, H.F. Ni, L.L. Lv, M.H. Zhang, A.H. Zhang, R.N. Tang, P.S. Chen, B.C. Liu, Improved mitochondrial function underlies the protective effect of pirfenidone against tubulointerstitial fibrosis in 5/6 nephrectomized rats, PLoS One 8 (2013) 1–15, https://doi.org/10.1371/journal.pone.0083593.
[33] H. Zhao, Y. jun Liu, Z. rui Liu, D. dong Tang, X. wen Chen, Y. hua Chen, R. ning Zhou, S. qi Chen, H. xin Niu, Role of mitochondrial dysfunction in renal fibrosis promoted by hypochlorite-modified albumin in a remnant kidney model and protective effects of antioxidant peptide SS-31, Eur. J. Pharmacol. 804 (2017) 57–67, https://doi.org/10.1016/j.ejphar.2017.03.037.
[34] E. Tapia, V. Soto, K.M. Ortiz-Vega, G. Zarco-Márquez, E. Molina-Jijón, M. Cristóbal-García, J. Santamaría, W.R. García-Niño, F. Correa, C. Zazueta, J. Pedraza-Chaverri, Curcumin induces Nrf2 nuclear translocation and prevents glomerular hypertension, hyperfiltration, oxidant stress, and the decrease in antioxidant enzymes in 5/6 nephrectomized rats, Oxid. Med. Cell. Longev. 2013 (2012) 269039, https://doi.org/10.1155/2012/269039.
[35] S. Granata, G. Zaza, S. Simone, G. Villani, D. Latorre, P. Pontrelli, M. Carella, F.P. Schena, G. Grandaliano, G. Pertosa, Mitochondrial dysregulation and oxidative stress in patients with chronic kidney disease, BMC Genom. 10 (2009) 1–13, https://doi.org/10.1186/1471-2164-10-388.
[36] O.E. Aparicio-Trejo, E. Tapia, E. Molina-Jijón, O.N. Medina-Campos, N.A. Macías-Ruvalcaba, J.C. León-Contreras, R. Hernández-Pando, F.E. García-Arroyo, M. Cristóbal, L.G. Sánchez-Lozada, J. Pedraza-Chaverri, Curcumin prevents mitochondrial dynamics disturbances in early 5/6 nephrectomy: relation to oxidative stress and mitochondrial bioenergetics, BioFactors 43 (2017) 293–310, https://doi.org/10.1002/biof.1338.
[37] F. Ursini, M. Maiorino, H.J. Forman, Redox homeostasis: the golden mean of healthy living, Redox Biol. 8 (2016) 205–215, https://doi.org/10.1016/j.redox.2016.01.010.
[38] M.S. Goligorsky, Oxidative stress and the kidney: riding on the curve of hormesis, Antioxid. Redox Signal. 25 (2016) 117–118, https://doi.org/10.1089/ars.2016.6794.
[39] R.J. Mailloux, J.R. Treberg, Protein S-glutathionlyation links energy metabolism to redox signaling in mitochondria, Redox Biol. 8 (2016) 110–118, https://doi.org/10.1016/j.redox.2015.12.010.
[40] R.J. Mailloux, X. Jin, W.G. Willmore, Redox regulation of mitochondrial function with emphasis on cysteine oxidation reactions, Redox Biol. 2 (2014) 123–139, https://doi.org/10.1016/j.redox.2013.12.011.
[41] P.T. Kang, C.L. Chen, Y.R. Chen, Increased mitochondrial prooxidant activity mediates up-regulation of Complex i S-glutathionylation via protein thiyl radical in the murine heart of eNOS-/-, Free Radic. Biol. Med. 79 (2015) 56–68, https://doi.org/10.1016/j.freeradbiomed.2014.11.016.
[42] M. Sharma, A. Sud, T. Kaur, C. Tandon, S.K. Singla, N-acetylcysteine with apocynin prevents hyperoxaluria-induced mitochondrial protein perturbations in nephrolithiasis, Free Radic. Res. 50 (2016) 1032–1044, https://doi.org/10.1080/10715762.2016.1221507.
[43] A. Amini, S. Masoumi-Moghaddam, D.L. Morris, Utility of Bromelain and N-acetylcysteine in Treatment of Peritoneal Dissemination of Gastrointestinal Mucin-producing Malignancies, first ed., Springer International, Switzerland, 2016, https://doi.org/10.1007/978-3-319-28570-2.
[44] G. Tamma, G. Valenti, Evaluating the oxidative stress in Renal diseases: what is the role for S-glutathionylation? Antioxid. Redox Signal. 25 (2016) 1–48, https://doi.org/10.1089/ars.2016.6794.
[45] X.L. Shen, Y. Zhang, W. Xu, R. Liang, J. Zheng, Y. Luo, Y. Wang, K. Huang, An iTRAQ-based mitoproteomics approach for profiling the nephrotoxicity mechanisms of ochratoxin A in HEK 293 cells, J. Proteom. 78 (2013) 398–415, https://doi.org/10.1016/j.jprot.2012.10.010.
[46] S. Terryn, Oxidative stress in the kidney: proximal tubule disorders, in: G. Marenzi, E. Sisillo, A.L. Bartorelli (Eds.), Stud. Ren. Disord., First, Springer, New York, 2011, pp. 179–203, , https://doi.org/10.1007/978-1-60761-857-7.
[47] L.J. Stallons, R.M. Whitaker, R.G. Schnellmann, Suppressed mitochondrial biogenesis in folic acid-induced acute kidney injury and early fibrosis, Toxicol. Lett. 224 (2014) 326–332.
[48] O. Ruiz-Andres, B. Suarez-Alvarez, C. Sánchez-Ramos, M. Monsalve, M.D. Sanchez-Niño, M. Ruiz-Ortega, J. Egido, A. Ortiz, A.B. Sanz, The inflammatory cytokine TWEAK decreases PGC-1α expression and mitochondrial function in acute kidney injury, Kidney Int. 89 (2016) 399–410, https://doi.org/10.1038/ki.2015.332.
[49] H.-Z. Wang, Z.-Y. Peng, X.-Y. Wen, T. Rimmelé, J.V. Bishop, J.A. Kellum, N-acetylcysteine is effective for prevention but not for treatment of folic acid-induced acute kidney injury in mice*, Crit. Care Med. 39 (2011) 2487–2494, https://doi.org/10.1097/CCM.0b013e31822575fc.
[50] C.M. Palmeira, A.J. Moreno, Mitochondrial Bioenergetics. Methods an Protocol, First, London, 2012.
[51] A. Briones-Herrera, S.H. Avila-Rojas, O.E. Aparicio-Trejo, M. Cristóbal, J.C. León-Contreras, R. Hernandez-Pando, E. Pinzón, J. Pedraza-Chaverri, L.G. Sánchez-Lozada, E. Tapia, Sulforaphane prevents maleic acid-induced nephropathy by modulating renal hemodynamics, mitochondrial bioenergetics and oxidative stress, Food Chem. Toxicol. 115 (2018) 185–197, https://doi.org/10.1016/j.fct.2018.03.016.
[52] K.J. Nelson, D. Parsonage, Measurement of peroxiredoxin activity, Curr. Protoc. Toxicol. (2011) 1–28, https://doi.org/10.1002/0471140856.tx0710s49.
[53] M. Negrette-Guzmán, W.R. García-Niño, E. Tapia, C. Zazueta, S. Huerta-Yepez, J.C. León-Contreras, R. Hernández-Pando, O.E. Aparicio-Trejo, M. Madero, J. Pedraza-Chaverri, Curcumin attenuates gentamicin-induced kidney mitochondrial alterations: possible role of a mitochondrial biogenesis mechanism, Evid.-Based Complement. Altern. Med. 2015 (2015) 1–16, https://doi.org/10.1155/2015/917435.
[54] J.E. Vela-Guajardo, P. Pérez-Treviño, I. Rivera-Álvarez, F.A. González-Mondellini, J. Altamirano, N. García, The 8-oxo-deoxyguanosine glycosylase increases its migration to mitochondria in compensated cardiac hypertrophy, J. Am. Soc. Hypertens. 11 (2017) 660–672, https://doi.org/10.1016/j.jash.2017.08.004.
[55] S. González-Reyes, S. Guzmán-Beltrán, O.N. Medina-Campos, J. Pedraza-Chaverri, Curcumin pretreatment induces Nrf2 and an antioxidant response and prevents hemin-induced toxicity in primary cultures of cerebellar granule neurons of rats, Oxid. Med. Cell. Longev. 2013 (2013) 801418, https://doi.org/10.1155/2013/801418.
[56] B. Wispriyono, M. Matsuoka, H. Igisu, K. Matsuno, Protection from cadmium cytotoxicity by N-acetylcysteine in LLC-PK1 cells, J. Pharmacol. Exp. Ther. 287 (1998) 344–351.
[57] S. Kröller-Schön, S. Steven, S. Kossmann, A. Scholz, S. Daub, M. Oelze, N. Xia, M. Hausding, Y. Mikhed, E. Zinssius, M. Mader, P. Stamm, N. Treiber, K. Scharffetter-Kochanek, H. Li, E. Schulz, P. Wenzel, T. Münzel, A. Daiber, Molecular mechanisms of the crosstalk between mitochondria and NADPH oxidase through reactive oxygen species-studies in white blood cells and in animal models, Antioxid. Redox Signal. 20 (2014) 247–266, https://doi.org/10.1089/ars.2012.4953.
[58] R.P. Brandes, N. Weissmann, K. Schröder, Nox family NADPH oxidases: molecular mechanisms of activation, Free Radic. Biol. Med. 76 (2014) 208–226, https://doi.org/10.1016/j.freeradbiomed.2014.07.046.
[59] M. Sedeek, R. Nasrallah, R.M. Touyz, R.L. Hébert, NADPH oxidases, reactive oxygen species, and the kidney: friend and foe, J. Am. Soc. Nephrol. 24 (2013) 1512–1518, https://doi.org/10.1681/ASN.2012111112.
[60] A.M. Garrido, K.K. Griendling, NADPH oxidases and angiotensin II receptor signaling, Mol. Cell. Endocrinol. 302 (2009) 148–158, https://doi.org/10.1016/j.mce.2008.11.003.
[61] F. Jiang, G.-S. Liu, G.J. Dusting, E.C. Chan, NADPH oxidase-dependent redox signaling in TGF-β-mediated fibrotic responses, Redox Biol. 2 (2014) 267–272, https://doi.org/10.1016/j.redox.2014.01.012.
[62] P. Gill, C. Wilcox, NADPH oxidases in the kidney, Antioxid. Redox Signal. 8 (2006) 1597–1607.
[63] T. Sekine, H. Endou, Solute transport, energy consumption, and production in the kidney, Seldin and Geibisch's the Kidney, fifth ed., Elsevier, London, UK, 2013, pp. 143–175, , https://doi.org/10.1016/B978-0-12-381462-3.00006-9.
[64] P. Bhargava, R.G. Schnellmann, Mitochondrial energetics in the kidney, Nat. Rev. Nephrol. 13 (2017) 629–646, https://doi.org/10.1038/nrneph.2017.107.
[65] J. Guo, M.J. Gaffrey, D. Su, T. Liu, D.G. Camp, R.D. Smith, W.J. Qian, Resin-Assisted enrichment of thiols as a general strategy for proteomic profiling of cysteine-based reversible modifications, Nat. Protoc. 9 (2014) 64–75, https://doi.org/10.1038/nprot.2013.161.

[66] M. Zhan, C. Brooks, F. Liu, L. Sun, Z. Dong, Mitochondrial dynamics: regulatory mechanisms and emerging role in renal pathophysiology, Kidney Int. 83 (2013) 568–581, https://doi.org/10.1038/ki.2012.441.
[67] H.M. Ni, J.A. Williams, W.X. Ding, Mitochondrial dynamics and mitochondrial quality control, Redox Biol. 4 (2015) 6–13, https://doi.org/10.1016/j.redox.2014.11.006.
[68] R.J. Youle, D.P. Narendra, Mechanisms of mitophagy, Nat. Rev. Mol. Cell Biol. 12 (2011) 9–14, https://doi.org/10.1038/nrm3028.
[69] A.R. Anzell, R. Maizy, K. Przyklenk, T.H. Sanderson, Mitochondrial quality control and disease: insights into Ischemia-reperfusion injury, Mol. Neurobiol. 55 (2018) 2547–2564, https://doi.org/10.1007/s12035-017-0503-9.
[70] G.S. Ducker, J.D. Rabinowitz, One-carbon metabolism in health and disease, Cell Metab. 25 (2017) 27–42, https://doi.org/10.1016/j.cmet.2016.08.009.
[71] F.H. Nazki, A.S. Sameer, B.A. Ganaie, Folate: metabolism, genes, polymorphisms and the associated diseases, Gene 533 (2014) 11–20, https://doi.org/10.1016/j.gene.2013.09.063.
[72] L.B. Bailey, Folate in Health and Disease, 2nd ed., Taylor & Francis, Washington, D.C., 2009.
[73] J.T. Fox, P.J. Stover, Folate-mediated one-carbon metabolism, Vitam. Horm. 79 (2008) 1–44, https://doi.org/10.1016/S0083-6729(08)00401-9.
[74] C.D. Chancy, R. Kekuda, W. Huang, P.D. Prasad, J.M. Kuhnel, F.M. Sirotnak, P. Roon, V. Ganapathy, S.B. Smith, Expression and differential polarization of the reduced-folate transporter-1 and the folate receptor α in mammalian retinal pigment epithelium, J. Biol. Chem. 275 (2000) 20676–20684, https://doi.org/10.1074/jbc.M002328200.
[75] M.E. Huguenin, A. Birbaumer, F.P. Brunner, J. Thorhorst, U. Schmidt, U.C. Dubach, G. Thiel, An evaluation of the role of tubular obstruction in Folic Acid-Induced Acute renal failure in the rat, Nephron 22 (1978) 41–45.
[76] A. Ortiz, C. Lorz, M.P. Catalan, T.M. Danoff, Y. Yamasaki, J. Egido, E.G. Neilson, Expression of apoptosis regulatory proteins in tubular epithelium stressed in culture or following acute renal failure, Kidney Int. 57 (2000) 969–981, https://doi.org/10.1046/j.1523-1755.2000.00925.x.
[77] C. Dai, J. Yang, Y. Liu, Single injection of naked plasmid encoding Hepatocyte growth factor prevents cell death and ameliorates acute renal failure in mice, J. Am. Soc. Nephrol. 13 (2002) 411–422 〈http://jasn.asnjournals.org/content/13/2/411%5Cnhttp://jasn.asnjournals.org/content/13/2/411.full.pdf%5Cnhttp://jasn.asnjournals.org/content/13/2/411.short%5Cnhttp://www.ncbi.nlm.nih.gov/pubmed/11805170〉.
[78] K. Doi, K. Okamoto, K. Negishi, Y. Suzuki, A. Nakao, T. Fujita, A. Toda, T. Yokomizo, Y. Kita, Y. Kihara, S. Ishii, T. Shimizu, E. Noiri, Attenuation of folic acid-induced renal inflammatory injury in platelet-activating factor receptor-deficient mice, Am. J. Pathol. 168 (2006) 1413–1424, https://doi.org/10.2353/ajpath.2006.050634.
[79] A. Ortega, D. Rámila, A. Izquierdo, L. González, A. Barat, R. Gazapo, R.J. Bosch, P. Esbrit, Role of the renin-angiotensin system on the parathyroid hormone-related protein overexpression induced by nephrotoxic acute renal failure in the rat, J. Am. Soc. Nephrol. 16 (2005) 939–949, https://doi.org/10.1681/ASN.2004040328.
[80] E.Y. Plotnikov, A.V. Kazachenko, M.Y. Vyssokikh, A.K. Vasileva, D.V. Tcvirkun, N.K. Isaev, V.I. Kirpatovsky, D.B. Zorov, The role of mitochondria in oxidative and nitrosative stress during ischemia/reperfusion in the rat kidney, Kidney Int. 72 (2007) 1493–1502, https://doi.org/10.1038/sj.ki.5002568.
[81] H.H. Szeto, S. Liu, Y. Soong, D. Wu, S.F. Darrah, F.-Y. Cheng, Z. Zhao, M. Ganger, C.Y. Tow, S.V. Seshan, Mitochondria-targeted peptide accelerates ATP recovery and reduces ischemic kidney injury, J. Am. Soc. Nephrol. 22 (2011) 1041–1052, https://doi.org/10.1681/ASN.2010080808.
[82] P.T. Kang, L. Zhang, C.L. Chen, J. Chen, K.B. Green, Y.R. Chen, Protein thiyl radical mediates S-glutathionylation of complex i, Free Radic. Biol. Med. 53 (2012) 962–973, https://doi.org/10.1016/j.freeradbiomed.2012.05.025.
[83] M. Forkink, F. Basit, J. Teixeira, H.G. Swarts, W.J.H. Koopman, P.H.G.M. Willems, Complex I and complex III inhibition specifically increase cytosolic hydrogen peroxide levels without inducing oxidative stress in HEK293 cells, Redox Biol. 6 (2015) 607–616, https://doi.org/10.1016/j.redox.2015.09.003.
[84] J. Garcia, D. Han, H. Sancheti, L.P. Yap, N. Kaplowitz, E. Cadenas, Regulation of mitochondrial glutathione redox status and protein glutathionylation by respiratory substrates, J. Biol. Chem. 285 (2010) 39646–39654, https://doi.org/10.1074/jbc.M110.164160.
[85] S.-B. Wang, C.I. Murray, H.S. Chung, J.E. Van Eyk, Redox regulation of mitochondrial ATP synthase, Trends Cardiovasc. Med. 23 (2013) 14–18, https://doi.org/10.1016/j.tcm.2012.08.005.
[86] S.-Y. Hwang, Y.L. Siow, K.K.W. Au-Yeung, J. House, K. O, Folic acid supplementation inhibits NADPH oxidase-mediated superoxide anion production in the kidney, Am. J. Physiol. Ren. Physiol. 300 (2011) F189–F198, https://doi.org/10.1152/ajprenal.00272.2010.
[87] M. Teschner, M. Kosch, R.M. Schaefer, Folate metabolism in renal failure, Nephrol. Dial. Transplant. 17 (Suppl. 5) (2002) S24–S27.
[88] C.M. Wyatt, J.D. Spence, Folic acid supplementation and chronic kidney disease progression, Kidney Int. 90 (2016) 1144–1145, https://doi.org/10.1016/j.kint.2016.09.019.
[89] H. Watanabe, Y. Miyamoto, D. Honda, H. Tanaka, Q. Wu, M. Endo, T. Noguchi, D. Kadowaki, Y. Ishima, S. Kotani, M. Nakajima, K. Kataoka, S. Kim-Mitsuyama, M. Tanaka, M. Fukagawa, M. Otagiri, T. Maruyama, p-Cresyl sulfate causes renal tubular cell damage by inducing oxidative stress by activation of NADPH oxidase, Kidney Int. 83 (2013) 582–592, https://doi.org/10.1038/ki.2012.448.
[90] T. Wai, T. Langer, Mitochondrial dynamics and metabolic regulation, Trends Endocrinol. Metab. 27 (2016) 105–117, https://doi.org/10.1016/j.tem.2015.12.001.
[91] T.M. Durcan, E.A. Fon, The three 'P' s of mitophagy: PARKIN, modifications, Genes Dev. 29 (2015) 989–999, https://doi.org/10.1101/gad.262758.115.GENES.
[92] B. Westermann, Mitochondrial fusion and fission in cell life and death, Nat. Rev. Mol. Cell Biol. 11 (2010) 872–884, https://doi.org/10.1038/nrm3013.
[93] G. Nowak, D. Bakajsova, A.M. Samarel, Protein kinase C-epsilon activation induces mitochondrial dysfunction and fragmentation in renal proximal tubules, Am. J. Physiol. Ren. Physiol. 301 (2011) F197–F208, https://doi.org/10.1152/ajprenal.00364.2010.
[94] L. Xiao, X. Xu, F. Zhang, M. Wang, Y. Xu, D. Tang, J. Wang, Y. Qin, Y. Liu, C. Tang, L. He, A. Greka, Z. Zhou, F. Liu, Z. Dong, L. Sun, The mitochondria-targeted antioxidant MitoQ ameliorated tubular injury mediated by mitophagy in diabetic kidney disease via Nrf2/PINK1, Redox Biol. 11 (2017) 297–311, https://doi.org/10.1016/j.redox.2016.12.022.
[95] Y. Zhao, Y. Guo, Y. Jiang, X. Zhu, Y. Liu, X. Zhang, Mitophagy regulates macrophage phenotype in diabetic nephropathy rats, Biochem. Biophys. Res. Commun. 494 (2017) 42–50, https://doi.org/10.1016/j.bbrc.2017.10.088.
[96] S. Hallan, K. Sharma, The role of mitochondria in diabetic kidney disease, Curr. Diab. Rep. 16 (2016) 1–9, https://doi.org/10.1007/s11892-016-0748-0.
[97] O.E. Aparicio-Trejo, E. Tapia, L.G. Sánchez-Lozada, J. Pedraza-Chaverri, Mitochondrial bioenergetics, redox state, dynamics and turnover alterations in renal mass reduction models of chronic kidney diseases and their possible implications in the progression of this illness, Pharmacol. Res. 135 (2018) 1–11, https://doi.org/10.1016/j.phrs.2018.07.015.

Free Radical Biology and Medicine 154 (2020) 18–32

Contents lists available at ScienceDirect

Free Radical Biology and Medicine

journal homepage: www.elsevier.com/locate/freeradbiomed

Original article

Chronic impairment of mitochondrial bioenergetics and β-oxidation promotes experimental AKI-to-CKD transition induced by folic acid

Omar Emiliano Aparicio-Trejo[a], Sabino Hazael Avila-Rojas[a], Edilia Tapia[b], Pedro Rojas-Morales[a], Juan Carlos León-Contreras[c], Elena Martínez-Klimova[a], Rogelio Hernández-Pando[c], Laura Gabriela Sánchez- Lozada[b], José Pedraza-Chaverri[a,*]

[a] Department of Biology, Faculty of Chemistry, National Autonomous University of Mexico (UNAM), Mexico City, 04510, Mexico
[b] Department of Cardio-Renal Physiopathology, National Institute of Cardiology "Ignacio Chávez", Mexico City, 14080, Mexico
[c] Experimental Pathology Section, National Institute of Medical Sciences and Nutrition "Salvador Zubirán", 14000, Mexico, Mexico City, Mexico

ARTICLE INFO

Keywords:
Renal damage progression
Folic acid
N-acetyl-cysteine
Mitochondrial bioenergetics
Mitochondrial oxidative stress

ABSTRACT

Recent studies suggest that mitochondrial bioenergetics and oxidative stress alterations may be common mechanisms involved in the progression of renal damage. However, the evolution of the mitochondrial alterations over time and the possible effects that their prevention could have in the progression of renal damage are not clear. Folic acid (FA)-induced kidney damage is a widely used experimental model to induce acute kidney injury (AKI), which can evolve to chronic kidney disease (CKD). Therefore, it has been extensively applied to study the mechanisms involved in AKI-to-CKD transition. We previously demonstrated that one day after FA administration, N-acetyl-cysteine (NAC) pre-administration prevented the development of AKI induced by FA. Such therapeutic effect was related to mitochondrial preservation. In the present study, we characterized the temporal course of mitochondrial bioenergetics and redox state alterations along the progression of renal damage induced by FA. Mitochondrial function was studied at different time points and showed a sustained impairment in oxidative phosphorylation capacity and a decrease in β-oxidation, decoupling, mitochondrial membrane potential depolarization and a pro-oxidative state, attributed to the reduction in activity of complexes I and III and mitochondrial cristae effacement, thus favoring the transition from AKI to CKD. Furthermore, the mitochondrial protection by NAC administration before AKI prevented not only the long-term deterioration of mitochondrial function at the chronic stage, but also CKD development. Taken together, our results support the idea that the prevention of mitochondrial dysfunction during an AKI event can be a useful strategy to prevent the transition to CKD.

1. Introduction

The term chronic kidney disease (CKD) describes a group of pathologies characterized by the progressive loss of renal function, resulting in a progressive decrement in the glomerular filtration rate (GFR), with or without an increment in the conventional clinical renal damage markers, like creatinine and blood urea nitrogen (BUN) [1,2]. In recent years, the number of patients with CKD has increased dramatically [3–7], representing a growing worldwide public health problem [8]. As a result of the lack of understanding of the complex pathological mechanisms involved in CKD development [9], the current clinical strategies and treatments do not significantly improve kidney function or prevent illness progression [10], thus highlighting the urgent need to investigate and understand the mechanisms involved in the generation and progression of CKD [11,12].

Furthermore, dysfunction in mitochondrial bioenergetics and redox state have recently emerged as key components of the sudden deterioration of renal functions in a relatively short time-interval, known as acute kidney injury (AKI). In fact, mitochondrial dysfunction in AKI is involved in tubular dysfunction, cell death, oxidative stress and inflammation [13–19]. Likewise, in both animal models and patients, a severe episode of AKI, or a series of them, results in CKD development [2,20–22]. The growing evidence suggests that renal mitochondrial alterations [9,23,24] favor hemodynamic alterations, Ca^{2+} deregulation, cell death, inflammation, fibrotic processes and epithelial-to-mesenchymal transition (EMT), which participate in the progression of several types of CKD in both non-diabetic and diabetic contexts [9,22–27]. However, currently there is no information about the

* Corresponding author.
E-mail address: pedraza@unam.mx (J. Pedraza-Chaverri).

https://doi.org/10.1016/j.freeradbiomed.2020.04.016
Received 13 February 2020; Received in revised form 27 March 2020; Accepted 17 April 2020
Available online 30 April 2020
0891-5849/

mitochondrial bioenergetics and redox state alterations over a time-course. Also, the possible effects of their attenuation in the progression of renal damage are not clear.

In this context, folic acid (FA)-induced kidney damage is a widely recurred to experimental model for AKI induction [28,29]. This model also induces chronic processes such as the persistence of cell death, EMT, cytokines release, inflammation and fibrosis, which lead to CKD transition usually in less than 28 days [28,30,31]. Furthermore, it re-creates the AKI pathology reported in the clinic [32] and is highly reproducible [28,29]. Together, these make the FA model good for the exploration of the mechanisms involved in AKI-to-CKD transition [28,30,31]. In the present work, we refer to "the acute stage" as the period that begins with the administration of FA and ends 72 h later, bringing about the AKI-to-CKD transition or "the chronic stage", which encompasses the time period between day 4 until day 28. It is important to highlight that although high doses of FA have pathological effects on kidney function [28,30,31], nephroprotective effects and the reduction of cardiovascular risk have also been reported by lower FA doses in CKD patients with elevated homocysteine levels, but with baseline vitamin B12 levels [33,34]. In fact, vitamin B12 and the metabolite of FA, 5-methyltetrahydrofolate (5-THF), act as cofactors of the enzyme methionine synthetase, that catalyzes the transfer to the methyl group from 5-THF to homocysteine, producing methionine [33]. Therefore, the protection in this context may be related to reduced homocysteine levels mediated by FA and vitamin B12 [35–37]. Additionally, it must be taken into account that the FA dose used in these papers (< 10 mg/day) is much lower compared to the dose used in the FA-induced renal damage models (> 250 mg/day) and it is well documented that FA at higher levels triggers prooxidant and proinflammatory states in kidneys [38,39]. So, a protective or prooxidant effect of FA could depend on the dose, the administration route and the preexistent kidney damage conditions.

In the case of renal damage induced by high levels of FA, the redox imbalance generated by FA metabolism is one of the main mechanisms involved in the genesis of the pathology [13,38,40], because FA metabolism requires higher levels of NADPH to reduce folate to THF [41,42], decreasing the antioxidant defense [13,38]. This redox imbalance is particularly harmful for kidney's mitochondria, due to the high internalization rates of folate in kidney [38,43,44] and because mitochondria store approximately 40% of folates [43,45]. Therefore, mitochondria are especially vulnerable to high doses of FA [13,46]. Additionally, the mitochondrial redox imbalance can be directly related to mitochondrial bioenergetics alterations [47]. In fact, we recently demonstrated that at 24 h after its administration FA induced in kidney mitochondria the decrease in glutathione (GSH) levels, the increase in glutathione disulfide (GSSG) and the decrease in total glutathione content (GSH + GSSG), that together with higher S-glutathionylation removal activity of mitochondrial glutaredoxin (Grx), leads to complex I (CI) dysfunction [13]. Furthermore, CI dysfunction induced by FA triggers the decrease in mitochondrial oxidative phosphorylation (OXPHOS) capacity, mitochondrial decoupling, loss of mitochondrial membrane potential ($\Delta\Psi m$), increased oxidative stress and mitochondrial hydrogen peroxide (H_2O_2) production. Such effects were associated with AKI development [13]. Additionally, we also demonstrated that the pretreatment with N-acetyl-cysteine (NAC), a donor of sulfhydryl groups and a precursor of GSH [48,49] prevented the mitochondrial bioenergetics and redox state impairment, which prevented the development of AKI 24 h after FA administration [13].

The progressive nature of the renal disease induced by FA was further evidenced by the reduction in mRNA levels of mitochondrial electron transport system (ETS) components in the days 2–14 after FA administration [39,46], the persistence of oxidative stress in kidneys after FA administration [38,50,51] and the inflammatory and fibrotic processes [52–55]. Interestingly, inflammatory and fibrotic processes have been related to mitochondrial impairment [56–58], suggesting that mitochondrial bioenergetics and redox state impairment is persistent in AKI-to-CKD transition in this model. However, such hypothesis has not yet been evaluated.

Therefore, in the present study, we characterize for the first time, the time course of mitochondrial bioenergetics and redox state alterations and their possible association to changes in mitochondrial mass and biogenesis in the AKI-to-CKD transition induced by FA. We also assess the effects of NAC pre-administration in the temporal evolution of mitochondrial bioenergetics and redox state alterations. Lastly, we evaluate if the prevention of mitochondrial dysfunction by NAC during AKI prevents transition to CKD in the FA model.

2. Materials and methods

2.1. Reagents

Adenosine 5′-diphosphate sodium salt (ADP), amplex red, antimycin A, L-arginine, fat free bovine serum albumin (BSA), bromophenol blue, β-mercaptoethanol, carbonyl cyanide m-chlorophenylhydrazone (CCCP), cytochrome *c* from equine heart, D-(+)-glucose, D-mannitol, decylubiquinone (DUB), 2,6-dichlorophenolindophenol sodium salt hydrate (DCPIP), 5,5′-dithio-bis-(2-nitrobenzoic acid) (DTNB), ethylene glycol-bis(2-aminoethylether)-N,N,N′,N'-tetraacetic acid (EGTA), glycerol, GSH, glucose-6-phosphate dehydrogenase, glutathione reductase (GR), glutamic acid, glutaraldehyde, hexokinase, 4-(2-hydroxyethyl)-1-piperazineethanesulfonic acid (HEPES), horseradish peroxidase (HRP), L-carnitine, Lead(II) citrate tribasic, K-lactobionate, manganese (II) chloride ($MgCl_2$) tetrahydrate, malic acid, NADPH, $NADP^+$, NADH, potassium cyanide (KCN), osmium tetroxide, palmitoyl-L-carnitine, paraformaldehyde, primary rotenone, safranin O, sodium chloride (NaCl), sodium succinate dibasic, sodium phosphate dibasic (Na_2HPO_4), sodium cacodylate trihydrate, sodium phosphate monobasic (NaH_2PO_4), sodium glutamate, sodium L-ascorbate, sodium malate, sodium dodecyl sulfate (SDS), sodium orthovanadate (Na_3VO_4), sodium pyruvate, sucrose, Tris-HCl, taurine, tetramethyl-p-phenylenediamine (TMPD) and uranyl acetate were purchased from Sigma-Aldrich (St. Louis, MO, USA). Calcium chloride ($CaCl_2$), ethanol, sodium bicarbonate ($NaHCO_3$), potassium dihydrogen phosphate (KH_2PO_4), and ethylenediaminetetraacetic acid disodium salt dihydrate (EDTA) were purchased from JT Baker (Xalostoc, Edo. Mexico, Mexico). Antibodies against actin, nuclear respiratory factor 1 (NRF2), tubulin and PTEN-induced putative kinase 1 (PINK1) were purchased from Santa Cruz Biotechnology (Dallas, TX, USA). Antibodies against voltage dependence anion channel (VDAC), peroxisome proliferator-activated receptor gamma coactivator 1-*alpha* (PGC-1α), total OXPHOS and 4-hydroxynonenal (4HNE) were purchased from Abcam (Cambridge, MA, USA). The sedative sodium pentobarbital (SedalphorteMR) was purchased from Salud y Bienestar Animal S.A. de C.V. (Mexico City, Mexico). Protease inhibitor cocktail was purchased from Roche Applied Science (Mannheim, Germany). Polyfructosan (Inutest®) was purchased from Fresenius-Kabi, (Linz, Austria). Trichloroacetic acid, sulphuric acid and anthrone were purchased from Merck (Naucalpan, Edo. Mexico, Mexico).

2.2. Experimental design

The experimental protocol was approved by the Institutional Animal Care Committee (Comité Institucional de Uso y Cuidado de Animales de Laboratorio, CICUAL) at the Faculty of Chemistry (FQ/CICUAL/260/18) and was conducted according to Mexican Official Norm Guides for the use and care of laboratory animals (NOM-062-ZOO-1999) and for the disposal of biological residues (NOM-087-SEMARNAT-SSA1-2002). Four groups of male Wistar rats with an initial body weight between 230 to 250 g were employed (n = 5–6 per group). Group 1: Vehicle, animals were injected with 300 mM $NaHCO_3$. Group 2: FA, animals were administered with one intraperitoneal dose of FA (300 mg/kg body weight) dissolved in 300 mM $NaHCO_3$. Group 3:

NAC + FA, animals were pre-treated with two doses of NAC (300 mg/kg) 24 and 2 h before FA administration. Group 4: NAC, animals only received two doses of NAC (300 mg/kg) 24 and 2 h before vehicle administration. The analysis was carried out on days 2, 4, 7, 14 and 28 after folic acid administration, with n = 6 per group for each time-period. The doses used of each compound followed our previous report [13]. The rats were housed in a temperature-controlled environment with a 12-12 h light-dark cycle and maintained with water and food *ad libitum*. At each time-point sacrifice, the animals were anesthetized with sodium pentobarbital (90 mg/kg). Blood was obtained from the abdominal aorta, plasma was separated and stored at 4 °C to determine BUN and plasma creatinine levels as markers of renal function.

2.3. Renal damage markers and hemodynamics parameters

Creatinine and BUN levels were assessed in plasma by commercial kits following manufacturer's instructions. The evaluation of hemodynamic parameters at 28 days after FA administration was carried out as previously described [15]. Briefly, the animals were anesthetized with sodium pentobarbital (50 mg/kg) and the femoral arteries, jugular veins, trachea and bladder were catheterized. The body temperature was maintained at 37 °C by means of a thermoregulated table. A femoral artery catheter was used to monitor mean arterial pressure (MAP) with a physiological pressure transducer MLT844 (ADInstruments, Colorado Springs, CO, USA), whereas the other femoral catheter was used for blood sampling. The blood samples were taken in microcapillaries and centrifuged in a hematocrit centrifuge (MICRO-MB, Thermo IEC, Thermo Fisher Scientific, Inc., Waltham, MA, USA) and the hematocrit was read with a microcapillary reader (Damon IEC Division). Sterile saline solution was infused through the vein to compensate body fluid loss and the bladder was catheterized to allow urine sampling. For the evaluation of GFR, rats received an infusion with 5% polyfructosan (in 0.9% saline solution) at a rate of 2.2 mL/h during a 60-min period for equilibrium reach. Then, a sample of blood was taken and the 30 min urine collection was started. In blood and urine samples, the concentration of polyfructosan was measured at 450 nm by the anthrone method [59] to calculate GFR. Later, the left kidney was exposed by a left subcostal flank incision, immobilized in a Lucite holder and sealed around 4% agar, covering the kidney surface with 0.9% saline solution. Renal blood flow (RBF) was also determined using a transit-time ultrasound flow probe TS420 (Transonic System, Ithaca, NY, USA) placed around the left renal artery. In addition, renal vascular resistance (RVR) was calculated according to the formula RVR = MAP/RBF. Renal plasma flow (RPF) was calculated with the formula RPF = RBF*(1-hematocrit). Whereas the filtration fraction (FF) was defined as FF = GFR/RPF.

2.4. Kidney histology

Immediately after euthanasia, kidneys were removed, sectioned in two halves and fixed by immersion in a mixed solution of 4% paraformaldehyde and 1.5% glutaraldehyde pH = 7.2. A thin tissue slide (1 mm width) was dehydrated and embedded in paraffin, sectioned at 5 μm and stained with hematoxylin/eosin (H&E) and Masson trichrome.

2.5. Protein extraction and western blot (WB)

For total protein extraction, the corresponding samples' pellets were resuspended in radioimmunoprecipitation buffer (RIPA): 40 mM Tris-HCl, 150 mM NaCl, 2 mM EDTA, 1 mM EGTA, 5 mM NaF, 1 mM Na_3VO_4, 1 mM PMSF, 0.5% sodium deoxycholate, 0.1% SDS pH 7.6 supplemented with protease inhibitor cocktail. The samples were homogenized using a Potter-Elvehjem homogenizer and centrifuged at 15,000 g for 10 min at 4 °C; the supernatants were collected. Total protein was quantified by the Lowry method, then the corresponding protein quantities were denatured by boiling for 10 min and diluted 1:5 in Laemmli sample buffer (60 mM Tris-Cl, pH = 6.8, 2% SDS, 10% glycerol, 5% β-mercaptoethanol, 0.01% bromophenol blue). Samples (20 μg) were loaded in SDS-polyacrylamide gels and electrophoresis was run. Molecular weight standards were run in parallel. Proteins were transferred to polyvinylidene fluoride (PVDF) membranes. Non-specific protein binding was blocked by incubation with 5% non-fat dry milk in TBS containing 0.4% Tween 20 for 1.5 h at room temperature. Membranes were incubated overnight at 4 °C, first with the appropriate primary antibody and then with the corresponding fluorescent secondary antibody (1:10,000) for 1.5 h in darkness. Protein bands were detected by fluorescence in an Odyssey scanner (LI-COR Biosciences, Lincoln, NE, USA). Protein band density was analyzed with the Image Studio™ Lite Software LI-COR Odyssey (LI-COR Biosciences).

2.6. Isolation of renal mitochondria

After sacrifice, kidneys were cooled by immersion in isolation buffer (225 mM D-mannitol, 75 mM sucrose, 1 mM EDTA, 5 mM HEPES, 0.1% BSA, pH = 7.4) at 4 °C and then cut into small pieces. Mitochondria were isolated from the whole renal mass; tissues were homogenized in a glass Potter–Elvehjem with a TeflonVR pestle in the same buffer. Mitochondria were obtained by differential centrifugation with Percoll gradients [60]. The pellet was resuspended in 180 μL of BSA-free isolation buffer and the mitochondrial total protein was measured by the Lowry method.

2.7. Mitochondrial O_2 consumption and membrane potential ($\Delta\Psi m$)

Evaluation of mitochondrial O_2 consumption was performed with a high-resolution respirometer (Oxygraph O2k, OROBOROS, Innsbruck, Austria) at 37 °C. Isolated mitochondria (200 μg of total protein) were loaded into the chamber with 2 mL of MiR05 respiration buffer (0.5 mM EGTA, 3 mM $MgCl_2$, 60 mM K-lactobionate, 20 mM taurine, 10 mM KH_2PO_4, 20 mM HEPES, 110 mM sucrose and 1 g/L essentially fatty acid free BSA pH 7.4). Electron transport was started by addition of complex I (CI)-linked substrates (5 mM sodium, 5 mM pyruvate, 2 mM malate and 10 mM glutamate), complex II (CII)-linked substrates (10 mM succinate plus 0.5 μM rotenone) or β-oxidation–linked substrates (2 mM L-carnitine, 2 μM palmitoyl-L-carnitine plus 2 mM malate). Respiration in state 3 (S3) was achieved by addition of 2.5 mM ADP. Oligomycin 2.5 μM was employed to induce state 4 (S4o) respiration. All parameters were corrected by residual respiration (ROX) obtained by addition of 1 μM rotenone plus 5 μM antimycin A. The respiratory control (RC) was defined as the S3/S4o ratio. The respiration directly attributable to OXPHOS (P) was defined as S3–S4o [13,61]. All values were normalized by total protein content determined by the Lowry method.

The ΔΨm in the different respiratory states was measured as previously reported [13]. Briefly, the changes in safranin O fluorescence (5 μM) were used to determine the ΔΨm. To stimulate CI, CII or β-oxidation–linked respiration, the respective substrates were added. Mitochondrial membrane potential in S3 was obtained by addition of 2.5 mM ADP and in S4o by addition of 2.5 μM oligomycin. CCCP 5 μM was added to completely dissipate the ΔΨm and to correct by the non-specific interactions. Results were expressed as the changes in the measurable concentration of safranin O (ΔμM of S) in S3 or S4o with respect to CCCP decoupling, and the results were normalized per milligram of protein (ΔμM of S/mg of protein).

2.8. Activity of mitochondrial respiratory complexes

Mitochondrial complexes' activities were assessed as previously described [13]. Briefly, CI oxidizes NADH while reducing DUb to $DUbH_2$, which is then oxidized by DCPIP; therefore, the decrease in the absorbance of DCPIP at 600 nm is proportional to the activity of CI. CII

activity was measured in presence of 2.5 μM rotenone, using CII's capacity to reduce DUb to $DUbH_2$; therefore, the decrease in the absorbance at 600 nm is proportional to the activity of CII. The activity of complex III (CIII) was evaluated using the increase in absorbance at 550 nm (cytochrome *c* reduction) by addition of $DUbH_2$. The activity of complex IV (CIV) was evaluated by addition of 0.5 mM TMPD plus 2 mM ascorbate to respiration medium MiR05 supplemented with 0.5 μM rotenone plus 2.5 μM antimycin A. Oxygen consumption rate was proportional to CIV activity [48]. Absorbance measurements were performed at 37 °C using a Synergy-Biotek microplate reader (Biotek Instruments, Winooski, VT, USA) and the oxygen consumption rate measurements were performed using a high-resolution respirometer (Oxygraph O2k). The specific activity of each complex was determined by the subtraction of the activity in the presence of the appropriate inhibitor from the non-inhibited one and the results were expressed as nmol/min/mg protein.

2.9. Mitochondrial H_2O_2 production

Mitochondrial H_2O_2 was measured as previously described [13] in an O2k-Fluorometer (OROBOROS, Innsbruck, Austria) using Amplex red as a probe. Fresh isolated mitochondria were resuspended in 2 mL of MiR05 plus HRP 0.5 U/mL. Calibration curves were employed to ensure the linearity of the assay and sequential additions were employed to determine the production rate in each state.

2.10. Activity of mitochondrial enzymes

Isolated mitochondria were used for the measurements of antioxidant enzymes as previously described [13]. Briefly, GR activity was determined by measuring the disappearance of NADPH at 340 nm. The glutathione peroxidase (GPx) activity was determined by measuring the disappearance of NADPH at 340 nm in a coupled reaction with GR. The inactivation of aconitase activity was evaluated as a mitochondrial oxidative stress marker by determining the rate of formation of the intermediate product *cis*-aconitate at 240 nm, as we previously described [13]. The lipoperoxidation markers were evaluated in mitochondria by Western blot (WB).

2.11. Electron microscopy

For the ultrastructural study, small tissue fragments from the kidney cortex were fixed with 2.5% glutaraldehyde in 0.15 M cacodylate buffer, post-fixed with 1% osmium tetroxide, dehydrated with ethyl alcohol in ascending concentrations and infiltrated in epoxy resin. Ultrathin sections were contrasted with uranyl acetate and lead citrate, and subsequently observed with an electron microscope (Tecnai Spirit BioTwin, FEI, Hillsboro, OR, USA).

2.12. Statistics

Data are presented as mean ± standard error of the mean (SEM). They were analyzed by Graph Pad Prism 6 (San Diego, CA, USA). The corresponding statistical tests are clarified in each figure legend.

3. Results

3.1. FA induces renal damage progression

Our first goal was to characterize the kidney damage progression induced by FA. Therefore, we evaluated the levels of the classic renal damage markers BUN and creatinine in plasma. As shown in Fig. 1A–C, at day 2 after its administration, FA induced a remarkable increase in BUN and creatinine plasma levels, as well as in the kidney weight/rat weight ratio compared to the control group. These alterations were prevented at day 2 by the pre-administration of NAC (Fig. 1A–C). Furthermore, histological analysis in sections stained with H&E from the FA group showed extensive damage in the proximal convoluted tubules, characterized by flattened epithelial cells alternating with necrotic cells. Some tubules showed hyaline casts in their lumen (Fig. 1D). The latter alterations were partially prevented by NAC preadministration. Furthermore, quantification of the damaged area observed by histology showed that NAC pre-adminstration at day two significantly reduced the injured area in the kidney cortex, which was also observed at 28 days (Fig. 1E). Additionally, NAC preadministration at day two maintained the tubules with normal morphology and with regeneration signs, whilst decreasing the tubules with necrotic morphology observed by histology (Fig. 1F). These results are consistent with our previous report, in which we demonstrated that FA induced AKI one day after its administration, and that NAC pre-administration protected kidney function at this time [13]. Interestingly, renal damage markers in the FA group remained high, even 4 days after FA administration and showed a tendency to decrease with time. This is in concordance with previous studies in mice, in which BUN and creatinine levels returned to control levels after 4 days of FA administration [38,46]. However, an increase in proinflammatory and profibrotic markers at 6 and 14 days after FA administration was also reported [38,46], suggesting the progression of the nephropathy.

As we found that systemic markers of renal damage progression returned to normal after 28 days of FA administration, we measured the GFR and other hemodynamic parameters 28 days after FA administration: FA decreased the GFR and increased the RVR, which triggers the decrease in RBF and RPF (Fig. 2A). Additionally, histological sections stained with Masson trichrome showed mild interstitial fibrosis in the FA group (Fig. 2B), confirming the progression to CKD in this model. Interestingly, the FF and MAP did not show changes with respect to the control group (Fig. 2A). On the other hand, NAC pre-administration prevented the GFR and RBF decrease, as well as the increase in RVR (Fig. 2A). Furthermore, NAC reduced at 28 days the injuries in the cortex (Fig. 1E), increased the number of tubules with regenerative signs (Fig. 1F) and prevented interstitial fibrosis (Fig. 2B), suggesting that this treatment partially blocked the progression of renal damage.

3.2. FA induces the persistence of mitochondrial bioenergetics impairment and renal damage progression

We previously demonstrated that FA induces, one day after its administration, mitochondrial decoupling and OXPHOS capacity reduction, which was mainly related to FA-induced CI dysfunction [13]. Furthermore, we also demonstrated that mitochondrial bioenergetics dysfunction favors the emergence of AKI in this model [13]. Therefore, to evaluate if the AKI-to-CKD transition is linked to the persistence of mitochondrial dysfunction, we evaluated the respiratory parameters in CI-linked respiration in isolated renal mitochondria. After mitochondrial addition (respiratory state 1), the ETS was stimulated by addition of CI-linked substrates generating the respiratory state 2 (Fig. 3A). Then, the addition of ADP stimulates oxygen consumption due to ATP synthesis generating the S3. Finally, OXPHOS inhibited by oligomycin generated S4o. As is observed in Fig. 3A, the vast majority of respiration in S3 is attributable to ATP synthesis (P = S3–S4o), meanwhile in the S4o, the leak of the respiration (L) is the main contributor to the oxygen consumption rate. For its part, the RC (S3/S4o) allows us to determine the degree of coupling between ETS and OXPHOS.

We found that FA induced the reduction of S3 and P respiration at the acute stage, which returned to control values after 14 and 7 days, respectively (Fig. 3B, D). These data indicate that the OXPHOS capacity reduction in CI-linked respiration persisted until day 7. Interestingly, FA induced a stepwise increase of S4o respiration (Fig. 3C), indicating a progressive increase in the leak over time. These effects eventually trigger the mitochondrial decoupling at all studied time points (Fig. 3E). Furthermore, FA also reduced $\Delta\Psi m$ in respiratory S3 (principally associated to OXPHOS) at the evaluated time interval (Fig. 3F),

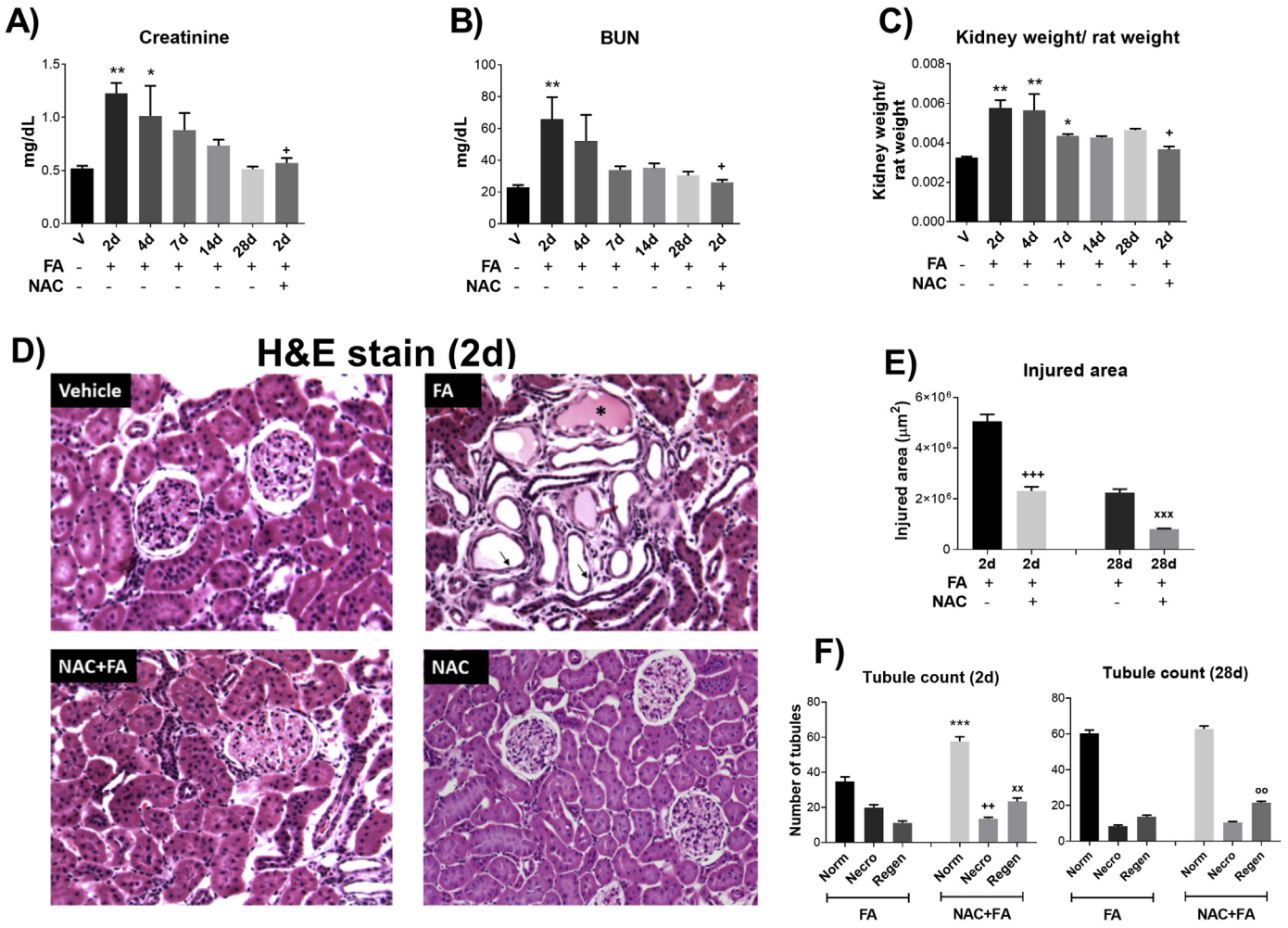

Fig. 1. Acute renal damage stage. Temporal course of the classical renal damage markers **(A)** creatinine and **(B)** blood urea nitrogen (BUN) in plasma, as well as **(C)** the kidney weight/total rat weight ratio. Data are mean ± SEM, n = 5–6. *p < 0.05 and **p < 0.01 Dunnet's *vs.* vehicle; $^{+}$p < 0.05 Student's T-test *vs.* FA 2 d. Representative kidney micrographs of the four experimental groups, 2 d after FA administration. **(D)** Normal histological kidney structure is seen in the representative micrograph of the control that received only the vehicle. In contrast, the group treated with FA showed numerous proximal convoluted tubules coated with flattened epithelium (arrows), some tubules showed hyaline casts in their lumens (asterisk). Animals treated with FA and NAC showed reduced tubular damage, while the treatment only with NAC did not produce any histological abnormalities. All micrographs 200x magnification, hematoxylin/eosin (H&E) staining. **(E)** Quantification of the damaged area observed by histology in the renal cortex at 2 d and 28 d $^{+++}$p < 0.001 Student's T-test *vs.* FA 2 d; ^{xxx}p < 0.001 Student's T-test *vs.* FA 2 d. **(F)** Tubule count per type in renal cortex at 2d and 28d. Norm = normal morphology, Necro = necrotic, Regen = in regeneration. ***p < 0.001 Student's T-test *vs.* Norm FA 2d. $^{++}$p < 0.01 Student's T-test *vs.* Necro FA 2d. ^{xx}p < 0.01 Student's T-test *vs.* Regen FA 2d. ^{oo}p < 0.01 Student's T-test *vs.* Regen FA 28d. V = vehicle, FA = folic acid, NAC= N-acetyl-cysteine, d = days after FA administration.

which agrees with the reduction in OXPHOS capacity. However, no changes were found in the ΔΨm in S4o between the groups (Fig. 3G).

On the other hand, NAC pre-administration prevented, at day two after FA administration, the decrease in S3 and P respiration and in the ΔΨm in respiratory S3, preventing mitochondrial decoupling (Fig. 3); which indicates that NAC preserved the OXPHOS capacity despite FA administration. Interestingly, NAC also partially preserved the mitochondrial respiratory parameters and ΔΨm at day 28 after FA administration (Fig. 3).

We previously demonstrated that at day one after its administration, FA-induced OXPHOS capacity reduction was strongly linked to CI dysfunction [13]. Furthermore, the observed respiratory alterations at all studied time points suggest that this reduction persisted from day 2 until day 28. Therefore, we separately evaluated the activity of CI and of the other ETS elements involved in CI-linked respiration. We observed that since day two, FA decreased the activity of CI, which tended to recover over time but without returning to baseline levels (Fig. 4A). Interestingly, NAC pre-administration prevented, at day two, the FA-induced CI activity decrease (Fig. 4A), which is consistent with our previously reported results at day one [13]. Additionally, FA induced the permanent reduction over time in CIII activity, which was also reversed by NAC pre-administration (Fig. 4B). Finally, no changes were observed between the different groups in CIV activity (Fig. 4C).

3.3. FA induces progressive β-oxidation dysfunction in the AKI-to-CKD transition

Although in the kidneys many substrates participate in ATP production, it is predominantly sustained by fatty acid β-oxidation [62,63]. Furthermore, the mRNA and the levels of β-oxidation proteins were reported deregulated in CKD animal models [64–66] and more recently in patients [66,67]. Therefore, in order to evaluate if the observed mitochondrial impairment was also linked to β-oxidation dysfunction, we evaluated the respiratory parameters by feeding with palmitate. FA administration reduced at all evaluated times the S3 respiration (Fig. 5A) and P (Fig. 5C). Additionally, FA also reduced RC since day two, which was recovered after 28 days of follow-up (Fig. 5D). However, it did not have a significative effect on S4o respiration (Fig. 5B).

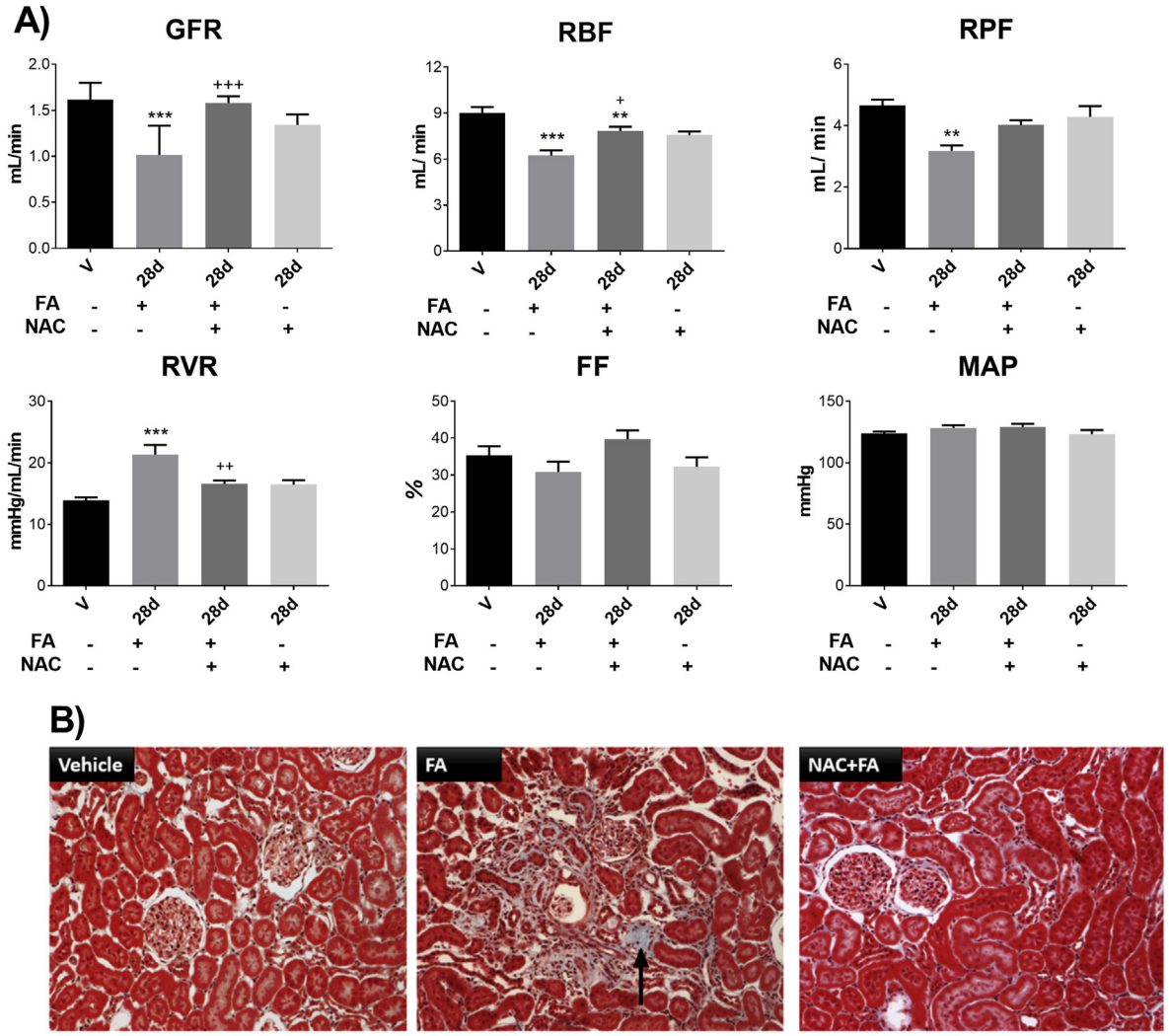

Fig. 2. Chronic renal damage stage at 28 days after FA administration. (A) Hemodynamic parameters of all experimental groups: glomerular filtration rate (GFR), renal blood flow (RBF), renal plasma flow (RPF), renal vascular resistance (RVR), filtration fraction (FF) and mean arterial pressure (MAP). The persistence in kidney hemodynamic alterations confirms the presence of chronic damage. Data are mean ± SEM, n = 4–5. $^{**}p < 0.01$ and $^{***}p < 0.001$ *vs.* V; $^{+}p < 0.05$, $^{++}p < 0.01$ and $^{+++}p < 0.001$ *vs.* FA 28 d; Tukey tests. **(B)** Representative kidney micrographs of trichrome Masson staining of the four experimental groups 28 d after FA administration. Control animals that received only the vehicle showed normal histology. In contrast, there is mild interstitial fibrosis (arrow) in the FA treated group, while administration of NAC totally prevented the fibrosis induced by FA. V = vehicle, FA = folic acid, NAC= N-acetyl-cysteine, d = days after FA administration.

These results suggest that FA administration affected β-oxidation mainly by the decrease in ATP production and mitochondrial decoupling even 28 days after FA administration. Therefore, we performed electron microscopy analysis at 28 days after FA administration to evaluate the mitochondrial ultrastructure. After 28 days the FA group showed in PT epithelial cells numerous mitochondria with irregular shape and smaller size with respect to the control group (Fig. 6). Furthermore, even at 28 days after FA administration, mitochondria displayed a mild cristae disruption and effacement (Fig. 6), which is in concordance with the reduction in the OXPHOS capacity observed by respirometry (Fig. 5 A, C).

On the other hand, results of the pre-administration of NAC, evaluated two days after FA administration, reveal that NAC effectively prevented the decrease in the respiration in S3 and P induced by FA (Fig. 5A, C). Furthermore, these protective effects were also present at day 28, when mitochondrial decoupling was also prevented (Fig. 5D), which is in agreement with the preservation of mitochondrial ultrastructure and cristae observed at day 28 in the NAC + FA group (Fig. 6), confirming that NAC pretreatment is able to preserve the OXPHOS capacity at the chronic stage.

3.4. FA induces a permanent pro-oxidative state in mitochondria during the AKI-to-CKD transition

It has been reported that FA-induced oxidative stress in the kidneys favors the progression of renal damage [38,50,51]. We previously demonstrated that FA induced at day one a prooxidant state in renal mitochondria, triggering the increase in mitochondrial H_2O_2 production, which promoted oxidative stress in the kidneys [13]. Therefore, in order to evaluate if the persistence in mitochondrial decoupling and the increase in S4o (Fig. 3) are linked to the persistence of a pro-oxidative state in mitochondria, we determined the aconitase activity (a sensitive mitochondrial target of ROS) as an oxidative stress marker, as well as the activity of the enzymes GR and GPx in isolated mitochondria.

FA strongly reduced the aconitase activity since day two and it remained below the control level even 28 days after FA administration (Fig. 7A). Likewise, the mitochondria of the FA group showed a reduction in the GPx (Fig. 7B) and GR (Fig. 7C) activities at the entire time-interval evaluated, which strongly supports the idea of a pro-oxidative state in mitochondria during the progression of renal damage. These data agree with the persistent elevation of mitochondrial H_2O_2 at

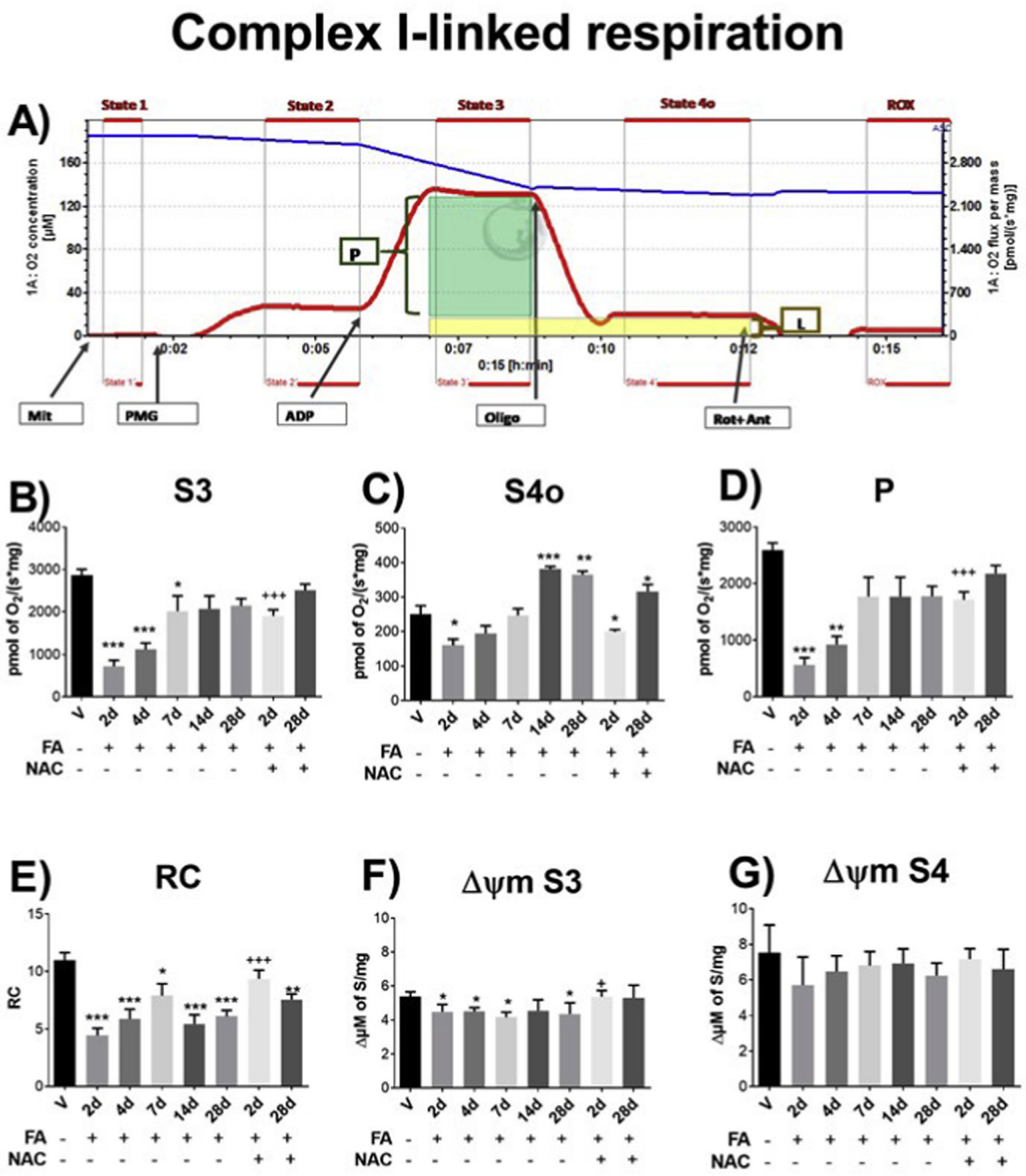

Fig. 3. Respiratory parameters and mitochondrial potential

Fig. 3. **Bioenergetics and mitochondrial membrane potential (ΔΨm) alterations. (A)** Schematic representations of the respiratory parameters. Blue line corresponds to O_2 concentration, red line corresponds to the rate of oxygen consumption. The additions are represented by gray arrows. L = leak of respiration, Mit = mitochondria, PMG = pyruvate–malate-glutamate, P= OXPHOS-associated respiration, Oligo = oligomycin, Rot = rotenone, Ant = antimycin A, ROX = residual non-mitochondrial respiration Temporal evaluation of mitochondrial respiratory parameters in complex I-linked respiration: **(B)** state 3 (S3), **(C)** state 4 induced by oligomycin (S4o), **(D)** P and **(E)** respiratory control (RC). Temporal evaluation of the changes in Δψm using safranin O as probe in the **(F)** S3 and **(G)** S4o respiratory states. Pyruvate–malate-glutamate were used as a substrate. V = vehicle, FA = folic acid, NAC= N-acetyl-cysteine, d = days after FA administration. Data are mean ± SEM, n = 6–7. *p < 0.05, **p < 0.01, ***p < 0.001 Dunnet's *vs.* V; $^{+}$p < 0.05 and $^{+++}$p < 0.001 Student's T-test *vs*. FA 2 d.

day 28 after FA administration (Fig. 7D) and are also supported by the higher levels of the oxidative stress marker 4-HNE in mitochondria at the chronic stage (Fig. 6E).

On the other hand, NAC pre-administration prevented, at day two, the decrease in activity of the aconitase (Fig. 7A) and antioxidant enzymes (Fig. 7B and C) as well as the increase in H_2O_2 levels at day 28 (Fig. 7D) and in the levels of 4-HNE in mitochondria (Fig. 7E). These results confirm that NAC prevented FA-induced mitochondrial oxidative stress.

3.5. *FA-induced mitochondrial dysfunction was not linked to mitochondrial mass changes in CKD*

It has been reported that at the acute stage after FA administration, there is a reduction in mitochondrial biogenesis [13,39,46], which could trigger a reduction in mitochondrial mass. To evaluate if the

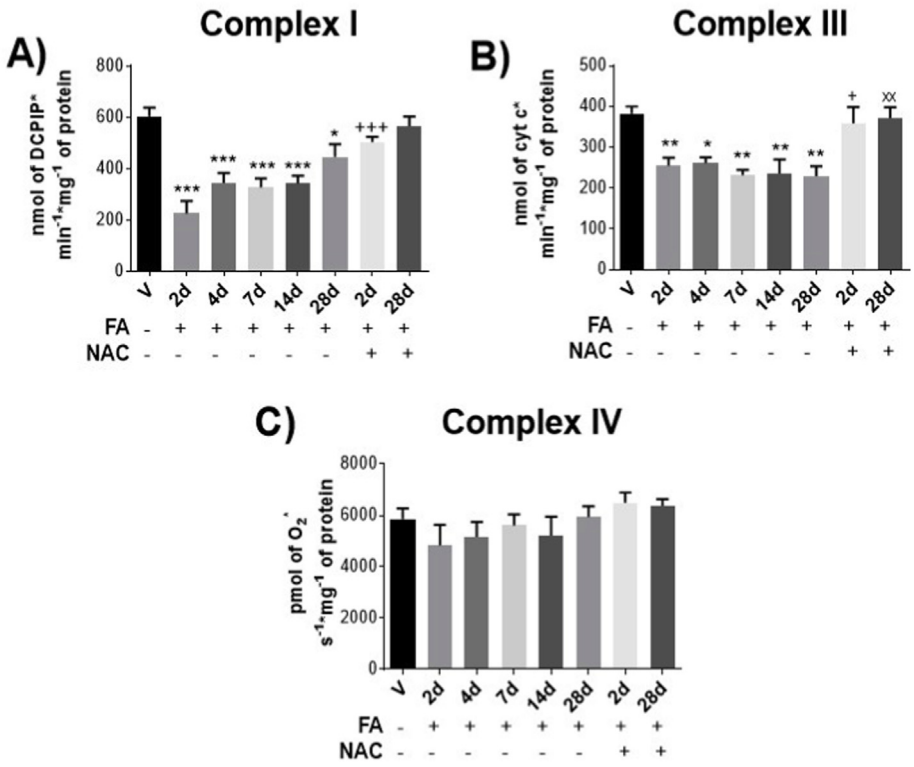

Fig. 4. Activity of mitochondrial complexes. Temporal evaluation of the activity of mitochondrial complexes involved in CI-linked respiration: **(A)** complex I, **(B)** complex III and **(C)** complex IV. V = vehicle, FA = folic acid, NAC= N-acetyl-cysteine, d = days after FA administration, cyt *c* = cytochrome *c* reduced, DCPIP = 2,6-dichlorophenolindophenol sodium salt hydrate, O_2 = oxygen. Data are mean ± SEM, n = 5–6. *P < 0.05, **P < 0.01, ***P < 0.001 Dunnet's *vs.* V; $^{+}$p < 0.05 and $^{+++}$p < 0.001 Student's T-test *vs.* FA 2 d ^{xx}p < 0.01 Student's T-test *vs.* FA 28 d.

observed mitochondrial alterations are linked to changes in mitochondrial biogenesis at the chronic stage, we evaluated the protein levels of the mitochondrial biogenesis markers PGC-1α and NRF2, as well as the levels of VDAC and a selected subunit of each of the mitochondrial complexes as a mass marker at seven days after FA administration.

We previously reported that after one day of its administration, FA decreased the mitochondrial biogenesis in kidney, by reducing the levels of PGC-1α and NRF2 [13]. However, when samples at 7, 14 and 28 days after FA administration were evaluated, as shown in Fig. 8, FA did not induce changes in the levels of the following proteins: NRF2, VDAC and the mitochondrial ETS subunits suggesting that the observed bioenergetic mitochondrial alterations are not linked to changes in mitochondrial mass, at least during the time period between day 7 and

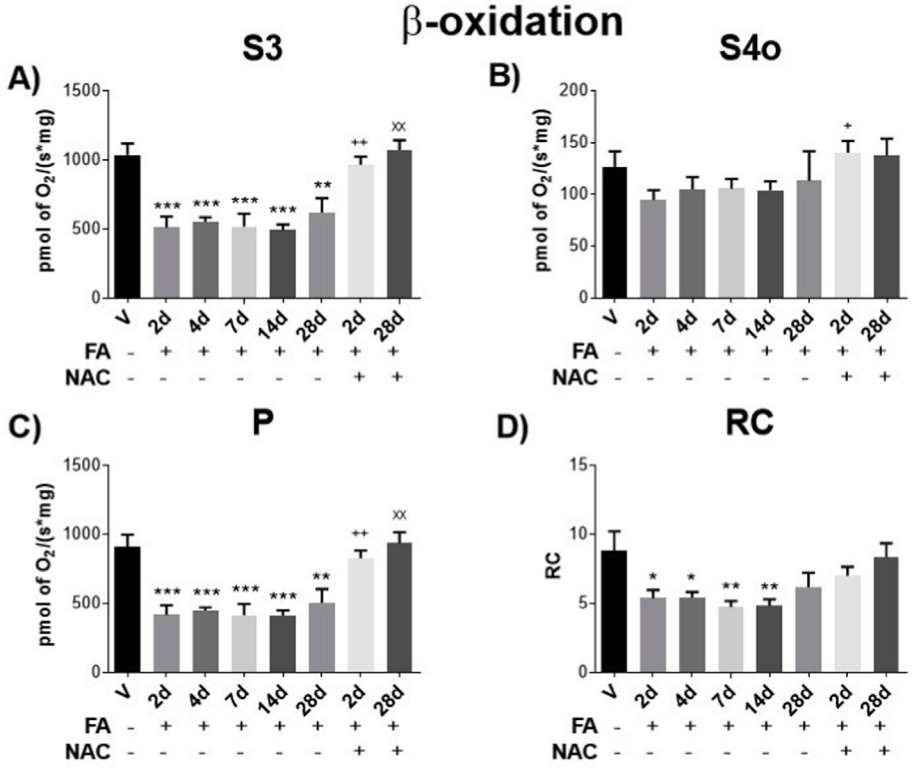

Fig. 5. Mitochondrial β-oxidation dysfunction. Temporal evaluation of the respiratory parameters associated to mitochondrial β-oxidation: **(A)** state 3 (S3), **(B)** state 4 induced by oligomycin (S4o), **(C)** OXPHOS-associated respiration (P) and **(D)** respiratory control (RC). 2 mM L-carnitine plus 2 μM palmitoyl-L-carnitine plus 2 mM malate (C/PC/M) were used as β-oxidation-linked substrates. V = vehicle, FA = folic acid, NAC= N-acetyl-cysteine, d = days after FA administration. Data are mean ± SEM, n = 5–6. *P < 0.05, **P < 0.01, ***P < 0.001 Dunnet *vs.* V; $^{+}$p < 0.05 and $^{++}$p < 0.01 Student's T-test *vs.* FA 2 d ^{xx}p < 0.01 Student's T-test *vs.* FA 28 d.

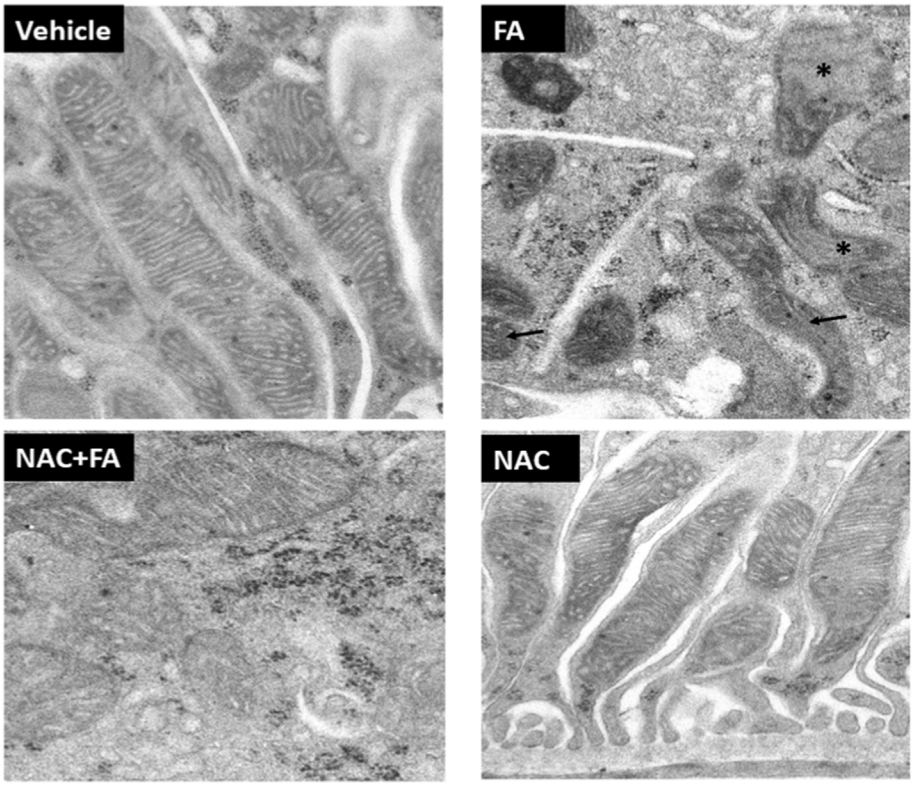

Fig. 6. Representative electron microscopy micrographs of mitochondria from the epithelial cells of the convoluted tubules at 28 d. Normal ultrastructural morphology of mitochondria from the control group that only received the vehicle. In contrast, mitochondria from rat treated with FA showed irregular size and shape with cristae disruption (arrow) or effacement (asterisk). Treatment with NAC partially prevented the mitochondrial damage induced by FA, while the treatment only with NAC did not induce any mitochondrial damage. FA = folic acid, NAC= N-acetyl-cysteine, d = days after FA administration.

day 28. Additionally, as we previously showed, one day after its administration, FA induced an impaired mitophagy process [13]. However, no significative changes were observed at 7, 14 and 28 days after FA administration in the levels of the mitophagy protein PINK1 in isolated mitochondria (Fig. 8E). These results, together with our previous report [13] suggest that the alterations induced by FA in biogenesis and mitophagy are mainly present in AKI, but they are reduced in the chronic state. However, since autophagy flow is a dynamic process, a more detailed evaluation of different autophagy proteins is still necessary to clarify the time evolution of mitophagy, which we are considering for a future work.

4. Discussion

The administration of high levels of FA leads to an increase of its metabolized product (tetrahydrofolate) in blood [42,43], which is then transported inside the cell by the reduced folate carrier exchanger and by the high-affinity folate receptor [42,43,45,68]. In the case of the kidney, folate metabolites accumulate in higher concentrations than in other tissues due to the expression of the high-affinity folate receptor in this organ, especially in PT cells [43]. The folate metabolites are immediately stored as polyglutamate derivatives impermeable to the cell membrane [45,68]. Although folates in the cell are distributed among the mitochondria, nucleus and cytosol, the mitochondria store 40% of the total cellular folate [43,45]. This process requires higher levels of NADPH to reduce folate to tetrahydrofolate [41,42], thus diminishing the antioxidant defense [13,38]. Therefore, mitochondria are especially vulnerable to high doses of folate [13,46]. Additionally, in FA-induced renal damage models, when high amounts of FA are administered and accumulate in the kidneys, the receptor and transporter of FA become saturated. These, together with the low solubility of FA in water, lead to folate crystals' precipitation in the lumen, enhancing tubular cell death, inflammation and fibrosis [38,39,44,46]. However, mitochondria have also been implicated in the promotion of these pathological processes that lead to CKD [9,23–27].

It has been well characterized that severe episodes of AKI trigger CKD development [2,20–22]. Furthermore, the severity of the injury during the AKI event is a highly effective indicator of how fast the CKD will progress [69]. We previously characterized that at day one after FA administration, there is a remarkable significative increase in creatinine and BUN plasma levels, as well as a higher urinary volume compared to the control group [13]. The time course evaluation showed that the increase in BUN and creatinine plasma levels reaches a peak at day two after FA administration and then decreases progressively with time (Fig. 1A and B). Furthermore, the histological alterations associated with AKI, like necrotic cell death, loss of brush border definition and PT's swollen cells were evident at days two (Fig. 1D). These results confirm that the peak in AKI is observed between day one and two after FA administration. The progressive decrease in these classical renal damage markers (Fig. 1A and B) has also been reported in mice administered with FA, signaling the end of the acute stage and the transition to CKD [38,46], which is characterized by progressive renal deterioration, as evidenced by the persistence of oxidative stress, cell death, inflammation, fibrosis, EMT transition and maladaptive repair of the tubular epithelium at the interval between days 2–14 after FA administration [39,46,52,70]. In fact, at 28 days we observed a decrease in the GFR (the major parameter of renal function), RBF and in RPF, as well as an increase in RVR (Fig. 2A). These results, together with the observed increase in the amount of fibrotic tissue (Fig. 2B), confirm the progression to CKD, which is congruent with studies that report CKD characteristics observed 14 days after FA administration [39,46,70].

It has been hypothesized that mitochondrial bioenergetics dysfunction could be related to the processes that favor renal damage progression in the FA model [13,46,70]. However, until now there had not been a time course study of the mitochondrial bioenergetics and oxidative stress alterations and their participation in the transition from AKI-to CKD. In this work, we have characterized for first time the temporal alterations in mitochondrial bioenergetics in the FA model. We show that at the AKI stage of the disease, there is a reduction in mitochondrial OXPHOS capacity (Fig. 3B, D) and mitochondrial decoupling in CI-linked respiration (Fig. 3E). Interestingly, from days 1–28, FA reduced the $\Delta\Psi m$ in respiratory S3 (Fig. 3F), respiration state

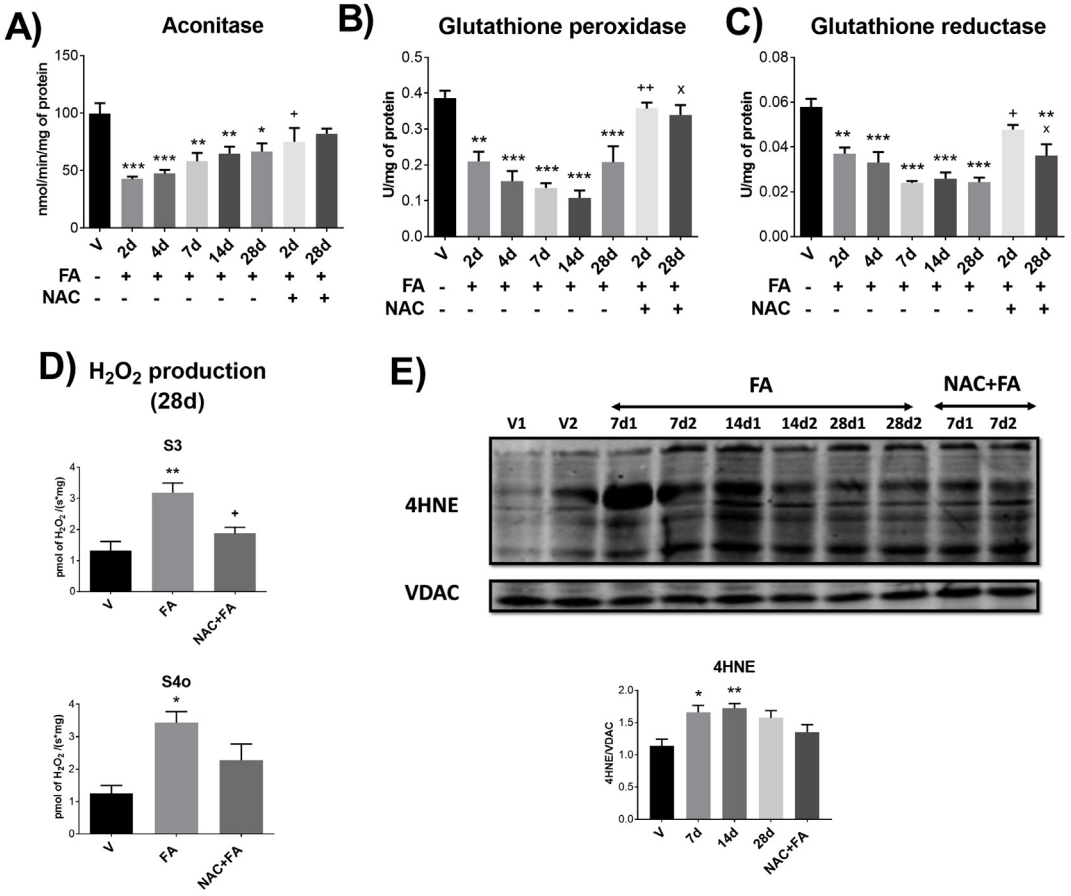

Fig. 7. Persistence of the prooxidative stage in mitochondria. Temporal evaluation of the enzymatic activity of **(A)** aconitase, **(B)** glutathione peroxidase (GPx) and **(C)** glutathione reductase (GR) in isolated mitochondria. V = vehicle, FA = folic acid, NAC= N-acetyl-cysteine, d = days after FA administration. Data are mean ± SEM, n = 5–6. *p < 0.05, **p < 0.01, ***p < 0.001 Dunnet's *vs.* V; $^{+}$p < 0.05 and $^{++}$p < 0.01 Student's T-test *vs.* FA 2d. ^{x}p < 0.05 Student's T-test *vs.* FA 28d. **(D)** Evaluation of mitochondrial hydrogen peroxide (H_2O_2) production in isolated mitochondria, 28 d after FA administration in respiratory state 3 (S3) and state 4 induced by oligomycin (S4o). Data are mean ± SEM, n = 5–6. *p < 0.05 and **p < 0.01 *vs.* V; $^{+}$p < 0.05 *vs.* FA 28 d; Tukey tests. **(E)** Oxidative stress marker 4-hydroxynonenal (4-HNE) in isolated mitochondria by Western blot and its quantification by densitometry. VDAC = voltage dependent anion channel. Data are mean ± SEM, n = 4. *p < 0.05, **p < 0.01 Dunnet's *vs.* V.

in which the presence of saturating levels of ADP generates the ΔΨm mainly used for ATP synthesis [71]. Meanwhile, FA did not induce significative changes in ΔΨm with respect to the control in respiratory S4o (Fig. 3G), resting respiration state of non-ATP production after inhibition of ATP synthesis by oligomycin, when ΔΨm is maintained and oxygen consumption is only stimulated to compensate the proton leak [71,72]. The results indicate that FA harmful effects occur only in conditions of high energy demand, when ATP production generates an additional stress to maintain ΔΨm, but also indicate that under resting conditions, the effect of FA on the ΔΨm dissipation is minimal. Therefore, ATP production is the principal process affected by FA administration. These changes can be associated mainly to CI- and CIII activity reduction at the acute stage (Fig. 4A and B). These results match our previous report at day 1 after FA administration, where CI inhibition was observed [13]. Interestingly, in that previous study, no change in CIII activity was observed at day one [13]. Alterations in CIII activity were observed only after day two (Fig. 4B), which implies that CI impairment precedes CIII impairment. This effect may be attributable to the higher susceptibility of CI to irreversible post-translational modifications at specific cysteine residues that decrease its activity [73,74]. In fact, we previously reported that at day one after FA administration, the reduction in CI activity was related to changes in the "S-glutathionylation" post-translational modification. Furthermore, a recent study showed that inhibition of CI by rotenone exacerbates renal damage 3 days after FA administration [75]. This study also showed that inhibition of CI enhanced the FA-induced inflammation and cell death processes [75], highlighting that mitochondrial CI dysfunction favors the progression of renal damage.

We observed a partial recuperation in S3 and P (Fig. 3B, D) at the chronic stage, which is consistent with partial CI recovery (Fig. 4A). However, the S4o progressive increase along the evaluated time-interval explains why even at the chronic stage, the RC remained reduced with respect to the control (Fig. 3E). Furthermore, the electron microscopy images showed that even at day 28 after FA administration, mitochondrial cristae disruption can be observed (Fig. 6). These results indicate that mitochondrial ATP production during the transition to CKD was only partially recovered and was accompanied by chronic mitochondrial decoupling. This permanent mitochondrial decoupling favors the increase in mitochondrial oxidative stress, as observed by the reduction in: aconitase activity (Fig. 7A), mitochondrial antioxidant enzymes activity (Fig. 7B and C) and in the mitochondrial 4-HNE levels (Fig. 7E). In effect, CI dysfunction and mitochondrial decoupling are related to the increase in mitochondrial ROS production [13,73,74], which is consistent with the observed mitochondrial H_2O_2 production in the FA group at day 28 (Fig. 7D). Moreover, we previously demonstrated that the increase in mitochondrial ROS triggers the pathological over-activation of NADPH oxidases (NOX) in mitochondria-rich segments like the PT [13]. Such effect is highly relevant because the over-activation of NOX has been proposed as a critical mechanism involved in the AKI-to-CKD transition induced by FA [29,39]. In fact, in other

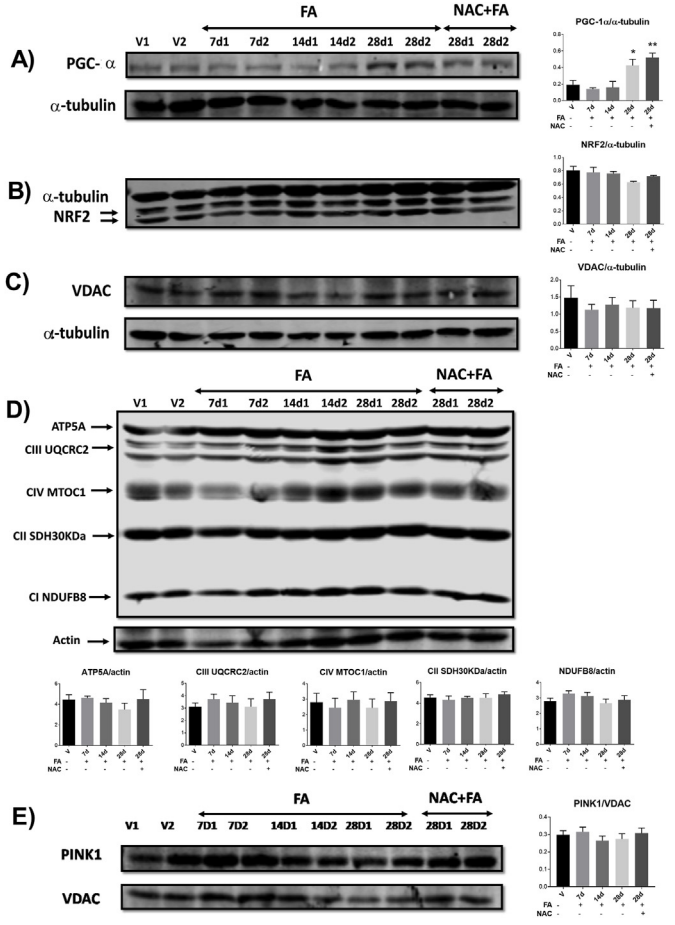

Fig. 8. Mitochondrial mass and biogenesis. Western blot and its quantification of the levels of mitochondrial biogenesis markers: **(A)** peroxisome proliferator-activated receptor *gamma* coactivator 1-*alpha* (PGC-1α) and **(B)** nuclear respiratory factor 2 (NRF2) proteins, as well as **(C)** voltage-dependent anion channel (VDAC) and **(D)** a subunit of each one of the mitochondrial complexes. **(E)** Levels of mitophagy protein PTEN-induced putative kinase 1 (PINK1) in isolated mitochondria. Data are mean ± SEM, n = 4. *p < 0.05, **p < 0.01 Dunnet's *vs.* V. V = vehicle, FA = folic acid, NAC= N-acetylcysteine, d = days after FA administration. Complex I subunit CI-NDUFB8, complex II 30-kDa subunit CII-SDHB30KDa, complex III-core protein 2 (CIII-UQCRC2), complex IV subunit I (CIV-MTCO1), and ATP synthase *alpha* subunit (ATP5A).

CKD models like 5/6 nephrectomy, the increase in mitochondrial ROS favors further pathological ROS production by NOX [60,76,77], enhancing the expression of proinflammatory cytokines and profibrotic factors, and thus triggering the progression of renal damage [78–81].

Furthermore, in the present work we have also described for the first time the temporal mitochondrial alterations in β-oxidation as a mechanism that contributes to the AKI-to-CKD transition in the FA model. In fact, we observed that since the AKI event, there is a reduction in the S3, RC and in the OXPHOS capacity associated to fatty acid β-oxidation (Fig. 5A, C, D). The data indicate that ATP production linked to fatty acid β-oxidation is permanently decreased after FA administration. This is particularly important for kidneys, where the vast majority of ATP production is attributed to fatty acid β-oxidation [62,63]. Therefore, our β-oxidation data (Fig. 5) suggests a permanent state of energetic stress during renal damage progression, which is supported by the mitochondrial irregular shape and cristae effacement observed at day 28 in the FA group (Fig. 6). In this regard, there is a consensus that mitochondria in CKD fail to respond to ATP demands [9,82,83], as shown by inorganic phosphate accumulation, lower ATP levels, increased oxygen uptake and decreased sodium transport in the kidneys. These changes have also been described in CKD patients [84–86]. Furthermore, the mRNA and β-oxidation protein levels are deregulated in CKD animal models [64–66] and in patients [66,67]. In addition, a recent work showed that the expression levels of genes related to fatty acid β-oxidation are markedly lower in samples of CKD patients and in FA-administered animals, with no changes in the mitochondrial DNA copy number between the groups [70].

The decrease in the levels of mitochondrial β-oxidation proteins appears to be a common pathology in CKD [10,65,85]. In fact, in FA models, the reduction in the expression of fatty acid β-oxidation preceded the increase in the expression of fibrosis marker [70]. This effect is consistent with the observed reduction of the respiratory parameter associated to the AKI event (Fig. 5), before renal fibrosis was observed (Fig. 2B). Furthermore, it was shown in Pax8rtTA/TRE-CD36 double-transgenic mice that reducing the expression of the fatty acid β-oxidation proteins alone is enough to reprogram tubular epithelial cells into a profibrotic phenotype, leading to CKD development [70]. In fact, the authors suggested that reduced fatty acid β-oxidation could be a manifestation of a broader mitochondrial dysfunction and/or oxidative phosphorylation defects [70]. These findings are consistent with our results, in which β-oxidation impairment (Fig. 5) is accompanied by a reduction in mitochondrial respiratory parameters in CI-linked respiration (Fig. 3), by a CI and CIII activity reduction and by enhanced mitochondrial ROS production. Notably, mitochondrial ROS are known to activate several targets related to CKD, especially fibrosis [56,58,87]. Together, these data suggest that early mitochondrial dysfunction triggers mitochondrial fatty acid β-oxidation reduction, which together with the mitochondrial ROS overproduction, promotes renal fibrosis.

On the other hand, FA administration leads, during the AKI stage, to a decrease in the mRNA levels of some mitochondrial biogenesis proteins in kidneys [39,46]. Indeed, we previously reported that at day one after FA administration, there is a reduction in PGC-1α and NRF2 protein levels, confirming the hypothesis that in the FA-induced AKI, mitochondrial biogenesis is restrained [13]. Interestingly, the NRF2, VDAC and the mitochondrial ETS subunit protein levels evaluated at days 7–28 after FA administration did not show significative changes compared to the control group (Fig. 8A–D). Together these data suggest that the FA-induced decrease in mitochondrial biogenesis is predominantly present at the acute stage of the disease.

On the other hand, NAC pre-administration was able to prevent the increase in the classic renal damage markers BUN and creatinine (Fig. 1A–B) and the histological alterations (Fig. 1D) at day 2, which is consistent with our previous study at day 1 [13]. We previously reported that NAC alone, 24 h after its administration, increased the GSH levels in kidney mitochondria, the GSH/GSSG ratio and the total S-glutathionylation levels with respect to the vehicle [13]. These effects were associated to NAC's capacity to preserve the redox state and the mitochondrial S-glutathionylation, especially in OXPHOS proteins, which prevents since day one after FA administration the loss of the activity of OXPHOS proteins in the posterior oxidative context induced by FA [13]. In the present work, we observed that the NAC protection observed at day one [13] remains at day two, preventing the FA-induced OXPHOS capacity dysfunction (Fig. 3B, D), ΔΨm decrease (Fig. 3F) and mitochondrial decoupling (Fig. 3E) in CI-linked respiration. Furthermore, it is extended even at day 28 (Fig. 3). Therefore, NAC's preservation of CI and CIII activities in AKI-to-CKD (Fig. 4A and B) would be a result of its effect at early time points. Interestingly, NAC pre-administration, in both AKI and AKI-to-CKD transition stages, also prevented the changes in FA-induced reduction in the S3, RC and in the OXPHOS capacity associated to fatty acid β-oxidation (Fig. 5A, C, D) and preserved the size and form of mitochondria, as well as their cristae definition (Fig. 6), confirming a general protection by NAC of mitochondrial ATP production.

The protective effects of NAC administration were previously shown in experimental models of kidney damage, like that induced by contrast [88]. In fact, in such model the beneficial effects of NAC and its

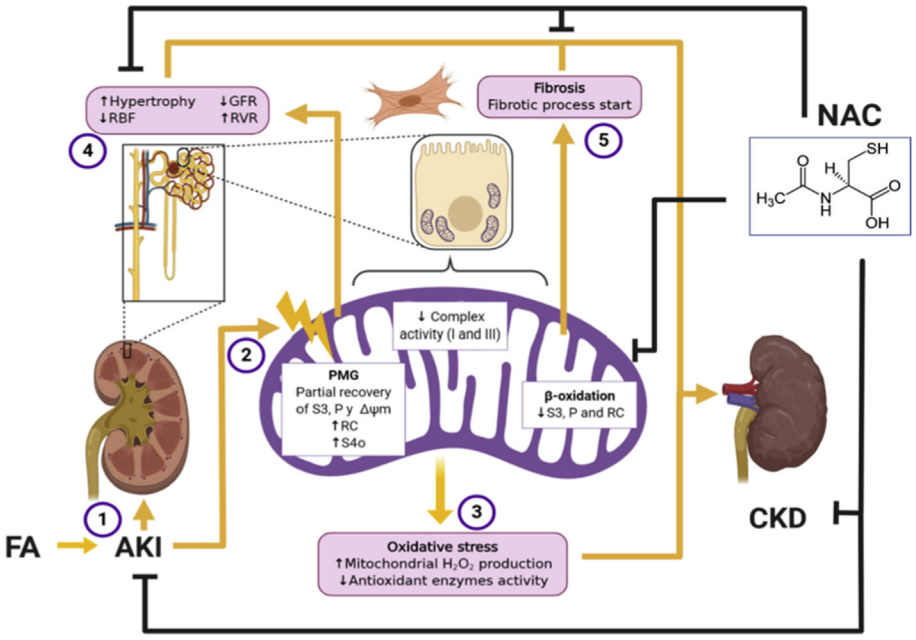

Fig. 9. Integrative scheme. FA induces early AKI (1). This is related to mitochondrial bioenergetics impairment (2). At the acute stage, there is CI and CIII activity reduction, leading to S3, S4o, P, RC and ΔΨm decrease in CI-linked respiration but also to a reduction in S3, P and RC in mitochondrial fatty acid β-oxidation. There is a partial recovery in S3, P and ΔΨm in CI-linked respiration. However, S4o and CI-linked respiration and the respiratory parameters linked to β-oxidation progressively decrease. This indicates a permanent reduction in ATP production and mitochondrial decoupling. The bioenergetics alterations favor persistent oxidative stress in mitochondria over time (3), reducing antioxidant activity and enhancing mitochondrial H_2O_2 production. Mitochondrial alteration as a whole favors processes such as hemodynamic alterations (4) and fibrosis (5), which are linked to CKD progression. Otherwise, NAC pre-administration (black lines) prevented the mitochondrial impairment in FA-induced AKI, thus avoiding the progression of mitochondrial dysfunction over time and fibrosis and hemodynamic alterations, which prevent CKD development. AKI = acute kidney injury, CKD = chronic kidney disease, FA = folic acid, GFR = glomerular filtration rate, NAC= N-acetylcysteine, P = respiration directly attributable to oxidative phosphorylation, PMG = pyruvate-malate-glutamate, CI-linked substrate, RBF = renal blood flow, RC = respiratory control, RVR = renal vascular resistance, S3 = respiratory state 3, S4o = respiratory state 4 induced by oligomycin, ΔΨm = mitochondrial membrane potential.

derivate, the N-acetylcysteine amide, are directly linked to the preservation of redox balance and GSH levels [88]. Likewise, in the AKI-to-CKD transition induced by cisplatin administration, the nephroprotective effects of NAC are due to its capacity to prevent oxidative stress, avoiding the renal senescence induced by the sirtuin 1 (SIRT1)-p53 pathway [89]. Although the vast majority of experimental models have reported NAC's protective effect in kidney damage [13,48,88–91], its utility is still under debate in the case of clinical studies [92]. Part of the controversy can be explained given the great heterogeneity in the literature regarding the route of administration, dose, frequency and treatment scheme, among other factors [49,92,93]. In this regard, the pre-treatment scheme seems to be the most effective approach to prevent kidney injury and to increase GSH levels than the post-treatment, which can help explain the differences in the data reported in the literature [94]. Additionally, clinical studies in most cases have a relatively small sample size, short periods of NAC use and they are non-randomized or not blinded [92,95]. Therefore, wider and longer studies are needed. Indeed, works like that made by Liao et al. [95], with 123,608 CKD patients followed during 10 years, showed that prolonged use of NAC significantly reduces the risk of end stage kidney disease and the CKD progression. Furthermore, NAC's protective effects are enhanced with a higher dose and longer treatment [95].

In this work, the preservation of mitochondrial function by NAC is related to the prevention of oxidative stress in mitochondria. These NAC protective effects are observed since day two, where NAC prevents the decrease in the activities of aconitase (Fig. 7A), GPx (Fig. 7B) and GR (Fig. 7C), and they extend until day 7, as demonstrated by the prevented-increase in MDA levels (Fig. 7E). Furthermore, even at 28 days of evolution, NAC also decreases mitochondrial oxidative stress, as shown by the lower levels of mitochondrial H_2O_2 production (Fig. 7D) and the higher aconitase and GPx activity (Fig. 7A–B) with respect to the FA group. Although at 28 days the GR activity in the NAC group does not return to control levels, it is higher than in the FA group at that time. Together these results indicated that NAC, prevent mitochondrial redox imbalance at both acute and chronic stages (Fig. 7A–D) which are related to the prevention of CKD evolution (Fig. 2A–B). In fact, NAC prevented, at day 28, the FA-induced decrease in the GFR and in RBF, the increase in RVR (Fig. 2A), as well as the fibrotic alterations observed by histology (Fig. 2B). Together our results suggest that preserving mitochondrial function over time can prevent the AKI-to-CKD transition in FA-induced injury. In other models of CKD, the use of compounds capable of preserving mitochondrial function could attenuate renal damage progression [9,83,96,97]. It was also recently suggested that restoring mitochondrial β-oxidation could be beneficial for CKD treatment [70]. It was shown that enhancing fatty acid β-oxidation enzymes' expression by genetic or pharmacological means protects animals from kidney fibrosis in FA and in unilateral ureteral obstruction (UUO)-induced CKD [70]. Although this study [70] exclusively evaluated the mRNA and protein levels in FA models, it is complementary and in agreement with the present results, in which we describe for the first time the temporal alterations in the activity of the mitochondrial β-oxidation (Fig. 5) and the therapeutic benefit of NAC pre-treatment to protect renal mitochondria in the AKI-to-CKD transition.

Finally, as we propose in the integrative scheme (Fig. 9), the AKI induced by FA (1) is related to mitochondrial bioenergetics impairment, characterized by CI and CIII activity reduction, which trigger a reduction in S3, S4o P, RC and ΔΨm in CI-linked respiration, as well as a reduction in respiratory parameters linked to β-oxidation. Despite the progressive recovery of S3 and P in CI-linked respiration attributable to CI activity's partial recovery over time, the alterations in respiratory parameters linked to β-oxidation and mitochondrial decoupling persist over time and there is progressive increase in S4o, related to leaking processes. Together bioenergetic and β-oxidation alterations favor the permanence of a pro-oxidative state in mitochondria (3), enhancing mitochondrial H_2O_2 production during the progression to CKD. This permanent mitochondrial oxidative stress (3) promotes hemodynamic alterations (4) and fibrotic processes (5), triggering CKD. On the other hand, NAC pre-administration prevents the acute and long-term mitochondrial bioenergetics alterations induced by FA, avoiding their persistence over time and the persistence of a mitochondrial pro-oxidative stage. In addition, by preventing β-oxidation dysfunction and CI-linked mitochondrial impairment, NAC prevents fibrosis and hemodynamic alterations, and therefore the development of CKD in the FA model. Taken together, our results suggest the idea that prevention of mitochondrial dysfunction during AKI can be a useful strategy to

prevent the progression to CKD. However, more studies are still necessary to confirm this hypothesis.

5. Conclusion

FA induces an acute stage of renal damage alterations in mitochondrial β-oxidation and CI-linked respiration. Although in a chronic stage of renal damage there is partial recovery in CI-linked respiration parameters, the mitochondrial β-oxidation alterations persist over time, triggering a permanent reduction in ATP production and mitochondrial decoupling, favoring the progression to CKD.

Finally, the renal mitochondrial preservation that results from NAC pre-treatment in FA-induced AKI may be a promising therapeutic strategy to prevent the transition to CKD.

Declaration of competing interestCOI

The authors report no conflict of interests.

Acknowledgements

Research conducted for this publication was supported by grants from “Consejo Nacional de Ciencia y Tecnología” (CONACyT, A1-S-7495 and 281967), Programa de Apoyo a Proyectos de Investigación e Innovación Tecnológica (PAPIIT, #IN202219) of Universidad Nacional Autónoma de México (UNAM), Programa de Apoyo a la Investigación y el Posgrado (PAIP, 5000-9105), and Fondos del Gasto Directo autorizado a la Subdirección de Investigación Básica from Instituto Nacional de Cardiología Ignacio Chávez to ET and LGSL. We thank Dr. Eneida Bailón-Vélez for inulin determinations and Dr. Ismael Torres for technical support with experimental animals. Special thanks to Programa de Apoyo a los Estudios de Posgrado (PAEP) from Programa de Maestría y Doctorado en Ciencias Bioquímicas, Universidad Nacional Autónoma de México (UNAM) for the support received. O. E. A-T. is a student of the Programa de Maestría y Doctorado en Ciencias Bioquímicas, Universidad Nacional Autónoma de México (UNAM) and received a fellowship from CONACyT. EMK is grateful for the postdoctoral scholarship from CONACyT with support from the Posgrado en Ciencias Biológicas at UNAM.

Appendix A. Supplementary data

Supplementary data to this article can be found online at https://doi.org/10.1016/j.freeradbiomed.2020.04.016.

References

[1] A.S. Levey, J. Coresh, Chronic kidney disease, Lancet 379 (2012) 165–180, https://doi.org/10.1016/S0140-6736(11)60178-5.
[2] T. Shafi, J. Coresh, Chronic kidney disease: definition, epidemiology, cost, and outcomes, in: J. Himmelfarb, M.H. Sayegh (Eds.), Chronic Kidney Dis. Dial. Transplant, third ed., Elsevier Inc., 2010, pp. 3–21, , https://doi.org/10.1016/B978-1-4377-0987-2.00001-7.
[3] E.D. Siew, A. Davenport, The growth of acute kidney injury: a rising tide or just closer attention to detail? Kidney Int. 87 (2015) 46–61, https://doi.org/10.1038/ki.2014.293.
[4] J.-J. Carrero, M. Hecking, I. Ulasi, L. Sola, B. Thomas, Chronic kidney disease, gender, and access to care: a global perspective, Semin. Nephrol. 37 (2017) 296–308, https://doi.org/10.1016/j.semnephrol.2017.02.009.
[5] A.C. Webster, E.V. Nagler, R.L. Morton, P. Masson, Chronic kidney disease, Lancet 389 (2017) 1238–1252, https://doi.org/10.1016/S0140-6736(16)32064-5.
[6] A. Khwaja, M. El Kossi, J. Floege, M. El Nahas, The management of CKD: a look into the future, Kidney Int. 72 (2007) 1316–1323, https://doi.org/10.1038/sj.ki.5002489.
[7] O. Akinlolu, Addressing the global burden of chronic kidney disease through clinical and translational research, Trans. Am. Clin. Climatol. Assoc. 125 (2014) 229–243 discussion 243-6.
[8] P.K.T. Li, E.A. Burdmann, R.L. Mehta, Acute kidney injury: global health alert, Hong Kong, J. Nephrol. 15 (2013) 1–5, https://doi.org/10.1016/j.hkjn.2013.03.001.
[9] J.M. Forbes, D.R. Thorburn, Mitochondrial dysfunction in diabetic kidney disease, Nat. Rev. Nephrol. 14 (2018) 291–312, https://doi.org/10.1038/nrneph.2018.9.
[10] B. Feng, R. Meng, B. Huang, Y. Bi, S. Shen, D. Zhu, Silymarin protects against renal injury through normalization of lipid metabolism and mitochondrial biogenesis in high fat-fed mice, Free Radic. Biol. Med. 110 (2017) 240–249, https://doi.org/10.1016/j.freeradbiomed.2017.06.009.
[11] A.A. Sharfuddin, S.D. Weisbord, P.M. Palevsky, B.A. Molitoris, Acute kidney injury, in: K. Skorecki, G.M. Chertow, P.A. Marsden, M.W. Taal, A.S.L. Yu (Eds.), Brenner and Rector's the Kidney, Ninth Edit, Elsevier, Philadelphia, 2012, pp. 1044–1099, , https://doi.org/10.1016/B978-1-4160-6193-9.10030-2.
[12] K. Doi, H. Rabb, Impact of acute kidney injury on distant organ function: recent findings and potential therapeutic targets, Kidney Int. 89 (2016) 555–564, https://doi.org/10.1016/j.kint.2015.11.019.
[13] O.E. Aparicio-Trejo, L.M. Reyes-Fermín, A. Briones-Herrera, E. Tapia, J.C. León-Contreras, R. Hernández-Pando, L.G. Sánchez-Lozada, J. Pedraza-Chaverri, Protective effects of N-acetyl-cysteine in mitochondria bioenergetics, oxidative stress, dynamics and S-glutathionylation alterations in acute kidney damage induced by folic acid, Free Radic. Biol. Med. 130 (2019) 379–396, https://doi.org/10.1016/j.freeradbiomed.2018.11.005.
[14] L.M. Reyes-Fermín, S.H. Avila-Rojas, O.E. Aparicio-Trejo, E. Tapia, I. Rivero, J. Pedraza-Chaverri, The protective effect of alpha-mangostin against cisplatin-induced cell death in LLC-PK1 cells is associated to mitochondrial function preservation, Antioxidants 8 (2019) 133, https://doi.org/10.3390/antiox8050133.
[15] S.H. Avila-Rojas, E. Tapia, A. Briones-Herrera, O.E. Aparicio-Trejo, J.C. León-Contreras, R. Hernández-Pando, J. Pedraza-Chaverri, Curcumin prevents potassium dichromate ($K_2Cr_2O_7$)-induced renal hypoxia, Food Chem. Toxicol. 121 (2018) 472–482, https://doi.org/10.1016/j.fct.2018.09.046.
[16] P. Rojas-Morales, J.C. León-Contreras, O.E. Aparicio-Trejo, J.G. Reyes-Ocampo, O.N. Medina-Campos, A.S. Jiménez-Osorio, S. González-Reyes, B. Marquina-Castillo, R. Hernández-Pando, D. Barrera-Oviedo, L.G. Sánchez-Lozada, J. Pedraza-Chaverri, E. Tapia, Fasting reduces oxidative stress, mitochondrial dysfunction and fibrosis induced by renal ischemia-reperfusion injury, Free Radic. Biol. Med. 135 (2019) 60–67, https://doi.org/10.1016/j.freeradbiomed.2019.02.018.
[17] E. Molina-Jijón, O.E. Aparicio-Trejo, R. Rodríguez-Muñoz, J.C. León-Contreras, M. del Carmen Cárdenas-Aguayo, O.N. Medina-Campos, E. Tapia, L.G. Sánchez-Lozada, R. Hernández-Pando, J.L. Reyes, L. Arreola-Mendoza, J. Pedraza-Chaverri, The nephroprotection exerted by curcumin in maleate-induced renal damage is associated with decreased mitochondrial fission and autophagy, Biofactors 42 (2016) 686–702, https://doi.org/10.1002/biof.1313.
[18] W. Ding, H. Guo, C. Xu, B. Wang, M. Zhang, F. Ding, Mitochondrial reactive oxygen species-mediated NLRP3 inflammasome activation contributes to aldosterone-induced renal tubular cells injury, Oncotarget 7 (2016), https://doi.org/10.18632/oncotarget.8243.
[19] Y. Ishimoto, R. Inagi, Mitochondria: a therapeutic target in acute kidney injury, Nephrol. Dial. Transplant. 31 (2015) 1062–1069, https://doi.org/10.1093/ndt/gfv317.
[20] A.B. Fogo, A.H. Cohen, R.B. Colvin, J.C. Jennette, C.E. Alpers, Fundamentals of Renal Pathology, first ed., Springer Berlin Heidelberg, Berlin, Heidelberg, 2014, https://doi.org/10.1007/978-3-642-39080-7.
[21] A.M. El Nahas, K.B. Aminu, Chronic kidney disease: the global challenge, Lancet 365 (2005) 331–340, https://doi.org/10.1016/S0140-6736(05)70199-9.
[22] M.W. Taal, B.M. Brenner, Adaptation to nephron loss and mechanisms of progression in chronic kidney disease, in: K. Skorecki, G.M. Chertow, P.A. Marsden, M.W. Taal, A.S.L. Yu (Eds.), Brenner & Rector's the Kidney, ninth ed., Elsevier, 2012, pp. 1918–1971, , https://doi.org/10.1016/B978-1-4160-6193-9.10051-X.
[23] O.E. Aparicio-Trejo, E. Tapia, L.G. Sánchez-Lozada, J. Pedraza-Chaverri, Mitochondrial bioenergetics, redox state, dynamics and turnover alterations in renal mass reduction models of chronic kidney diseases and their possible implications in the progression of this illness, Pharmacol. Res. 135 (2018) 1–11, https://doi.org/10.1016/j.phrs.2018.07.015.
[24] D. Mafra, E.K. Gidlund, N.A. Borges, D.C. Magliano, B. Lindholm, P. Stenvinkel, F. von Walden, Bioactive food and exercise in chronic kidney disease: targeting the mitochondria, Eur. J. Clin. Invest. 48 (2018), https://doi.org/10.1111/eci.13020.
[25] S. Hallan, K. Sharma, The role of mitochondria in diabetic kidney disease, Curr. Diabetes Rep. 16 (2016) 1–9, https://doi.org/10.1007/s11892-016-0748-0.
[26] B. Benipal, L.H. Lash, Influence of renal compensatory hypertrophy on mitochondrial energetics and redox status, Biochem. Pharmacol. 81 (2011) 295–303, https://doi.org/10.1016/j.bcp.2010.10.010.
[27] M. Tamaki, K. Miyashita, S. Wakino, M. Mitsuishi, K. Hayashi, H. Itoh, Chronic kidney disease reduces muscle mitochondria and exercise endurance and its exacerbation by dietary protein through inactivation of pyruvate dehydrogenase, Kidney Int. 85 (2014) 1330–1339, https://doi.org/10.1038/ki.2013.473.
[28] A. Ortiz, M.D. Sanchez-Niño, M.C. Izquierdo, C. Martin-Cleary, L. Garcia-Bermejo, J.A. Moreno, M. Ruiz-Ortega, J. Draibe, J.M. Cruzado, M.A. Garcia-Gonzalez, J.M. Lopez-Novoa, M.J. Soler, A.B. Sanz, Translational value of animal models of kidney failure, Eur. J. Pharmacol. 759 (2015) 205–220, https://doi.org/10.1016/j.ejphar.2015.03.026.
[29] D. Chunsun, P.K. Lawrence, L. Youhua, Animal models of kidney diseases, Model. Biomed. Res. (2008) 657–664.
[30] S. He, N. Liu, G. Bayliss, S. Zhuang, EGFR activity is required for renal tubular cell dedifferentiation and proliferation in a murine model of folic acid-induced acute kidney injury, AJP Ren. Physiol. 304 (2013) F356–F366, https://doi.org/10.1152/ajprenal.00553.2012.
[31] T.-C. Fang, Proliferation of bone marrow-derived cells contributes to regeneration after folic acid-induced acute tubular injury, J. Am. Soc. Nephrol. 16 (2005) 1723–1732, https://doi.org/10.1681/ASN.2004121089.
[32] M.S. Szczypka, A.J. Westover, S.G. Clouthier, J.L.M. Ferrara, H.D. Humes, Rare incorporation of bone marrow-derived cells into kidney after folic acid-induced

injury, Stem Cell. 23 (2005) 44–54, https://doi.org/10.1634/stemcells.2004–0111.
[33] I. Capelli, G. Cianciolo, L. Gasperoni, F. Zappulo, F. Tondolo, M. Cappuccilli, G. La Manna, Folic acid and vitamin B12 administration in CKD, why not? Nutrients 11 (2019), https://doi.org/10.3390/nu11020383.
[34] C.M. Wyatt, J.D. Spence, Folic acid supplementation and chronic kidney disease progression, Kidney Int. 90 (2016) 1144–1145, https://doi.org/10.1016/j.kint.2016.09.019.
[35] S.-Y. Hwang, Y.L. Siow, K.K.W. Au-Yeung, J. House, K. O, Folic acid supplementation inhibits NADPH oxidase-mediated superoxide anion production in the kidney, Am. J. Physiol. Ren. Physiol. 300 (2011) F189–F198, https://doi.org/10.1152/ajprenal.00272.2010.
[36] M. Teschner, M. Kosch, R.M. Schaefer, Folate metabolism in renal failure, Nephrol. Dial. Transplant. 17 (Suppl 5) (2002) 24–27.
[37] C.M. Wyatt, J.D. Spence, Folic acid supplementation and chronic kidney disease progression, Kidney Int. 90 (2016) 1144–1145, https://doi.org/10.1016/j.kint.2016.09.019.
[38] A. Gupta, V. Puri, R. Sharma, S. Puri, Folic acid induces acute renal failure (ARF) by enhancing renal prooxidant state, Exp. Toxicol. Pathol. 64 (2012) 225–232, https://doi.org/10.1016/j.etp.2010.08.010.
[39] O. Ruiz-Andres, B. Suarez-Alvarez, C. Sánchez-Ramos, M. Monsalve, M.D. Sanchez-Niño, M. Ruiz-Ortega, J. Egido, A. Ortiz, A.B. Sanz, The inflammatory cytokine TWEAK decreases PGC-1α expression and mitochondrial function in acute kidney injury, Kidney Int. 89 (2016) 399–410, https://doi.org/10.1038/ki.2015.332.
[40] D. Martin-Sanchez, O. Ruiz-Andres, J. Poveda, S. Carrasco, P. Cannata-Ortiz, M.D. Sanchez-Niño, M. Ruiz Ortega, J. Egido, A. Linkermann, A. Ortiz, A.B. Sanz, Ferroptosis, but not necroptosis, is important in nephrotoxic folic acid–induced AKI, J. Am. Soc. Nephrol. 28 (2017) 218–229, https://doi.org/10.1681/ASN.2015121376.
[41] G.S. Ducker, J.D. Rabinowitz, One-carbon metabolism in health and disease, Cell Metabol. 25 (2017) 27–42, https://doi.org/10.1016/j.cmet.2016.08.009.
[42] F.H. Nazki, A.S. Sameer, B.A. Ganaie, Folate: metabolism, genes, polymorphisms and the associated diseases, Gene 533 (2014) 11–20, https://doi.org/10.1016/j.gene.2013.09.063.
[43] L.B. Bailey, Folate in Health and Disease, second ed., Taylor & Francis, Washington, D.C., 2009.
[44] M.E. Huguenin, A. Birbaumer, F.P. Brunner, J. Thorhorst, U. Schmidt, U.C. Dubach, G. Thiel, An evaluation of the role of tubular obstruction in folic acid-induced acute renal failure in the rat, Nephron 22 (1978) 41–45.
[45] J.T. Fox, P.J. Stover, Folate-mediated one-carbon metabolism, Vitam. Horm. 79 (2008) 1–44, https://doi.org/10.1016/S0083-6729(08)00401-9.
[46] L.J. Stallons, R.M. Whitaker, R.G. Schnellmann, Suppressed mitochondrial biogenesis in folic acid-induced acute kidney injury and early fibrosis, Toxicol. Lett. 224 (2014) 326–332, https://doi.org/10.1016/j.toxlet.2013.11.014.
[47] R.J. Mailloux, X. Jin, W.G. Willmore, Redox regulation of mitochondrial function with emphasis on cysteine oxidation reactions, Redox Biol. 2 (2014) 123–139, https://doi.org/10.1016/j.redox.2013.12.011.
[48] M. Sharma, A. Sud, T. Kaur, C. Tandon, S.K. Singla, N-acetylcysteine with apocynin prevents hyperoxaluria-induced mitochondrial protein perturbations in nephrolithiasis, Free Radic. Res. 50 (2016) 1032–1044, https://doi.org/10.1080/10715762.2016.1221507.
[49] A. Amini, S. Masoumi-Moghaddam, D.L. Morris, Utility of Bromelain and N-Acetylcysteine in Treatment of Peritoneal Dissemination of Gastrointestinal Mucin-Producing Malignancies, first ed.di, Springer International, Switzerland, 2016, https://doi.org/10.1007/978-3-319-28570-2.
[50] E.Y. Plotnikov, A.V. Kazachenko, M.Y. Vyssokikh, A.K. Vasileva, D.V. Tcvirkun, N.K. Isaev, V.I. Kirpatovsky, D.B. Zorov, The role of mitochondria in oxidative and nitrosative stress during ischemia/reperfusion in the rat kidney, Kidney Int. 72 (2007) 1493–1502, https://doi.org/10.1038/sj.ki.5002568.
[51] H.H. Szeto, S. Liu, Y. Soong, D. Wu, S.F. Darrah, F.-Y. Cheng, Z. Zhao, M. Ganger, C.Y. Tow, S.V. Seshan, Mitochondria-targeted peptide accelerates ATP recovery and reduces ischemic kidney injury, J. Am. Soc. Nephrol. 22 (2011) 1041–1052, https://doi.org/10.1681/ASN.2010080808.
[52] A. Ortiz, C. Lorz, M.P. Catalan, T.M. Danoff, Y. Yamasaki, J. Egido, E.G. Neilson, Expression of apoptosis regulatory proteins in tubular epithelium stressed in culture or following acute renal failure, Kidney Int. 57 (2000) 969–981, https://doi.org/10.1046/j.1523-1755.2000.00925.x.
[53] C. Dai, J. Yang, Y. Liu, Single injection of naked plasmid encoding hepatocyte growth factor prevents cell death and ameliorates acute renal failure in mice, J. Am. Soc. Nephrol. 13 (2002) 411–422 http://jasn.asnjournals.org/content/13/2/411%5Cnhttp://jasn.asnjournals.org/content/13/2/411.full.pdf%5Cnhttp://jasn.asnjournals.org/content/13/2/411.short%5Cnhttp://www.ncbi.nlm.nih.gov/pubmed/11805170.
[54] K. Doi, K. Okamoto, K. Negishi, Y. Suzuki, A. Nakao, T. Fujita, A. Toda, T. Yokomizo, Y. Kita, Y. Kihara, S. Ishii, T. Shimizu, E. Noiri, Attenuation of folic acid-induced renal inflammatory injury in platelet-activating factor receptor-deficient mice, Am. J. Pathol. 168 (2006) 1413–1424, https://doi.org/10.2353/ajpath.2006.050634.
[55] A. Ortega, D. Rámila, A. Izquierdo, L. González, A. Barat, R. Gazapo, R.J. Bosch, P. Esbrit, Role of the renin-angiotensin system on the parathyroid hormone-related protein overexpression induced by nephrotoxic acute renal failure in the rat, J. Am. Soc. Nephrol. 16 (2005) 939–949, https://doi.org/10.1681/ASN.2004040328.
[56] B.-Z. Shao, Z.-Q. Xu, B.-Z. Han, D.-F. Su, C. Liu, NLRP3 inflammasome and its inhibitors: a review, Front. Pharmacol. 6 (2015) 262, https://doi.org/10.3389/fphar.2015.00262.
[57] H. Zhao, Y. jun Liu, Z. rui Liu, D. dong Tang, X. wen Chen, Y. hua Chen, R. ning Zhou, S. qi Chen, H. xin Niu, Role of mitochondrial dysfunction in renal fibrosis promoted by hypochlorite-modified albumin in a remnant kidney model and protective effects of antioxidant peptide SS-31, Eur. J. Pharmacol. 804 (2017) 57–67, https://doi.org/10.1016/j.ejphar.2017.03.037.
[58] Y. Yuan, Y. Chen, P. Zhang, S. Huang, C. Zhu, G. Ding, B. Liu, T. Yang, A. Zhang, Mitochondrial dysfunction accounts for aldosterone-induced epithelial-to-mesenchymal transition of renal proximal tubular epithelial cells, Free Radic. Biol. Med. 53 (2012) 30–43, https://doi.org/10.1016/j.freeradbiomed.2012.03.015.
[59] E. Tapia, V. Soto, K.M. Ortiz-Vega, G. Zarco-Márquez, E. Molina-Jijón, M. Cristóbal-García, J. Santamaría, W.R. García-Niño, F. Correa, C. Zazueta, J. Pedraza-Chaverri, Curcumin induces Nrf2 nuclear translocation and prevents glomerular hypertension, hyperfiltration, oxidant stress, and the decrease in antioxidant enzymes in 5/6 nephrectomized rats, Oxid. Med. Cell. Longev. (2013) 1–14, https://doi.org/10.1155/2012/269039 2012.
[60] O.E. Aparicio-Trejo, E. Tapia, E. Molina-Jijón, O.N. Medina-Campos, N.A. Macías-Ruvalcaba, J.C. León-Contreras, R. Hernández-Pando, F.E. García-Arroyo, M. Cristóbal, L.G. Sánchez-Lozada, J. Pedraza-Chaverri, Curcumin prevents mitochondrial dynamics disturbances in early 5/6 nephrectomy: relation to oxidative stress and mitochondrial bioenergetics, Biofactors 43 (2017) 293–310, https://doi.org/10.1002/biof.1338.
[61] E. Ojuka, B. Andrew, N. Bezuidenhout, S. George, G. Maarman, H.P. Madlala, A. Mendham, P.O. Osiki, Measurement of β-oxidation capacity of biological samples by respirometry: a review of principles and substrates, Am. J. Physiol. Metab. 310 (2016) E715–E723, https://doi.org/10.1152/ajpendo.00475.2015.
[62] T. Sekine, H. Endou, Solute Transport, Energy consumption, and production in the kidney, Seldin and Geibisch's the Kidney, fifth ed., Elsevier, 2013, pp. 143–175, , https://doi.org/10.1016/B978-0-12-381462-3.00006-9.
[63] O.E. Aparicio-Trejo, E. Tapia, L.G. Sánchez-Lozada, J. Pedraza-Chaverri, Mitochondrial bioenergetics, redox state, dynamics and turnover alterations in renal mass reduction models of chronic kidney diseases and their possible implications in the progression of this illness, Pharmacol. Res. 135 (2018) 1–11, https://doi.org/10.1016/j.phrs.2018.07.015.
[64] K. Stadler, I.J. Goldberg, K. Susztak, The evolving understanding of the contribution of lipid metabolism to diabetic kidney disease, Curr. Diabetes Rep. 15 (2015), https://doi.org/10.1007/s11892-015-0611-8.
[65] L. V Fedorova, A. Tamirisa, D.J. Kennedy, S.T. Haller, G. Budnyy, J.I. Shapiro, D. Malhotra, Mitochondrial impairment in the five-sixth nephrectomy model of chronic renal failure: proteomic approach, BMC Nephrol. 14 (2013) 209–230 http://www.pubmedcentral.nih.gov/articlerender.fcgi?artid=3851543&tool=pmcentrez&rendertype=abstract.
[66] H.M. Kang, S.H. Ahn, P. Choi, Y.A. Ko, S.H. Han, F. Chinga, A.S.D. Park, J. Tao, K. Sharma, J. Pullman, E.P. Bottinger, I.J. Goldberg, K. Susztak, Defective fatty acid oxidation in renal tubular epithelial cells has a key role in kidney fibrosis development, Nat. Med. 21 (2015) 37–46, https://doi.org/10.1038/nm.3762.
[67] F. Afshinnia, T.M. Rajendiran, T. Soni, J. Byun, S. Wernisch, K.M. Sas, J. Hawkins, K. Bellovich, D. Gipson, G. Michailidis, S. Pennathur, Impaired β-oxidation and altered complex lipid fatty acid partitioning with advancing CKD, J. Am. Soc. Nephrol. 29 (2018) 295–306, https://doi.org/10.1681/asn.2017030350.
[68] C.D. Chancy, R. Kekuda, W. Huang, P.D. Prasad, J.M. Kuhnel, F.M. Sirotnak, P. Roon, V. Ganapathy, S.B. Smith, Expression and differential polarization of the reduced-folate transporter-1 and the folate receptor α in mammalian retinal pigment epithelium, J. Biol. Chem. 275 (2000) 20676–20684, https://doi.org/10.1074/jbc.M002328200.
[69] L.S. Chawla, R.L. Amdur, S. Amodeo, P.L. Kimmel, C.E. Palant, The severity of acute kidney injury predicts progression to chronic kidney disease, Kidney Int. 79 (2011) 1361–1369, https://doi.org/10.1038/ki.2011.42.
[70] H.M. Kang, S.H. Ahn, P. Choi, Y.A. Ko, S.H. Han, F. Chinga, A.S.D. Park, J. Tao, K. Sharma, J. Pullman, E.P. Bottinger, I.J. Goldberg, K. Susztak, Defective fatty acid oxidation in renal tubular epithelial cells has a key role in kidney fibrosis development, Nat. Med. 21 (2015) 37–46, https://doi.org/10.1038/nm.3762.
[71] E. Gnaiger, Mitochondrial pathways and respiratory control an Introduction to OXPHOS Analysis, http://wiki.oroboros.at/images/f/fc/Gnaiger_2014_Mitochondr_Physiol_Network_MitoPathways.pdf, (2014).
[72] M. Makrecka-Kuka, G. Krumschnabel, E. Gnaiger, High-resolution respirometry for simultaneous measurement of oxygen and hydrogen peroxide fluxes in permeabilized cells, Tissue Homogenate and Isolated Mitochondria, Biomolecules 5 (2015) 1319–1338, https://doi.org/10.3390/biom5031319.
[73] P.T. Kang, L. Zhang, C.L. Chen, J. Chen, K.B. Green, Y.R. Chen, Protein thiyl radical mediates S-glutathionylation of complex i, Free Radic. Biol. Med. 53 (2012) 962–973, https://doi.org/10.1016/j.freeradbiomed.2012.05.025.
[74] M. Forkink, F. Basit, J. Teixeira, H.G. Swarts, W.J.H. Koopman, P.H.G.M. Willems, Complex I and complex III inhibition specifically increase cytosolic hydrogen peroxide levels without inducing oxidative stress in HEK293 cells, Redox Biol. 6 (2015) 607–616, https://doi.org/10.1016/j.redox.2015.09.003.
[75] W. Zhang, Y. Yang, H. Gao, Y. Zhang, Z. Jia, S. Huang, Inhibition of Mitochondrial Complex I Aggravates Folic Acid-Induced Acute Kidney Injury, (2019), pp. 1002–1013, https://doi.org/10.1159/000501934 210008.
[76] S. Kröller-Schön, S. Steven, S. Kossmann, A. Scholz, S. Daub, M. Oelze, N. Xia, M. Hausding, Y. Mikhed, E. Zinßius, M. Mader, P. Stamm, N. Treiber, K. Scharffetter-Kochanek, H. Li, E. Schulz, P. Wenzel, T. Münzel, A. Daiber, Molecular mechanisms of the crosstalk between mitochondria and NADPH oxidase through reactive oxygen species—studies in white blood cells and in animal models, Antioxidants Redox Signal. 20 (2013) 247–266, https://doi.org/10.1089/ars.2012.4953.
[77] R.P. Brandes, N. Weissmann, K. Schröder, Nox family NADPH oxidases: molecular mechanisms of activation, Free Radic. Biol. Med. 76 (2014) 208–226, https://doi.org/10.1016/j.freeradbiomed.2014.07.046.

[78] M. Sedeek, R. Nasrallah, R.M. Touyz, R.L. Hébert, NADPH oxidases, reactive oxygen species, and the kidney: friend and foe, J. Am. Soc. Nephrol. 24 (2013) 1512–1518, https://doi.org/10.1681/ASN.2012111112.
[79] A.M. Garrido, K.K. Griendling, NADPH oxidases and angiotensin II receptor signaling, Mol. Cell. Endocrinol. 302 (2009) 148–158, https://doi.org/10.1016/j.mce.2008.11.003.
[80] F. Jiang, G.-S. Liu, G.J. Dusting, E.C. Chan, NADPH oxidase-dependent redox signaling in TGF-β-mediated fibrotic responses, Redox Biol. 2 (2014) 267–272, https://doi.org/10.1016/j.redox.2014.01.012.
[81] P. Gill, C. Wilcox, NADPH oxidases in the kidney, Antioxidants Redox Signal. 8 (2006) 1597–1607.
[82] S. Hwang, R. Bohman, P. Navas, J.T. Norman, T. Bradley, L.G. Fine, Hypertrophy of renal mitochondria, J. Am. Soc. Nephrol. 1 (1990) 822–827.
[83] O.E. Aparicio-Trejo, E. Tapia, E. Molina-Jijón, O.N. Medina-Campos, N.A. Macías-Ruvalcaba, J.C. León-Contreras, R. Hernández-Pando, F.E. García-Arroyo, M. Cristóbal, L.G. Sánchez-Lozada, J. Pedraza-Chaverri, Curcumin prevents mitochondrial dynamics disturbances in early 5/6 nephrectomy: relation to oxidative stress and mitochondrial bioenergetics, Biofactors 43 (2017) 293–310, https://doi.org/10.1002/biof.1338.
[84] S. Kume, T. Uzu, S. Araki, T. Sugimoto, K. Isshiki, M. Chin-Kanasaki, M. Sakaguchi, N. Kubota, Y. Terauchi, T. Kadowaki, M. Haneda, A. Kashiwagi, D. Koya, Role of altered renal lipid metabolism in the development of renal injury induced by a high-fat diet, J. Am. Soc. Nephrol. 18 (2007) 2715–2723, https://doi.org/10.1681/ASN.2007010089.
[85] H.H. Szeto, S. Liu, Y. Soong, N. Alam, G.T. Prusky, S.V. Seshan, Protection of mitochondria prevents high-fat diet induced glomerulopathy and proximal tubular injury, Kidney Int. 90 (2016) 997–1011, https://doi.org/10.1016/j.kint.2016.06.013.
[86] S. Hallan, M. Afkarian, L.R. Zelnick, B. Kestenbaum, S. Sharma, R. Saito, M. Darshi, G. Barding, D. Raftery, W. Ju, M. Kretzler, K. Sharma, I.H. de Boer, Metabolomics and gene expression analysis reveal down-regulation of the citric acid (TCA) cycle in non-diabetic CKD patients, EBioMed. 26 (2017) 68–77, https://doi.org/10.1016/j.ebiom.2017.10.027.
[87] A. Voulgaris, O. Marrone, M.R. Bonsignore, P. Steiropoulos, Chronic kidney disease in patients with obstructive sleep apnea. A narrative review, Sleep Med. Rev. 47 (2019) 74–89, https://doi.org/10.1016/j.smrv.2019.07.001.
[88] X. Gong, Y. Duan, J. Zheng, Y. Wang, G. Wang, S. Norgren, T.K. Hei, Nephroprotective effects of N-acetylcysteine amide against contrast-induced nephropathy through upregulating thioredoxin-1, inhibiting ASK1/p38MAPK pathway, and suppressing oxidative stress and apoptosis in rats, Oxid. Med. Cell. Longev. (2016), https://doi.org/10.1155/2016/8715185 2016.
[89] C. Li, N. Xie, Y. Li, C. Liu, F.F. Hou, J. Wang, N-acetylcysteine ameliorates cisplatin-induced renal senescence and renal interstitial fibrosis through sirtuin1 activation and p53 deacetylation, Free Radic. Biol. Med. 130 (2019) 512–527, https://doi.org/10.1016/j.freeradbiomed.2018.11.006.
[90] G. Marenzi, E. Sisillo, A.L. Bartorelli, Studies on Renal Sisorders, (2011), https://doi.org/10.1007/978-1-60761-857-7.
[91] B. Wispriyono, M. Matsuoka, H. Igisu, K. Matsuno, Protection from cadmium cytotoxicity by N-acetylcysteine in LLC-PK1 cells, J. Pharmacol. Exp. Therapeut. 287 (1998) 344–351.
[92] G. Marenzi, E. Sisillo, A.L. Bartorelli, N -Acetylcysteine in kidney disease, (n.d.) 367–388. doi:10.1007/978-1-60761-857-7.
[93] H.-Z. Wang, Z.-Y. Peng, X.-Y. Wen, T. Rimmelé, J.V. Bishop, J.A. Kellum, N-acetylcysteine is effective for prevention but not for treatment of folic acid-induced acute kidney injury in mice*, Crit. Care Med. 39 (2011) 2487–2494, https://doi.org/10.1097/CCM.0b013e31822575fc.
[94] H.Z. Wang, Z.Y. Peng, X.Y. Wen, T. Rimmelé, J.V. Bishop, J.A. Kellum, N-acetylcysteine is effective for prevention but not for treatment of folic acid-induced acute kidney injury in mice, Crit. Care Med. 39 (2011) 2487–2494, https://doi.org/10.1097/CCM.0b013e31822575fc.
[95] C.Y. Liao, C.H. Chung, C.C. Wu, F.H. Lin, C.H. Tsao, C.C. Wang, W.C. Chien, Protective effect of N-acetylcysteine on progression to end-stage renal disease: necessity for prospective clinical trial, Eur. J. Intern. Med. 44 (2017) 67–73, https://doi.org/10.1016/j.ejim.2017.06.011.
[96] S. Granata, A. Dalla Gassa, P. Tomei, A. Lupo, G. Zaza, Mitochondria: a new therapeutic target in chronic kidney disease, Nutr. Metab. (Lond). 12 (2015) 1–21, https://doi.org/10.1186/s12986-015-0044-z.
[97] L. Xiao, X. Xu, F. Zhang, M. Wang, Y. Xu, D. Tang, J. Wang, Y. Qin, Y. Liu, C. Tang, L. He, A. Greka, Z. Zhou, F. Liu, Z. Dong, L. Sun, The mitochondria-targeted antioxidant MitoQ ameliorated tubular injury mediated by mitophagy in diabetic kidney disease via Nrf2/PINK1, Redox Biol. 11 (2017) 297–311, https://doi.org/10.1016/j.redox.2016.12.022.

Pharmacological Research 135 (2018) 1–11

Contents lists available at ScienceDirect

Pharmacological Research

journal homepage: www.elsevier.com/locate/yphrs

Review

Mitochondrial bioenergetics, redox state, dynamics and turnover alterations in renal mass reduction models of chronic kidney diseases and their possible implications in the progression of this illness

Omar Emiliano Aparicio-Trejo[a], Edilia Tapia[b], Laura Gabriela Sánchez-Lozada[b], José Pedraza-Chaverri[a,*]

[a] Department of Biology, Faculty of Chemistry, National Autonomous University of Mexico (UNAM), Mexico City 04510, Mexico
[b] Department of Nephrology and Laboratory of Renal Pathophysiology, National Institute of Cardiology "Ignacio Chávez", Mexico City 14080, Mexico

ARTICLE INFO

Chemical compounds studied in this article:
Adenosine triphosphate (CID 5957)
Curcumin (CID 969516)
Elamipretide: Szeto–Schiller peptides 31 (CID 11764719)
Glutathione (CID 124886)
L-cysteine (CID 60960)
L-glutamate (CID 33032)
Malate (CID 525)
Succinate (CID 1110)
Resveratrol (CID 445154)
Rotenone (CID 6758)

Keywords:
Chronic kidney disease
Mitochondria bioenergetics
Mitochondrial dynamic
Nephrectomy
Oxidative stress
Renal mass reduction

ABSTRACT

Nowadays, chronic kidney disease (CKD) is considered a worldwide public health problem. CKD is a term used to describe a set of pathologies that structurally and functionally affect the kidney, it is mostly characterized by the progressive loss of kidney function. Current therapeutic approaches are insufficient to avoid the development of this disease, which highlights the necessity of developing new strategies to reverse or at least delay CKD progression. Kidney is highly dependent on mitochondrial homeostasis and function, consequently, the idea that mitochondrial pathologies could play a pivotal role in the genesis and development of kidney diseases has risen. Although many research groups have recently published studies of mitochondrial function in acute kidney disease models, the existing information about CKD is still limited, especially in renal mass reduction (RMR) models. This paper focuses on reviewing current experimental information about the bioenergetics, dynamics (fission and fusion processes), turnover (mitophagy and biogenesis) and redox mitochondrial alterations in RMR, to discuss and integrate the mitochondrial changes triggered by nephron loss, as well as its relationship with loss of kidney function in CKD, in these models. Understanding these mechanisms would allow us to design new therapies that target these mitochondrial alterations.

1. Introduction: renal mitochondria and its importance in the development of new therapies to prevent the CKD progression

The term chronic kidney disease (CKD) is used to include a broad range of disorders characterized by progressive nephron loss, glomerular filtration rate (GFR) reduced to less than 60 ml /min/ 1.73 m^2 for at least 3 months and increased renal damage markers (such as blood creatinine and blood urea nitrogen, BUN) [1]. CKD can be developed by a series of acute insults, such as ischemic episodes or by exposure to nephrotoxic agents, which generate the initial nephron loss. In an attempt to adapt this nephron loss, the kidney triggers hemodynamic, vascular and inflammatory changes [2,3] (see Taal & Brenner [3] for more details), which lead to further nephron loss, thus promoting progressive deterioration of renal function. Within the last decades, the number of patients with CKD has increased dramatically, moving from the 27th (in 1990) to the 18th place (in 2014) in the list of worldwide death causes and its death rate is expected to continue increasing [4,5]. In addition, its medical treatment cost is high, since patients with CKD usually have other complications, such as cardiovascular diseases, hypertension, obesity and diabetes [1,2]. Therefore, there is an urgent need for the development of new treatments and strategies to prevent or at least delay CKD progression.

In the kidney, ATP production is predominantly sustained by oxidative phosphorylation (OXPHOS) of fatty acids β-oxidation [6], although other substrates like lactic acid and ketone bodies are also oxidized [7]. Due to the different energy requirements along the nephron, each nephron segment has different mitochondrial abundance [6–8]. So, the nephron shows a higher mitochondrial density in the

* Corresponding author.
E-mail address: pedraza@unam.mx (J. Pedraza-Chaverri).

https://doi.org/10.1016/j.phrs.2018.07.015
Received 8 June 2018; Received in revised form 10 July 2018; Accepted 16 July 2018
Available online 17 July 2018

most energy demanding segments [6,8], such as the proximal convoluted tubule (PCT) and the thick ascending loop of Henle (TAL) [8], because mitochondria is responsible of the maintenance of high reabsorption rates in these segments [6]. Mitochondrial membrane potential (ΔΨm) also changes along the nephron, multiphotonic excitatory confocal microscopy studies in anesthetized mice demonstrated a notably higher ΔΨm in proximal tubule (PT) and TAL [9,10]. Additionally, in pathologic states (like hypoxia), ΔΨm alterations are different along the tubular segments, which is consistent with the poor PT capacity for obtaining energy from anaerobic glycolysis.

Since renal function highly depends on mitochondrial ATP production and, hence, on the balance between the processes that regulate mitochondrial dynamics (fission and fusion) and turnover (biogenesis and mitophagy) [6,11] mitochondrial alterations have been related to the development of kidney pathologies and have been considered as a therapeutic target [12]. In the case of acute kidney disease (AKD) there is a correlation between tubular damage and mitochondrial alterations in models of cisplatin [13], ischemia / reperfusion[9], gentamicin [14], dichromate [15] and maleate [16]. In addition, the excessive increase in mitochondrial reactive oxygen species (ROS) production leads to the loss of integrity of mitochondrial membrane, inducing its permeability and the release of pro-apoptotic proteins [17], thus contributing to cell death in these models. Furthermore, mitochondrial alterations are related to tubular defects in patients with renal pathologies, such as Fanconi syndrome, Bartter-like syndrome and cystic renal disease, among others [17,18]. In the case of CKD, many evidences suggest that mitochondrial dysfunction may be involved in the pathophysiology of these diseases, although the precise role of mitochondria in those changes, especially in non-diabetic conditions, is largely unknown [12]. It is believed that, after the original damage, an increase in the metabolism rate and ATP consumption generate mitochondria bioenergetics stress, which together with the increase in ROS production [3,19,20] contribute to CKD progression. However, nowadays there is not a theory that describes, in a temporal course way, the changes that occur in the mitochondria along CKD progression [12].

Renal mass reduction (RMR) models, like uninephrectomy, 3/4 nephrectomy, and 5/6 nephrectomy (5/6Nx) models are widely used techniques for studying CKD progression [3,21]. This procedure induces nephron hypertrophy and hyperfunction and an increase in single nephron GFR (snGFR), however, it leads to a higher injury in the remnant renal mass, decreasing total GFR and producing a circle of progressive deterioration in the kidney, which emulates clinical CKD [3,21]. Therefore, RMR models are powerful tools for studying the mechanisms involved in CKD progression [3,21].

Since RMR models are powerful tools for studying the mechanisms involved in CKD progression in a non-diabetic context [3,21], in this review, we will first analyze the current information about mitochondrial bioenergetics alterations triggered by nephron loss in these models. Then, we will discuss the current information of mitochondrial oxidative stress and mitochondrial dynamics and turnover alterations in these models, to discuss and try to integrate along time the mitochondrial changes, as well as their relationship with the illness development. This would suggest possible mitochondrial proteins or mechanisms that may be used as targets to develop new therapies to prevent CKD progression.

2. Mitochondrial bioenergetics alterations in RMR models

According to the unified theory postulated by Taal & Brenner [3], in CKD (as well as in the RMR models), the progression is linear with respect to time and it results from a set of common mechanisms, which include hemodynamic, oxidative stress, hypertrophy and bioenergetics changes [3]. In RMR models, hemodynamic alterations appear immediately after the renal mass loss, which include an early increase in renal vascular resistance and glomerular capillaries pressure, as well as a decrease in plasma blood flow [22,23]. Together these changes lead to an increase in snGFR, which peaks between the first and fourth week after the damage (depending of the magnitude of the renal mass loss) [3].

Hypertrophy processes and biomacromolecular synthesis rise also appear in early stages of the disease [3]. Hypertrophy triggers DNA, mRNA, rRNA and lipid synthesis, especially in PT. Further, pro-apoptotic genes are suppressed and growth factors levels rise in the first days [24–26]. During the first 24 h after RMR, the elevated snGFR leads to higher solute reabsorption rates and an increase in Na^+/K^+ ATPase activity, which further drives the basolateral membrane growth, particularly in PT. These changes, together with the dramatic molecular biosynthesis increase, lead to a higher energy expenditure [27,28]. Moreover, vasoactive and tropic factors such as aldosterone, vascular endothelial growth factor and insulin-like growth factor-1, lead to a further kidney growth which could persist until the 2nd or 3rd month [3,22,25,26,29]. Briefly, in the first period after nephrectomy, the increase in snGFR and solute reabsorption together with the biosynthetic rise and hypertrophy process generate an excessive energy demand in the tubular segment of the nephron, especially in PT. It has been hypothesized that this hypermetabolic state in the remnant renal mass induces stress in ATP sources, especially in mitochondria [3,30,31].

In RMR models, there is an early increase in mitochondrial volume per cell, which persists until the 14th day [30,32]. This increase in the mitochondrial volume was associated with higher size (mitochondrial hypertrophy) but not with mitochondrial proliferation, since an increase in mitochondrial DNA (mtDNA) or in expression of nuclear-encoded mitochondrial genes [with exception of glutathione (GSH)/glutathione disulfide (GSSG) transporter] was not observed in this interval [30,32–34]. However, as we will be discussing later, the current evidence suggests that mitochondrial fusion has a pivotal role in the mitochondrial hypertrophy, associated with a failed compensatory response to the higher kidney energy demand [32], since inorganic phosphate accumulation, increase in oxygen uptake and sodium transport alterations have been observed in PT [23,35,36]. This suggests that in the early stage after RMR, bioenergetics imbalance is particularly greater in PT.

These changes also occur in patients with CKD, where it has been proposed that mitochondria is not able to maintain the ATP production in PT and TAL segments [37,38]. These observations have led to the hypothesis that the increase in energy demand triggers mitochondria stressful hypermetabolic state along all the tubular segments. Moreover, since PT segment is not able to obtain energy by non-mitochondrial pathway [33], this segment is particularly more vulnerable to mitochondrial dysfunction.

In accordance with this, recently, our research group has demonstrated important bioenergetics mitochondrial alterations at 24 h after 5/6Nx. We confirmed that isolated mitochondria from remnant kidney tissue have decreased respiratory state 3 (S3) and ADP/oxygen (ADP/O) ratio and increased respiratory state 4 (S4), which leads to a reduction in the respiratory control index (RCI = S3/S4) in complex I-linked respiration (malate-glutamate feeding). The activities of complex I (CI) and ATP synthase also decrease, however, no changes in the subunit protein levels of these complexes were observed [30]. On the other hand, Lash et al. [33] observed an increase in S3 in complex II (CII)-linked respiration (using succinate) at 10 days post-nephrectomy; however, they were not able to observe changes in any other bioenergetics parameters. This contrasts with a recent work made by Thomas et al. [39] at 1 week, that reported a slight increase in S3, S4 and uncoupled respiration (badly called by them S3u) in the respirations fed by malate-glutamate, pyruvate-malate and succinate + rotenone, without changes in RCI or in the mitochondrial ATP production. These findings need to be interpreted with caution. It is true that the increase in energy demand drives an increase in OXPHOS capacity, higher values of S3, mitochondria coupling, respiration leak decrease [40,41] and mitochondrial biogenesis [42] in a physiologic context, such as during exercise. However, in RMR models, the energy demand increase

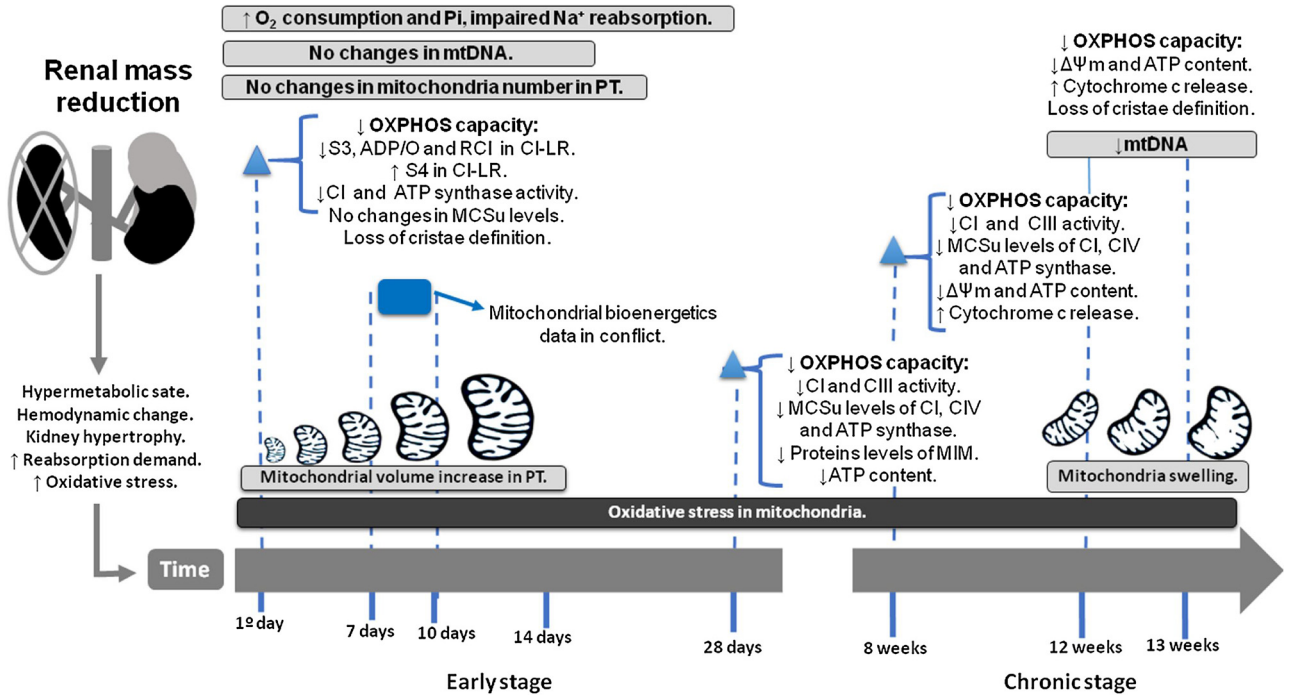

Fig. 1. Mitochondrial bioenergetics alterations over time in RMR models of CKD. The initial nephron loss induces immediately in remnant kidney hemodynamic changes, hypertrophy process, reabsorption rate increase, and oxidative stress that finally trigger pathological mitochondrial bioenergetics alterations. To facilitate its analysis, two stages can be identified, an early stage (from first hours after renal injury to the 28th day) and a chronic stage (after the first month and hereafter). The early stage is characterized by mitochondrial OXPHOS capacity loss, attributable to mitochondrial complexes and ATP synthase activity drop; this is associated with mitochondrial volume rise, (gray bars) especially in PT. Nonetheless changes in mitochondria number and mtDNA are not observed. The mitochondrial growth eventually stops, however, the reduction in the OXPHOS remains until the end of the early stage, now as a result of both mitochondrial complexes diminished activity and decrease in their subunits protein levels. On the other hand, the chronic stage is characterized by damaged mitochondria accumulation, decreased OXPHOS capacity and drop in mitochondrial membrane potential. These alterations drive to cristae shape loss, mitochondrial swelling and cytochrome c release. The persistence of changes over time are shown as a bar in this figure, blue triangles represent the data at a specific time point; blue square represents the time lapse where the available data show discrepancy. The figure construction was carried out following the next guideline "Guidelines for preparing color figures for everyone including the colorblind" [130]. CI = mitochondrial complex I; CIII = mitochondrial complex III; CIV = mitochondrial complex IV; mtDNA = mitochondrial DNA; PT = proximal tubule; Pi = inorganic phosphate; S3 = respiratory state 3; S4 = respiratory state 4; ADP/O = ADP/oxygen ratio; RCI = respiratory control index; CI-LR = complex I linked respiration; MCSu = mitochondrial complexes subunits; MIM = mitochondrial inner membrane; ΔΨm = mitochondrial membrane potential. (For interpretation of the references to colour in this figure legend, the reader is referred to the web version of this article.)

is accompanied by oxidative stress and by inflammatory processes, that are able to induce mitochondrial damage [19,30,33], which lead to bioenergetics alterations, like mitochondria uncoupling, and therefore to a reduction in OXPHOS capacity. This has been demonstrated in non-renal tissues, like skeletal [42,43] and cardiac [44] ones, in nephrectomized animals. In fact, alterations in kidney levels of GSH, the principal mitochondrial non-enzymatic antioxidant, and in its oxidized form, GSSG, can be observed in the first week after nephrectomy. Further, an increase in the GSH/GSSG re-uptake in nephrectomized rats, with respect to sham-operated ones, has been reported [19,33]. These observations, along with higher lipid peroxidation in isolated mitochondria, are considered as signals of a mitochondrial pro-oxidant state [19,30,33]. Although this is widely discussed in the next section, most of the literature agree with the concept of a mitochondrial early oxidative stress state after nephrectomy [19,30,31,33,45], that should affect OXPHOS capacity and therefore trigger the observed decrease in S3 and the increase in S4. At least in the first 24 h, this can be mainly attributed to the drop in CI and ATP synthase activities [30].

Ten days after nephrectomy the mitochondrial volume per cell, as well as the overexpression of GSH/GSSG mitochondrial transporter remain elevated, however, mtDNA stays unchanged [46]. Four weeks after 5/6 Nx, the compensatory kidney hypertrophy rate (evaluated by the increase in the tubular segment size), starts decreasing [32]. Nevertheless, at this time it was also observed that the activities of CI and complex III (CIII), as well as the ATP content decrease [45]. These data, together with the reported lower levels of β subunit of ATP synthase [45], suggest that alterations in the synthetic activity of the enzyme which are observed at 24 h [30] remain until the 4th week.

Proteomic and Western blot analyses of the renal cortex of 5/6Nx rats evidenced a downregulation of mitochondrial proteins like medium chain acetyl dehydrogenase (MCAD), the phosphoglycerate kinase 1 (PGK-1), and glucose-regulated protein-75 (GRP-75) [31]. Nonetheless, the most relevant protein levels which are decreased are the NADH dehydrogenase-ubiquinone 1 beta subcomplex subunit 8 (NDUFB8) and cytochrome c oxidase subunits I (COXI) and IV (COXIV) [31]. All these proteins are located in the mitochondrial inner membrane (MIM). Contrary, the protein voltage-dependent anion channel (VDAC), in the mitochondrial outer membrane (MOM), did not show changes [31]. In fact, patients with CKD present low complex IV (CIV) activity and high 8-hydroxydeoxyguanosine levels, as compared to controls [45]. Although there is no available information regarding mitochondrial respiratory state, the observed decrease in mitochondrial CI, CIII and ATP synthase activities, along with diminished levels of respiratory complexes subunits, suggest that OXPHOS capacity is drastically reduced. Furthermore, changes such as increased oxygen consumption, inorganic phosphate accumulation, and ineffective sodium reabsorption are observed at these times [23,31,35,47] implying a continuous renal bioenergetics disruption from the first hours to the 4th week after the RMR.

On the other hand, there is scarce information regarding mitochondrial respiratory state changes occurring in the remnant kidney mass at a longer time. A study using low-resolution respirometry, at 30 days after 5/6Nx, did not find alterations in the respiration rates using

malate-glutamate or succinate [48], however, the oxidative stress, along with hemodynamic changes and the inflammatory processes, that have been linked to mitochondrial dysfunction are still present in this advanced stage [3,21,48,49] implying that mitochondrial alteration could be present. This agrees with other reports in which 5/6Nx rats after 8, 12 and 13 weeks show a drop in ATP content in renal cortex, lower ΔΨm, as well as loss of cristae definition and mitochondrial swelling, in comparison to sham-operated rats [50–52]. Also, a decline in CI and CIII activities, and lower levels of ATP synthase β subunit, COXI and NDUFB8 were detected at the 8th week in 5/6Nx rats [50]. In comparison, advanced stage of CKD induced by ischemia (at nine months after the original kidney damage), shows an accumulation of smaller mitochondria with abnormal cristae and also signs of proteolytic degradation [53,54]. Altogether, these data, suggest that CKD mitochondrial bioenergetics alterations, specially the OXPHOS capacity decrease, is still present even at long times after kidney injury, however, further studies are needed to clarify this point.

To sum up, early changes triggered by RMR such as hypermetabolic state, hemodynamic changes, hypertrophy and reabsorption rate increase, together with oxidative stress, lead to a pathologic state in the mitochondria (Fig. 1). This pathologic state is characterized by respiratory alterations, uncoupling and OXPHOS capacity loss, which are mainly caused by decreased activities of mitochondrial complexes and ATP synthase (possibly induced by oxidative stress). However, these alterations are not linked to a decrease in subunits complexes levels. The bioenergetics alterations induce an increase in mitochondrial volume (especially in PT), in an attempt to restore mitochondrial function. Eventually, the increase in the mitochondria size stops. In chronic stages mitochondrial growth is not observed, however, the reduced OXPHOS capacity remains caused by both lower activities and subunits levels of mitochondrial complexes and ATP synthase. Finally, the progressive accumulation of damaged mitochondria and the inefficient ATP supply have been strongly linked to the progressive kidney function deterioration in these models, as well as in clinical CKD.

3. Mitochondrial redox changes in RMR models

In the kidney, recent studies have shown that ROS play fundamental roles, at low concentrations, as second messengers [55], since these molecules regulate processes like gluconeogenesis, solute reabsorption, glucose transport and tubuloglomerular feedback [56,57]. However, the notion that ROS have a harmful effect at elevated concentrations is a well-accepted concept [57]. Oxidative stress is an imbalance between ROS production and their detoxification [58], which is well-known to be involved in the progression of diverse renal pathologies [15,59,60], including CKD [61]. In this section, we will discuss the role of mitochondrial oxidative stress in RMR models of CKD. Then we will analyze the role of NADPH oxidase (Nox) in the mitochondrial redox imbalance, in these models.

3.1. Alterations in ROS production and oxidative stress in mitochondria

Mitochondria are one of the most important redox cellular centers [62,63]. In both, pathologic and non-pathologic conditions, the mitochondrial ROS production is linked to the function of oxidoreductases of the electron transport system (ETS), β-oxidation and the Krebs cycle [64,65]. However, ROS production by proteins not involved in the ATP generation system, like Romo1 and dihydroorotate dehydrogenase [66,67] has also been reported. In fact, nowadays at least nine ROS production sites in mitochondria have been identified [41,65] and the contribution of each site can change depending on the conditions [65]. It is estimated that under physiologic conditions only 0.2–0.5% of the oxygen consumed by mitochondria produces ROS [68], however, these values can change depending on diverse factors. The first ROS produced by mitochondria is the superoxide anion (O_2^-) [69] and its generation needs chemical groups able to donate one electron at the time, like the semiquinone radical (Q) and the reduced flavin (F) [70], which are found in different proteins of the ETS, like F in the NADH-oxidizing site (site I-F). However, its half life is short (approximately 10^{-6} s), due to its chemical or enzymatic (by superoxide dismutase, SOD) dismutation, which generates hydrogen peroxide (H_2O_2) [71]. Due to H_2O_2 stability, its membrane permeability and probes accessibility, H_2O_2 is the most common specie used to evaluate the mitochondrial ROS production [71,72].

At low levels, ROS tightly regulate mitochondrial function [73], since these organelles have different redox sensors which quickly detect the redox changes in the environment [55,57]. The thiol groups of cysteines are among the most sensitive redox sensors since they possess a wide spectrum of redox posttranslational modifications (PTM) that strongly depend on the microenvironment [74,75]. Mitochondria possess a broad amount of proteins whose activity is mostly regulated by reversible PTM induced by low ROS levels, such as protein S-glutathionylation (RS-SG) and S-nitrosylation (RS-NO) [76,77], involved in processes like Krebs cycle, β-oxidation, ETS, OXPHOS, mitochondrial morphology, solute transport and apoptosis [55,57,74,76]. In the ETS, the RS-SG and the RS-NO at low levels are associated with a decline in ROS production and a slight CI activity decrease, preventing further ROS production [76,78] and protecting cysteines from irreversible PTM [79]. Therefore, many authors thought that these reversible PTM could be a mitochondrial homeostasis regulation mechanism which links energy metabolism to mitochondrial redox state [74,76]. Nevertheless, an excessive increase in these PTM induced by higher ROS has also been traditionally considered as an oxidative stress marker [80], confirming that the mechanisms involved in mitochondria redox homeostasis are not fully understood [79].

In nephrectomy models, the hypermetabolic state and the hemodynamic changes trigger oxidative stress in mitochondria [33,46]. Recently, we demonstrated that 24 h after nephrectomy, there is an increase in mitochondrial H_2O_2 production in CI-linked respiration (using malate-glutamate) along with CII-linked respiration (using succinate), and higher malondialdehyde (MDA) mitochondrial levels [30]. The mitochondrial GSH uptake rates also increase as a result of the elevated levels of dicarboxylate and oxoglutarate mitochondrial carriers [19,33]. Furthermore, the activities of SOD and glutathione peroxidase (GPx) in isolated mitochondria are reduced [30]. Additionally, mitochondria are also more susceptible to damage by external oxidants and alkylating agents [33], confirming a redox mitochondrial imbalance on the first days after renal ablation. Actually, at seven days after nephrectomy, O_2^- levels, evaluated by electron paramagnetic resonance, are still elevated. Moreover, after 10 days a decrease in the aconitase activity (a mitochondrial oxidative stress indicator) was reported, as well as increased levels of 4-hydroxy-2-nonenal [19] and, at 28 days, mitochondrial ROS measured using 2,7-dichlorofuorescin diacetate continue high [45]. Taken together, these data suggest persistent mitochondrial oxidative stress in the early stage of nephrectomy. Further, increased mitochondrial ROS production, elevated MDA levels, decreased GSH levels and reduced SOD activity and protein levels at weeks 8, 12 and 13 after nephrectomy were reported [45,47,50–52]. This implies that even at chronic stages, the mitochondrial pro-oxidant state is still present.

The mitochondrial redox imbalance has been extensively associated with mitochondrial bioenergetics alterations [19,30,33], so it has been hypothesized that the decrease in the ETS complexes activity at 24 h in nephrectomized rats could be attributable to ROS-induced irreversible PTM. In cardiac mitochondria, Kang et al. [81] showed that oxidative stress induces irreversible PTM in 51 and 75 kDa subunits of CI (near to IQ site), decreasing its activity and also increasing ROS production associated to CI. In fact, CI cysteine residues can undergo S-sulfenylation (R-SOH), and if oxidative stress persists they can suffer S-sulfinylation ($R\text{-}SO_2H$) and even S-sulfonylation ($R\text{-}SO_3H$), which irreversibly inactivate CI [74]. These modifications compete for CI cysteines against RS-SG and although all of them reduce CI activity, only RS-SG can be

reversed, restoring totally CI activity [62]. CII Cys90 RS-SG is also necessary to avoid its inactivation by oxidative stress [82]. Moreover, S-glutathionylation of ATP synthase prevents R-SOH of the Cys^{294} and Cys^{103}, which triggers a disulfide bond formation and irreversibly decrease ATP production [83,84].

Outstanding information about oxidative stress role in mitochondrial bioenergetics came from the use of antioxidants in AKD models [58]. In these models, antioxidants prevented mitochondrial oxidative stress and also avoided bioenergetics alterations, like S3 decrease, leak respiration rise, decline in ADP/O ratio and ATP, RCI rate reduction, decrease in mitochondrial complexes and ATP synthase activity and ΔΨm alterations [13,15,59,85,86]. Hence, prevention of mitochondrial oxidative stress may be a good approach to avoid mitochondrial bioenergetics alterations in RMR models. In fact, preadministration of curcumin (a bifunctional antioxidant) in a 5/6 Nx model substantially reduces mitochondrial and PT oxidative stress at 24 h and also prevents CI activity loss, ATP synthase activity decrease, as well as uncoupling and alterations in mitochondrial respiratory states [30]. Similarly, resveratrol post-administration at the 4th week, increases ATP, decreases mitochondrial ROS production and prevents the drop in CI and CIII activity induced by nephrectomy [45]. The use of mitochondria-targeted antioxidants, such as MitoQ, MitoTEMPO or Szeto–Schiller (SS) peptides protects the mitochondria and preserve kidney function in AKD models [54,87–89]; however, their use in CKD models is just beginning to be explored. A recent study showed that, after 13 weeks, in a 5/6 Nx model, the post-surgery administration of the SS-31 peptide avoided the mitochondrial SOD activity drop, decline in ATP levels, decrease in the ΔΨm, ROS increment and cytochrome c release [52]. Taken together, these data confirm the role of redox imbalance in mitochondrial alterations and suggest that prevention of mitochondrial oxidative stress can be a good approach to preserve mitochondrial bioenergetics [30,52].

Additionally, the mitochondrial redox imbalance not only generates bioenergetics alterations [19,30,33], but also favors other mechanisms involved in CKD progression. For instance, mitochondrial ROS are able to activate NLRP3 inflammasome and further contribute to CKD inflammatory and fibrotic processes [90]. It has been demonstrated *in vitro* (in human renal proximal tubular epithelial cells, HK2) and *in vivo* (in 5/6NX rats) that mitochondrial redox imbalance is an early event that prompts the fibrotic process [51]. Furthermore, mitochondrial ROS, together with aldosterone, mediate the epithelial-mesenchymal transition of tubular cells [91], favoring fibrotic processes. Moreover, the formation of hypochlorite-modified albumin by mitochondrial ROS triggers renal fibrosis, modulated by the transforming growth factor beta 1 (TGF-β1) signal transduction pathway, and generates renal macrophage infiltration [52]. Although, CI ROS generation has been implicated in this mechanism [52,91], more studies are needed to elucidate this mechanism.

In brief (see Fig. 2), the mitochondrial redox imbalance and oxidative stress appears since the first stages after RMR and it persists at even CKD advanced stages. Notably, redox imbalance has a strong relationship with mitochondrial bioenergetics alterations over time [19,30,33,51,52]. These alterations contribute to the intricate network of mechanisms that lead to progressive renal function deterioration. Since the mitochondrial balance is highly dependent on the redox state [55,57,74,76], proteomic approaches of ROS-induced PTM could help us to understand the molecular mechanisms involved in redox state and mitochondrial bioenergetics interdependence, generating a new approach to develop strategies to prevent the genesis and development of CKD.

3.2. Nox and its role in mitochondrial oxidative stress in RMR models

The Nox family group includes seven homolog proteins present in humans: Nox1 to Nox5, and Duox1 and Duox2 [92], which catalyze the electron transfer from NADPH to oxygen producing O_2^-. The kidney possesses a wide distribution of Nox isoforms along the tubular segments (being Nox4 the predominant isoform) and vasculature [93]. Nox-derived ROS are implicated in the regulation of several kidney physiologic processes, such as the tubuloglomerular feedback, gluconeogenesis [56], regulation of active transport and Na^+/K^+ ATPase activity [93].

Several reports have associated Nox upregulation with kidney disease development [56]. In CKD models, Watanabe et al. [49] showed that Nox4-derived ROS are tubular damage mediators, which increase the expression of proinflammatory cytokines and profibrotic factors. In addition, in RMR models, it was seen that p47 phox deletion (Nox activating subunit) protects mice from glomerulosclerosis [94]. It has been suggested that angiotensin II is able to activate Nox in a chronic state, contributing to systemic hypertension [95] in CKD models, although the mechanism is still not fully understood. In RMR models, Nox subunits overexpression enhances kidney function deterioration by increasing oxidative stress and inflammation and promoting hemodynamic changes [96,97]. Furthermore, in 5/6Nx models, increased levels (20% to 40%) of gp91phox, p22phox, and p47phox Nox subunits have been reported at the 8th week, which was further correlated with the rise in proteinuria and plasma creatinine levels [97,98]. Recently, we reported higher O_2^- production by Nox at 24 h in 5/6 Nx rats, compared to control group. Interestingly, this increase was found to be different along the nephron segments, being especially high at PT [30]. Usually, this increase in O_2^- production by Nox has been linked to Nox4 and Nox2 isoforms activity and it has a strong correlation with loss of renal function in CKD models [56].

Further, it has been reported that an increase in O_2^- production by Nox can induce ETS system dysfunction [99]. Nox4 overexpression decreases the activity of mitochondrial CI, increases H_2O_2 production and leads to mitochondrial network disruption in smooth muscle cells [100]. Furthermore, mitochondrial ROS can drive quick activation of kinases such as protein kinase C (PKC) β and ε, which in turn enhance Nox activity [101], this mechanism has been reported in AKD models [86], but not yet in CKD models. Both PKCβ and PKCε have structural motifs sensitive to ROS modification, which leads to p47phox Nox subunit phosphorylation and activation [101,102]. Twenty-four hours after 5/6 NX, the PKC-βII levels in PT of nephrectomized rats did not show significant changes with respect to the sham-operated group. Nevertheless, there was a significant increase in p47phox subunit phosphorylation in serine 304; this phosphorylation has been linked to its activation by ROS [92,103], implying that the observed O_2^- production rise by Nox is related to its activation by mitochondrial ROS.

Similar to another authors in other models [99,101], we propose an integral feedback mechanism which involves mitochondrial Nox activation in RMR models at early stages (Fig. 3). In this mechanism and according to the overload hypothesis [3], nephrectomy induces alterations in renal hemodynamics, in reabsorption processes, as well as in the renal metabolism [3,22–26,29]. These alterations lead to an energy stress [19,30,33,37,38] and to kidney Nox activation, which is able to trigger mitochondrial redox imbalance and subsequent loss of the activity of mitochondrial complexes [19,30,45,47,51,52]. These alterations in mitochondrial ROS production lead to the activation of PKC isoforms, which trigger a higher activation of Nox, thus enhancing oxidative stress [19,30,33,37,38,95–98] and causing subsequent damage to mitochondria and nephron segments. These alterations altogether induce a feedback loop of rising oxidative stress and thus contribute to CKD progression.

4. Mitochondrial dynamics and turnover alterations in RMR models

Mitochondria is a highly dynamic organelle, it is constantly under fission (fragmentation) or fusion (joining) processes, as well as under degradation of damaged mitochondrial components and synthesis of new components (biogenesis). All these processes determine its

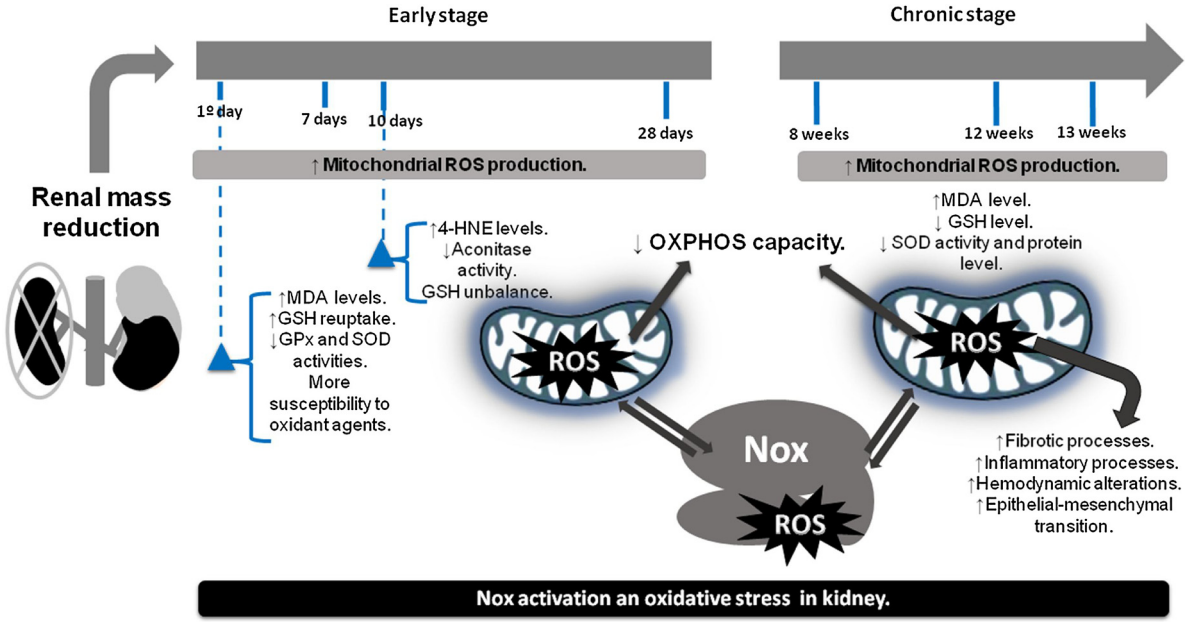

Fig. 2. Mitochondrial redox alterations over time, and the role of NOX in mitochondrial dysfunction. Renal mass reduction immediately induces in the remnant kidney mass a mitochondria redox unbalance, characterized by a mitochondrial ROS production increase (grey bar), seen in both stages (early and chronic). The mitochondrial redox unbalance is related to a permanent oxidative stress and to Nox overregulation (especially in PT). In both stages, Nox and mitochondria establish feedback loop of ROS production increase, leading to mitochondrial pathological alterations. These mitochondrial pathological alterations promote mechanisms over time that contributes to CDK development and progression. The conservation of changes along the time is shown as bars; blue triangles represent the analyzed data at a specific time point. The figure construction was carried out following the next guideline "Guidelines for preparing color figures for everyone including the colorblind" [130]. GSH = glutathione; GPx = glutathione peroxidase; MDA = malondialdehyde; Nox = NADPH oxidase; OXPHOS = oxidative phosphorylation system; ROS = reactive oxygen species; SOD = superoxide dismutase; 4-HNE = 4-hydroxynonenal. (For interpretation of the references to colour in this figure legend, the reader is referred to the web version of this article.)

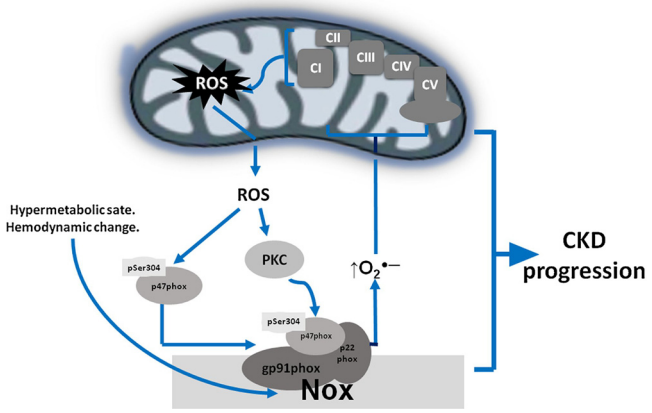

Fig. 3. Proposed mitochondria-Nox mechanism of ROS production rise. The hypermetabolic state and the hemodynamic alterations trigger Nox overactivation (particularly in PT), increasing its superoxide production and generating a prooxidant state in mitochondria. This prooxidant state promotes irreversible PTMs in mitochondrial proteins especially in ETS components, uncoupling and enhancing mitochondrial ROS production. Additionally, mitochondrial ROS activate Nox by mechanisms such as the PKC isoforms activation which triggers the p47phox phosphorylation and increases more the Nox activation. This vicious ROS production circle induces oxidative stress and contributes to CKD progression. The figure construction was carried out following the next guideline "Guidelines for preparing color figures for everyone including the colorblind" [130]. CI–CV = mitochondrial complex I to IV; PKC = protein kinase C; pSer304 = phosphorylation of serine 304.

morphology, size, and distribution along the cell [104,105]. Mitochondrial fusion is regulated by the proteins implicated in MOM fusion: Mitofusin 1 (Mfn1) and 2 (Mfn2); and by the protein that participates in MIM: fusion Optic atrophy 1 (Opa1) [11]. On the other hand, the fission process is regulated by Dynamin-related protein 1 (Drp1) and four adapter proteins: fission protein 1 (Fis1), mitochondrial fission factor (Mff), and the mitochondrial elongation factors 1 (Mief) and 2 (Mief2) [11,106]. Mitochondrial bioenergetics is tightly coordinated with dynamics, favors fission or fusion depending of the energy demands [107,108]. In addition, ROS are able to regulate mitochondrial morphology and dynamics. For example, H_2O_2 stimulates Mfn1 and Mfn2 ubiquitination, promoting their degradation, and also activates Drp1, triggering mitochondrial fragmentation [106]. Actually, a decrease in CI activity induces mitochondrial ROS production and leads to mitochondria fragmentation [108]. So there is a tight relation between bioenergetics, redox and dynamics processes in mitochondria [109].

Concerning mitophagy, this process is regulated by the phosphatase and tensin homolog (PTEN)-induced putative kinase 1 (Pink1), whose accumulation in MOM is caused by mitochondria depolarization [110]. Pink1 activates Parkin E3-ubiquitin ligase allowing protein ubiquitination, which is a marker of autophagy machinery recruitment [108]. The importance of this process relies on eliminating damaged mitochondria, avoiding the harmful organelle accumulation [111]. However, mitophagy must be preceded by mitochondrial fission, in order to reach an organelle size capable of being encapsulated by the autophagosomes [110].

In the kidney, most of the mitochondrial dynamics alterations have been reported in AKD models, where there is a shift to fission at early stages after injury [11]. However, CKD models have just begun to draw attention. At a chronic stage in ischemia kidney injury (9 months), a reduction of mitochondria number and an accumulation of these organelles in autophagy bodies has been reported [53,54]. This has been related to an impairment in mitophagy [88]. Likewise, diabetic nephrectomy is characterized by high levels of apoptosis induced by mitochondrial cytochrome c release, mitochondrial fragmentation and Drp1 activation [88,112].

Nonetheless, the mitochondrial dynamics alterations in RMR models have been less characterized and cannot give us a full

perspective [30]. At 24 h after 5/6 Nx, there is shift of mitochondrial dynamics to fusion, characterized by Mfn1 and Opa1 increase and decrease in Fis1 and Drp1 levels in mitochondria, as well as mitochondria swelling, loss of cristae definition and higher mitochondrial size in PT [30]. In agreement with this, morphometric analysis in PT, reported mitochondrial volume rise after nephrectomy, reaching its maximum at the 14th day (66% compared to control) [32]. Due to the absence of mtDNA or mitochondrial protein increase in this time lapse, the authors concluded that at early stages, mitochondria undergo a pathologic hypertrophy (size rise) rather than proliferation [22,32]. According to this, other studies did not find increase in mtDNA, in mtRNA, in mitochondrial complexes subunits or in transporters levels at 1, 10, and 14 days after nephrectomy [19,32,33,46].

These type of changes are found in other energy stress conditions associated with mitochondrial hyperfusion state [104], for example, profusion state is typically observed in starvation and exercise [111]. Nonetheless, in a pathologic context, hyperfusion has been linked to apoptosis resistance state and to oxidative stress [104]. That is the case of nephrectomy at early stage, where it is observed apoptosis resistance in epithelial cells [3], mitochondrial oxidative stress [19,30,33,37,38,95–98] and mitochondrial size rise [30,32]. Altogether and considering mitochondrial bioenergetics alterations [19,30,45,47,51,52] and the kidney energy demand rise [3], this suggest that mitochondrial size increase is more attributable to mitochondrial fusion rather than biogenesis (see Fig. 4).

Studies in later stages are also scarce. It was reported, at 28 days after 5/6 Nx, a change in mitochondrial dynamics markers tendency, with an increase in Fis1 and a decrease in Opa1 and Mfn2 levels, although mtDNA remain without changes [45]. That tendency persist until the 8th week [50]. Besides, at the 28th day, the peroxisome proliferator-activated receptor gamma coactivator 1-alpha (PGC-1α), the master mitochondrial biogenesis protein, was downregulated and the MIM proteins MCAD, PGK-1, GRP-75 NDUFB8 and COXI were also downregulated [31,46]. Interestingly, NDUFB8 and COX remained low even at 8th week [50]. Furthermore, at the 12th and 13th week there is a decrease in mtDNA in 5/6NX rats a, as well as mitochondria swelling and cristae definition loss, which was associated to impaired biogenesis induced by the increase in TGF-β1 level [51,52], suggesting a mitochondrial biogenesis disruption in chronic stages (see Fig. 5). A study in CKD patients submitted to dialysis also showed lower levels of mRNA of mitochondrial biogenesis factors PGC-1α, nuclear respiration factor 1 and mitochondrial transcription factor A (TFAM), and a downregulation of PGC-1α downstream genes (TFAM, COX6C, COX7C, UQCRH and MCAD) [18], supporting the idea that mitochondrial biogenesis is impaired in CKD.

Finally, it has been hypothesized that mitophagy might also be disrupted in RMR models, due to the hyperfusion state, lower mitochondria levels of fission and increase in mitochondrial size [30,32]. Taken as a whole, the above information suggests that damaged mitochondria are not being degraded by autophagy [110]. This is supported by the damaged mitochondria accumulation observed in these models [30,32]. Furthermore, after 28 days Beclin 1 (essential protein for autophagosome formation) and BCL2/adenovirus E1B 19 kDa protein-interacting protein (3BNIP3, necessary for mitophagy process) proteins levels rise, however, autophagy factor microtubule-associated protein 1 light chain 3 (LC3) that mediates later autography steps did not show significant changes [31]. The lack of LC3-II changes along with undisturbed mitochondrial VDAC levels and the fact that autophagy is inhibited in PT [113,114], led authors to suggest that mitophagy flux is disrupted in this model (Figs. 4 and 5). However, there is not enough information to support this idea and sequential studies are needed to clarify the correlation within dynamics and mitophagy in these models.

The aim of this work was to review mitochondrial dysfunction in models of non-diabetic acquired nephropathy, since, for diabetic nephropathy, mitochondrial alterations have been widely documented in recent reviews [115,116]. Nevertheless, it is important to mention that, like in non-diabetic models, in diabetic nephropathy and especially in chronic stages the following changes have been observed: decrease in expression of mitochondrial biogenesis factors, such as of PGC-1α, increase in mitochondrial fragmentation produced by the shift of mitochondrial dynamics to fission and impaired mitophagy flux [115,117,118]. Furthermore, CI dysfunction leads to increased mitochondrial ROS production, which was recently confirmed using a redox-sensitive green fluorescent protein biosensor expressed in mitochondrial matrix in diabetic mice [119]. Additionally, reduction in expression and activity of Krebs cycle enzymes in kidney has been reported in both, patients with type 2 diabetes and animal models of diabetes [115]. So, the current data indicate that in diabetic nephropathy there is an accumulation of damaged mitochondria in the kidney, which will be a primary factor responsible for tubule and vascular damage, oxidative stress, cell death, inflammation and fibrosis, which

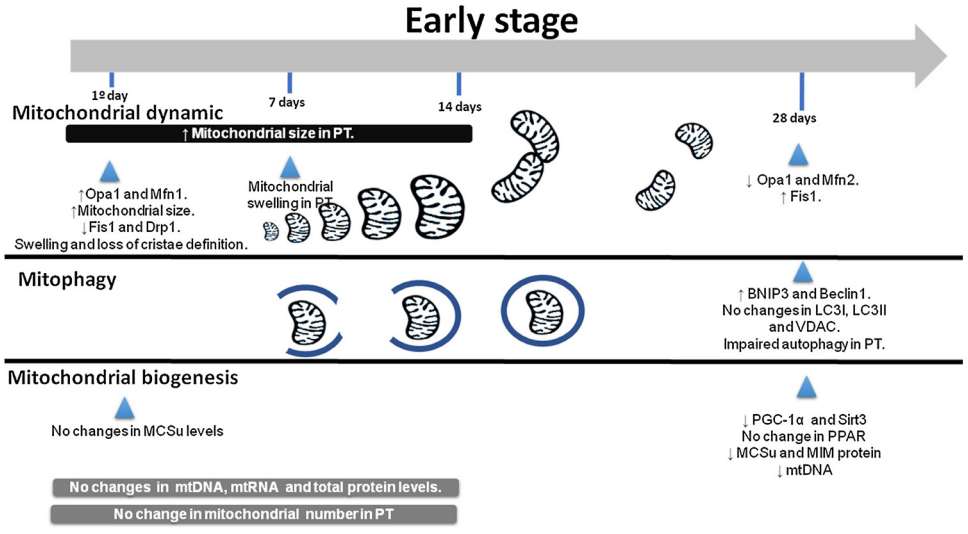

Fig. 4. Mitochondrial alterations in dynamics, biogenesis and mitophagy in RMR models at early stages. At early stage the observed mitochondrial size rise (black bar) is related to mitochondrial dynamics shift to fusion. Due to no changes in mitochondria number, mtRNA, mtDNA, and protein levels (gray bars) are observed between the 1 st and the 14th day. Mitochondrial fusion increase could be an attempt to face the bioenergetics unbalance in high energy demands conditions. This shift to fusion together with an impaired autophagy prevents impaired mitochondria degradation by mitophagy. Nevertheless, more data are necessary to confirm this hypothesis. Interestingly, after 28 days is observed an increase in Fis1 and a decrease in Opa1 an Mfn2, suggesting a shift to fusion, additionally mitophagy and biogenesis are still impaired. The figure construction was carried out following the next guideline "Guidelines for preparing color figures for everyone including the color-blind" [130]. PT = proximal tubule; MCSu = mitochondrial complexes subunits; Mfn (1/2) = mitofusin (1/2); Opa1 = optic atrophy 1 protein; Fis 1 = fission protein 1; Drp1 = dynamin-related protein 1; BNIP3 = BCL2/adenovirus E1B 19 kDa protein-interacting protein 3; LC3 (I/II) = Microtubule-associated protein 1 A/1B-light chain 3 (I/II); Sirt3 = Sirtuin 3; MIM = mitochondrial inner membrane; mtDNA = mitochondrial DNA; mtRNA = mitochondrial RNA; PGC-1α = peroxisome proliferator-activated receptor gamma coactivator 1-alpha, PPAR = peroxisome proliferator-activated receptors; VDAC = voltage depending anion channel.

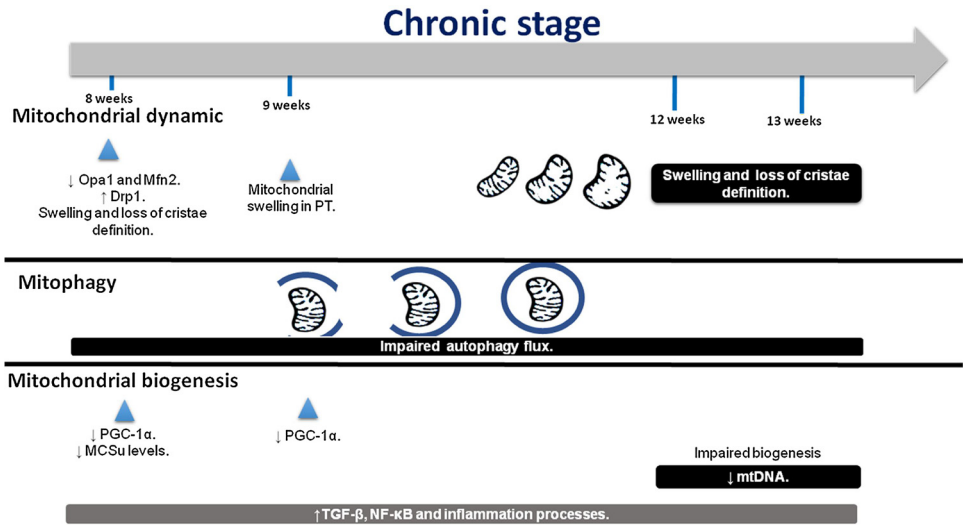

Fig. 5. Mitochondrial alterations in dynamics, biogenesis and mitophagy in RMR models at chronic stages. A persistent mitochondrial swelling and cristae shape loss are observed in chronic stages. However mitochondrial fusion proteins have been reported to decrease. Impaired mitochondrial biogenesis seems to remain, but the current data are insufficient to establish which mitochondrial changes occur at chronic stages. The figure construction was carried out following the next guideline "Guidelines for preparing color figures for everyone including the colorblind" [130]. PT = proximal tubule; MCSu = mitochondrial complexes subunits; Mfn2 = mitofusin2; Opa1 = optic atrophy 1 protein; Drp1 = dynamin-related protein 1; mtDNA = mitochondrial DNA; PGC-1α = peroxisome proliferator-activated receptor gamma coactivator 1-alpha; TGF-β = Transforming growth factor beta; NF-κB = nuclear factor kappa-light-chain-enhancer of activated B cells.

contribute to the CKD progression [115–120].

Despite the direct comparison between data of mitochondrial alterations in non-diabetic and in diabetic nephropathy, this must be made with care, because the high levels of glucose in plasma in diabetes generate a different bioenergetics context [116,120]. Many similar mitochondrial alterations have been found in both types of models, especially in chronic stages. As discussed above, both are characterized by a reduction in the OXPHOS capacity, especially in mitochondrial CI activity that triggers an increase in ROS production by this organelle. Additional to the mitochondrial and renal pro-oxidant state, in both types of models there is a shift of the mitochondrial dynamics towards the fission process (in the chronic stage), as well as evidence of a reduction of mitochondrial biogenesis and a defective mitophagy flux. In *in vivo* models of diabetic nephropathy, the use of antioxidants aimed at preventing these mitochondrial alterations has been shown to significantly prevent the increase in kidney damage markers, the structural alterations in the kidney and the progression of CKD [115,117,121], highlighting the role of mitochondria in this illness. However, especially in non-diabetic models, more information and sequential studies are needed to support this idea and to clarify the correlation within dynamics and mitophagy in these models.

5. Mitochondrial alterations in patients with CKD

The correlation of the information obtained in the experimental models with clinical data of patients with CKD is still poor [12]. The existing clinical data principally comes from studies of *Mitochondrial nephropathys,* term used to encompass kidney illness triggered by mutations in mitochondrial proteins encoded by mtDNA or nuclear genes [122,123]. Although these *Mitochondrial nephropathys* are rare genetic diseases, they usually have poor prognosis, because quickly lead to CKD development and end stage renal disease [122]. Among the genetic defects there are mutations in tRNA, in the enzymes involved in coenzyme Q10 synthesis and in CIII and CIV that lead to a decrease in their activities [12,122,124]. In kidney, these mitochondrial mutations trigger mainly tubular dysfunction and also interstitial nephritis, cystic renal disease and glomerulosclerosis [123,125,126], however, renal alterations are rarely isolated and are usually part of a systemic disorder [122].

On the other hand, in the case of acquired CKD, there is still a lack of human clinical data of mitochondrial bioenergetics and dynamics alterations in kidney tissue of patients in early and chronic stage [12], this is mainly given by the difficulty of obtaining renal biopsies for mitochondrial studies, making problematic the correlation with the experimental data. However, in CKD patients, important studies have been made on biopsies of muscle tissue [127] and in peripheral blood mononuclear cells [128]. In the case of muscle biopsies, it has been found decreased mitochondrial density, mtDNA copies, maximal oxygen consumption by tissues and activity of mitochondrial enzymes citrate synthase and hydroxyacyl-CoA dehydrogenase, implying an impaired mitochondrial bioenergetics function [127]. Additionally, the observed mitochondria fragmentation together with the increase in mitophagy protein BNIP3, suggest that the mitochondrial reduction in skeletal muscle in patients with CKD would be related to an increase in mitophagy [127]. In peripheral blood mononuclear cells of patients with CKD, there is a decrease in the expression of mitochondrial biogenesis markers of NRF1, PGC1-α and TFAM and in cytochrome c oxidase subunit 6C, in cytochrome c oxidase and in mtDNA, tightly associated with enhanced oxidative stress [127,128].

The importance of mitochondrial dysfunction in patients with CKD is confirmed by studies that show a correlation between the mitochondrial reduction in muscle and blood mononuclear cells with the advance of CKD and with the increase of risk of mortality [127,128]. In these studies, an impaired mitochondrial bioenergetics and turnover in patients is suggested, which is also observed in the kidney in the chronic stages in the experimental models in animals (Figs. 4 and 5). However, the lack of human clinical data in kidney tissues makes difficult the correlation between data in experimental models and in humans. Nevertheless, first studies with the Q10 supplementation therapy, a mitochondria focus therapy, decreases proteinuria, a renal damage marker, in patients [122,129]. Considering all the above information, mitochondria-focused therapy could be emerging strategies to mitigate the progression of CKD in patients.

6. Conclusion and perspectives

In summary, the current information about mitochondrial changes in RMR models suggests a temporary accumulation of damaged mitochondria, which highly contributes to CKD progression. This mitochondrial impairment is characterized at early stages by OXPHOS reduced capacity, mitochondrial volume rise, shift to fusion process and oxidative stress. However, the progression of these mitochondrial alterations over time in CKD stages is not totally clear. Current information suggests persistence of impaired OXPHOS capacity, mitophagy and mitochondrial biogenesis, as well as of mitochondrial prooxidant state, which contributes to kidney deterioration. Additionally, the use of mitochondria-targeted antioxidants could be a good alternative to reverse both bioenergetics alterations and oxidative

stress in mitochondria; however their effects in mitochondrial dynamics and turnover balance are still unknown. Since the information existing in the literature about the mitochondrial changes along the progression to CKD is lacking and fragmented, well-conducted temporal studies of bioenergetics, redox state, dynamics, mitophagy, and biogenesis are needed to clarify and unify the theories of mitochondrial dysfunction progression. Future experiments should be directed to unravel which proteins are key in imbalance of these mechanisms, to point them as possible targets with therapeutic potential, opening the possibility of developing strategies to mitigate the progression of this disease. Finally, renal mitochondrial proteomics studies focused on redox-induced PTMs are needed to describe at a molecular level the mechanisms involved in mitochondrial and renal function deterioration in CKD.

Conflict of interest

We have no conflict of interest to declare.

Acknowledgements

Special thanks to Dianelena Eugenio-Pérez for her assistance on the review and refinement of the present text and to *Programa de Apoyo a los Estudios de Posgrado* (PAEP) for the support received. This article was supported by *Consejo Nacional de Ciencia y Tecnología* (CONACyT) Grant number 220046 and *Programa de Apoyo a Proyectos de Investigación e Innovación Tecnológica (*UNAM*)* Grant number IN201316.

References

[1] A.S. Levey, J. Coresh, Chronic kidney disease, Lancet 379 (2012) 165–180, https://doi.org/10.1016/S0140-6736(11)60178-5.
[2] A.M. El Nahas, K.B. Aminu, Chronic kidney disease: the global challenge, Lancet 365 (2005) 331–340, https://doi.org/10.1016/S0140-6736(05)70199-9.
[3] M.W. Taal, B.M. Brenner, Adaptation to Nephron Loss and Mechanisms of Progression in Chronic Kidney Disease, fifth edit, Elsevier, 2013, pp. 1918–1971, https://doi.org/10.1016/B978-1-4160-6193-9.10051-X.
[4] J.-J. Carrero, M. Hecking, I. Ulasi, L. Sola, B. Thomas, Chronic kidney disease, gender, and access to care: a global perspective, Semin. Nephrol. 37 (2017) 296–308, https://doi.org/10.1016/j.semnephrol.2017.02.009.
[5] A. Khwaja, M. El Kossi, J. Floege, M. El Nahas, The management of CKD: a look into the future, Kidney Int. 72 (2007) 1316–1323, https://doi.org/10.1038/sj.ki.5002489.
[6] T. Sekine, H. Endou, Solute transport, energy consumption, and production in the kidney, Seldin and Geibisch's The Kidney, fifth edit, Elsevier, 2013, pp. 143–175, https://doi.org/10.1016/B978-0-12-381462-3.00006-9.
[7] K. Klein, W. Maw-Song, S. Torikai, D.D. Warren, K. Kurakawa, Substrate oxidation by isolated single nephron segments of the rat, Kidney Int. 20 (1981) 29–35.
[8] W. Pfaller, M. Rittinger, Quantitative morphology of the rat kidney, Int. J. Biochem. 12 (1980) 17–22.
[9] A.M. Hall, G.J. Rhodes, R.M. Sandoval, P.R. Corridon, B.A. Molitoris, In vivo multiphoton imaging of mitochondrial structure and function during acute kidney injury, Kidney Int. 83 (2014) 72–83, https://doi.org/10.1038/ki.2012.328.In.
[10] A.M. Hall, R.J. Unwin, N. Parker, M.R. Duchen, Multiphoton imaging reveals differences in mitochondrial function between nephron segments, J. Am. Soc. Nephrol. 20 (2009) 1293–1302, https://doi.org/10.1681/ASN.2008070759.
[11] M. Zhan, C. Brooks, F. Liu, L. Sun, Z. Dong, Mitochondrial dynamics: regulatory mechanisms and emerging role in renal pathophysiology, Kidney Int. 83 (2013) 568–581, https://doi.org/10.1038/ki.2012.441.
[12] J. Pedraza-Chaverri, L.G. Sánchez-Lozada, H. Osorio-Alonso, E. Tapia, A. Scholze, New pathogenic concepts and therapeutic approaches to oxidative stress in chronic kidney disease, Oxid. Med. Cell. Longev. 2016 (2016) 6043601, , https://doi.org/10.1155/2016/6043601.
[13] B. Ortega-Domínguez, O.E. Aparicio-Trejo, F.E. García-Arroyo, J.C. León-Contreras, E. Tapia, E. Molina-Jijón, R. Hernández-Pando, L.G. Sánchez-Lozada, D. Barrera-Oviedo, J. Pedraza-Chaverri, Curcumin prevents cisplatin-induced renal alterations in mitochondrial bioenergetics and dynamic, Food Chem. Toxicol. 107 (2017) 373–385, https://doi.org/10.1016/j.fct.2017.07.018.
[14] M. Negrette-Guzmán, W.R. García-Niño, E. Tapia, C. Zazueta, S. Huerta-Yepez, J.C. León-Contreras, R. Hernández-Pando, O.E. Aparicio-Trejo, M. Madero, J. Pedraza-Chaverri, Curcumin attenuates gentamicin-induced kidney mitochondrial alterations: possible role of a mitochondrial biogenesis mechanism, evidence-based complement, Altern. Med. 2015 (2015) 917435, , https://doi.org/10.1155/2015/917435.
[15] E. Molina-Jijón, E. Tapia, C. Zazueta, M. El Hafidi, Z.L. Zatarain-Barrón, R. Hernández-Pando, O.N. Medina-Campos, G. Zarco-Márquez, I. Torres, J. Pedraza-Chaverri, Curcumin prevents Cr(VI)-induced renal oxidant damage by a mitochondrial pathway, Free Radic. Biol. Med. 51 (2011) 1543–1557, https://doi.org/10.1016/j.freeradbiomed.2011.07.018.
[16] E. Molina-Jijón, O.E. Aparicio-Trejo, R. Rodríguez-Muñoz, J.C. León-Contreras, M. del Carmen Cárdenas-Aguayo, O.N. Medina-Campos, E. Tapia, L.G. Sánchez-Lozada, R. Hernández-Pando, J.L. Reyes, L. Arreola-Mendoza, J. Pedraza-Chaverri, The nephroprotection exerted by curcumin in maleate-induced renal damage is associated with decreased mitochondrial fission and autophagy, Biofactors 42 (2016) 686–702, https://doi.org/10.1002/biof.1313.
[17] Y. Ishimoto, R. Inagi, Mitochondria: a therapeutic target in acute kidney injury, Nephrol. Dial. Transplant. 31 (2015) 1062–1069, https://doi.org/10.1093/ndt/gfv317.
[18] G. Zaza, S. Granata, V. Masola, C. Rugiu, F. Fantin, L. Gesualdo, F.P. Schena, A. Lupo, Downregulation of nuclear-encoded genes of oxidative metabolism in dialyzed chronic kidney disease patients, PLoS ONE 8 (2013) e77847, , https://doi.org/10.1371/journal.pone.0077847.
[19] B. Benipal, L.H. Lash, Influence of renal compensatory hypertrophy on mitochondrial energetics and redox status, Biochem. Pharmacol. 81 (2011) 295–303, https://doi.org/10.1016/j.bcp.2010.10.010.
[20] M. Tamaki, K. Miyashita, S. Wakino, M. Mitsuishi, K. Hayashi, H. Itoh, Chronic kidney disease reduces muscle mitochondria and exercise endurance and its exacerbation by dietary protein through inactivation of pyruvate dehydrogenase, Kidney Int. 85 (2014) 1330–1339, https://doi.org/10.1038/ki.2013.473.
[21] E. Tapia, Z.L. Zatarain-Barrón, R. Hernández-Pando, G. Zarco-Márquez, E. Molina-Jijón, M. Cristóbal-García, J. Santamaría, J. Pedraza-Chaverri, Curcumin reverses glomerular hemodynamic alterations and oxidant stress in 5/6 nephrectomized rats, Phytomedicine 20 (2013) 359–366, https://doi.org/10.1016/j.phymed.2012.11.014.
[22] T.H. Hostetter, J.L. Olson, H.G. Renke, M.A. Venkatachalam, B.M. Brenner, Hyperfiltration in remnant nephrons: a potentially adverse response to renal ablation, J. Am. Soc. Nephrol. 12 (2001) 1315–1325, https://doi.org/10.1681/ASN.2009020171.
[23] B.M. Brenner, Nephron adaptation to renal injury or ablation, Ren. Fluid Electrolyte Physiol. 18 (1985) F324–37.
[24] I. Sinuani, Z. Averbukh, I. Gitelman, M.J. Rapoport, J. Sandbank, M. Albeck, B. Sredni, J. Weissgarten, Mesangial cells initiate compensatory renal tubular hypertrophy via IL-10-induced TGF-beta secretion: effect of the immunomodulator AS101 on this process, Am. J. Physiol. Renal Physiol. 291 (2006) F384–F394, https://doi.org/10.1152/ajprenal.00418.2005.
[25] P. Hauser, A. Kainz, P. Perco, H. Bergmeister, C. Mitterbauer, C. Schwarz, H.M. Regele, B. Mayer, T.W. Meyer, R. Oberbauer, Transcriptional response in the unaffected kidney after contralateral hydronephrosis or nephrectomy, Kidney Int. 68 (2005) 2497–2507, https://doi.org/10.1111/j.1523-1755.2005.00725.x.
[26] G. Wolf, F.N. Ziyadeh, Molecular mechanisms of diabetic renal hypertrophy, Kidney Int. 56 (1999) 393–405, https://doi.org/10.1046/j.1523-1755.1999.00590.x.
[27] J.P. Hayslett, M. Kashgarian, F.H. Epstein, Functional correlates of compensatory renal hypertrophy, J. Clin. Invest. 47 (1968) 774–799, https://doi.org/10.1172/JCI105772.
[28] K. Tabei, D.J. Levenson, B.M. Brenner, Early enhancement of fluid transport in rabbit proximal straight tubules after loss of contralateral renal excretory function, J. Clin. Invest. 72 (1983) 871–881, https://doi.org/10.1172/JCI111058.
[29] M.M. Schwartz, M. Churchill, a Bidani, P.C. Churchill, Reversible compensatory hypertrophy in rat kidneys: morphometric characterization, Kidney Int. 43 (1993) 610–614, https://doi.org/10.1038/ki.1993.89.
[30] O.E. Aparicio-Trejo, E. Tapia, E. Molina-Jijón, O.N. Medina-Campos, N.A. Macías-Ruvalcaba, J.C. León-Contreras, R. Hernández-Pando, F.E. García-Arroyo, M. Cristóbal, L.G. Sánchez-Lozada, J. Pedraza-Chaverri, Curcumin prevents mitochondrial dynamics disturbances in early 5/6 nephrectomy: relation to oxidative stress and mitochondrial bioenergetics, Biofactors 43 (2017) 293–310, https://doi.org/10.1002/biof.1338.
[31] L.V. Fedorova, A. Tamirisa, D.J. Kennedy, S.T. Haller, G. Budnyy, J.I. Shapiro, D. Malhotra, Mitochondrial impairment in the five-sixth nephrectomy model of chronic renal failure: proteomic approach, BMC Nephrol. 14 (2013) 209 http://www.pubmedcentral.nih.gov/articlerender.fcgi?artid=3851543&tool=pmcentrez&rendertype=abstract.
[32] J.T. Norman, S. Hwang, L.G. Fine, D. Nephrology, T. Bradley, Hypertrophy of renal mitochondria, J. Am. Soc. Nephrol. I (1990) 822–827.
[33] L.H. Lash, D.A. Putt, S.J. Horky, R.K. Zalups, Functional and toxicological characteristics of isolated renal mitochondria: impact of compensatory renal growth, Biochem. Pharmacol. 62 (2001) 383–395, https://doi.org/10.1016/S0006-2952(01)00673-6.
[34] J.A. Funk, R.G. Schnellmann, Persistent disruption of mitochondrial homeostasis after acute kidney injury, Am. J. Physiol. Renal Physiol. 302 (2012) F853–F864, https://doi.org/10.1152/ajprenal.00035.2011.
[35] Mackenzie Walser, Progression of chronic renal failure in man, Kidney Int. 37 (1990) 1195–1210.
[36] A. Priyadarshi, S. Periyasamy, T.J. Burke, S.L. Britton, D. Malhotra, J.I. Shapiro, Effects of reduction of renal mass on renal oxygen tension and erythropoietin production in the rat, Kidney Int. 61 (2002) 542–546, https://doi.org/10.1046/j.1523-1755.2002.00140.x.
[37] S. Kume, T. Uzu, S. Araki, T. Sugimoto, K. Isshiki, M. Chin-Kanasaki, M. Sakaguchi, N. Kubota, Y. Terauchi, T. Kadowaki, M. Haneda, A. Kashiwagi, D. Koya, Role of altered renal lipid metabolism in the development of renal injury induced by a high-fat diet, J. Am. Soc. Nephrol. 18 (2007) 2715–2723, https://doi.org/10.1681/ASN.2007010089.
[38] H.H. Szeto, S. Liu, Y. Soong, N. Alam, G.T. Prusky, S.V. Seshan, Protection of mitochondria prevents high-fat diet induced glomerulopathy and proximal tubular

injury, Kidney Int. 90 (2016) 997–1011, https://doi.org/10.1016/j.kint.2016.06.013.
[39] J.L. Thomas, H. Pham, Y. Li, E. Hall, G.A. Perkins, S.S. Ali, H.H. Patel, P. Singh, Hypoxia-inducible factor-1α activation improves renal oxygenation and mitochondrial function in early chronic kidney disease, Am. J. Physiol. - Ren. Physiol. 313 (2017) F282–F290, https://doi.org/10.1152/ajprenal.00579.2016.
[40] C. Kang, W. Lim, Data on mitochondrial function in skeletal muscle of old mice in response to different exercise intensity, Data Br. 7 (2016) 1519–1523, https://doi.org/10.1016/j.dib.2016.04.043.
[41] R.L.S. Goncalves, C.L. Quinlan, I.V. Perevoshchikova, M. Hey-Mogensen, M.D. Brand, Sites of superoxide and hydrogen peroxide production by muscle mitochondria assessed ex vivo under conditions mimicking rest and exercise, J. Biol. Chem. 290 (2015) 209–227, https://doi.org/10.1074/jbc.M114.619072.
[42] Z. Yan, V.A. Lira, N.P. Greene, Exercise training-induced regulation of mitochondrial quality, Exerc. Sport Sci. Rev. 40 (2012) 159–164, https://doi.org/10.1097/JES.0b013e3182575599.
[43] C. Lundby, R.A. Jacobs, Adaptations of skeletal muscle mitochondria to exercise training, Exp. Physiol. 101 (2015) 17–22, https://doi.org/10.1113/EP085319.
[44] F. Correa, M. Buelna-Chontal, S. Hernández-Reséndiz, W.R. García-Niño, F.J. Roldán, V. Soto, A. Silva-Palacios, A. Amador, J. Pedraza-Chaverrí, E. Tapia, C. Zazueta, Curcumin maintains cardiac and mitochondrial function in chronic kidney disease, Free Radic. Biol. Med. 61 (2013) 119–129, https://doi.org/10.1016/j.freeradbiomed.2013.03.017.
[45] Y. Hui, M. Lu, Y. Han, H. Zhou, W. Liu, L. Li, R. Jin, Resveratrol improves mitochondrial function in the remnant kidney from 5/6 nephrectomized rats, Acta Histochem. 119 (2017) 392–399, https://doi.org/10.1016/j.acthis.2017.04.002.
[46] B. Benipal, L.H. Lash, Modulation of mitochondrial glutathione status and cellular energetics in primary cultures of proximal tubular cells from remnant kidney of uninephrectomized rats, Biochem. Pharmacol. 85 (2013) 1379–1388, https://doi.org/10.1016/j.bcp.2013.02.013.
[47] K.A. Nath, A.J. Croatt, T.H. Hostetter, Oxygen consumption and oxidant stress in surviving nephrons, Am. J. Physiol. 258 (1990) F1354–F1362.
[48] E. Tapia, V. Soto, K.M. Ortiz-Vega, G. Zarco-Márquez, E. Molina-Jijón, M. Cristóbal-García, J. Santamaría, W.R. García-Niño, F. Correa, C. Zazueta, J. Pedraza-Chaverri, Curcumin induces Nrf2 nuclear translocation and prevents glomerular hypertension, hyperfiltration, oxidant stress, and the decrease in antioxidant enzymes in 5/6 nephrectomized rats, Oxid. Med. Cell. Longev. 2013 (2012) 269039, , https://doi.org/10.1155/2012/269039.
[49] H. Watanabe, Y. Miyamoto, D. Honda, H. Tanaka, Q. Wu, M. Endo, T. Noguchi, D. Kadowaki, Y. Ishima, S. Kotani, M. Nakajima, K. Kataoka, S. Kim-Mitsuyama, M. Tanaka, M. Fukagawa, M. Otagiri, T. Maruyama, p-Cresyl sulfate causes renal tubular cell damage by inducing oxidative stress by activation of NADPH oxidase, Kidney Int. 83 (2013) 582–592, https://doi.org/10.1038/ki.2012.448.
[50] L. Sun, Q. Yuan, T. Xu, L. Yao, J. Feng, J. Ma, L. Wang, C. Lu, D. Wang, Pioglitazone improves mitochondrial function in the remnant kidney and protects against renal fibrosis in 5/6 nephrectomized rats, Front. Pharmacol. 8 (2017) 545, https://doi.org/10.3389/fphar.2017.00545.
[51] J.F. Chen, H. Liu, H.F. Ni, L.L. Lv, M.H. Zhang, A.H. Zhang, R.N. Tang, P.S. Chen, B.C. Liu, Improved mitochondrial function underlies the protective effect of pirfenidone against tubulointerstitial fibrosis in 5/6 nephrectomized rats, PLoS One 8 (2013) e83593, , https://doi.org/10.1371/journal.pone.0083593.
[52] H. Zhao, Y. jun Liu, Z. rui Liu, D. dong Tang, X. wen Chen, Y. hua Chen, R. ning Zhou, S. qi Chen, H. xin Niu, Role of mitochondrial dysfunction in renal fibrosis promoted by hypochlorite-modified albumin in a remnant kidney model and protective effects of antioxidant peptide SS-31, Eur. J. Pharmacol. 804 (2017) 57–67, https://doi.org/10.1016/j.ejphar.2017.03.037.
[53] H.H. Szeto, S. Liu, Y. Soong, S.V. Seshan, L. Cohen-Gould, V. Manichev, L.C. Feldman, T. Gustafsson, Mitochondria protection after acute ischemia prevents prolonged upregulation of IL-1 β and IL-18 and arrests CKD, J. Am. Soc. Nephrol. 28 (2017) 1437–1449, https://doi.org/10.1681/ASN.2016070761.
[54] M.T. Sweetwyne, J.W. Pippin, D.G. Eng, K.L. Hudkins, Y.A. Chiao, M.D. Campbell, D.J. Marcinek, C.E. Alpers, H.H. Szeto, P.S. Rabinovitch, S.J. Shankland, The mitochondrial-targeted peptide, SS-31, improves glomerular architecture in mice of advanced age, Kidney Int. 91 (2017) 1126–1145, https://doi.org/10.1016/j.kint.2016.10.036.
[55] F. Ursini, M. Maiorino, H.J. Forman, Redox homeostasis: the golden mean of healthy living, Redox Biol. 8 (2016) 205–215, https://doi.org/10.1016/j.redox.2016.01.010.
[56] M. Sedeek, R. Nasrallah, R.M. Touyz, R.L. Hébert, NADPH oxidases, reactive oxygen species, and the kidney: friend and foe, J. Am. Soc. Nephrol. 24 (2013) 1512–1518, https://doi.org/10.1681/ASN.2012111112.
[57] M.S. Goligorsky, Oxidative stress and the kidney: riding on the curve of Hormesis, Antioxid. Redox Signal. 25 (2016) 117–118, https://doi.org/10.1089/ars.2016.6794.
[58] J. Trujillo, Y.I. Chirino, E. Molina-Jijón, A.C. Andérica-Romero, E. Tapia, J. Pedraza-Chaverrí, Renoprotective effect of the antioxidant curcumin: recent findings, Redox Biol. 1 (2013) 448–456, https://doi.org/10.1016/j.redox.2013.09.003.
[59] E. Tapia, L.G. Sánchez-Lozada, W.R. García-Niño, E. García, A. Cerecedo, F.E. García-Arroyo, H. Osorio, A. Arellano, M. Cristóbal-García, M.L. Loredo, E. Molina-Jijón, J. Hernández-Damián, M. Negrette-Guzmán, C. Zazueta, S. Huerta-Yepez, J.L. Reyes, M. Madero, J. Pedraza-Chaverrí, Curcumin prevents maleate-induced nephrotoxicity: relation to hemodynamic alterations, oxidative stress, mitochondrial oxygen consumption and activity of respiratory complex I, Free Radic. Res. 48 (2014) 1342–1354, https://doi.org/10.3109/10715762.2014.954109.
[60] J. Trujillo, L.F. Granados-Castro, C. Zazueta, A.C. Andérica-Romero, Y.I. Chirino, J. Pedraza-Chaverrí, Mitochondria as a target in the therapeutic properties of curcumin, Arch. Pharm. (Weinheim). 347 (2014) 873–884, https://doi.org/10.1002/ardp.201400266.
[61] C.J. Martin, C.M. Goeddeke-Merickel, Oxidative stress in chronic kidney disease, Iran. J. Kidney Dis. 9 (2015) 165–179.
[62] R.J. Mailloux, W.G. Willmore, S-glutathionylation reactions in mitochondrial function and disease, Front. Cell Dev. Biol. 2 (2014) 68, https://doi.org/10.3389/fcell.2014.00068.
[63] S. Granata, A. Dalla Gassa, P. Tomei, A. Lupo, G. Zaza, Mitochondria: a new therapeutic target in chronic kidney disease, Nutr. Metab. (Lond). 12 (2015) 49, https://doi.org/10.1186/s12986-015-0044-z.
[64] C.L. Quinlan, J.R. Treberg, I.V. Perevoshchikova, A.L. Orr, M.D. Brand, Native rates of superoxide production from multiple sites in isolated mitochondria measured using endogenous reporters, Free Radic. Biol. Med. 53 (2012) 1807–1817, https://doi.org/10.1016/j.freeradbiomed.2012.08.015.
[65] C.L. Quinlan, I.V. Perevoshchikova, M. Hey-Mogensen, A.L. Orr, M.D. Brand, Sites of reactive oxygen species generation by mitochondria oxidizing different substrates, Redox Biol. 1 (2013) 304–312, https://doi.org/10.1016/j.redox.2013.04.005.
[66] L. Sun, L. Xiao, J. Nie, F.-Y. Liu, G.-H. Ling, X.-J. Zhu, W.-B. Tang, W.-C. Chen, Y.-C. Xia, M. Zhan, M.-M. Ma, Y.-M. Peng, H. Liu, Y.-H. Liu, Y.S. Kanwar, p66Shc mediates high-glucose and angiotensin II-induced oxidative stress renal tubular injury via mitochondrial-dependent apoptotic pathway, Am. J. Physiol. Renal Physiol. 299 (2010) F1014–F1025, https://doi.org/10.1152/ajprenal.00414.2010.
[67] Y.M. Chung, J.S. Kim, Y. Do Yoo, A novel protein, Romo1, induces ROS production in the mitochondria, Biochem. Biophys. Res. Commun. 347 (2006) 649–655, https://doi.org/10.1016/j.bbrc.2006.06.140.
[68] B. Chance, H. Sies, a Boveris, Hydroperoxide metabolism in mammalian organs, Physiol. Rev. 59 (1979) 527–605.
[69] M.P. Murphy, How mitochondria produce reactive oxygen species, Biochem. J. 417 (2009) 1–13, https://doi.org/10.1042/BJ20081386.
[70] M. Jastroch, A.S. Divakaruni, S. Mookerjee, J.R. Treberg, D. Martin, Mitochondrial proton and electron leaks, Essays Biochem. 47 (2011) 53–67, https://doi.org/10.1042/bse0470053.Mitochondrial.
[71] M. Forkink, Ja M. Smeitink, R. Brock, P.H.G.M. Willems, W.J.H. Koopman, Detection and manipulation of mitochondrial reactive oxygen species in mammalian cells, Biochim. Biophys. Acta 1797 (2010) 1034–1044, https://doi.org/10.1016/j.bbabio.2010.01.022.
[72] M. Makrecka-kuka, G. Krumschnabel, E. Gnaiger, High-resolution respirometry for simultaneous measurement of oxygen and hydrogen peroxide fluxes in permeabilized cells, tissue homogenate and isolated mitochondria, Biomolecules 5 (2015) 1319–1338, https://doi.org/10.3390/biom5031319.
[73] G.S. Shadel, T.L. Horvath, Mitochondrial ROS signaling in Organismal Homeostasis, Cell 163 (2015) 560–569, https://doi.org/10.1016/j.cell.2015.10.001.
[74] R.J. Mailloux, X. Jin, W.G. Willmore, Redox regulation of mitochondrial function with emphasis on cysteine oxidation reactions, Redox Biol. 2 (2014) 123–139, https://doi.org/10.1016/j.redox.2013.12.011.
[75] Y. Xiong, J.D. Uys, K.D. Tew, D.M. Townsend, S-glutathionylation: from molecular mechanisms to health outcomes, Antioxid. Redox Signal. 15 (2011) 233–270, https://doi.org/10.1089/ars.2010.3540.
[76] R.J. Mailloux, J.R. Treberg, Protein S-glutathionlyation links energy metabolism to redox signaling in mitochondria, Redox Biol. 8 (2016) 110–118, https://doi.org/10.1016/j.redox.2015.12.010.
[77] C.A. Piantadosi, Regulation of mitochondrial processes by protein S-nitrosylation, Biochim. Biophys. Acta - Gen. Subj. 1820 (2012) 712–721, https://doi.org/10.1016/j.bbagen.2011.03.008.
[78] P.T. Kang, C.L. Chen, Y.R. Chen, Increased mitochondrial prooxidant activity mediates up-regulation of Complex i S-glutathionylation via protein thiyl radical in the murine heart of eNOS-/-, Free Radic. Biol. Med. 79 (2015) 56–68, https://doi.org/10.1016/j.freeradbiomed.2014.11.016.
[79] G. Tamma, G. Valenti, Evaluating the Oxidative stress in Renal diseases: What is the role for S-glutathionylation? Antioxid. Redox Signal. 25 (2016) 147–164, https://doi.org/10.1089/ars.2016.6656.
[80] J.J. Mieyal, P.B. Chock, Posttranslational modification of cysteine in redox signaling and oxidative stress: focus on s-glutathionylation, Antioxid. Redox Signal. 16 (2012) 471–475, https://doi.org/10.1089/ars.2011.4454.
[81] P.T. Kang, L. Zhang, C.L. Chen, J. Chen, K.B. Green, Y.R. Chen, Protein thiyl radical mediates S-glutathionylation of complex i, Free Radic, Biol. Med. 53 (2012) 962–973, https://doi.org/10.1016/j.freeradbiomed.2012.05.025.
[82] Y.-R. Chen, C.-L. Chen, D.R. Pfeiffer, J.L. Zweier, Mitochondrial Complex II in the Post-ischemic Heart: oxidative injury and the role of protein s-glutathionylation, J. Biol. Chem. 282 (2007) 32640–32654, https://doi.org/10.1074/jbc.M702294200.
[83] J. Garcia, D. Han, H. Sancheti, L.P. Yap, N. Kaplowitz, E. Cadenas, Regulation of mitochondrial glutathione redox status and protein glutathionylation by respiratory substrates, J. Biol. Chem. 285 (2010) 39646–39654, https://doi.org/10.1074/jbc.M110.164160.
[84] S.-B. Wang, C.I. Murray, H.S. Chung, J.E. Van Eyk, Redox regulation of mitochondrial ATP synthase, Trends Cardiovasc. Med. 23 (2013) 14–18, https://doi.org/10.1016/j.tcm.2012.08.005.
[85] J. Trujillo, E. Molina-Jijón, O.N. Medina-Campos, R. Rodríguez-Muñoz, J.L. Reyes, M.L. Loredo, D. Barrera-Oviedo, E. Pinzón, D.S. Rodríguez-Rangel, J. Pedraza-Chaverri, Curcumin prevents cisplatin-induced decrease in the tight and adherens junctions: relation to oxidative stress, Food Funct. 7 (2016) 279–293 http://xlink.

rsc.org/?DOI=C5F148O00624D.
[86] B. Fernández-Rojas, D.S. Rodríguez-Rangel, L.F. Granados-Castro, M. Negrette-Guzmán, J.C. León-Contreras, R. Hernández-Pando, E. Molina-Jijón, J.L. Reyes, C. Zazueta, J. Pedraza-Chaverri, C-phycocyanin prevents cisplatin-induced mitochondrial dysfunction and oxidative stress, Mol. Cell. Biochem. 406 (2015) 183–197, https://doi.org/10.1007/s11010-015-2436-9.
[87] H.H. Szeto, Pharmacologic approaches to improve mitochondrial function in AKI and CKD, J. Am. Soc. Nephrol. 28 (2017) 2856–2865, https://doi.org/10.1681/ASN.2017030247.
[88] B.D. Fink, J.A. Herlein, M.A. Yorek, A.M. Fenner, R.J. Kerns, W.I. Sivitz, Bioenergetic effects of mitochondrial-targeted coenzyme q analogs in endothelial cells, J. Pharmacol. Exp. Ther. 342 (2012) 709–719, https://doi.org/10.1124/jpet.112.195586.
[89] N.K. Patil, N. Parajuli, L.A. MacMillan-Crow, P.R. Mayeux, Inactivation of renal mitochondrial respiratory complexes and manganese superoxide dismutase during sepsis: mitochondria-targeted antioxidant mitigates injury, AJP Ren. Physiol. 306 (2014) F734–F743, https://doi.org/10.1152/ajprenal.00643.2013.
[90] S. Granata, V. Masola, E. Zoratti, M.T. Scupoli, A. Baruzzi, M. Messa, F. Sallustio, L. Gesualdo, A. Lupo, G. Zaza, NLRP3 inflammasome activation in dialyzed chronic kidney disease patients, PLoS One 10 (2015) e012272, , https://doi.org/10.1371/journal.pone.0122272.
[91] Y. Yuan, Y. Chen, P. Zhang, S. Huang, C. Zhu, G. Ding, B. Liu, T. Yang, A. Zhang, Mitochondrial dysfunction accounts for aldosterone-induced epithelial-to-mesenchymal transition of renal proximal tubular epithelial cells, Free Radic. Biol. Med. 53 (2012) 30–43, https://doi.org/10.1016/j.freeradbiomed.2012.03.015.
[92] R.P. Brandes, N. Weissmann, K. Schröder, Nox family NADPH oxidases: Molecular mechanisms of activation, Free Radic. Biol. Med. 76 (2014) 208–226, https://doi.org/10.1016/j.freeradbiomed.2014.07.046.
[93] P. Gill, C. Wilcox, NADPH oxidases in the kidney, Antioxid. Redox Signal. 8 (2006) 1597–1607.
[94] H. Wang, X. Chen, Y. Su, P. Paueksakon, W. Hu, M.-Z. Zhang, R.C. Harris, T.S. Blackwell, R. Zent, A. Pozzi, P47(Phox) contributes to Albuminuria and kidney fibrosis in mice, Kidney Int. 87 (2015) 948–962, https://doi.org/10.1038/ki.2014.386.
[95] A.M. Garrido, K.K. Griendling, NADPH oxidases and angiotensin II receptor signaling, Mol. Cell. Endocrinol. 302 (2009) 148–158, https://doi.org/10.1016/j.mce.2008.11.003.
[96] H.J. Kim, N.D. Vaziri, Contribution of impaired Nrf2-Keap1 pathway to oxidative stress and inflammation in chronic renal failure, Am. J. Physiol. Renal Physiol. 298 (2010) F662–F671, https://doi.org/10.1152/ajprenal.00421.2009.
[97] N.D. Vaziri, Y. Bai, Z. Ni, Y. Quiroz, R. Pandian, B. Rodriguez-Iturbe, Intra-renal angiotensin II/AT1 receptor, oxidative stress, inflammation, and progressive injury in renal mass reduction, J. Pharmacol. Exp. Ther. 323 (2007) 85–93, https://doi.org/10.1124/jpet.107.123638.
[98] Y. Gorin, Nox4 as a potential therapeutic target for treatment of uremic toxicity associated to chronic kidney disease, Kidney Int. 83 (2013) 541–543, https://doi.org/10.1038/ki.2012.434.
[99] A. Daiber, Redox signaling (cross-talk) from and to mitochondria involves mitochondrial pores and reactive oxygen species, Biochim. Biophys. Acta 1797 (2010) 897–906, https://doi.org/10.1016/j.bbabio.2010.01.032.
[100] R. Kozieł, H. Pircher, M. Kratochwil, B. Lener, M. Hermann, N. a Dencher, P. Jansen-Dürr, Mitochondrial respiratory chain complex I is inactivated by NADPH oxidase Nox4, Biochem. J. 452 (2013) 231–239, https://doi.org/10.1042/BJ20121778.
[101] P. Wenzel, H. Mollnau, M. Oelze, E. Schulz, J.M.D. Wickramanayake, J. Müller, S. Schuhmacher, M. Hortmann, S. Baldus, T. Gori, R.P. Brandes, T. Münzel, A. Daiber, First evidence for a crosstalk between mitochondrial and NADPH oxidase-derived reactive oxygen species in nitroglycerin-triggered vascular dysfunction, Antioxid. Redox Signal. 10 (2008) 1435–1447, https://doi.org/10.1089/ars.2007.1969.
[102] R. Rathore, Y. Zheng, C. Niu, Hypoxia activates NADPH oxidase to increase i and i through mitochondrial ROS–PKCε signaling axis in pulmonary artery smooth muscle cells, Free Radic. Biol. 45 (2008) 1223–1231, https://doi.org/10.1016/j.freeradbiomed.2008.06.012.Hypoxia.
[103] A. Fontayne, P.M.C. Dang, M.A. Gougerot-Pocidalo, J. El Benna, Phosphorylation of p47phox sites by PKC α, βII, δ, and ζ: effect on binding to p22phox and on NADPH oxidase activation, Biochemistry 41 (2002) 7743–7750, https://doi.org/10.1021/bi011953s.
[104] P.H.G.M. Willems, R. Rossignol, C.E.J. Dieteren, M.P. Murphy, W.J.H. Koopman, Redox homeostasis and mitochondrial dynamics, Cell Metab. 22 (2015) 207–218, https://doi.org/10.1016/j.cmet.2015.06.006.
[105] H.M. Ni, J.A. Williams, W.X. Ding, Mitochondrial dynamics and mitochondrial quality control, Redox Biol. 4 (2015) 6–13, https://doi.org/10.1016/j.redox.2014.11.006.
[106] B. Westermann, Mitochondrial fusion and fission in cell life and death, Nat. Rev. Mol. Cell Biol. 11 (2010) 872–884, https://doi.org/10.1038/nrm3013.
[107] T. Wai, T. Langer, Mitochondrial dynamics and metabolic regulation, Trends Endocrinol. Metab. 27 (2016) 105–117, https://doi.org/10.1016/j.tem.2015.12.001.
[108] T.M. Durcan, E.A. Fon, The three 'P' s of mitophagy : PARKIN, modifications, Genes Dev. 29 (2015) 989–999, https://doi.org/10.1101/gad.262758.115.GENES.
[109] G. Nowak, D. Bakajsova, A.M. Samarel, Protein kinase C-epsilon activation induces mitochondrial dysfunction and fragmentation in renal proximal tubules, Am. J. Physiol. Renal Physiol. 301 (2011) F197–F208, https://doi.org/10.1152/ajprenal.00364.2010.
[110] R.J. Youle, D.P. Narendra, Mechanisms of mitophagy, Nat. Rev. Mol. Cell Biol. 12 (2011) 9–14, https://doi.org/10.1038/nrm3028.
[111] S. Rovira-Llopis, C. Bañuls, N. Diaz-Morales, A. Hernandez-Mijares, M. Rocha, V.M. Victor, Mitochondrial dynamics in type 2 diabetes: pathophysiological implications, Redox Biol. 11 (2017) 637–645, https://doi.org/10.1016/j.redox.2017.01.013.
[112] P. Bhargava, R.G. Schnellmann, Mitochondrial energetics in the kidney, Nat. Rev. Nephrol. 13 (2017) 629–646, https://doi.org/10.1038/nrneph.2017.107.
[113] S. Kume, T. Uzu, K. Horiike, M. Chin-kanasaki, K. Isshiki, S. Araki, T. Sugimoto, M. Haneda, A. Kashiwagi, D. Koya, Calorie restriction enhances cell adaptation to hypoxia through Sirt1-dependent mitochondrial autophagy in mouse aged kidney, J. Clin. Invest. 120 (2010) 1043–1055, https://doi.org/10.1172/JCI41376DS1.
[114] J. Cui, S. Shi, X. Sun, G. Cai, S. Cui, Q. Hong, X. Chen, X.Y. Bai, PLoS One. 8 (2013) e69720, , https://doi.org/10.1371/journal.pone.0069720.
[115] S. Hallan, K. Sharma, The role of mitochondria in diabetic kidney disease, Curr. Diab. Rep. 16 (2016) 61, https://doi.org/10.1007/s11892-016-0748-0.
[116] D.L. Galvan, N.H. Green, F.R. Danesh, The hallmarks of mitochondrial dysfunction in chronic kidney disease, Kidney Int. 92 (2017) 1051–1057, https://doi.org/10.1016/j.kint.2017.05.034.
[117] L. Xiao, X. Xu, F. Zhang, M. Wang, Y. Xu, D. Tang, J. Wang, Y. Qin, Y. Liu, C. Tang, L. He, A. Greka, Z. Zhou, F. Liu, Z. Dong, L. Sun, The mitochondria-targeted antioxidant MitoQ ameliorated tubular injury mediated by mitophagy in diabetic kidney disease via Nrf2/PINK1, Redox Biol. 11 (2017) 297–311, https://doi.org/10.1016/j.redox.2016.12.022.
[118] Y. Zhao, Y. Guo, Y. Jiang, X. Zhu, Y. Liu, X. Zhang, Mitophagy regulates macrophage phenotype in diabetic nephropathy rats, Biochem. Biophys. Res. Commun. 494 (2017) 42–50, https://doi.org/10.1016/j.bbrc.2017.10.088.
[119] D.L. Galvan, S.S. Badal, J. Long, B.H. Chang, P.T. Schumacker, P.A. Overbeek, F.R. Danesh, Real-time in vivo mitochondrial redox assessment confirms enhanced mitochondrial reactive oxygen species in diabetic nephropathy, Kidney Int. 92 (2017) 1282–1287, https://doi.org/10.1016/j.kint.2017.05.015.
[120] A. Czajka, A.N. Malik, Hyperglycemia induced damage to mitochondrial respiration in renal mesangial and tubular cells: implications for diabetic nephropathy, Redox Biol. 10 (2016) 100–107, https://doi.org/10.1016/j.redox.2016.09.007.
[121] O. Ortiz-Avila, M. del C. Figueroa-García, C.I. García-Berumen, E. Calderón-Cortés, J.A. Mejía-Barajas, A.R. Rodriguez-Orozco, R. Mejía-Zepeda, A. Saavedra-Molina, C. Cortés-Rojo, Avocado oil induces long-term alleviation of oxidative damage in kidney mitochondria from type 2 diabetic rats by improving glutathione status, J. Bioenerg. Biomembr. 49 (2017) 205–214, https://doi.org/10.1007/s10863-017-9697-9.
[122] C. Feng, Q. Wang, J. Wang, F. Liu, H. Shen, H. Fu, J. Mao, Coenzyme Q10 supplementation therapy for 2 children with proteinuria renal disease and ADCK4 mutation, Medicine (United States) 96 (2017) e8880, , https://doi.org/10.1097/MD.0000000000008880.
[123] F. Emma, G. Montini, S.M. Parikh, L. Salviati, Mitochondrial dysfunction in inherited renal disease and acute kidney injury, Nat. Rev. Nephrol. 12 (2016) 267–280, https://doi.org/10.1038/nrneph.2015.214nrneph.2015.214 [pii]..
[124] R. Che, Y. Yuan, S. Huang, A. Zhang, Mitochondrial dysfunction in the pathophysiology of renal diseases, Am. J. Physiol. Renal Physiol. 306 (2014) F367–F378, https://doi.org/10.1152/ajprenal.00571.2013.
[125] K.E. D'Aco, M. Manno, C. Clarke, J. Ganesh, K.E.C. Meyers, N. Sondheimer, Mitochondrial tRNAPhe mutation as a cause of end-stage renal disease in childhood, Pediatr. Nephrol. 28 (2013) 515–519, https://doi.org/10.1007/s00467-012-2354-y.
[126] K.M. Au, S.C. Lau, Y.F. Mak, W.M. Lai, T.C. Chow, M.L. Chen, M.C. Chiu, A.Y.W. Chan, Mitochondrial DNA deletion in a girl with Fanconi's syndrome, Pediatr. Nephrol. 22 (2007) 136–140, https://doi.org/10.1007/s00467-006-0288-y.
[127] J.L. Gamboa, F.T. Billings, M.T. Bojanowski, L.A. Gilliam, C. Yu, B. Roshanravan, L.J. Roberts, J. Himmelfarb, T.A. Ikizler, N.J. Brown, Mitochondrial dysfunction and oxidative stress in patients with chronic kidney disease, Physiol. Rep. 4 (2016) e12780, , https://doi.org/10.14814/phy2.12780.
[128] S. Granata, G. Zaza, S. Simone, G. Villani, D. Latorre, P. Pontrelli, M. Carella, F.P. Schena, G. Grandaliano, G. Pertosa, Mitochondrial dysregulation and oxidative stress in patients with chronic kidney disease, BMC Genomics 10 (388) (2009), https://doi.org/10.1186/1471-2164-10-388.
[129] F. Emma, L. Salviati, Mitochondrial cytopathies and the kidney, Nephrol. Ther. 13 (2017) S23–S28, https://doi.org/10.1016/j.nephro.2017.01.014.
[130] R. Roskoski, Guidelines for preparing color figures for everyone including the colorblind, Pharmacol. Res. 119 (2017) 240–241, https://doi.org/10.1016/j.phrs.2017.02.005.